3d Transition Metal Catalyzed Dehydrogenation of Alcohols

Miao, Yulong

Publication date:
2021

Document Version
Publisher's PDF, also known as Version of record

DTU Chemistry
Technical University of Denmark

3d Transition Metal Catalyzed Dehydrogenation of Alcohols

Yulong Miao (苗玉龙)

Ph.D. Thesis

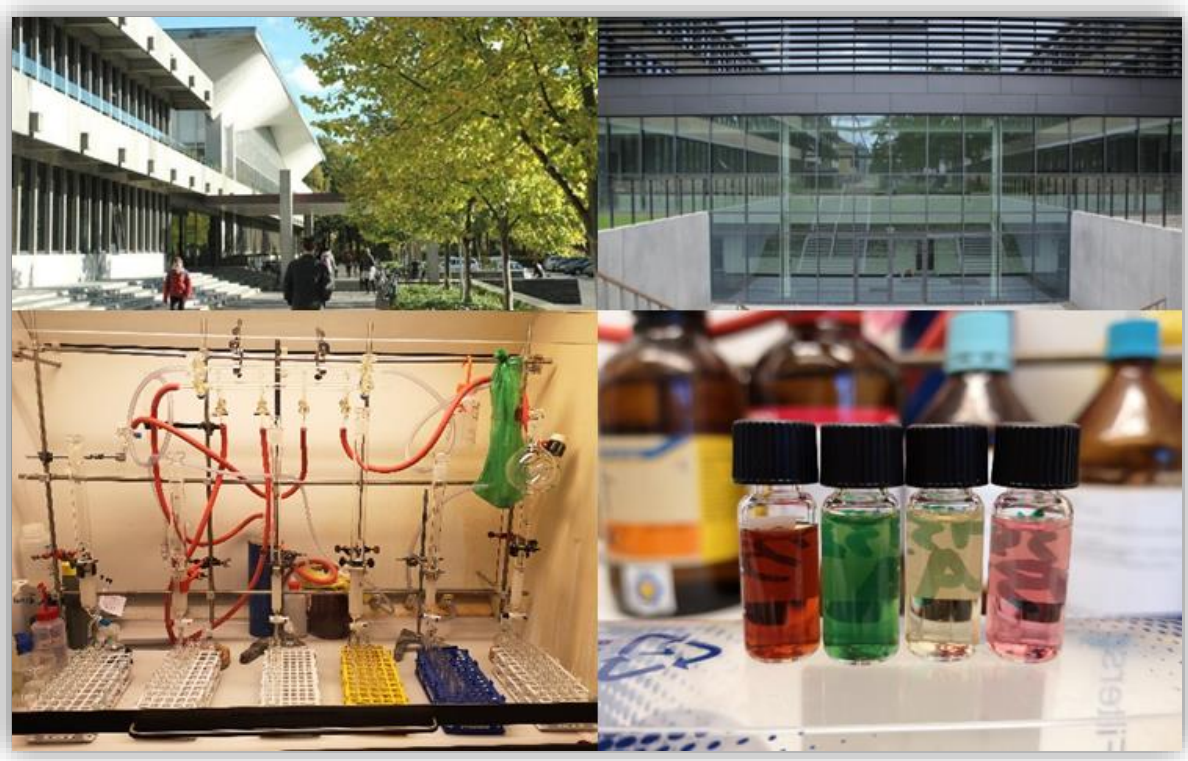

August 2021

3d Transition Metal Catalyzed Dehydrogenation of Alcohols

PhD Thesis 2021

Yulong Miao (苗玉龙)

Supervisor: Prof. Robert Madsen

Co-Supervisor: Prof. Mads H. Clausen

Technical University of Denmark, Department of Chemistry

Kongens Lyngby, 2021

Title: 3d Transition Metal Catalyzed Dehydrogenation of Alcohols

Website: Library.DTU.dk

Designed by Yulong Miao

Printed in Denmark 2021

ISBN: 978-87-DTU-20180827-1014

Cover designed by Yulong Miao

Department of Chemistry

Technical University of Denmark

www.kemi.dtu.dk

Kemitorvet, Building 207

2800 Kgs Lyngby, Denmark

Phone: +45 52788909

Email: yumi@kemi.dtu.dk

Print: Technical University of Denmark

Edition: Sept. 2021

It is the time you have wasted for your rose

that makes your rose so important.

Antoine de Saint-Exupéry, The Little Prince

Preface

This thesis presents the work conducted during my Ph.D. study at the Department of Chemistry, the Technical University of Denmark under the supervision of Professor Robert Madsen as the main supervisor and Professor Mads H. Clausen as the co-supervisor.

The project was supported from the funding of Robert's group and the Chinese Scholarship Council (CSC). The PhD program included courses for 31.5 ECTS and a minimum of 420 hours spent on dissemination of knowledge, including teaching. Additionally, a two months' external stay at Haldor Topsøe A/S was conducted under the supervision of R&D director Dr. Esben Taarning and R&D manager Dr. Søren Tolborg.

The dissertation includes two projects regarding the development of new catalysts based on Earth-abundant transition metals for acceptorless dehydrogenation of alcohols. Two catalysts based on chromium and vanadium have been described and studied, respectively.

So far, the work has resulted in one scientific publication. A full paper has been published in Organometallics. The other manuscript has been submitted to my supervisor. Further applications of the catalysts are currently under investigation.

Acknowledgement

I had read Hans Christian Andersen's fairy tales before starting primary school, but I never imagined that I could come to his home country Denmark and pursue my Ph.D. at DTU Chemistry. Now I have lived in Denmark for almost three years. My mind is filled with appreciations when I look back.

First of all, I would like to express my sincere gratitude to my supervisor Prof. Dr. Robert Madsen. Robert provided me an opportunity to start a different and colorful life out of my home country. He has given me lots of patience, support, and encouragement throughout the length of my Ph.D. I did not perform my research smoothly during the past three years and failed many times. I would have experienced more storms without Robert's supervision.

Three thousand thanks to my former and present colleagues in the group. Especially thanks to Simone, the Fabrizios, Eli, Emil, Kassem, and Nicolai for the introductions to a new field of chemistry, the professional guides, the unselfish help, and the enjoyable company whenever at beginning of the Ph.D. or in the post-COVID-19 era. I like the atmosphere of our group and enjoy the time we have spent together.

I also would like to express my gratitude to the lecturers who gave me courses at DTU, particularly to David Ackland Tanner, Søren Kramer, Charlotte Held Gotfredsen, Sebastian Meier, and Mads H. Clausen. They all used simple words to make me understand complicated knowledge. A special thanks to my co-supervisor, Prof. Mads H. Clausen. He always came up with some critical questions to push me to think further on the Monday Morning Meeting.

I would like to give thanks to the technical staff and people in the building center for keeping the department on its feet. Special thanks to Charlie and Anne, who ensured that the samples could be in the line or tested at any time. I thank Lars and John, who provided enough consumable items at the department.

I also want to thank Esben Taarning and Søren Tolborg for giving me the opportunity to carry out my external stay at Haldor Topsøe A/S. It was nice to have an excellent experience at Haldor Topsøe.

I sincerely thank postdoc Dr. Hao Jiang from Mads'group, who gave me lots of guidance and help both in academics and in life. We visited each other for many times and I enjoyed the time we spent in Copenhagen. I also thank my former lab-mate Weiguang Jin. We talked and shared a lot with each other. It was a good time to spend together.

Many thanks to colleagues, friends and the people I have met here at the department. In particular, the people from our social group: lunch group “Pasta with olives”, Friday breakfast, and international dinners from Chemclub. It was so enjoyable to have a nice conversation and share funny experiments and stories. I miss the happy time, delicious cookies, and (pan)cakes. The badminton group is also deserved to thank. Thanks to Dr. Huili Cao’s introduction, I made new friends with Xin, Yaoxin, Dr. Gu, and Dr. Dong.

At this point, I would also thank Hao, Eli and Kassem who has helped me proofread my thesis. I also thank Nicolai for the help on the Hammett study and LCMS.

I am particularly grateful to my neighbors, Huili, Iben, and Noell in Lundtoftegårdsvej. They were generous to give me a warm welcome and provide help when I moved in. We talked, cooked together and shared a lot of lovely time.

I also thank my friends in China and other countries, Dr. Li (Yuwen), Dr. Yang (Liangtao), Adeng, Pan, and Yunze. They have always given me company, support and encouragement when I need. It is an honor to be friends with them.

Here, I gratefully acknowledge the China Scholarship Council (CSC) to give financial support for my living expense in Denmark.

Finally, a great thanks to my family and parents. You have always given me support, concern, encouragement, understanding, and trust throughout my education, and have constantly believed in me, which are endless powers for me.

Kgs. Lyngby, DTU Kemi, August 2021

Yulong Miao (苗玉龙)

Abstract

Alcohols are a good energy source from biomass and can be converted to functional groups, such as amides, amines, carboxylic acids, esters, and imines. One of the key transformations is the dehydrogenation of alcohols. The common method is to use traditional oxidants, or use catalysts based on precious metals. However, these two methods are either not “green” or sustainable. The 3d transition metals are cheap and relatively nontoxic, and they have a high abundance and a large annual production. Catalysts based on these metals could have a good performance on the dehydrogenation.

The acceptorless dehydrogenation of alcohols means that alcohol, catalyzed by metal complexes, undergoes formal oxidation to the corresponding carbonyl compound accompanied by the removal of H_2 gas. The advantage of these dehydrogenative transformations is that alcohol oxidation occurs in the absence of an oxidizing agent, which leads to less waste and more environmentally friendly reaction conversions.

Two catalysts based on Earth-abundant transition metals for acceptorless alcohol dehydrogenation are described in this Ph.D. thesis. Both catalysts mediate the dehydrogenative coupling of primary alcohols and amines to form imines.

The first developed catalyst is chromium(III) tetraphenylporphyrin chloride (Cr(TPP)Cl). This is the first time for Cr(TPP)Cl to be applied for acceptorless alcohol dehydrogenation. The catalyst has a good performance on the dehydrogenation of alcohols with amines to form imines. The reaction mechanism has been investigated by various practical experiments, and a metal-ligand cooperative pathway has been proposed.

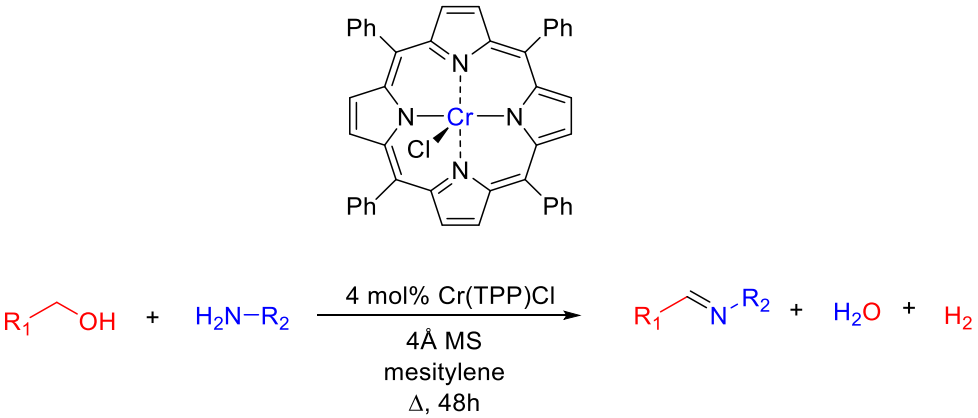

Scheme I: Dehydrogenative imine synthesis catalyzed by Cr(TPP)Cl.

The second developed catalyst is vanadium(IV) salen chloride. The catalyst indeed has a good performance on the dehydrogenation of alcohols, and the mechanism is believed to involve a metal-ligand cooperation pathway.

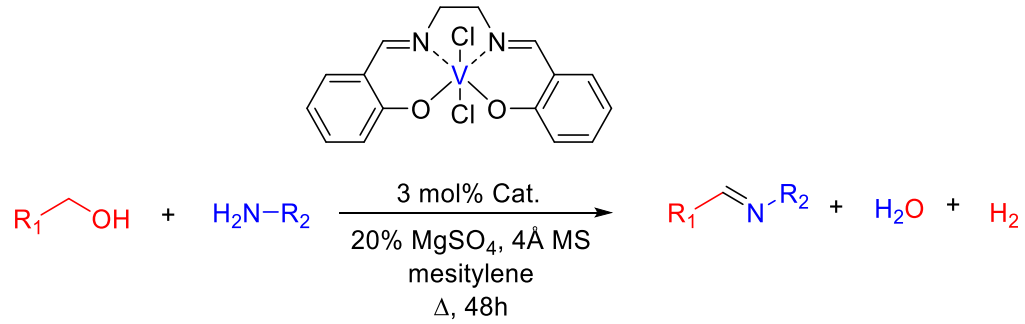

Scheme II: Vanadium-catalyzed dehydrogenative coupling of primary alcohols and amines into imines.

The thesis begins with four short chapters regarding the aim of the project, introduction to alcohols, imines, and acceptorless alcohol dehydrogenation. Subsequently, the development of the two novel catalysts is described and discussed in two chapters, followed by a conclusion on the entire project.

Resumé (Danish)

Alkoholer er gode energikilder fra biomasse, og kan omdannes til mange funktionelle grupper, som amider, aminer, carboxylsyrer, estere og iminer. En af nøgletransformationerne er dehydrogenering af alkoholer. Den almindelige metode er at bruge traditionelle oxidanter eller bruge katalysatorer baseret på ædel metaller. Disse to metoder er imidlertid enten ikke "grønne" eller bæredygtige. 3d-overgangsmetaller er billige og forholdsvis ugiftige, og de har stor forekomst og en stor årlig produktion. Katalysatorer baseret på disse metaller kan have en god indvirkning på dehydrogeneringen.

Den acceptorfrie dehydrogenering af alkoholer betyder, at en alkohol katalyseret af metalkomplekser gennemgår en formel oxidation til den tilsvarende carbonylforbindelse, der medfører fjernelsen af H_2 gas. Fordelen ved disse dehydrogenative transformationer er, at alkohol oxidationen finder sted i fravær af et oxidationsmiddel, hvilket fører til mindre spild og mere miljøvenlige reaktionsbetingelser.

To katalysatorer baseret på almindeligt forekommende overgangsmetaller til acceptorfri alkoholdehydrogenering er beskrevet i denne ph.d. afhandling. Begge katalysatorer formidler en dehydrogenativ kobling af primære alkoholer og aminer til at danne iminer.

Den første udviklede katalysator er chrom(III) tetraphenylporphyrinchlorid (Cr(TPP)Cl). Dette er første gang, at Cr(TPP)Cl anvendes til acceptorfri alkoholdehydrogenering. Katalysatoren har en god ydeevne ved dehydrogenering af alkoholer med aminer til dannelse af iminer. Reaktionsmekanismen er blevet undersøgt ved forskellige praktiske eksperimenter, og en metal-ligand-kooperativ vej er blevet foreslået.

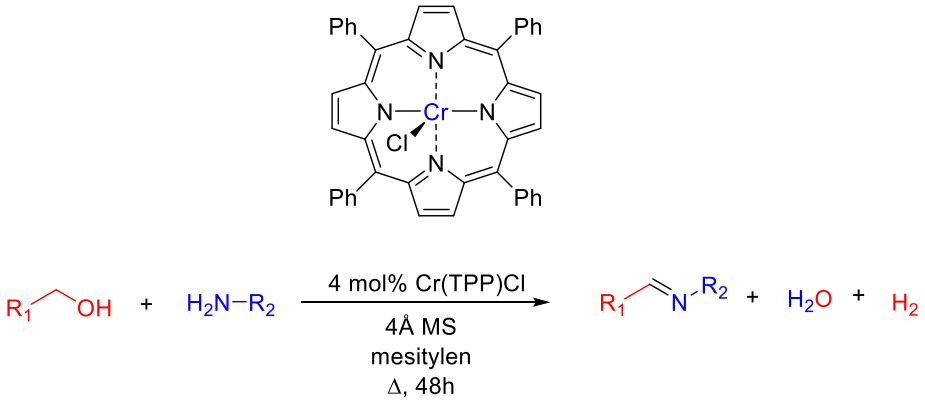

Skema I: Dehydrogenativ iminsyntese katalyseret af Cr (TPP) Cl.

Den anden udviklede katalysator er vanadium (IV) salenchlorid. Katalysatoren har en god ydeevne med hensyn til dehydrogenering af alkoholer, og mekanismen antages at gå gennem en metal-ligand-kooperativ vej.

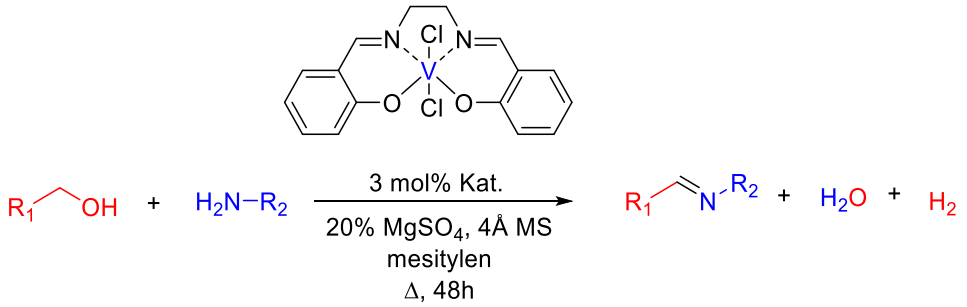

Skema II: Vanadium-katalyseret dehydrogenativ kobling af primære alkoholer og aminer til dannelse af iminer.

Afhandlingen begynder med fire korte kapitler om projektets formål, som omhandler introduktion til alkoholer, iminer og acceptorfri alkoholdehydrogenering. Derefter beskrives og diskuteres udviklingen af de to nye katalysatorer i to kapitler efterfulgt af en konklusion på hele projektet.

List of abbreviations

AAD	Acceptorless alcohol dehydrogenation
ABNO	9-Azabicyclo[3.3.1]nonan-*N*-oxyl
ACN	Acetonitrile
AD	Acceptorless dehydrogenation
BH	Borrowing hydrogen
BHT	Butylated hydroxytoluene
Bipy	2,2'-Bipyridine
Bn	Benzyl
^{t}Bu	*tert*-Butyl
Cat	Catalyst
Cp*	1,2,3,4,5-Pentamethylcyclopentadienyl
CrMCM-41	Chromium containing mesoporous molecular sieve
Cy	Cyclohexyl
DCE	1,1-Dichloroethane
DCM	Dichloromethane
DFT	Density functional theory
DIBAL-H	Diisobutylaluminium hydride
DMF	*N*,*N*-Dimethylmethanamide
DMP	Dess-Martin periodinane
DPMP	2,4-Diphenyl-4-methyl-1-pentane
dtbpy	4,4'-Di-*tert*-butyl-2,2'-bipyridine
FT-IR	Fourier-transform infrared spectroscopy
GC-MS	Gas chromatography mass spectrometry
ICP-MS	Inductively coupled plasma mass spectrometry
KIE	Kinetic isotope effect
L	Ligand
LCMS	Liquid chromatography mass spectrometry
M	Metal
Mes	Mesityl
MLC	Metal-ligand cooperation
MS	Molecular sieves
NHC	N-heterocyclic carbene
NMR	Nuclear magnetic resonance

o	Ortho
p	Para
PFTB	Perfluoro-*tert*-butoxide
PLM	Pillared montmorillonite
PNP	Diphosphinoamine
^{i}Pr	Isopropyl
RDS	Rate-determining step
Ref	Reference
rt	Room temperature
TEMPO	(2,2,6,6-Tetramethylpiperidin-1-yl)oxyl
THF	Tetrahydrofuran
TOF	Turnover frequency
TPP	Tetraphenylporphyrin

For additional abbreviations, readers are referred to JOC's list of standard abbreviations and Acronyms. https://www.cas.org/support/documentation/references/cas-standard-abbreviations

Table of Contents

1. Aim of the project

An alcohol group is one of the main functional groups in organic chemistry. Chemical reactions involving alcohols include oxidation to carbonyl compounds as well the formation of ethers and olefins, which belong to the core of organic synthesis. Oxidation of alcohols in the presence of some traditional inorganic oxidizing agents could give stoichiometric amounts of toxic waste.

Metal-catalyzed dehydrogenation of alcohols has received much interest, because of the current challenge of sustainability. This has led to the development of dehydrogenative reactions, where a metal catalyst removes hydrogen gas from an alcohol, producing the corresponding carbonyl group, which can subsequently undergo a variety of transformations into other functional groups, such as amides, amines, imines, esters, and carboxylic acids with the removal of hydrogen gas in the absence of oxidants. Hydrogen gas as the only by-product is also a much valuable commodity.

Dehydrogenative reactions with the catalysts based on metals from the platinum group, such as ruthenium, iridium and rhodium have been well established since the last century. However, these precious metals suffer from toxic effects, high prices, and low global productions. As a result, there has been a new trend and interest to focus on cheaper and more abundant metals with similar catalytic activities (Scheme 1.1).

Hence, this project will focus on the development of catalysts based on Earth-abundant metals to perform dehydrogenative reactions to convert inexpensive, simple and widely available alcohols into more valuable compounds.

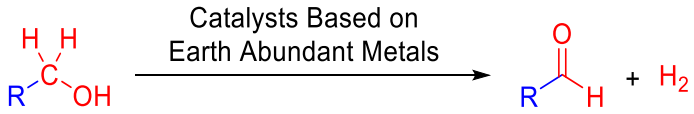

Scheme 1.1. Acceptorless dehydrogenation of primary alcohol catalyzed by Earth-abundant metals.

2. Alcohols and applications

Alcohols are good raw material for industrial processes. The source of the alcohols can be petroleum, although, petroleum is a non-renewable fossil material. It can also come from biomass,[1] which is renewable and continuously available in large amounts.

Wood, as the most abundant source of renewable carbon on the planet, is an accessible target for catalytic conversion to liquid transportation fuels or platform industrial chemicals. Potential sources of this "carbon-neutral" feedstock include forests and farms as well as municipal, agricultural, and forest waste products. Lignocellulose constitutes the woody cell walls of dry plant matter, which is composed of the biopolymers cellulose, hemicellulose, and lignin (Scheme 2.1), and it can be converted to many high-value industrial compounds.[2,3]

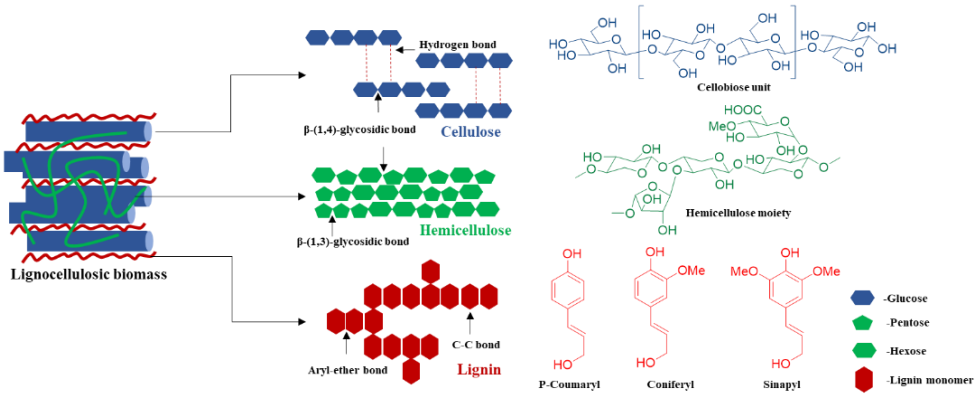

Scheme 2.1. Main components of woody biomass and their chemical structures.[3]

There have been prepared many industrially important alcohols from lignocellulose (Scheme 2.2). Ethanol and methanol, as simple and common industrial chemicals, are low boiling and volatile alcohols, which are widely reported for the fractionation of lignocellulosic biomass in organosolv processes as shown in Table 2.1. The fractionation processes are conducted at elevated temperatures with or without the addition of catalysts.

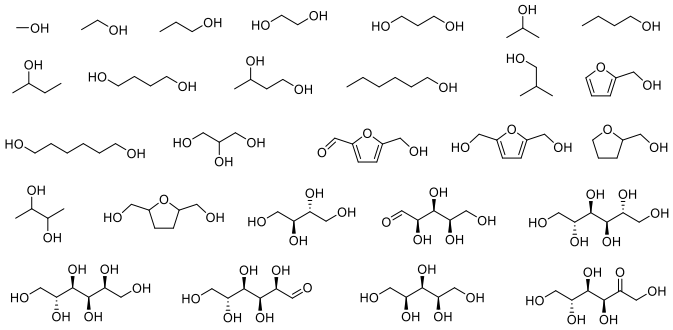

Scheme 2.2. Industrially important alcohols available from lignocellulose.[4]

Table 2.1. Different methods to use ethanol and methanol in the organosolv fractionation.[5]

Entry	Fractiona -tion process	Raw material	Fractionation conditions	Main results
1[6]	Ethanol	Eucalyptus globulus	Ethanol 60%, liquor/solid ratio 6/1(v/w), 180-200 ºC and 30-120 min	Glucose yields 69-77% after enzymatic hydrolysis (20 FPU/g Celluclast 1.5 L and 20 CBU β-glucosidase (Novozymes, USA)), and glucose to ethanol conversion 51% after fermentation (Saccharomyces cerevisiae IR2-9a, Celluclast and β-glucosidase).
2[7]	Ethanol	Wheat straw (hydrothermal ly treated)	Ethanol 60%, liquor/solid ratio 10/1(v/w), 220 ºC and 60 min	Xylose yield 67% and glucose yield 93% after enzymatic hydrolysis (20 FPU/g Celluclast Accellerase 1500).
3[8]	Ethanol	Wheat bran	Ethanol 30%, liquor/solid ratio 4/1(v/w), 180 ºC and 30 min	Glucose yield of 75%, hemicelluloses to xylose conversion 60%, and hemicelluloses to arabinose conversion 45% after enzymatic hydrolysis (Cellulase (0.017 units/mg), endo-1,3(4) β-glucanase (0.017 units/mg) and endo-1,4-β-xylanase (1 unit/mg) from Trichoderma longibrachiatum (Sigma Aldrich)).
4[9]	Ethanol	Sweet sorghum stalks	Ethanol 50%, sulfuric acid 1%, liquor/solid ratio 10/1(v/w), 140 ºC and 30 min	Biomethane 92% theoretical yield after anaerobic digestion, and sugar yield 77.0% after enzymatic hydrolysis (20 FPU/g cellulose (Celluclast 1.5 L, Novozyme, Denmark) and 50 IU β-glucosidase (Novozyme 188, Novozyme, Denmark)).
5[10]	Ethanol/ H_2SO_4	Miscanthus (enzyme hydrolyzed)	Ethanol 80%, H_2SO_4 1%, liquid/solid ratio 8/1, 170 ºC and 60 min	Delignification 93% and enzymatic cellulose-to-glucose conversion 75% (Celluclast R 1.5 L (E.C. 3.2.1.4) from T. Reesei supplemented with β-glucosidase preparation (Novozyme 188 R, E.C. 3.2.1.21)).
6[11]	Ethanol/ H_2SO_4	Wheat straw	Ethanol 60%, H_2SO_4 30 mM, liquid/solid ratio 10/1, 190 ºC and 60 min	Lignin yield 84% and glucose yield 86% after enzymatic hydrolysis (20 FPU/g Accellerase 1500 (Leiden, NL)).
7[12]	Ethanol/ H_2SO_4	Pine and elm	Ethanol 75%, H_2SO_4 1%, liquor/solid ratio 8/1 (w/w), 150-180 ºC and 30-60 min	Acetone-butanol-ethanol yield 14.2-87.9 g/per kg pine (25 FPU/g cellulase and 40 IU β-glucosidase) and 70.1-121.2 g/kg of elm after fermentation (growing culture (optical density of 1.2-1.6 at 610 nm)).
8[13]	Ethanol/ H_2SO_4 or HCl	Willow wood And wheat straw	Ethanol 55%, H_2SO_4 0.01 mol/L or HCl 0.02 mol/L, liquor/solid ratio 9.5/1 (w/w), 190 ºC and 180 min	Cellulose to glucose conversion 87% (willow wood) and 99% (wheat straw) after enzymatic hydrolysis (Accellerase 1500 and 62 FPU/g cellulase).
9[14]	Ethanol/ HCl	Chamaecypar isobtusa	Ethanol 50%, HCl 0.4%, liquor/solid ratio 5.3/1 (v/w), 170 ºC and 45 min	Glucose yield 70% after enzymatic hydrolysis (cellulases from Trichoderma reesei ATCC 26921 (Celluclast 1.5 L) and β-glucosidase (Novozyme 188) from Aspergillus niger (both Novozymes, Bagsværd, Denmark)).
10[15]	Ethanol/a cetic acid	Sugarcane bagasse	Ethanol 60%, acetic acid 5%, liquor/solid ratio 8/1(v/w), 190 ºC and 45 min	Xylose yield 11.83% and cellulose conversion 93.8% after enzymatic hydrolysis (20 FPU/g cellulase mixture provided by Genencor (Shanghai, China)).
11[16]	Ethnol/gr een liquor	Sugarcane bagasse	Ethanol 50%, green liquor 1.5 mL/g raw material, 0.01 g anthraquinone, liquor/solid ratio 10/1(v/w), 140 ºC and 3 h	Lignin removal 77.9%, glucose yield 97.7%, and xylose yield 94.1% (cellulase (Celluclast 1.5 L, Sigma Co., St. Louis, MO, USA), 18 FPU/g cellulose for cellulase and 27 CBU/g cellulose for β-glucosidase).
12[17]	Methanol	Pressed pericarp fibers	Methanol 65%, liquor/solid ratio 8/1(v/w), 180 ºC and 75 min	Lignin removal 44.6% and cellulose-to-glucose conversion 42.5% after enzymatic hydrolysis (Celluclast 1.5 L (Novozymes, Denmark), β-glucosidase (Novozyme 188, Novozymes), at loadings of 60 FPU/g cellulose and 64 pNPGU/g cellulose, respectively).
13[18]	Methanol /H_2SO_4	Hemp hurds	Methanol 45%, H_2SO_4 3%, liquor/solid ratio 25/1(v/w), 165 ºC and 20 min	Hemicellulose removal 75%, lignin removal 75%, and cellulose-toglucose conversion 60% after enzymatic hydrolysis (cellulose enzyme Cellic CTec2 (Novozymes, Bagsværd, Denmark)).
14[19]	Methanol /NaOH	Populus tomentosa Carr	Methanol 70%, NaOH 1%, 80 ºC and 5 h	Cellulosic fraction yield 80.3% and bioethanol concentration 5.09 g/L after fermentation (15 FPU/g Celluclast 1.5 L (cellulase) and 17.5 IU/g Novozyme 188 (β-glucosidase)).

The production-scale synthesis of chemicals from plant extracts is usually limited for the chemical industry. In contrast, the chain degradation of cellulose could open an avenue for sustainable large-scale alcohol production (Scheme 2.1), and some have been extensively used in the chemical industry as intermediates (Scheme 2.2).

The preparation of alcohols from biomass has been developed for many years, and the research about biomass and alcohols is still a hot topic. There is a huge increase in the research area in past 30 years, in terms of published articles (Figure 2.1). Despite the fact that alcohols can be used as a good fuel source, they can also be converted into different compounds, such as amides, amines, imines, carboxylic acids, and esters. The key step during this transformation is the dehydrogenation of alcohols (Scheme 2.3).

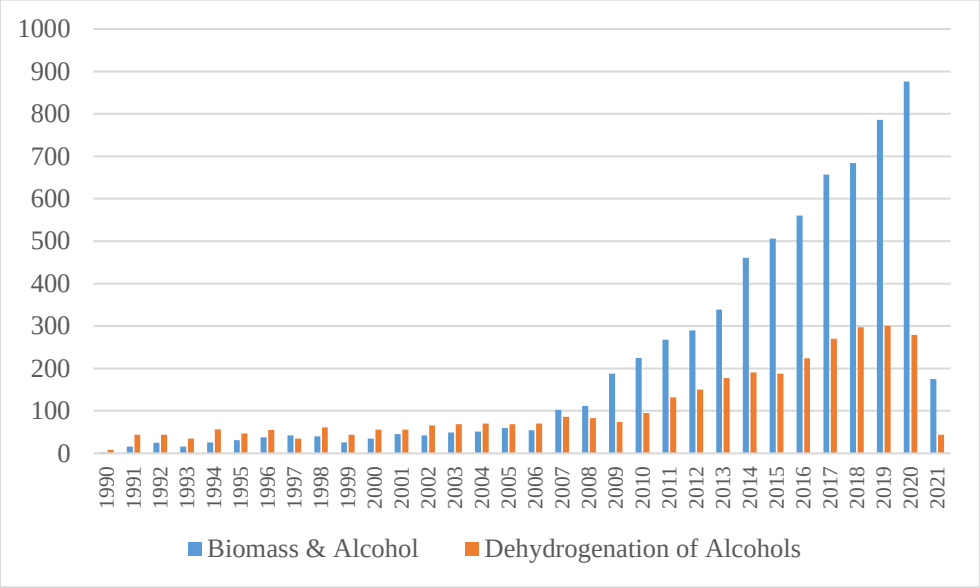

Figure 2.1. Evolution of published articles about biomass and alcohols, and dehydrogenation of alcohols per year (data compiled through the web of science website on 22 April 2021, using "biomass and alcohols" and "dehydrogenation of alcohols" respectively, as topics).

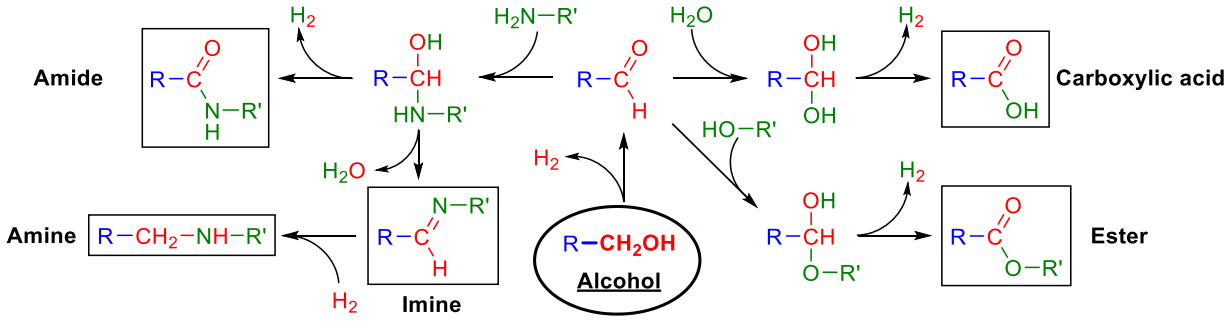

Scheme 2.3. Pathways for dehydrogenative reactions from alcohols.

3. Synthesis of imines

3.1 Introduction to imines

Imines have the formula $R_1R_2C=NR_3$, and the functionality is well known as a Schiff base. The functionality was discovered and named by Hugo Schiff in 1864, if R_3 is not a hydrogen atom.[20] The N atom is easy to facilitate coordination to various metals, which can make molecules containing the imine group feasible ligands in homogeneous catalysis, because of the presence of a lone pair of electrons on the nitrogen atom of an imine group.[21] Imines are important intermediates. They are not only widely applied in the synthesis of active compounds, such as pharmaceuticals, dyes, fragrances, fungicides, and agricultural chemicals,[21,22] but also involved in a variety of organic transformations, such as reduction, addition, condensation, cyclization, and aziridination reactions in industrial synthetic processes.[23] From Figure 3.1, it can be seen that imines have been well studied in different fields.

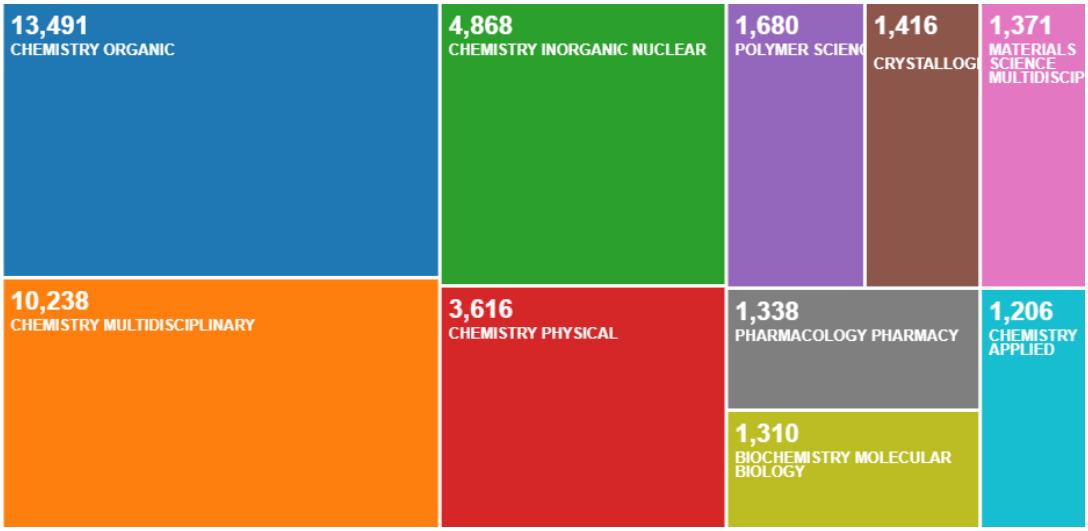

Figure 3.1. Evolution of published articles about imines (data compiled through the web of science on 14 June 2021 using imine as topic from 1990-2021, and there are total 36590 records).

Schiff originally reported the preparation of imines by the condensation of amines with carbonyl compounds (Scheme 3.1).[23] This reaction proceeds by nucleophilic addition of the amine nitrogen to the carbonyl carbon, and then gives a hemiaminal intermediate followed by elimination of water to yield the imine. This procedure has been applied for the preparation of various imines, where neither a catalyst, an additive nor a solvent is needed.[24,25]

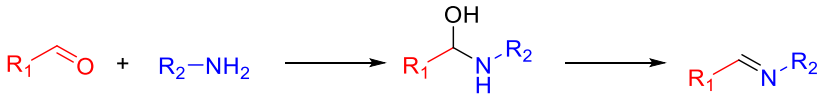

Scheme 3.1. Traditional method to synthesize imines.

3.2 Synthesis of imines by catalytic oxidations of primary alcohols and/or amines

However, there are some disadvantages for the traditional method: (a) it often involves unstable aldehydes and the equilibrium usually favors the reverse reaction; (b) the reaction of aliphatic aldehydes and amines does not necessarily lead to the desired imine; (c) ketones react with amines slowly and often require harsh conditions. In general, it is limited for the traditional procedure to react between highly nucleophilic amines and strongly electrophilic aldehydes/ketones.[21] Therefore, it is necessary and highly appealing to develop an alternative, efficient and sustainable procedure with a broad scope of imine products.

Different methods to prepare imines have been developed since Hugo Schiff's discovery. These methods include hydroamination of alkynes with amines,[26] coupling of aldehydes with alkyl bromides and ammonia,[27] coupling of aldimines with boronates,[28] addition of organometallic reagents to nitriles,[29] arylation of nitriles[30], decarboxylative amine couplings,[31] addition of arenes or boronic acids to nitriles,[32] reductive imination of nitro compounds,[33] reduction of secondary amides,[34] coupling of aryl halides with isonitriles and organometallic reagents,[35] hydrogen transfer from amines to alkynes,[36] addition of isocyanides to electron-rich arenes,[37] and coupling of vinyl bromide with amines.[38]

Although many methods have been reported, three approaches have obtained much attention, as shown in Scheme 3.2: (a) oxidative dehydrogenation of secondary amines; (b) oxidative self-coupling of primary amines; and (c) oxidative cross-coupling of alcohols with amines.

The oxidative dehydrogenation of secondary amines gives high selectivity, because the substrates can not be further dehydrogenated into nitriles. Yet, the substrate conversion efficiency is affected by the steric hindrance around the N-H bond and no new C-N bond is formed. In 1933, the Ritter group reported the dehydrogenation of amines to form imines.[39] For the homo-coupled imines from the self-coupling of primary amines, they are easily obtained, whereas hetero-coupled imines are less accessible. Additionally, there is a potential risk in the reaction for the transformation of the primary amine into a nitrile, amide or azo compound as by-products, because of the possibility of over-oxidation in the presence of an oxidant.

a) Oxidative dehydrogenation of secondary amines

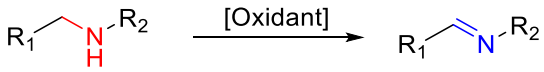

b) Self-coupling of primary amines

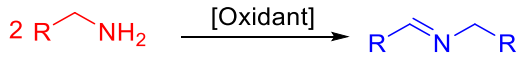

c) Cross-coupling of alcohols with amine

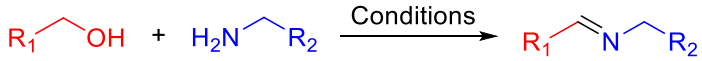

Scheme 3.2. New approaches to synthesize imines.

In 1909, the direct N-alkylation of amines with alcohols to produce secondary amines as the final products with imines as intermediates was reported by Sabatier.[40,41] Later, this approach was applied in the selective synthesis of the imine product. For the cross-coupling of alcohols with amines, the advantage is that both symmetric and asymmetric imines can be readily synthesized by choosing different starting materials. In addition, alcohols are desirable starting materials, because they are inexpensive, easily available by various industrial processes as stated in Chapter 1. Therefore, it is considered to be of high importance to develop catalytic reactions for synthesizing different compounds from alcohols, which can reduce CO_2 emissions and prevent the use of fossil carbon feedstock. Hence, "the use of renewable feedstocks" is also one of the principles of green chemistry.[42,43] Therefore, the cross-coupling of alcohols with amines is regarded as an environmentally benign protocol.

The biggest problem with this approach is that alcohols are quite unreactive, because the hydroxy group is a poor leaving group, which means that it often has to be converted into a better leaving group by protonation, sulfonation or halogenation to be able to participate in different reactions. However, these modifications usually require harsh reaction conditions. The acidic environment that is required for the protonation of the alcohol may also protonate, and thereby deactivate the incoming nucleophile (especially amines). Many alkyl sulfonates and alkyl halides are known to be mutagenic.[44] A potential solution to circumvent the problem is to oxidize the alcohol into the corresponding and more reactive carbonyl group. In this case, the major challenge is the selective oxidation of the alcohol into the corresponding aldehyde or ketone intermediate under mild conditions. Traditional methods to oxidize alcohols into aldehydes are to use stoichiometric or excess amounts of inorganic oxidants, such as CrO_3Py_2 (Collins reagent),[45] Dess-Martin Periodinane (DMP),[46] activated DMSO (Swern oxidation),[47] tetrapropylammonium perruthenate (TPAP)/*N*-methylmorpholine *N*-oxide (NMO) (Ley oxidation),[48] and (2,2,6,6-

tetramethylpiperidin-1-yl)oxyl (TEMPO)/NaOCl.[49] However, these inorganic oxidants would lead to the generation of a copious stoichiometric amount of toxic waste. Furthermore, they can also oxidize the amine starting material,[50–52] and lead to undesirable byproducts, as the case with the self-coupling of amines.

Because of all these challenges mentioned above, a wide range of catalysts has been developed for these transformations during the past years, which include transition metal, photo-, electro-, and organo-catalysts. In the case of photo-,[53–56] electro-,[57,58] and organo-catalysts[59–62], they have often been achieved with a limitted substrate scope.[55]

Additionally, a catalyst based on transition metals has also been reported. Various transition metals have been shown to catalyze the oxidative coupling of amines and alcohols in the presence of an environmentally friendly and cheap oxidant (air/O_2). Some examples are shown in Table 3.1.

Moreover, simple bases, such as NaOH (10 mol%), have been shown to catalyze the oxidative coupling of amines and alcohols in the presence of air at 90-100 ºC.[63] Coupling of primary amines can be achieved by refluxing the amines in water under one atmosphere of oxygen pressure, the so-called “on-water” reaction.[64]

Air and O_2 are environmentally friendly oxidants, but they can not avoid the possibility of over-oxidation of the substrates, leading to various possible byproducts. Furthermore, pressurized oxygen could also give potential explosion hazards. Therefore, another solution is desired. Reactions employing metal catalysts to catalyze the alcohol to aldehyde or ketone conversion with the removal of hydrogen gas could be a better option, in comparison to the use of stoichiometric reagents.

Table 3.1. Various catalysts applied in the oxidative cross-coupling of alcohols with amines in the presence of mild oxidants.

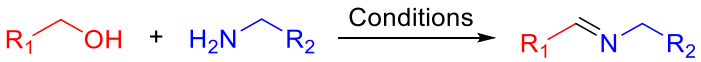

Entry	Catalyst	Oxidant	Additive	Solvent	T (°C)	t (h)
1[65]	1 mol% $Pd(OAc)_2$	air	4 % TEMPO 15 % NEt_3 20 % ^tBuOK	neat	rt	72
2[66]	0.3g γ-Fe_2O_3	air	-	toluene	80	8
3[67]	5 mol% $Cu(ClO_4)_2 \cdot 6H_2O$	O_2 (balloon)	150 mol% KOH	toluene	70	19
4[68]	0.3 g/mmol CeO_2 on mesoporous carbon	air	-	toluene	80	2
5[69]	20 mg/mmol FeCu@NPC porous N-doped carbon	air	-	neat	120	4
6[70]	5 mol% Ru nanoparticles on carbon	O_2	-	toluene	90	15-36
7[71]	3 mol% ABNO 9-azabicyclo[3.3.1] nonan-N-oxyl (ABNO)	air	30 mol% KOH	toluene	80	4-12
8[72]	5.0 wt% MnOx/HAP hydroxyapatite	air	-	toluene	80	24
9[73]	1000 mol% MnO_2	-	4Å MS (200 mg)	DCM	reflux	24-48
10[74]	20 mol% $CsOH \cdot H_2O$	air	-	toluene	70	18
11[75]	120 mol% KOH	air	-	toluene	90	20
12 [76]	50 mg/mmol Cs/MnOx	air	-	toluene	110	3
13[77]	0.02 % Au/TiO_2	1 atm O_2	10 % $KOCH_3$	methanol	rt	24
14[78]	5 % Ag/Al_2O_3	air	-	toluene	100	24
15[79]	0.3 % Pt-Sn/γ-Al_2O_3	0.1 MPa O_2	-	ethylbenzene	138	24
16[80]	1 % CuI	air	2 % TEMPO 1 % Bipy	acetonitrile	rt	12
17[81]	2 % Pd/AlO(OH)	1 atm O_2	-	heptane	90	20
18[82]	1 % Pd/ZrO_2	air	10 % KOH	alcohol substrate	30	6
19[83]	5 mol% $La(NO_3)_3 \cdot 6H_2O$	O_2	KOH	toluene	90	19
20[84]	20 mg/CeO_2	air	-	mesitylene	100-140	24-48

4. Dehydrogenation of alcohols and imination from alcohols with metal catalysts

4.1 Catalysis

The 9th principle of green chemistry that catalytic reagents are superior to stoichiometric reagents is catalysis.[42,43] A substance known as a catalyst can be used to accelerate the rate of a chemical reaction by providing an alternative reaction pathway with lower activation energy, and without affecting the overall Gibbs free energy of the reaction (Figure 4.1). The catalyst itself is not consumed during the transformation and proceeds through a cyclic process consisting of different steps called a catalytic cycle, which means that the catalyst can act repeatedly and be regenerated after the end of the reaction. Hence, in contrast to the use of stoichiometric reagents, which are a major source of waste, only a small amount of catalyst required for a reaction could have a similar performance.[42] In addition, catalytic reactions often have low E-factors,[43,85] and are very atom-economic and makes it possible to perform reactions efficiently that would maybe otherwise be impossible or very expensive. Today, up to 90% of the production of all commercial products relies on catalysts,[86,87] which gives a clear prospect of the importance of catalysis.

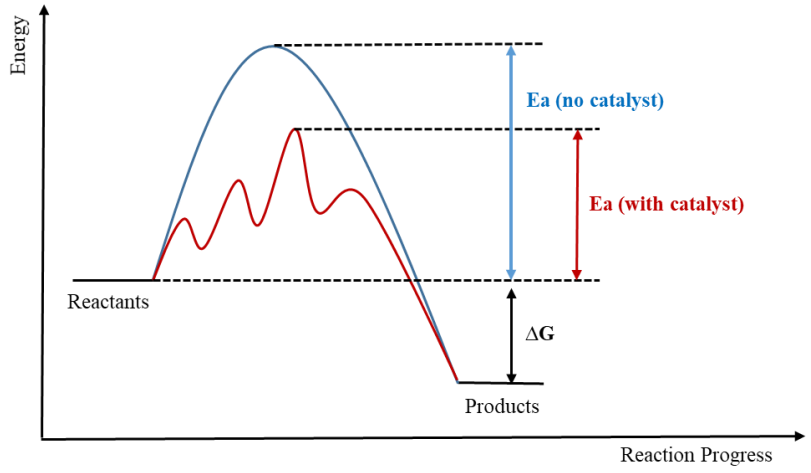

Figure 4.1. Potential energy diagram showing the effect of a catalyst in a chemical reaction.

A catalytic cycle is a multistep reaction mechanism, which is used to describe the role of a catalyst in the conversion of reactants into the desired product. Often a precursor to the catalyst, called a pre-catalyst, is used in the reactions. In the reaction mixture, the pre-catalyst is converted to the active catalyst. Pre-catalysts are normally more stable than the active catalysts, and therefore easier to handle. The catalyst activation is not a part of the actual cycle. After activation, the catalyst can

bind one or more reactants, followed by several steps, leading to the release of the desired product and regeneration of the catalyst, as shown in Scheme 4.1.

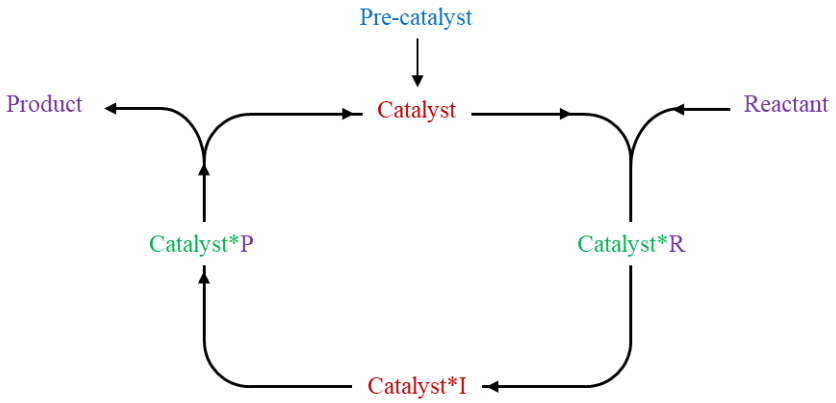

Scheme 4.1. Catalytic cycle for conversion of reactant into product through intermediate I.

In 1812, Gottlieb Kirchhoff reported the first example of a catalyst applied in the field of chemistry, where he discovered the acid-catalyzed conversion of starch into sugar moieties.[88] The term catalysis was first introduced by Jöns Jacob Bérzelius in 1836.[89] The modern definition of catalysis, as we know it today, was presented by Wilhelm Ostwald in 1895.[90]

Catalysts can be classified as either homogeneous or heterogeneous. A homogeneous catalyst is in the same phase with the reactants, whereas a heterogeneous catalyst acts in different phases with the reactants. One of the greatest advantages of heterogeneous catalysis is that they can be easily separated from the reactions and then reused. However, heterogeneous catalysts often suffer from limited activity and selectivity. Homogeneous catalysts are easy to access for the reactants and promote high catalytic activity as well as selectivity towards the desired product.[91] It is estimated that 10-15% of the current catalytic processes in industry are homogeneous, and the development of homogeneous catalysts is continuously growing.[92] In addition, catalysts can also be classified according to their structure. The most common types are organo-, photo- and electro-catalysts as well as metal catalysts.

4.2 Coordination complex

In 1911, Werner first resolved the coordination complex hexol ($[Co(Co(NH_3)_4(OH)_2)_3]^{6+}(SO_4^{2-})_3$) into optical isomers, overthrowing the theory that only carbon compounds could possess chirality.[93] Werner developed the basis for modern coordination chemistry and won the Nobel

Prize in Chemistry for proposing the octahedral configuration of transition metal complexes in 1913.[94]

A coordination complex consists of a central atom or ion, which is usually metallic and is called the coordination centre and a surrounding array of bound molecules or ions, that are in turn known as ligands or complexing agents.[95] Many metal-containing compounds are coordination complexes, especially those of transition metals (d block elements).

Coordination complexes are so pervasive that their structures and reactions are described in many ways. The atom within a ligand that is bonded to the central metal atom or ion is called the donor atom. In a typical complex, a metal ion is bonded to several donor atoms, which can be the same or different. A polydentate (multiple bonded) ligand is a molecule or ion that bonds to the central atom through several of the ligand's atoms. Ligands with 2, 3, 4 or even 6 bonds to the central atom are common. These complexes are called chelate complexes, and the formation of such complexes is called chelation, complexation and coordination.

In coordination chemistry, a structure is first described by its coordination number, i.e. the number of ligands attached to the metal (more specifically, the number of donor atoms). Coordination numbers are normally between two and nine, but large numbers of ligands are common for the lanthanides and actinides. The number of bonds depends on the size, charge, and electron configuration of the metal ion and ligands. Metal ions may have more than one coordination number.

Typically, the chemistry of transition metal complexes is dominated by interactions between s and p molecular orbitals of the donor-atoms in the ligands and the d orbitals of the metal ions. The s, p and d orbitals of the metal can accommodate 18 electrons.[96,97] The maximum coordination number for a certain metal is thus related to the electronic configuration of the metal ion (to be more specific, the number of empty orbitals). Large metals and small ligands lead to high coordination numbers, such as $[Mo(CN)_8]^{4-}$. Small metals with large ligands lead to low coordination numbers, such as $Pt[P(CMe_3)]_2$. Due to their large size, lanthanides, and actinides tend to have high coordination numbers.

Most structures follow the points on a sphere pattern (or, as if the central atom is in the middle of a polyhedron where the corners of the shape are the locations of the ligands), where orbital overlap (between ligand and metal orbitals) and ligand-ligand repulsion tend to lead to certain regular geometries. The most observed geometries are listed below (Scheme 4.2). However, due to the use of ligands of diverse types, the size of ligands, electronic effects, the geometries can be irregular. Different structures and examples are given as shown as follows.[95]

(a) Linear for two-coordination, such as $AuCl(PPh_3)$.

(b) Trigonal planar for three-coordination, such as $Pt(PPh_3)_3$.

(c) Tetrahedral for four-coordination, such as $RhCl(PPh_3)_3$.

(d) Square planar for four-coordination, such as $Ni(CO)_4$.

(e) Trigonal bipyramidal for five-coordination, such as $Fe(CO)_5$.

(f) Square pyramidal for five-coordination, such as $[VOCl_4]^{2-}$.

(g) Octahedral for six-coordination, such as $Mo(CO)_6$.

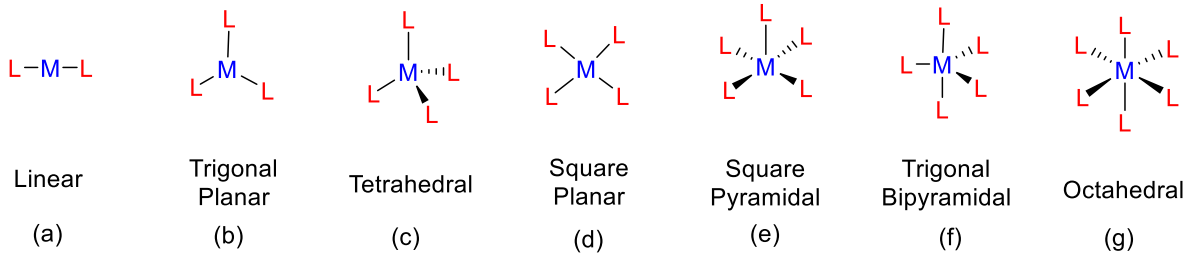

Scheme 4.2. Common structures of coordinate complexes (M = metal, L = ligand).

The descriptions of 5-, 7-, 8-, and 9- coordination are often indistinct geometrically from alternative structures with slightly differing L-M-L (ligand-metal-ligand) angles, as for example the difference between square pyramidal and trigonal bipyramidal structures.[95]

In systems with low d electron count, due to special electronic effects, such as Jahn-Teller stabilization,[98] certain geometries (in which the coordination atoms do not follow a points-on-a-sphere pattern) are stabilized relative to the other possibilities, therefore for some compounds, the trigonal prismatic geometry is stabilized relative to octahedral structures for six-coordination.

Coordinate complexes as homogeneous catalysts have been widely applied in the production of organic substances. Processes include hydrogenation, hydroformylation, and oxidation. A combination of titanium trichloride and triethylaluminium gives rise to Ziegler-Natta catalysts[99] used for the polymerization of ethylene and propylene to give polymers of great commercial importance as fibers, films, and plastics.

Nickel, cobalt, and copper can be extracted using hydrometallurgical processes involving complex ions. They are extracted from their ores as ammine complexes. Metals can also be separated using the selective precipitation and solubility of complex ions. Cyanide is used chiefly for the extraction of gold and silver from their ores.[100]

Many coupling reactions based on metal complexes have been developed in the past decades, such as the Kumada coupling,[101,102] the Mizoroki-Heck reaction,[103–105] the Sonogashira coupling,[106,107] the Negishi coupling,[108–111] the Stille reaction,[112] the Suzuki-Miyaura reaction,[113–115] the Hiyama coupling,[116,117] and the Buchwald-Hartwig amination.[118]

In metal catalysis, the catalyst consists of at least one metal, usually, a transition metal, to which organic and/or inorganic ligands often are coordinated. The transition metal can have multiple oxidation states and coordination sites to the ligands, which makes them a good choice as metal catalysts. During the catalytic cycle, the catalyst can undergo various transformations, such as ligand exchange, oxidative addition, reductive elimination, migratory insertion, elimination and transmetalation (Table 4.1).[95]

Table 4.1. Schematic presentation of common steps in a catalytic cycle.

Reaction type	Examples	Remarks
Ligand exchange	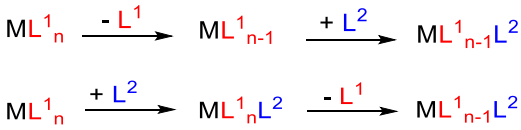	Dissociative mechanism
		Associative mechanism
Migration insertion	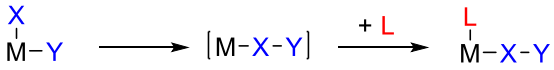	
Oxidative addition	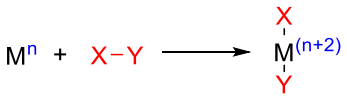	
Reductive elimination	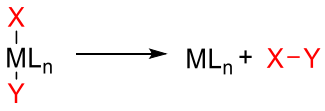	
	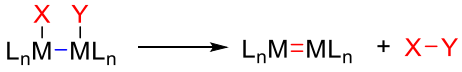	
		
β-Elimination	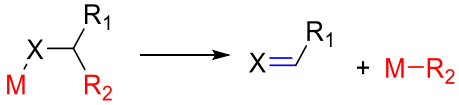	Relative rates: R_2 = H > R_2 ≥ alkyl or aryl For X = CH_2, studied for R_2 = H, alkyl, Ar, OR, and Cl For X = O or NR, studied for R_2 = H and aryl
α-Elimination	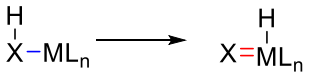	X = O, NR, CR_2
Transmetalation	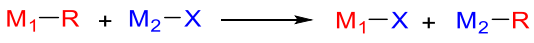	R = aryl, vinyl, alkyl X = halide, pseudohalide

To understand the common steps in a catalytic cycle, an example is shown in Scheme 4.3.[119] This is a common catalytic cycle for the Sonogashira reaction, and there are two cycles, i.e. the palladium cycle and the copper cycle.

In the palladium cycle, the palladium pre-catalyst species is activated to form a reactive Pd^0 complex **1**. This $[Pd(0)L_2]$ complex can be formed from Pd(0) complexes, such as $Pd(PPh_3)_4$, or can be created from Pd(II) complexes, such as $PdCl_2(PPh_3)_2$, through the formation of a $[Pd(II)L_2(C{\equiv}CR_2)_2]$ species.[120] The active Pd^0 catalyst is involved in the oxidative addition step with the aryl or vinyl halide substrate to produce Pd^{II} species **2**. This step is believed to be the rate-limiting step of the reaction. Complex **2** reacts with copper acetylide complex **6** in a transmetalation step, yielding complex **3** and regenerating the copper catalyst **4**. The structure of complex **3** depends on the properties of the ligands. For the facile reductive elimination to occur, the substrate motifs need to be in close vicinity, such as cis-orientation, therefore trans-cis isomerization can be involved. In the reductive elimination step, the product is expelled from the complex and the active Pd catalytic species is regenerated.

For the copper cycle, the details are poorly known. It is suggested that the presence of a base results in the formation of a π-alkyne complex **5**. This increases the acidity of terminal proton and leads to the formation of the copper acetylide, complex **6**, upon deprotonation. Acetylide **6** is then involved in the transmetalation reaction with palladium intermediate **2**.

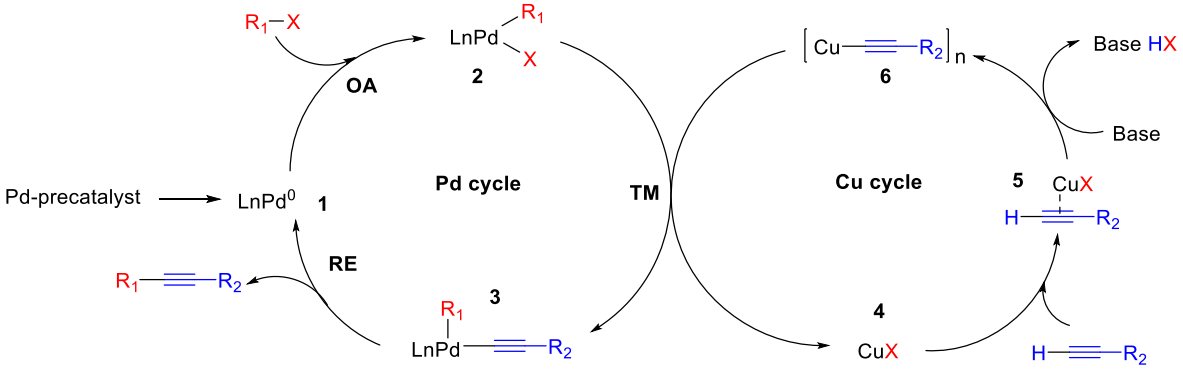

Scheme 4.3. Catalytic cycle for the Sonogashira reaction.[118]

4.3 Dehydrogenation of alcohols and imination from alcohols using metal catalysts

4.3.1 Catalysts based on platinium group metals

One of the earliest dehydrogentation of alcohols was reported by Duson and Robinson.[121] The authors discovered that the complex was active in the dehydrogenation of a series of primary and secondary alcohols.

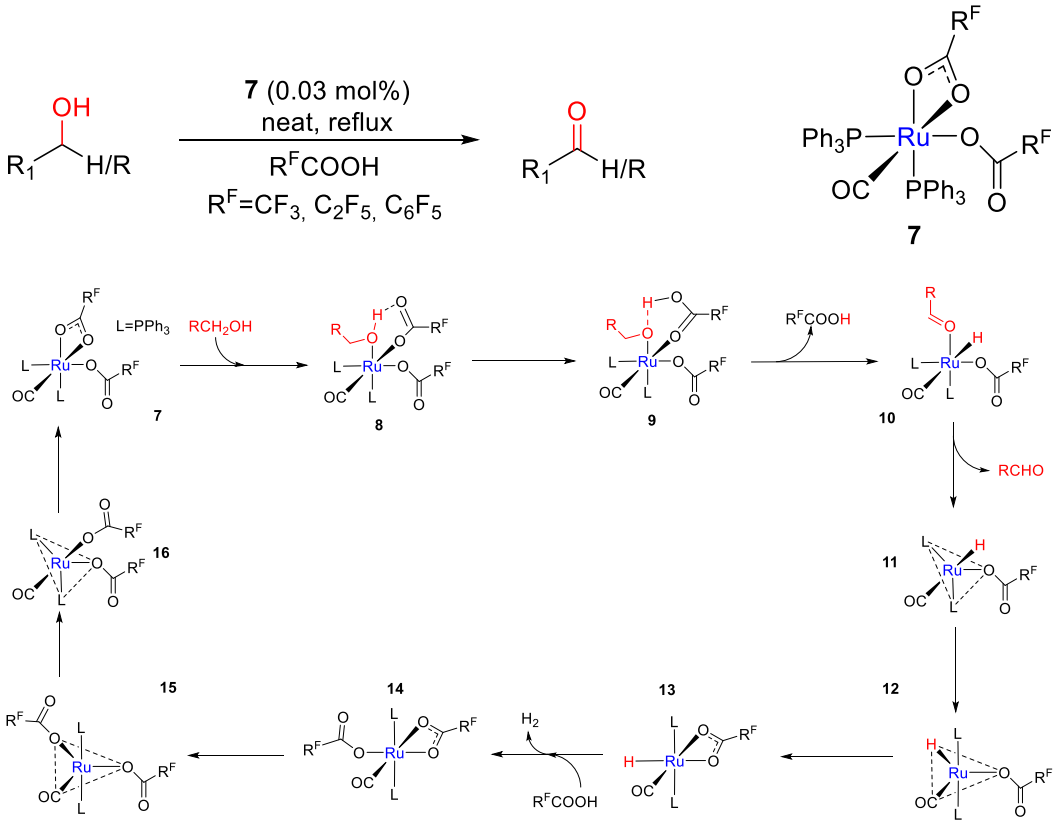

Scheme 4.4. Early example of dehydrogenation of primary and secondary alcohols employing a metal catalyst and the catalytic cycle.

In Scheme 4.4, the mechanism shows a detailed version of the outlined dehydrogenative reaction including the stereochemical information. The initial step was thought to involve coordination of the alcohol to form adduct **8**, with a structure analogous to that found for the methanol solvate $[Ru(OCOCF_3)_2(MeOH)(CO)(PPh_3)_2]$. The crystal structure of $[Ru(OCOCF_3)_2(MeOH)(CO)(PPh_3)_2]$ also proved the hydrogen bonding between the CF_3CO_2 and the OMe moieties,[120] which pointed to a mechanism for facile interligand proton transfer (**8** - **9**).

A similar finding was reported for a metal-assisted proton transfer between coordinated water and amino acid ligands. The resulting alkoxide complex **9** presumably underwent a rapid elimination step with the proton migrating to the coordination site vacated by the departing perfluorocarboxylic acid ligand.[122] Loss of the weakly coordinated aldehyde (or ketone) ligand, followed by a reverse Berry pseudorotation (**11 - 12**) on the resultant five-coordinate square-pyramidal (d_6) intermediate and subsequent rechelation of a carboxylate group, could account for formation of the observed hydride (**13**). The proposed form of a reverse Berry pseudorotation (**11 - 12**) minimizes steric interactions between the bulky triphenylphosphine ligands. The course of the reaction leading to regeneration of catalyst **7** is more difficult to elucidate. It was presumed that acid (R^FCOOH) attack on the hydrides $[RuH(OCOR^F)(CO)(PPh_3)_2]$ occurred with retention of stereochemistry and led to formation of dicarboxylato complexes $[Ru(OCOR^F)_2(CO)(PPh_3)_2]$ with mutual trans triphenylphosphine ligands. Regeneration of the observed isomeric species **7** could then occur by a further reverse Berry pseudorotation sequence (**15 - 16**). Alternatively, the conversion of the hydrides $[RuH(OCOR^F)(CO)(PPh_3)_2]$ to the dicarboxylate $[Ru(OCOR^F)_2(CO)(PPh_3)_2]$ with acid R^FCOOH may involve a protonation step leading to the formation of seven-coordinate ruthenium(IV) species $[RuH_2(OCOR^F)(CO)(PPh_3)_2]^+$ or $[RuH_2(OCOR^F)_2(CO)(PPh_3)_2]$, which can undergo reductive elimination of dihydrogen to yield the observed isomer of $[Ru(OCOR^F)_2(CO)(PPh_3)_2]$ directly.

The inhibitory effect of accumulated aldehyde (or ketone) was similar to what had previously been observed in related alcohol dehydrogenation and hydrogen-transfer processes.[123–125] It was presumably attributable to competition between the alcohol and the carbonyl product in the initial coordination step (**7 - 8**). Synthesis of ketone solvates supported this suggestion. The low concentrations of dihydrogen should ensure that the reverse hydrogenation of the aldehyde or the ketone did not play a significant role. The observed acid dependence of the catalyst system can be explained, if the acid-promoted catalyst regeneration reaction (**13 - 14**) is superseded by the solvolysis process (**9** >> **10**) as the rate-determining step at acid concentrations greater than about 12 mol/mol of catalyst. Weakly bound perfluorocarboxylate ligands of exceptional lability appeared to be a characteristic and essential feature of the catalytic complex $[Ru(OCOR^F)_2(CO)(PPh_3)_2]$. It was, therefore, useful to consider the origin of this phenomenon, and two plausible explanations, trans influence and available sites for alcohol coordination, merited special consideration.

In addition, there are some other catalysts based on Ru for dehydrogenation of alcohols in Scheme 4.5.[126–130]

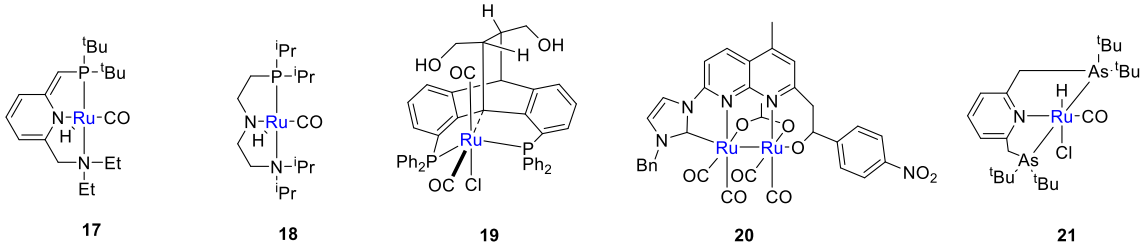

Scheme 4.5. Different catalysts based on Ru for dehydrogenation.

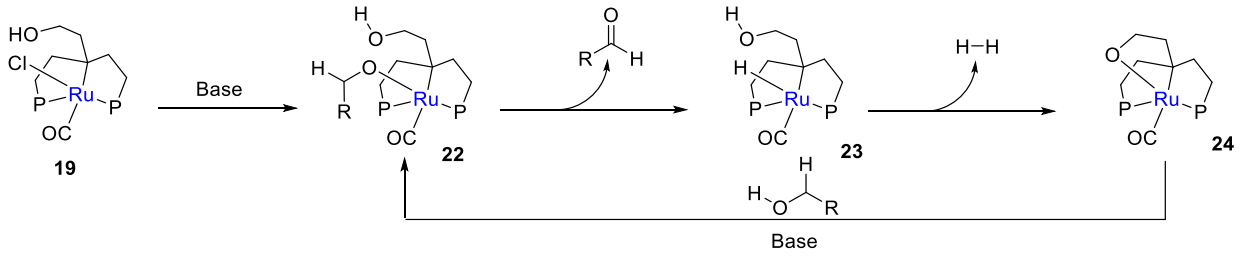

Scheme 4.6. Proposed mechanism for imine formation based on catalyst **19**.

For the catalyst **19**, the mechanistic transformation was likely to proceed via three steps[128] in Scheme 4.6 : (a) a ligand exchange step, leading to the arm-opened ruthenium alkoxide species **22**; (b) generation of the Ru-H species via β-hydride elimination with subsequent formation of the hydride product **23**; (c) a H_2-forming step, leading to the formation of the catalytically active arm-closed ruthenium species **24**.[131] Hydrogen formation was observed upon stoichiometric interaction of **19** with 1-phenylethanol.

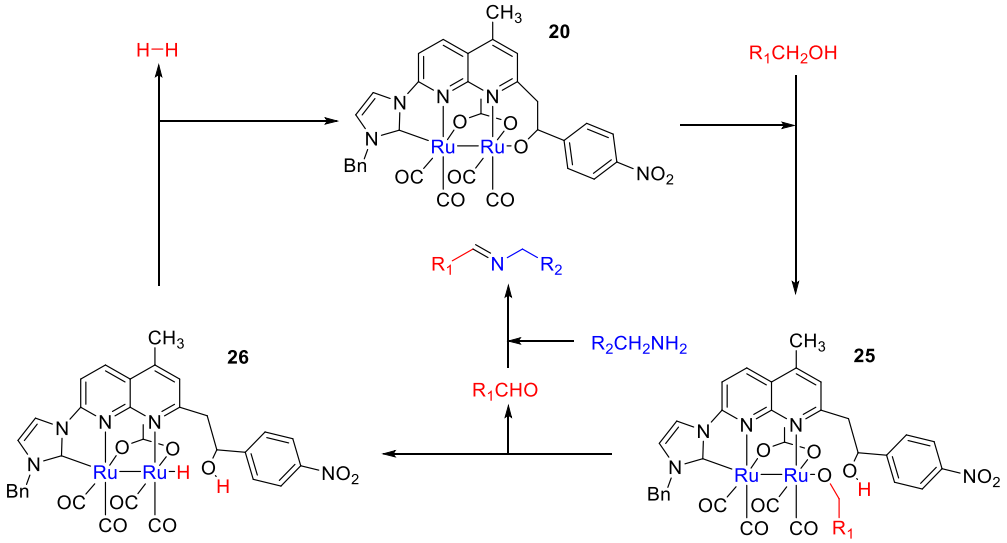

Scheme 4.7. Proposed mechanism for imine formation based on catalyst **20**.

For the catalyst **20**, a bifunctional mechanism to account for the conversion of the alcohol into the aldehyde was proposed.[129] The alcohol was activated in a bifunctional manner to form an axial diruthenium-alkoxide **25**, causing the hydroxy arm to open up (Scheme 4.7). Subsequent β-hydride elimination of the alkoxide produced the aldehyde and the [Ru-Ru]-H intermediate **26**. In the absence of the amine, the hydride intermediate was identified by a characteristic signal at δ = -7.37 ppm in the ^{1}H-NMR spectrum. The active catalyst **20** was regenerated with the liberation of hydrogen and the extruded aldehyde reacted with the amine to give the imine as the final product.[132–134]

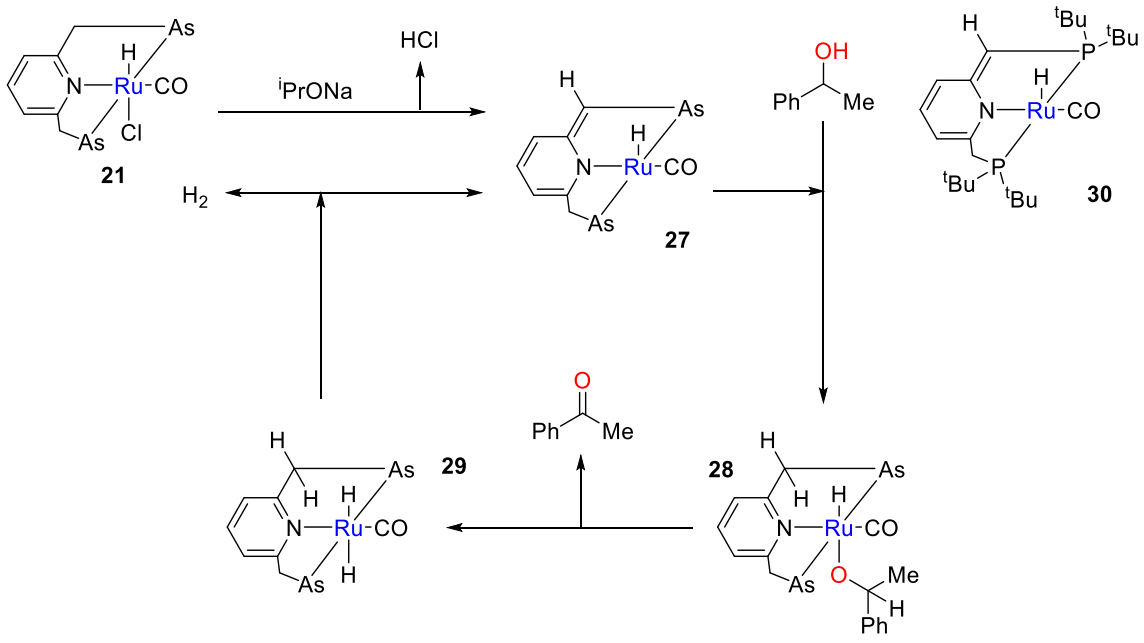

Scheme 4.8. Possible reaction pathway for the dehydrogenation of 1-phenylethanol.

The dearomatized species **27** shown in Scheme 4.8, which was formed via deprotonation of **21** with base, may play an important role to promote the catalytic transformations of alcohols.[130] The presence of arsine instead of phosphine (compared with complex **30**) in the pincer ligand may lower the reaction rate to form the dearomatized species **27**, where the arsine attached to the deprotonated methylene group unit may function as a weaker π-acceptor. Then an insertion reaction occurred between 1-phenylethanol and species **27** to give species **28**, where the pyridine ring was formed again. Hydrogen abstraction happened through species **28**, and then afforded hydride species **29**, from which hydrogen gas can be liberated to regenerate species **27**.

Besides the Ru-based catalyst, there are also some reports about dehydrogenation of alcohols using iridium catalysts.

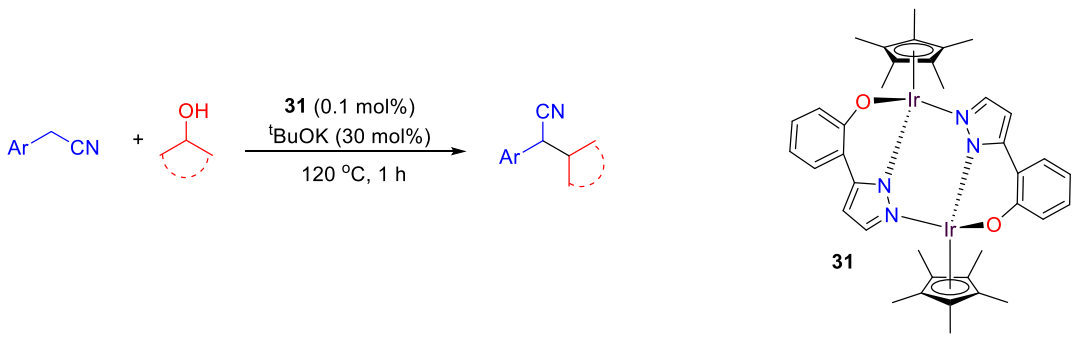

Scheme 4.9. Alkylation of alcohols with an iridium catalyst.

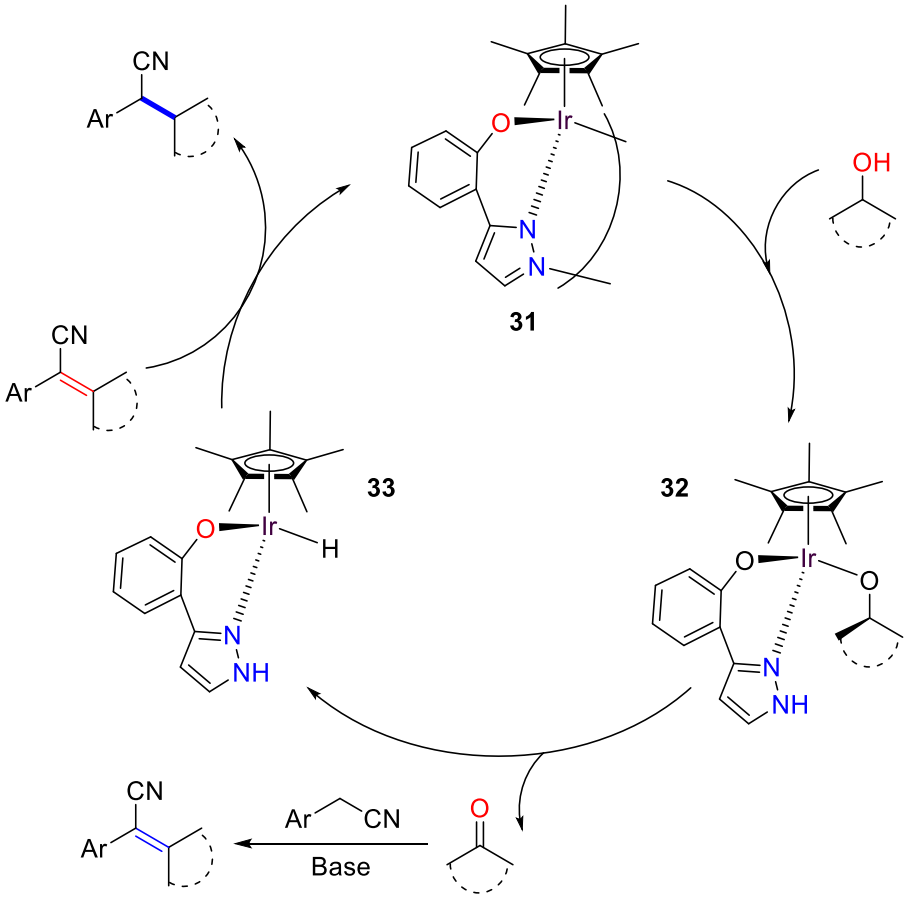

Scheme 4.10. Possible reaction mechanism.

In Scheme 4.9, the α-alkylations of nitriles were efficiently performed at 120 °C under solvent-free conditions with a very low (0.1-0.01 mol%) catalyst loading.[135] A plausible mechanism based on the experimental evidence and previous reports was proposed in Scheme 4.10.[136–143] Initially, the alcohol interacted with the iridium dimer **31**, and the O-H activation of the alcohol via proton transfer to the pyrazolato moiety yielded an alkoxy intermediate **32**. A similar example with a nitrogen atom in the pyrazolato moiety abstracting a hydrogen atom was reported: a related

iridium-pyrazolato complex activated the N-H bond of tosyl amine via proton transfer to the pyrazolato moiety.[144] Thereafter, the β-hydride elimination of intermediate **32** resulted in the formation of the ketone and the hydride intermediate **33**, which was isolated and fully characterized. As β-hydride elimination requires a vacant site at the metal center, this second step might also undergo a Cp^* ring slippage from η^5 to η^3 coordination. However, the proposed β-hydride elimination in saturated complexes has also been reported.[142,143,145,146] Thereafter, the ketone and the arylnitrile underwent a Knoevenagel condensation in the presence of a base to form the vinyl nitrile with the elimination of water. Finally, hydrogen transferred from the hydride intermediate **33** to the vinyl nitrile yielding α-alkylated arylacetonitrile with the regeneration of iridium complex **31**.

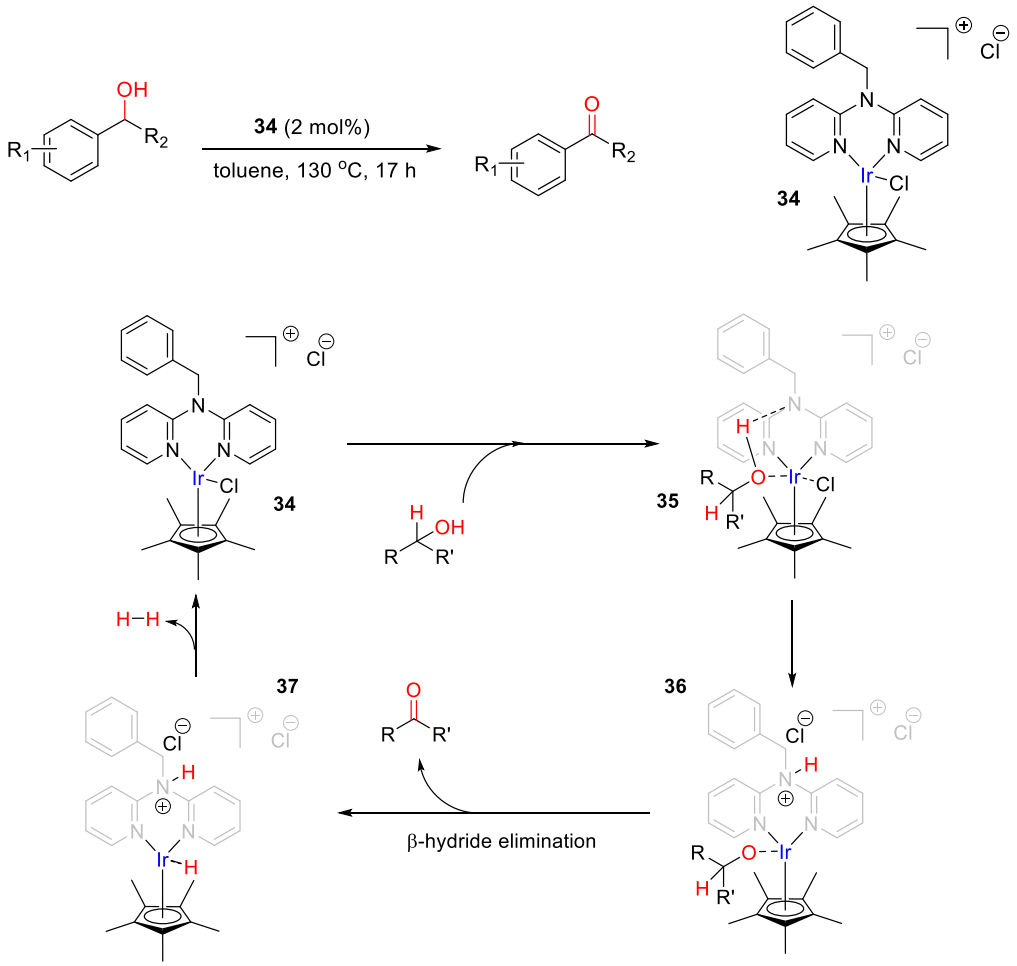

Scheme 4.11. Dehydrogenation of alcohols and proposed mechanism.

An iridium catalyst for the acceptorless and base-free dehydrogenation of alcohols has also been implemented (Scheme 4.11).[147] The catalyst displayed high efficiency in a number of alcohol dehydrogenation reactions. A possible reaction mechanism is presented in Scheme 4.11. The

activity of catalyst was drastically improved when the dipyridylamine ligand was made into a bridging tertiary amine in comparison to a secondary amine. A mechanism was proposed in which the basicity of the bridging nitrogen was a key parameter. Similar to other bifunctional catalysts based on pincer ligands, the bridging nitrogen would play the role of a base abstracting the acidic proton of the alcohol, and thus leading to the possible intermediate **36**. Subsequently, hydride elimination would release the ketone product leading to **37**, and hydrogen extrusion would then regenerate catalyst **34**. Another mechanism involving the decoordination of one of the pyridine rings, which would act as a basic center, was also conceivable.

Other metals, such as Os,[148–150] Pd,[151,152] and Rh,[153] also perform well on the dehydrogenation of alcohols.

4.3.2 Comparison between platinium group metals and 3d transition metals

Although the platinium group metals have good performances on the dehydrogenation of alcohols, they are all precious metals. From Figure 4.2,[154] it can be seen that the prices of the platinium group metals are very high. For the metal Rh, the price is about 70000 €/mol. Even though the price of Pt is relatively low, it is still about 10000 €/mol. For the 3d transition metals, their prices are very low, with Ni being the most expensive, but with a price lower than 1 €/mol.

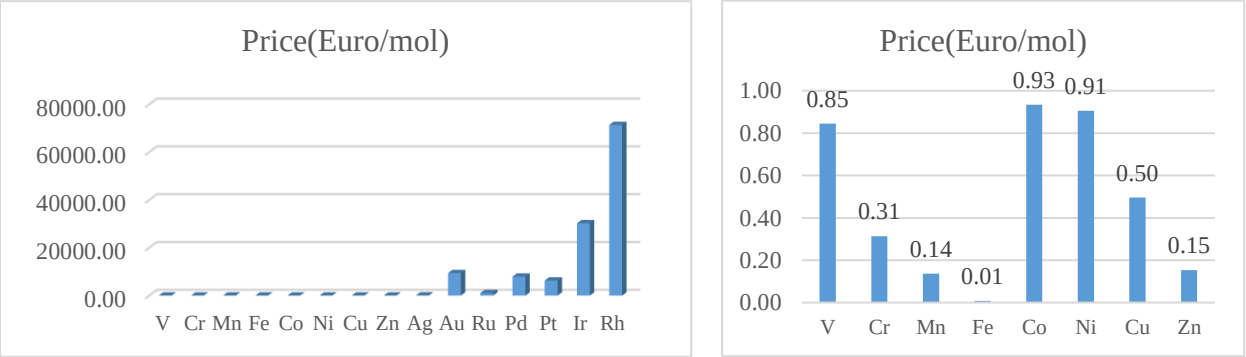

Figure 4.2. Prices of different transition metals.

In addition, the permitted daily oral exposure of 3d transition metals are magnitudes higher than the values for the of platinium group metals as shown in Figure 4.3.[154,155] Moreover, there is a limited amount in the human body of 3d transition metals as shown in Table 4.2.[156,157]

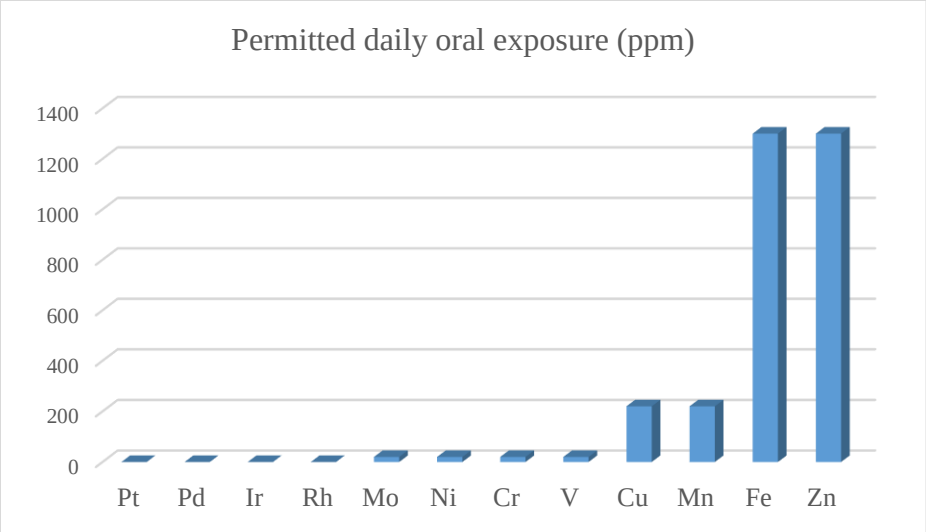

Figure 4.3. Permitted daily oral exposure of different transition metals.

Table 4.2. Concentrations of transition metals in the human plasma.

Element	Human plasma (M) × 10^8
Fe	2230
Zn	1720
Cu	1650
Mo	1000
Co	0.0025
Cr	5.5
V	17.7
Mn	10.9
Ni	4.4

Furthermore, the natural abundance in the Earth's crust of the platinium group metals is very low compared with that of the 3d transition metals as seen in Figure 4.4.[154] 3d Transition metals are the most abundant transition metals in Earth's crust and Fe is the most abundant metal among the 3d transition metals as seen from Figure 4.5.[154]

Therefore, the annual productions of 3d transition metals are thousands of times higher than that of the platinium group metals as shown in Figure 4.6.[158]

Based on the facts introduced above, 3d transition metals have a low price, a high permitted daily oral exposure, a high abundance and annual production, and therefore it is interesting to investigate whether they can be applied into dehydrogenation reactions, and have similar performances as the platinum group metals.

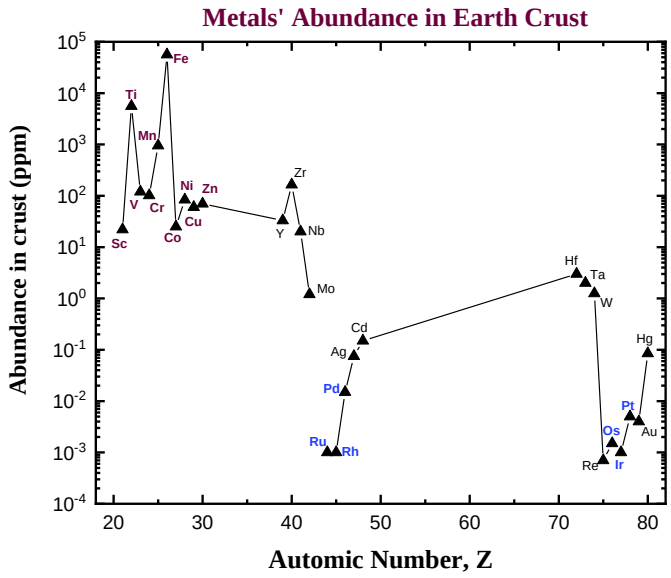

Figure 4.4. Natural abundance of different transition metals in the Earth's crust.

Figure 4.5. Natural abundance of 3d, 4d, 5d transition metals (left) and abundance of 3d transition metals (right).

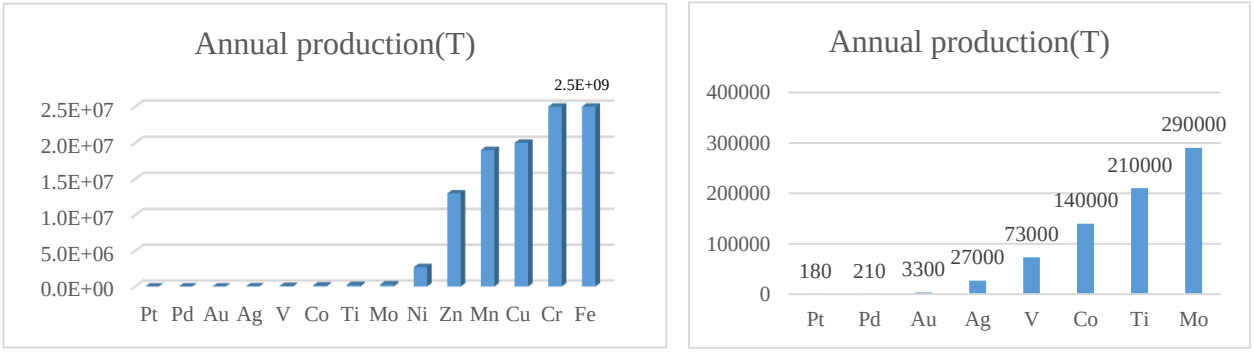

Figure 4.6. Annual production of different transition metals.

4.3.3 3d Transition metals in dehydrogenation reactions

The catalytic dehydrogenative coupling of alcohols and amines to form imines represents an environmentally benign methodology in organic chemistry. This has previously been mainly accomplished with catalysts based on precious metals. However, 3d-transition-metal-based catalysts have indeed made much progress in recent years, and they can also have good performances. There have been many reports about manganese since the first Mn complex was developed for dehydrogenation in the Milstein group in 2016.[22]

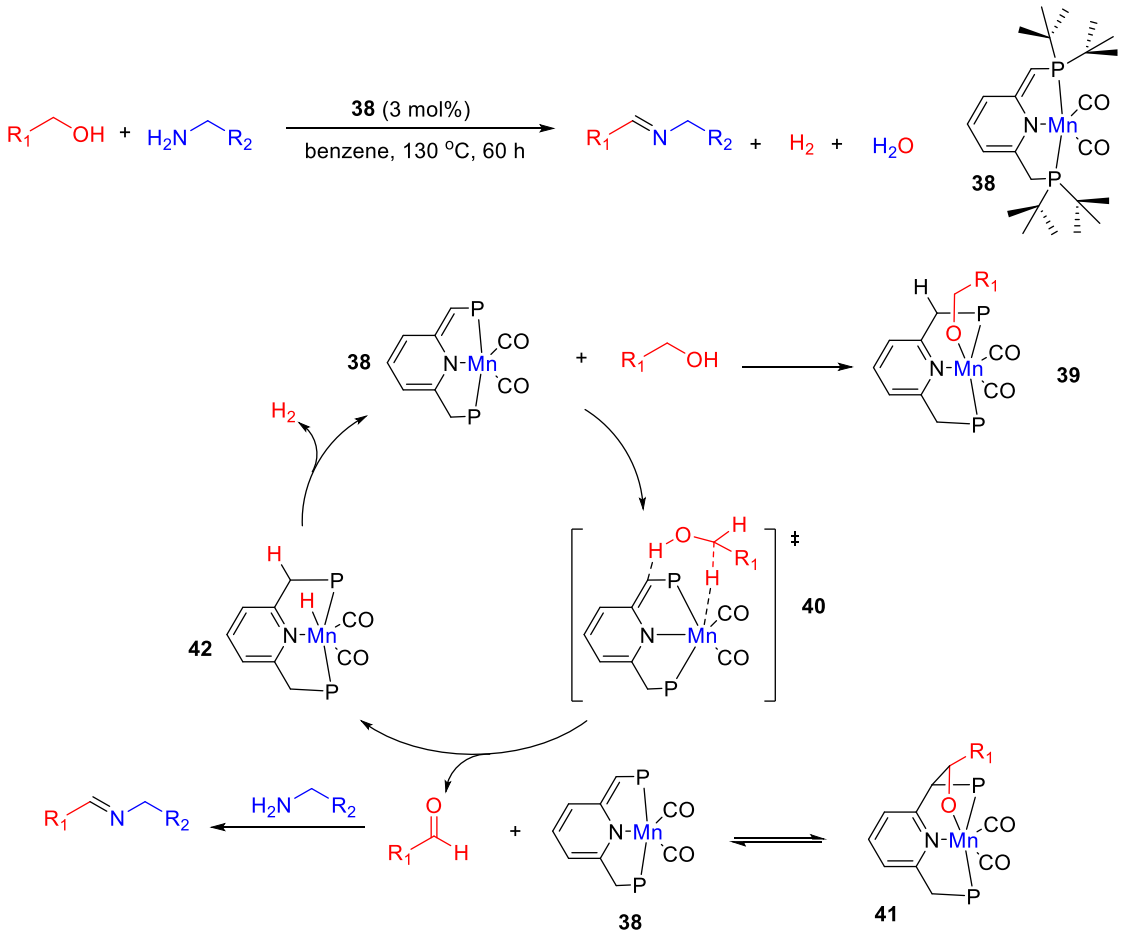

Scheme 4.12. Reaction with catalyst based on Mn and proposed mechanism.

The dehydrogenative coupling of alcohols and amines to form imines and H_2 reported by Milstein is shown in Scheme 4.12. This was the first catalyst with a complex composed of the Earth-abundant Mn for the dehydrogenation of alcohols.

The proposed mechanism for the Mn-catalyzed process followed a pathway similar to that of the PNP Ru-catalyzed reactions. The dehydrogenation of the alcohol likely proceeded through a

bifunctional proton and hydride transfer step, illustrated as transition state species **40** (Scheme 4.12).[159] Formation of the aldehyde by direct β-H elimination of the alkoxy ligand of coordinatively saturated species **39** (reversibly formed under the reaction conditions) was less likely. Complex **42** then underwent dehydrogenation under the catalytic conditions to regenerate active complex **38**, which then reentered into the catalytic cycle.

The crystal structure of the intermediate was determined and examined. Treating a saturated THF solution of **38** with two equivalents of benzaldehyde, followed by exposure to pentane vapor, yielded after 72 h at 25 °C single crystals of complex **41**. The X-ray structure of complex **41** indicated the product of aldehyde binding to the ligand framework with formation of Mn-O and C-O bonds. ^{31}P-NMR of complex **41** in neat benzyl alcohol was found to be in accordance with the NMR experiment. This eliminated the possibility of subsequent attack of the alcohol on complex **41**.

Moreover, there are multiple additional articles about dehydrogenation of alcohols based on Mn in Milstein's group. Another example is catalytic α-olefination of nitriles using primary alcohols via dehydrogenative coupling of alcohols with nitriles (Scheme 4.13).[160] The reaction was catalyzed by a pincer complex of an Earth-abundant metal (manganese) in the absence of any additives, base, or hydrogen acceptor, liberating dihydrogen gas and water as the only byproducts.

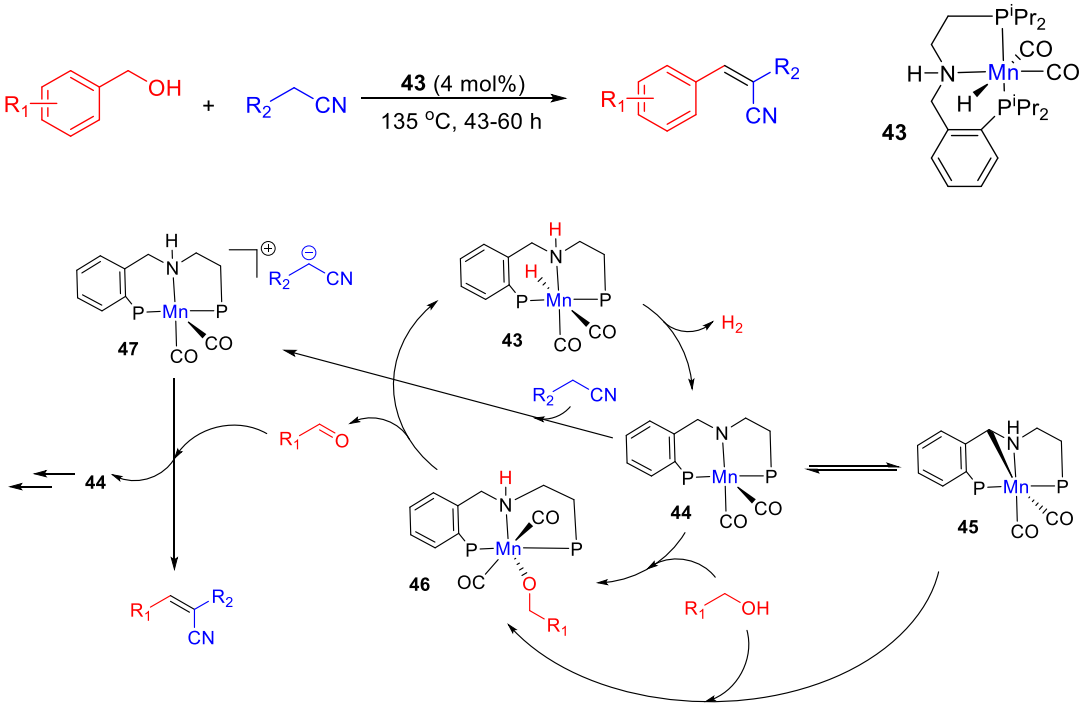

Scheme 4.13. α-Olefination of nitriles with catalyst based on Mn and proposed mechanism.

Regarding the mechanism, it was believed that the amido complex **44** was involved in the catalytic cycle.[161] Indeed, when freshly prepared **44** was employed as a catalyst in the dehydrogenative coupling of benzyl alcohol and benzyl cyanide, a 73% yield of 2,3-diphenylacrylonitrile was obtained after 40 h, whereas complex **45** also catalyzed the reaction giving a slightly lower yield (52%) compared to complex **43** or **44**. To obtain more information about complex **44**, NMR experiments were performed. Treatment of **44** with 4-fluorophenylacetonitrile (1 equiv) in toluene-d_8 at room temperature resulted in partial formation of a new complex, which exhibited two broad ^{31}P-NMR signals at δ = 59 and 91 ppm. Cooling to -40 °C resulted in sharpening of the broad signals to form two doublet signals at δ = 59.8 ($^2J_{PP}$ = 89 Hz) and 91.8 ($^2J_{PP}$ = 89 Hz) ppm, indicating reversibility of the reaction at room temperature.

This new complex was plausibly a cationic complex **47**, in which abstraction of the acidic α-proton from 4-fluorophenylacetonitrile by the basic amido moiety of complex **44** generated a nitrile carbanion, which may be stabilized by coordination to the cationic metal center or remain as a counteranion. In the ^{1}H-NMR spectrum, a singlet signal at 4.3 ppm was likely due to a CH proton of the nitrile carbanion. In the ^{19}F-NMR spectrum, a signal at 133.6 ppm was observed for the fluorine atom of the likely carbanion, along with the signal of 4-fluorophenylacetonitrile at 116 ppm.

To further support these assignments, 4-fluorophenylacetonitrile was reacted with KH in THF at room temperature and the observed ^{1}H-NMR (4.4 ppm) and ^{19}F-NMR (133.7 ppm) signals were in accordance with the suggested nitrile carbanion. Thus, these observations represented a rare direct observation of a C-H activation of arylacetonitrile by an amido-amine metal-ligand cooperation. In addition, the author has previously reported that the amido complex **44** reacted with excess 4-methoxybenzyl alcohol to form the alkoxo complex **46** (Scheme 4.12) along with 4-methoxybenzaldehyde at room temperature and the hydride complex **43** as revealed by ^{1}H- and ^{31}P-NMR spectra.[162]

Based on recent mechanistic investigations of the Mn-catalyzed dehydrogenative coupling of amines and methanol,[161] and on deoxygenation of primary alcohols catalyzed by **43**,[162] the catalytic cycle depicted in Scheme 4.13 was plausible. Initial dihydrogen liberation from complex **43** lead to the amido complex **44**, which underwent intramolecular C-H activation to form the thermodynamically more stable C-metalated complex **45**.[161] O-H activation of the alcohol by complex **44** or **45** via proton transfer, to either the amido nitrogen or benzylic carbon, resulted in the formation of the alkoxo complex **46**. The following β-hydride elimination step released the aldehyde, unlike the dearomatized Mn(PNP^{t}Bu) system, which did not bind with the amido complex **44**.[22] In a competitive pathway, the nitrile bearing α-hydrogen likely formed complex **47**

by ligand-based deprotonation, generating a nitrile carbanion. Intermediates **46** and **47** were expected to be in equilibrium with the amido complex **44**. Nucleophilic attack of the carbanion at the aldehyde followed by water elimination lead to the α,β-unsaturated nitriles and regenerates the amido complex **44**, thus completing the catalytic cycle.

The Madsen group has also focused on dehydrogention of alcohols with catalysts based on Ir, Ru, Mn and Mo for many years, leading to a number of publications.[163–169] A catalyst based on Mn is shown in Scheme 4.14.[167] Different imines were prepared through dehydrogenation of different alcohols with amines in the presence of catalyst **48**.

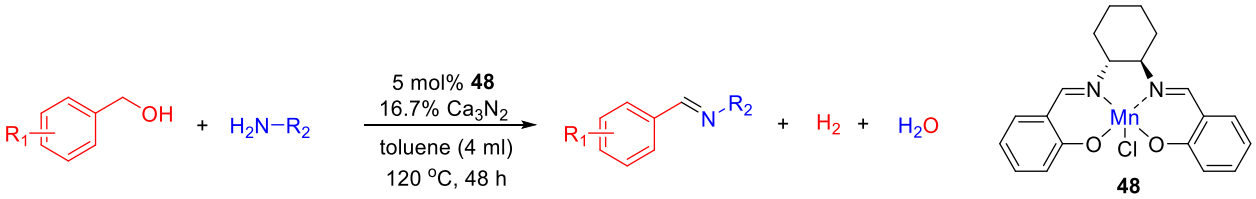

Scheme 4.14. Dehydrogenation of alcohols with amines to form imines.

The catalyst **48** is a Mn(salen)Cl complex, and the activation of the catalyst is shown in Scheme 4.15. The initial idea was that complex **49** underwent β-hydride elimination. However, the activation energy for this process was found to be prohibitively high (at 37.9 kcal mol^{-1} relative to **49**), which was partly due to the lack of an available coordination site. Instead, an alternative reaction was found, where the hydride was transferred from the benzylic carbon to the imine carbon of the salen ligand. The activation energy was merely 17.6 kcal mol^{-1} and the product complex **51** was at 6.6 kcal mol^{-1}. A similar pathway has been identified in the activation of (PNNP)Fe(II) eneamido complexes with isopropanol.[170] The product benzaldehyde was then replaced by benzyl alcohol, from which a proton was transferred to the amide nitrogen of the reduced salen ligand. The resulting complex where one imine of the salen is hydrogenated was at -5.2 kcal mol^{-1} relative to **49**. The lowest activation energy found from the hydrogenated intermediate was for another hydride transfer to the second imine of the salen ligand, with a transition state at 14.5 kcal mol^{-1} (maximum ΔG act = 19.7 kcal mol^{-1}).

After complete dissociation of benzaldehyde, a key species **53** was formed, where one imine was hydrogenated to the amine and the other was reduced to an amide ligand. This species resembled intermediates from alcohol dehydrogenations with (PNP)Ru(II), (PNP)Mn(I), (PNNP)Fe(II) and (PNP)Ir(III) catalysts,[171,172] which had an amide ligand that can act as a Brønsted base and a metal that can serve as a hydride acceptor. They have all been proposed to react via an outer-sphere hydrogen transfer mechanism.[171,172] The main difference was the metal and the oxidation state, which in the current case was manganese(III). The same outer-sphere hydrogen transfer was

identified, and the activation energy was 26.7 kcal mol^{-1} relative to **53** and 27.2 kcal mol^{-1} relative to **56**, which corresponded to a TOF of 83 h^{-1} at the reaction conditions.

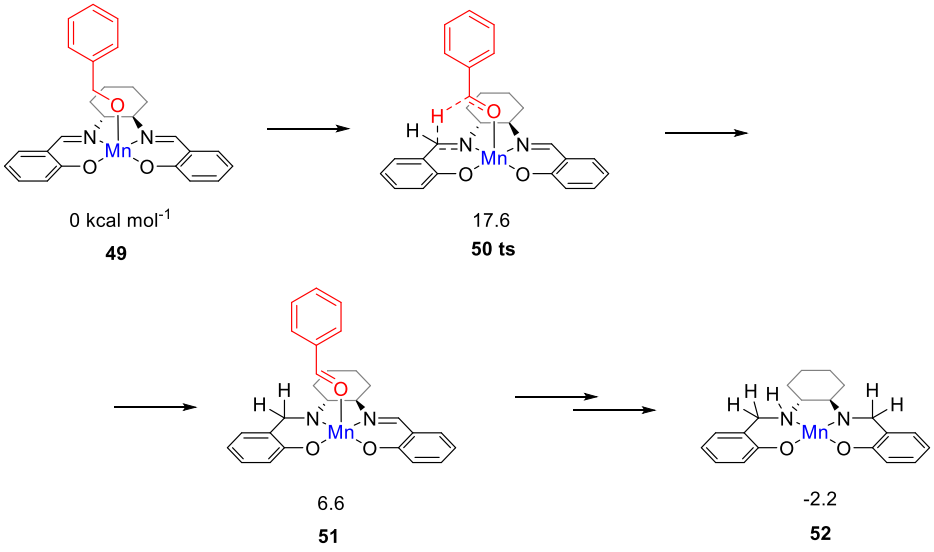

Scheme 4.15. Activation of Mn(III)(salen)OBn to form the active amido complex.

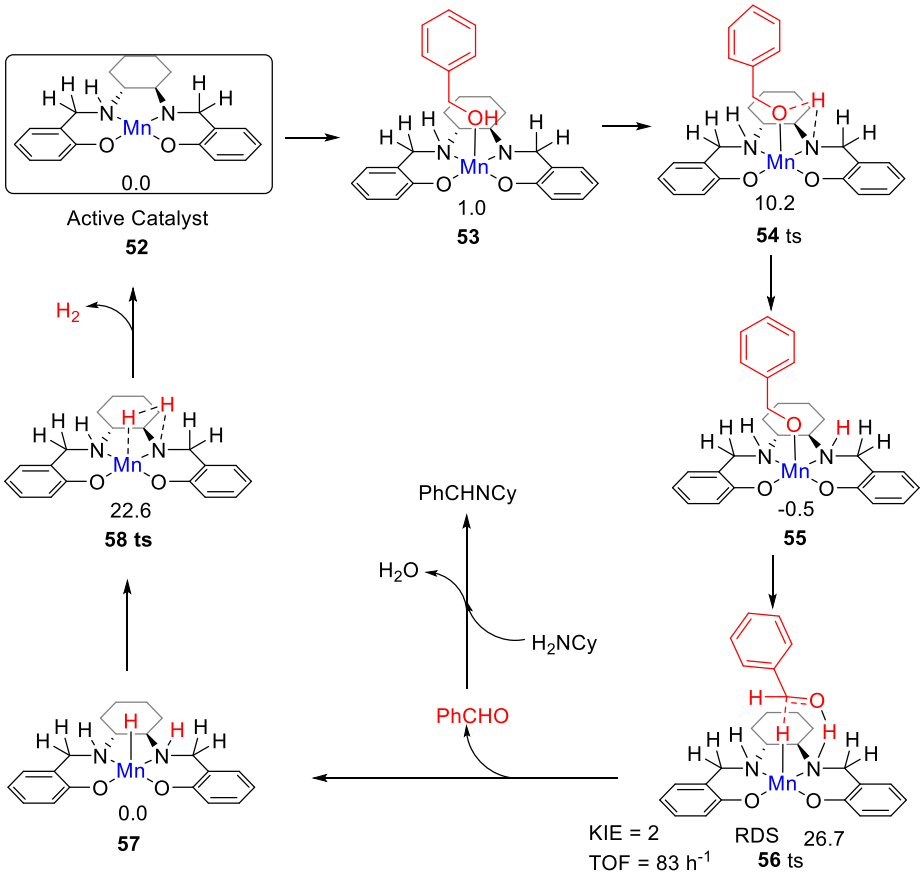

Scheme 4.16. Proposed catalytic cycle and relative Gibbs free energies.

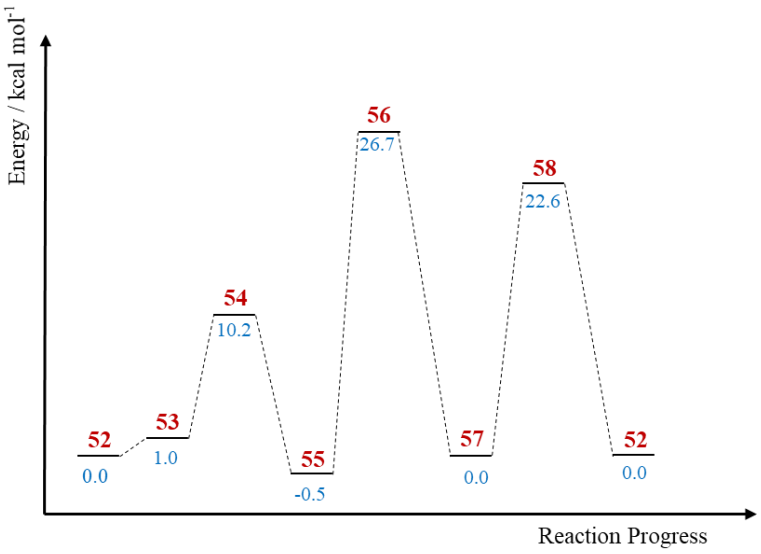

Scheme 4.17. Potential energy diagram of catalytic cycle.

The relative rates were calculated from the pre-reactive complex **55** and a good agreement was found with the experimental results, giving a very similar ρ value. After the formation of the manganese(III) hydride intermediate **57**, benzaldehyde was assumed to react irreversibly with the amine. From complex **57** the formation of hydrogen gas required an activation energy of 22.6 kcal mol^{-1}, in a step that regenerated the active catalyst as shown in Scheme 4.16. The potential energy diagram is shown as Scheme 4.17, if the catalytic cycle is converted to reaction progress.

In addition, Matthias Beller,[173] Karl Kirchner,[174,175] and Rhett Kempe[176,177] also reported different catalysts based on Mn for dehydrogenation of alcohols.

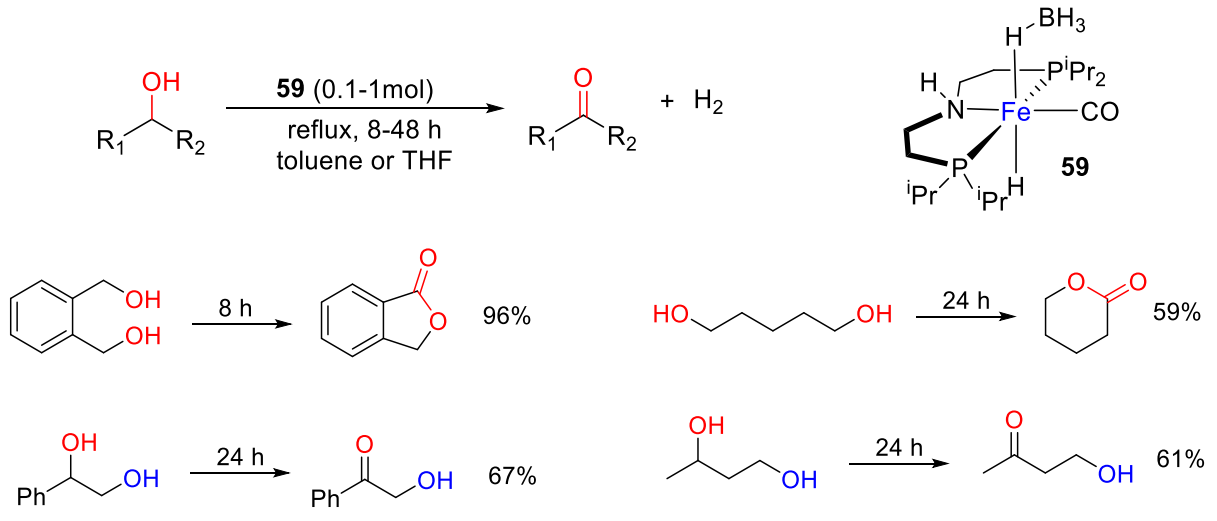

Scheme 4.18. Dehydrogenation of alcohols with catalyst based on Fe.

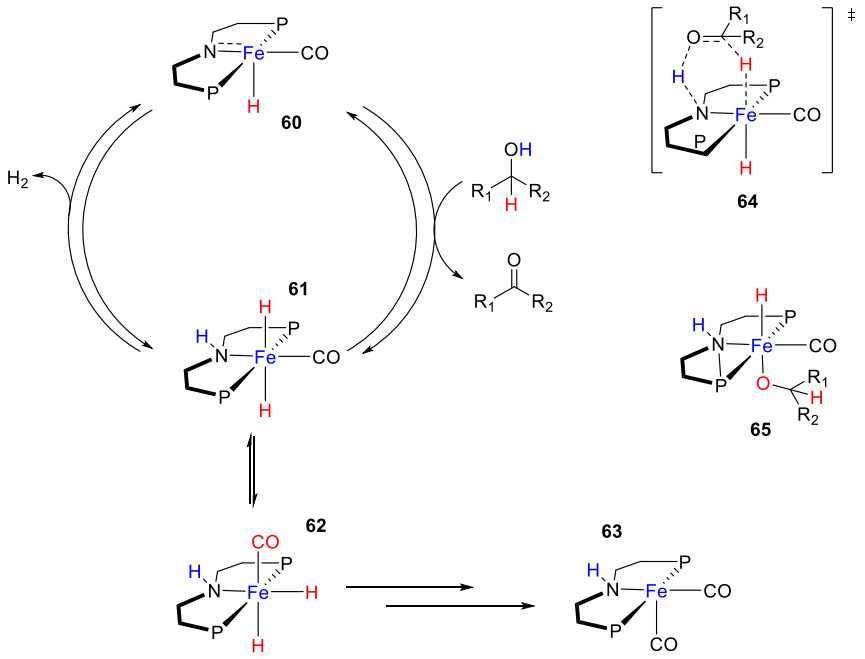

Scheme 4.19. Proposed catalytic mechanism.

Iron, as the cheapest metal, has also been well established as a common metal catalyst. As shown in Scheme 4.18, an iron catalyst performs on different alcohols, including aliphatic alcohols and diol substrates.[178]

A plausible homogeneous mechanism for the iron-catalyzed alcohol dehydrogenation is outlined in Scheme 4.19. It was proposed that complex **60** was involved in the catalytic cycle.[179,180] Previously, it was established that complex **60** reversibly added H_2 to give mainly trans-dihydride complex **61** and smaller amounts of cis-dihydride complex **62**, which was in equilibrium with **61** in accordance with EXSY-NMR experiments.[181] Minor quantities of free $HN(CH_2CH_2P^iPr_2)_2$ and iron(0) complex **63** ($Fe(CO)_2(HN(CH_2CH_2P^iPr_2)_2)$) were also observed.[179] The relevance of species **60** within the catalytic cycle of AAD was supported by a stoichiometric control reaction of species **60** with 2 equiv of 1-butanol at room temperature. Slow, selective substrate conversion to *n*-butyl-butanoate was accompanied by formation of the same iron products (complex **61** - **63**) and free ligand as determined by a ^{31}P-NMR spectra without detection of other intermediates. Hydrogen transfer from the substrate to species **60** was conceivable either by a concerted pathway via **64** or stepwise **65** through an alkoxide intermediate, which remained at this point unresolved on experimental grounds. However, the computational results indicated low barriers for a concerted mechanism. Comparison of the stoichiometric reactions of species **60** with H_2 and 1-butanol, respectively, indicated faster catalyst degradation to iron(0) and free ligand with the alcohol as the hydrogen source. This observation suggested that formation of inactive **63** might be initiated by

H_2 reductive elimination from **62** at low H_2 concentrations. In contrast, H_2 elimination from **61** to amide **60** was shown under vacuum[180,181] and closed the cycle.

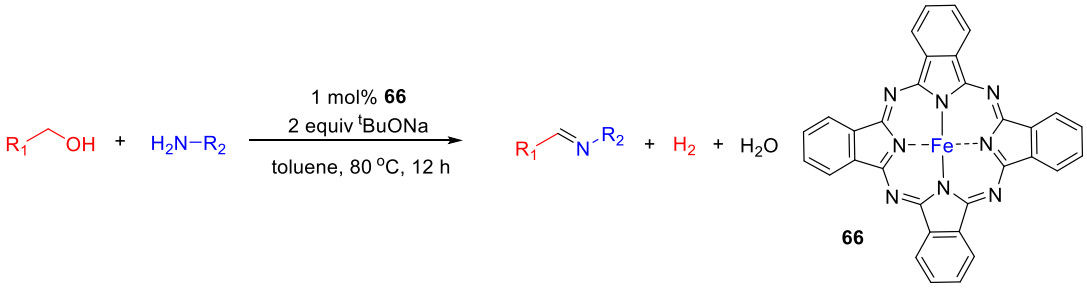

Scheme 4.20. Dehydrogenation of alcohols with catalyst based on Fe.

Scheme 4.20 shows another iron comples that also performed well on benzyl alcohols and aliphatic alcohols with a low temperature and a short reaction time.[182]

Cobalt, as a common metal, has also been well established as a metal catalyst. As shown in Scheme 4.21, a cobalt catalyst performs on dehydrogenation of 1-phenylethanol with the liberation of hydrogen gas.[183]

A reaction mechanism is proposed and shown in Scheme 4.22. In the proposed catalytic cycle, a complex **67** was a resting state. Starting from **67**, reductive elimination of acetophenone generated a cobalt(I) intermediate **68** and allowed for ligand exchange at the cobalt center. Exchange of the bound acetophenone-d_8 in complex **67**-d_8 with free acetophenone occurred rapidly at 60 °C, verifying the possibility of such a reductive elimination step. Replacement of the coordinated acetophenone with 1-phenylethanol could occur by either associative or dissociative ligand substitution (Scheme 4.22). Once 1-phenylethanol entered the cobalt(I) coordination sphere, oxidative addition of the O-H bond generated a cobalt(III) alkoxide complex **70**. The cobalt(III) alkoxide complex **70** underwent β-hydride elimination to generate a cobalt(III) dihydride complex **69**.[184–188] Loss of hydrogen and coordination of acetophenone or 1-phenylethanol completed the catalytic cycle. The overall reaction was reversible, as demonstrated experimentally.

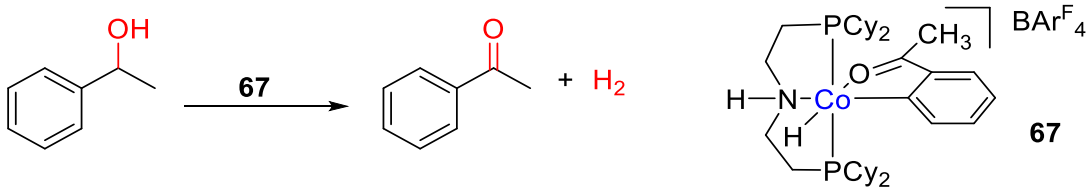

Scheme 4.21. Dehydrogenation of 1-phenylethanol with catalyst based on Co.

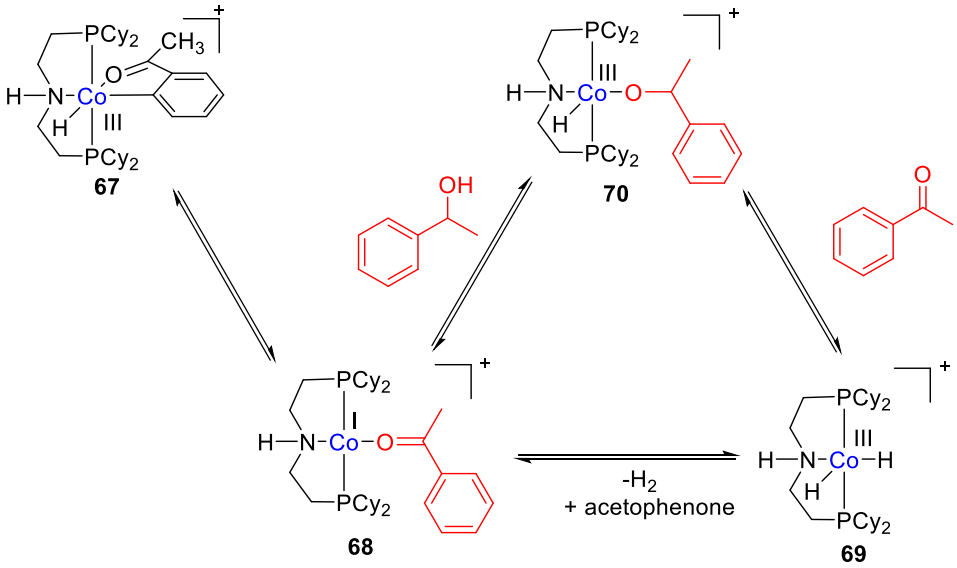

Scheme 4.22. Proposed mechanism for cobalt catalyzed dehydrogenation of 1-phenylethanol.

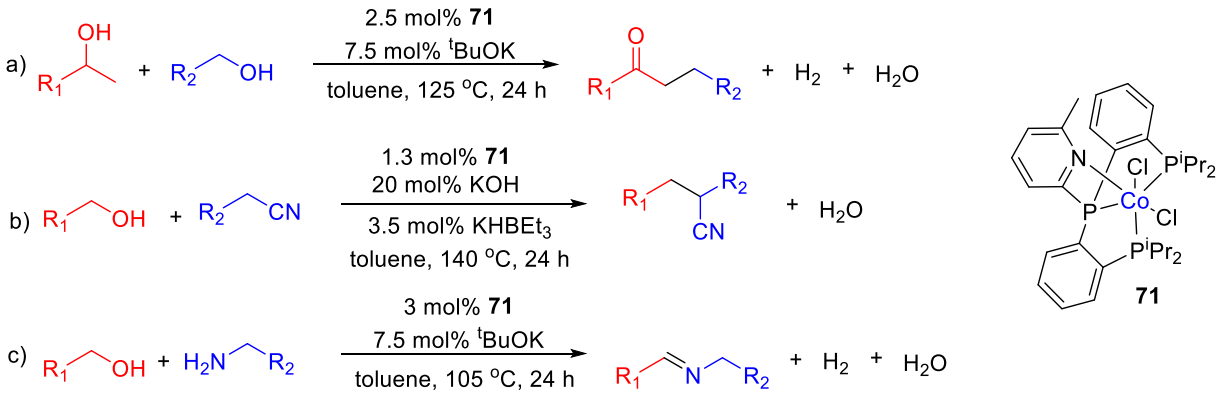

Scheme 4.23. Dehydrogenative reactions with catalyst based on Co.

In addition, the Co complexes can also be employed for dehydrogenation and alkylation reactions. In Scheme 4.23a, a homogeneous cobalt-catalyzed β-alkylation of secondary alcohols with primary alcohols to selectively synthesize ketones via acceptorless dehydrogenative coupling is reported for the first time. Notably, this transformation only yielded water and hydrogen gas as the byproducts.[189] In Scheme 4.23b, the α-alkylation of nitriles with primary alcohols to selectively synthesize nitriles by a well-defined molecular homogeneous cobalt catalyst is presented.[190] Remarkably, this transformation was environmentally friendly and atom economical with water as the only byproduct. In Scheme 4.23c, the dehydrogenation of alcohols with amines to form imines is shown.[191]

Other groups also have made achievements on the dehydrogenation of alcohols with cobalt catalysts, such as Kempe,[192] Zhang,[193] Kirchner,[194] and Milstein.[195,196]

Cu and Ni, as cheap 3d transition metals, have also been applied in the dehydrogenation of alcohols with some examples shown in Scheme 4.24.[197–199]

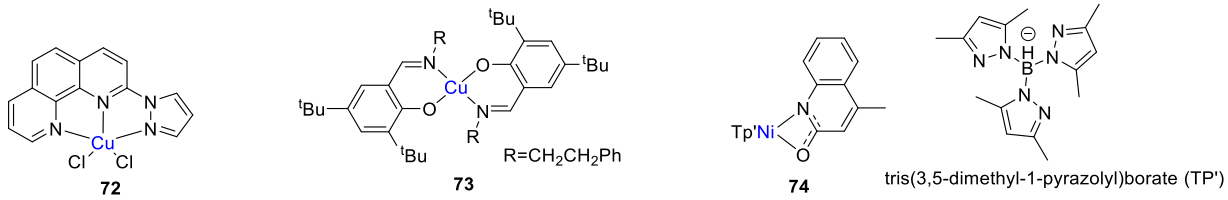

Scheme 4.24. Different catalysts based on Cu and Ni.

4.4 The classical AAD reaction mechanism & metal-ligand cooperation (MLC)

Many AAD reactions are introduced above, and many of the early examples have turned out to be operating through a Shrock-Osborn inner-sphere reaction mechanism,[200] which is now divided into a "monohydride" and a "dihydride" version[201–203] (Scheme 4.25). The two reaction mechanisms are different in various aspects, but the most obvious difference is that for the "dihydride" mechanism, two hydrogens are transferred to the metal center (the O-H and C_α-H from the alcohol substrate), whereas the metal only receives one hydride in the "monohydride" mechanism (the C_α-H from the alcohol substrate). In case of reversibility, scrambling between the two different hydrogens is observed in the "dihydride" mechanism, whereas scrambling between the two hydrogens will not occur in the "monohydride" mechanism, which makes it possible to distinguish between the two pathways with the use of deuterium-labelled substrates. Another difference between the two mechanisms is that the oxidation state of the metal is changing during the "dihydride" cycle, whereas the oxidation state of the metal remains the same in the "monohydride" pathway.

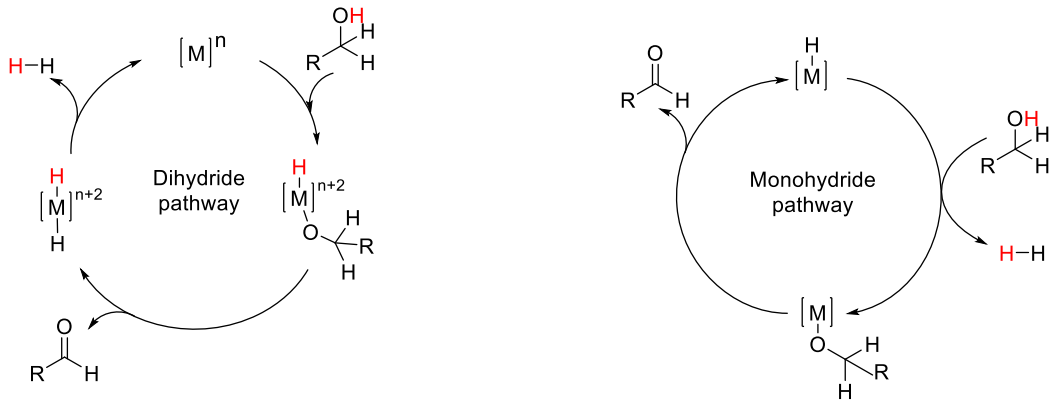

Scheme 4.25. Representation of dihydride pathway (on the left) and monohydride pathway (on the right).

In the most recent examples of AAD reactions, a new concept of catalysis has turned up, where the role of the ligands has changed. In contrast to "classical" transition metal catalysis, where all key transformations take place at the metal center, and the ligand acts as a simple spectator, MLC, also regarded as a bifunctional pathway, suggests that both the metal and the ligand participate in the bond activation processes. In many examples of homogeneous catalysis, oxidative addition, reductive elimination and β-hydride elimination occur at the metal center, while the ligand stays unaltered throughout the reaction as shown above (Scheme 4.25). The introduced examples of Ru complexes,[129] Mn complexes[22] and Fe complexes[178] belong to the MLC.

The bifunctional pathway is possible for catalysts possessing a metal center as a Lewis acid and a cooperative site in the ligand as a Brønsted base, enabling acid-base functionality. The most common MLC systems are based on N-donor ligands, but also other donor atoms such as carbon, oxygen, sulfur and boron have demonstrated a great potential for MLC reactivity. The classical mechanism proceeds through direct participation of the ligand in the catalytic reaction by a reversible proton transfer through cleavage/formation of one of its X-H bonds and the formation of a metal-hydride complex. H-H and H-heteroatom bond activations are among the most well studied and widely used in catalysis. Bifunctional catalysts can be classified as α, β or γ-functionalized, depending on the location of the cooperative site in the ligand framework with respect to the metal center. Furthermore, MLC can be divided into two classes, where metal-ligand cooperation proceeds either through M-L bonds or aromatization/dearomatization (Scheme 4.26).[204,205]

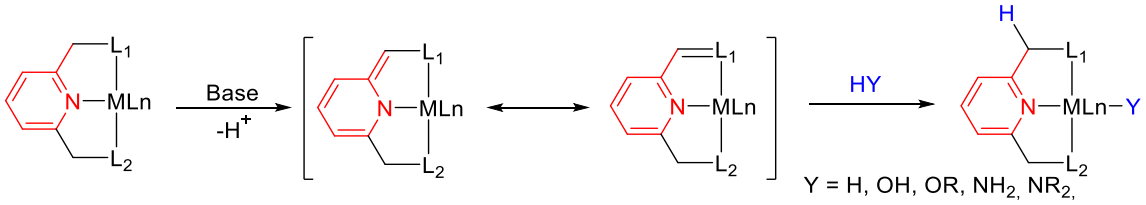

Scheme 4.26. Metal-ligand cooperation through aromatization/dearomatization.

The transfer of the proton and the hydride can occur either by a stepwise inner-sphere reaction mechanism or by a concerted outer-sphere reaction mechanism (Scheme 4.27). As the name implies that the transfer of the proton to the ligand and the hydride to the metal is concerted in the outer-sphere mechanism. In contrast, in the case of the inner-sphere mechanism, abstraction of the proton by the ligand leads to the formation of a metal alkoxide intermediate, which is subsequently converted to the metal hydride during the β-hydride elimination. Hence, the transfer of the proton and the hydride is stepwise.

Cooperative action of a reactive heteroatom center in a ligand and a metal center may offer a suitable acid-base bifunctionality and spatial arrangement for selective bond activation processes under mild conditions, resembling bond activation reactions that occur in enzymes.[203]

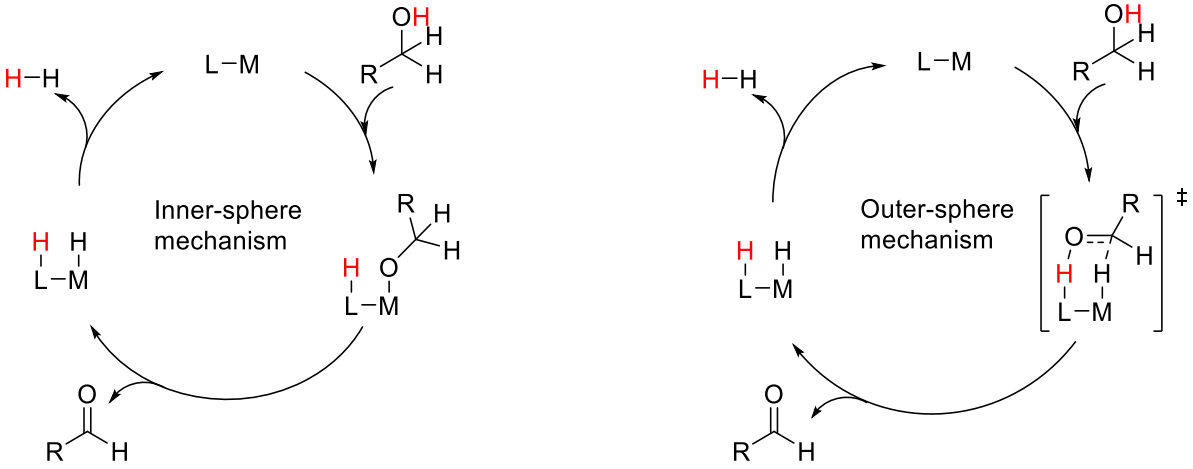

Scheme 4.27. Inner-sphere (on the left) and outer-sphere (on the right) mechanism in bifunctional pathways.

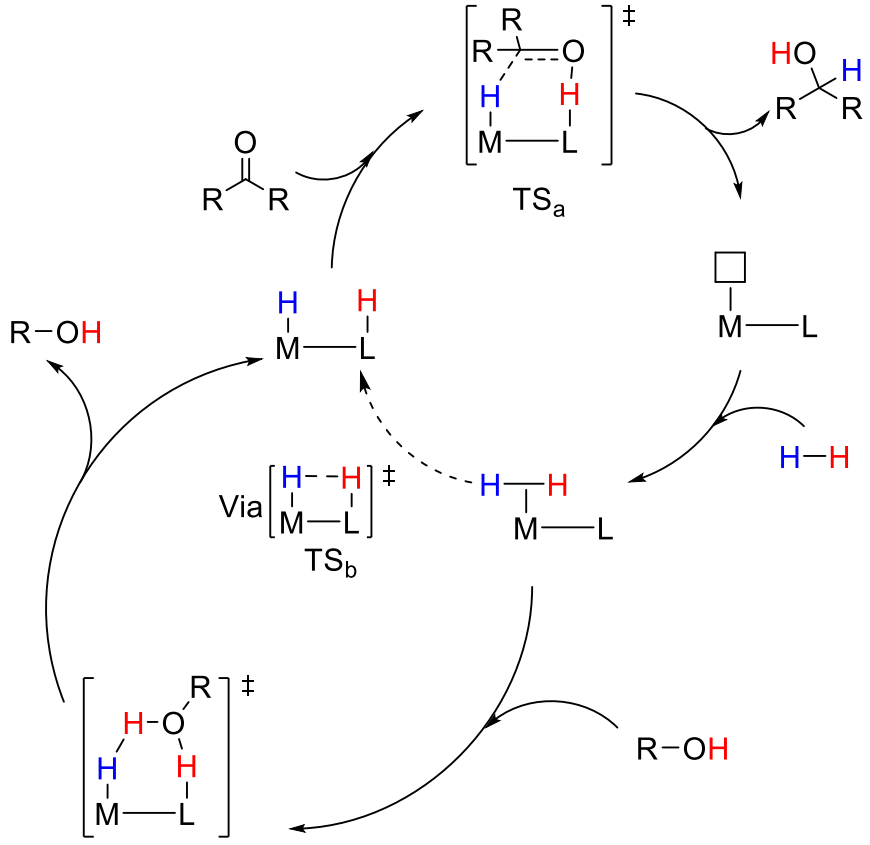

Scheme 4.28. Noyori mechanism for the hydrogenation of ketones.

In 1985, Shvo reported the first "chemically non-innocent" ligand.[206] About ten years later, Noyori proposed an outer-sphere bifunctional mechanism for the hydrogenation of ketones (Scheme 4.28), which is the most commonly accepted bifunctional mechanism.[148,207,208] Since then, the particular mechanism has been revised[209] and many other examples of complexes capable of MLC have been published,[204,207,209] both with AD systems and new hydrogenation reactions.

In conclusion, AAD could be considered as a green alternative to traditional methods to synthesize various functional groups, including imines. Moving towards the use of catalysts based on Earth-abundant metals will make AAD more valuable. In the development of new catalysts, it is important to keep in mind the advantages of complexes capable of MLC.

5. Chromium porphyrin catalyzed dehydrogenation of alcohols to form imines

This chapter is based on the part in the following article:

Yulong Miao, Simone V. Samuelsen, Robert Madsen, Vanadium- and Chromium-Catalyzed Dehydrogenative Synthesis of Imines from Alcohols and Amines, *Organometallics* **2021**, 40, 1328-1335. Published by the American Chemical Society.

5.1 Background

5.1.1 Introduction to chromium

Chromium is the seventh most abundant transition metal in the Earth's crust and the 21th most abundant among all elements. Chromium is a cheap metal with a price of around 5.17 €/kg and a worldwide production estimated at 440000 tons per year.[154,158] Chromium is predominately used for the production of stainless steel.[210] The common oxidation states of chromium compounds range from 0 to +VI, thereby encompassing both reductive and oxidative transformations in synthetic chemistry.

Chromium has gained less attention in organic synthesis and catalysis among many metal candidates to promote sustainable catalytic reactions. Nerveless, the employment of chromium as a metal source has been a hot topic in recent years, because of its low price and huge annual production. Furthermore, trivalent chromium compounds show a low order of toxicity in humans (contrary to hexavalent species), due to their poor ability to pass through cell membranes.[211]

Inorganic chromium compounds have been applied in heterogeneous catalysis for many years. Several examples are shown in the following:

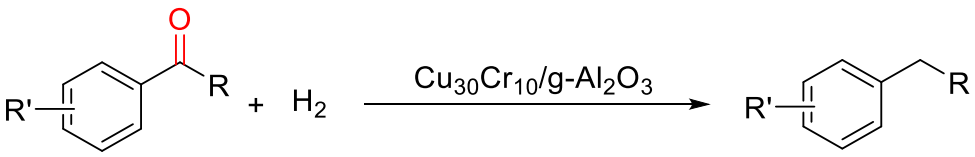

Scheme 5.1. Deoxygenation of aromatic ketones.

In Scheme 5.1, chromium is an important part of nanoparticles, which have a good performance in the reductive deoxygenation of aromatic ketones.[212]

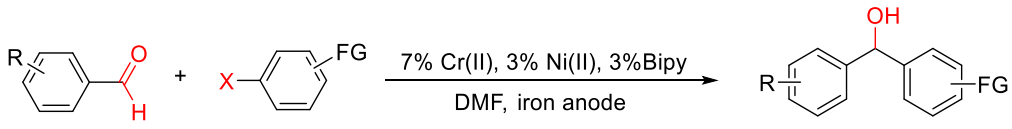

Scheme 5.2. Catalyzed reaction with Cr and Ni.

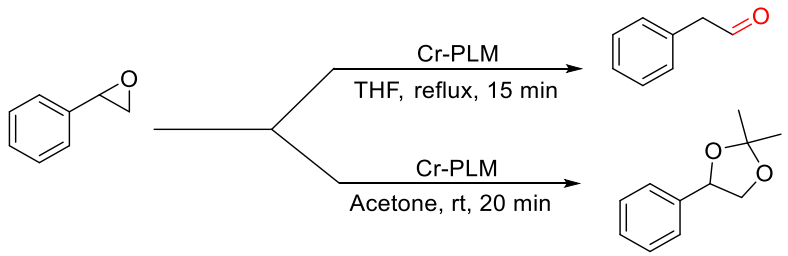

Scheme 5.3. Catalyzed reaction with Cr-PLM.

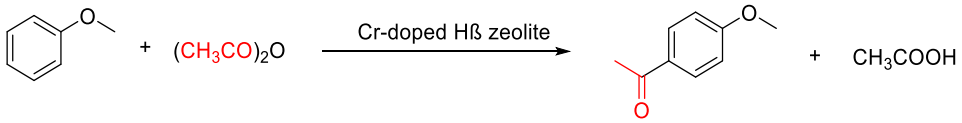

Scheme 5.4. Catalyzed reaction with Cr-doped Hβ zeolite.

In Scheme 5.2, the electrochemical addition of vinyl, allyl, or aryl halides to aldehydes via an intermediate chromium (III) species is achieved by using catalytic amounts of $CrCl_2$ and $NiBr_2$, which is an importance part of the Nozaki-Hiyama-Kishi reaction.[213]

In Scheme 5.3, chromium-pillared montmorillonite (Cr-PLM) is synthesized and efficiently utilized for styrene oxide transformations. The target aldehyde product could be quantitatively achieved from the isomerization of styrene oxide by using 10 wt% of Cr-PLM under reflux temperature for 15 min. The acetonide product could be achieved in excellent yield from the reaction of styrene oxide and acetone by using 10 wt% of Cr-PLM at room temperature for 20 min.[214] Cr-PLM performs well in these transformations in a short reaction time.

In Scheme 5.4, Cr-doped Hβ zeolite is found to have better catalytic performance than Hβ zeolite in the Friedel-Crafts acylation of anisole, with acetic anhydride conversion of over 99% and nearly 100% selectivity to furnish *para*-methoxyacetophenone under the optimized reaction conditions. This is attributed to the increase of weak and moderately strong acid sites, caused by the Cr addition.[215]

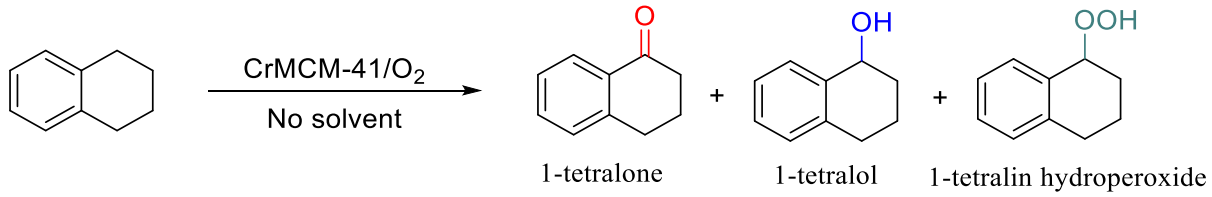

Scheme 5.5. Catalyzed oxidation of tetralin with O_2.

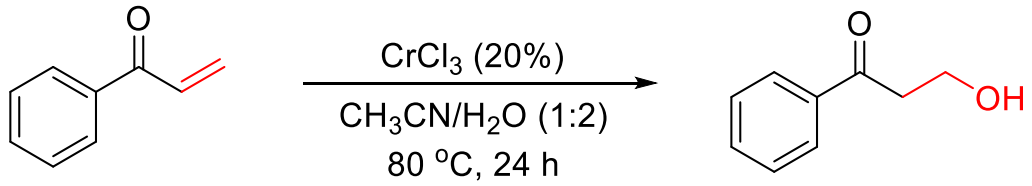

Scheme 5.6. Catalyzed reaction with $CrCl_3$.

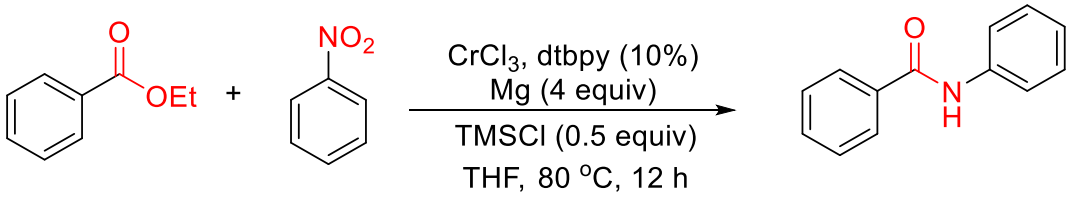

Scheme 5.7. Coupling reaction with $CrCl_3$.

In Scheme 5.5, solvent-free selective oxidation of benzylic compounds is effectively performed over a chromium-containing mesoporous molecular sieve (CrMCM-41) catalyst at 1 atm O_2 under mild reaction conditions (<100 °C). The catalyst has a good selectivity for 1-tetralone.[216]

Chromium salts can sometimes also be employed.

In Scheme 5.6, an efficient chromium(III) chloride-catalyzed Michael-type reaction of water (or alcohol) with α,β-unsaturated ketones was developed.[217]

In Scheme 5.7, the chromium salt can activate acyl C-O bonds for the amidation of esters with nitroarenes. Low-cost chromium(III) chloride showed high reactivity in promoting the amidation by using magnesium as a reductant and chlorotrimethylsilane as an additive.[218]

In Scheme 5.8, an efficient protocol for chromium(III)-catalyzed $C(sp^2)$-$C(sp^3)$ cross-coupling was reported. The alkylations of halo-quinoline and phenacyl derivatives proceed at room temperature within minutes using the tetrahydrofuran-soluble chromium(III) complex $CrCl_3 \cdot 3THF$.[219]

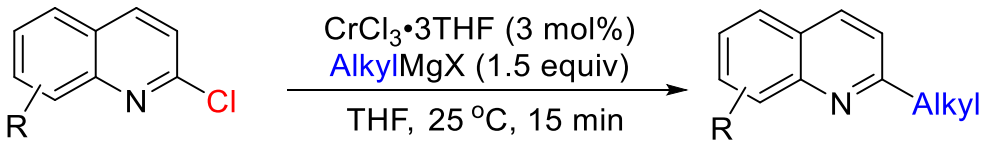

Scheme 5.8. Cross-coupling reaction with $CrCl_3$.

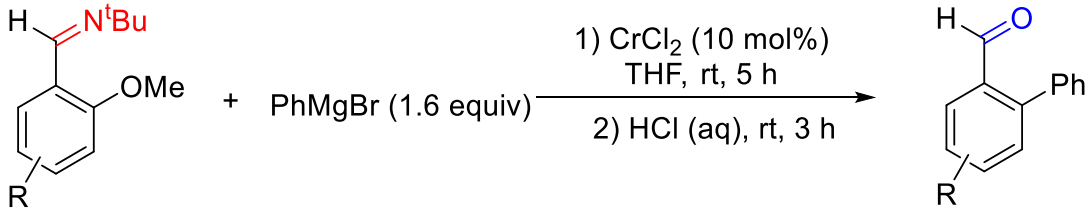

Scheme 5.9. Catalyzed reaction with $CrCl_2$.

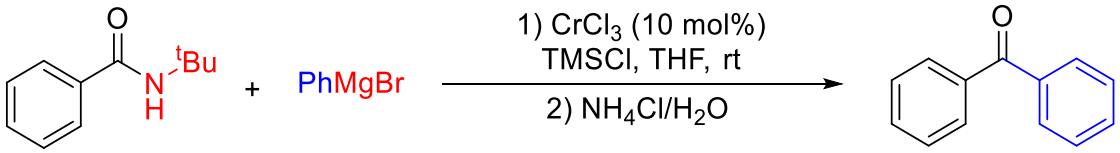

Scheme 5.10. Cross-coupling reaction with $CrCl_3$ salt.

The first chromium-catalyzed selective cross-coupling reaction of aryl ethers with Grignard reagents by the cleavage of C-O bonds is shown in Scheme 5.9. Diverse transformations were achieved using simple, inexpensive chromium(II) pre-catalyst combined with the imino auxiliary at room temperature.[220]

In Scheme 5.10, the synthesis of aromatic ketones by chromium-catalyzed Kumada arylation of secondary amides with organomagnesium reagents is described. This reaction is enabled by using a low-cost chromium(III) salt as a pre-catalyst, combined with trimethylsilyl chloride as an additive, and presents a rare example of a catalytic transformation of secondary amides to ketones at room temperature. It is shown that catalytically active low-valent chromium species might be responsible for the amide-ketone exchange by a mechanism involving the activation of the benzimidate intermediate.[221]

Chromium can also be inducted into metal complexes. In Scheme 5.11, the first example of a well-defined, supported organometallic chromium hydrogenation pre-catalyst was reported. In the reaction, the well-defined, four-coordinate, eleven-electron Cr(III) centers bound to catecholate porous organic polymers were demonstrated to be active hydrogenation catalysts for nonpolar unsaturated organic substrates under mild conditions (5 mol% of Cr, 200 psi of H_2, 60 °C).[222,223]

In Scheme 5.12, a new, stoichiometric activation mode is presented for Cr-PNP (PNP = diphosphinoamine) complexes for ethylene tetramerization catalysis. To access suitable pre-catalysts, two robust Cr(III) multiaryl compounds were synthesized as THF adducts. These complexes are supported by a facially coordinated bis(aryl) ligand with an additional ether donor. From these precursors, Cr-PNP tris(hydrocarbyl) complexes were synthesized. With 1 equiv of a Brønsted acid as an activator, an active species for the catalytic tetramerization of ethylene was produced, without the need for excess alkylaluminum reagents.[224,225]

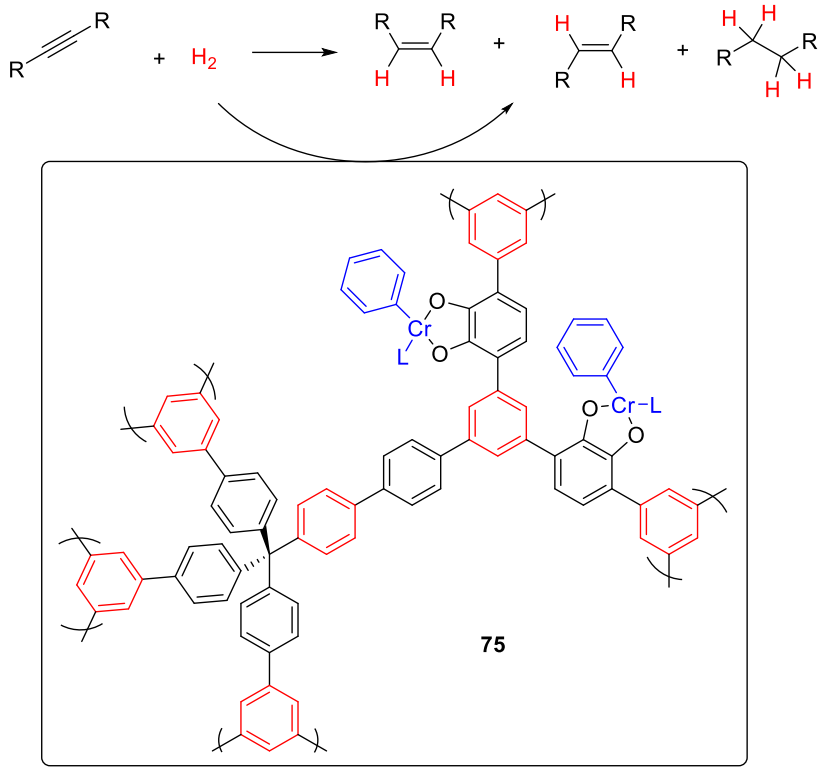

Scheme 5.11. Hydrogenation of alkyne with a catalyst based on Cr.

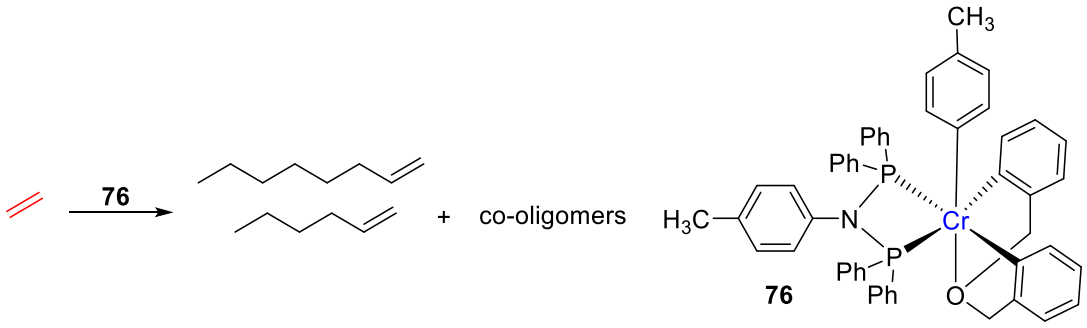

Scheme 5.12. Tetramerization of ethylene with a catalyst based on Cr.

Chromium complexes have found very few applications as hydrogenation catalysts, but a Cr-catalyzed semihydrogenation of internal alkynes to the corresponding Z-alkenes with good stereocontrol (up to 99/1 for dialkyl alkynes) is reported in Scheme 5.13. The active catalyst is generated from the commercial reagent chromium(III) acetylacetonate ($Cr(acac)_3$) and diisobutylaluminium hydride (DIBAL-H) in THF. The semi-hydrogenation operates at mild conditions (1-5 bar H_2, 30 °C).[226]

In Scheme 5.14, the Cr complex can catalyze the C-N bond formation reaction. The catalyst can tolerate numerous functional groups, including hydrogenation-sensitive moieties. Compared to many other alcohol-based amine alkylation methods, where a stoichiometric amount of base is required, the Cr-based catalyst system gives yields higher than 90% for various alkyl amines with a catalytic amount of base. The research indicates that Cr complexes can catalyze borrowing hydrogen or hydrogen auto-transfer reactions and could thus be an alternative to Fe, Co, and Mn, or noble metals in (de)hydrogenation catalysis, which could rouse great interest to researchers for exploration of dehydrogenations based on chromium.[227]

Even though chromium has been applied in catalysis for many years, the applications in homogeneous catalysis are limited, and only one previous example exists where a dehydrogenation is involved.

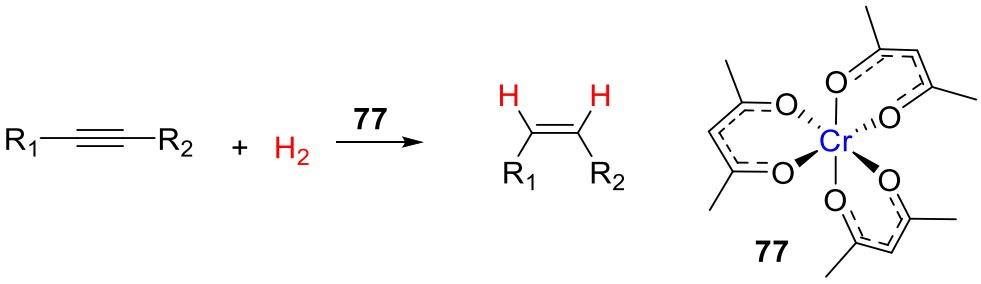

Scheme 5.13. Hydrogenation of alkyne with catalyst **77**.

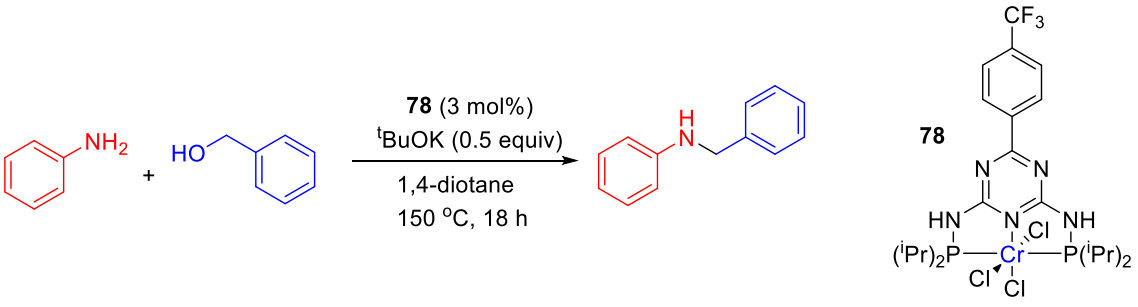

Scheme 5.14. C-N coupling reaction with a Cr catalyst.

5.1.2 Metalloporphyrin-catalyzed AAD reactions

Metalloporphyrin derivatives are naturally occurring macrocyclic compounds, which play key roles in several life processes. Metalloporphyrins have been well applied in many fields, such as conductive materials, medicine, magnetism, and solar energy conversion. Since the past decades, the development of metalloporphyrins as catalysts in organic synthesis has evolved considerably.[228,229] The simplest metalloporphyrins with no substituent at the meso positions are rarely used as catalysts, since they easily undergo oxidative degradation.[230] To solve this problem, different substituents have been introduced at the meso positions as well as at the β-positions (Scheme 5.15). The most common porphyrin derivative is the tetraphenylporphyrin (TPP), which has aryl moieties at the meso positions. Substituted aldehydes and substituted pyrroles are usually used to prepare different porphyrins in the presence of propionic acid (Scheme 5.16).[231] Considering the general overall synthetic reaction, the method to prepare metalloporphyrins can be written as:

$$M^{n+} + PH_2 \rightleftharpoons [MP]^{(n-2)+} + 2H^+$$

Where M is a metal and P is a porphyrinic material.[232]

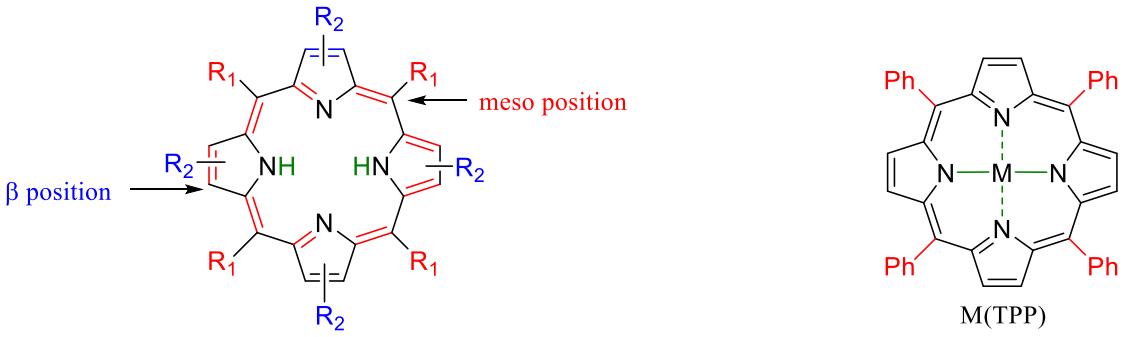

Scheme 5.15. Structure of general substituted porphyrin (left) and M(TPP) (right).

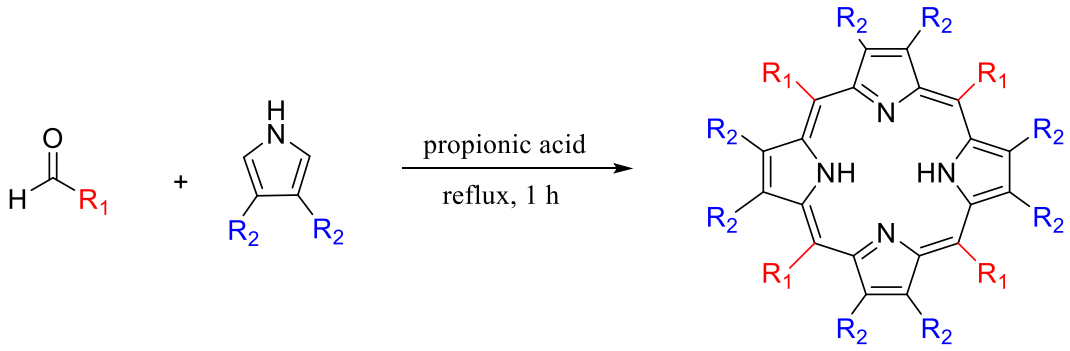

Scheme 5.16. General method to prepare substituted porphyrins.

Metalloporphyrins based on different metals have been used to catalyze several organic transformations, including epoxidations,[233] sulfoxidations,[234] hydroxylations,[235] and carbonylations,[236] although most commonly in the presence of an oxidant. However, metalloporphyrins have also been used as catalysts in AAD reactions. One of the very first examples was published by Yasukazu Saito and coworkers in 1983,[237] who demonstrated that the photocatalyst Rh(TPP)Cl could dehydrogenate both cyclohexanol and isopropanol into the corresponding carbonyl compounds as shown in Scheme 5.17.

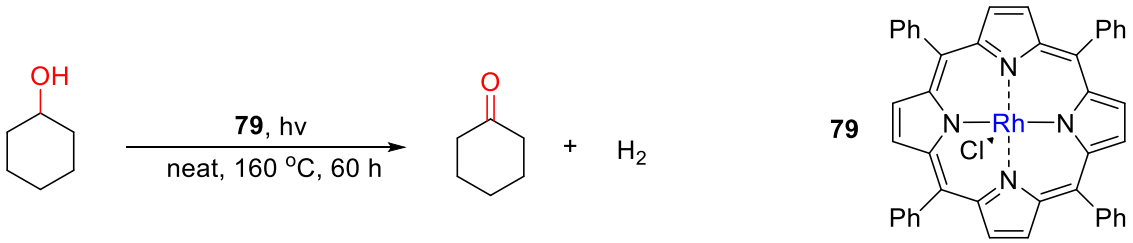

Scheme 5.17. Photocatalytic acceptorless dehydrogenation of cyclohexanol with Rh(TPP)Cl.

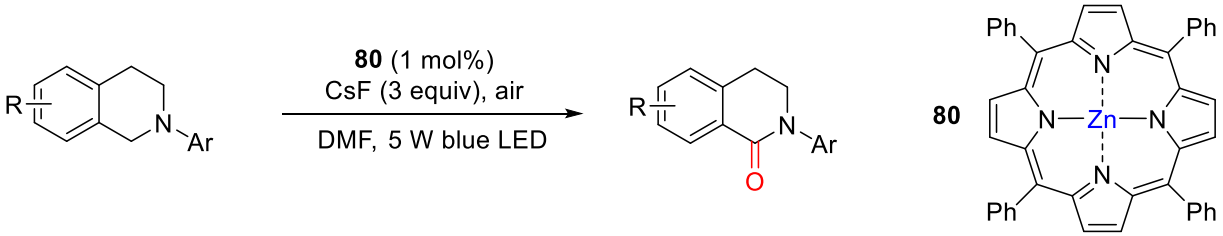

Scheme 5.18. Catalyzed reaction with Zn(TPP).

There are also several examples with metal porphyrin complexes, where they perform well in different reactions and with different roles.

In Scheme 5.18, a visible-light-induced direct-oxygenation of N-substituted 1,2,3,4-tetrahydroisoquinoline derivatives has been successfully developed. Zinc(II) tetraphenylporphyrin (Zn(TPP)) has been identified as an effective and inexpensive photocatalyst for the transformation with a wide range of substrates.[238]

In Scheme 5.19, iron(III) tetraphenylporphyrin (Fe(TPP)Cl) as an effective catalyst for promoting arene C-H amidation through intramolecular cyclization of N-tosyloxyarylcarbamate substrates is reported. The reaction proceeds via a nitrene (outer sphere pathway) C(sp^2)-H insertion to yield benzoxazolones under external-oxidant-free conditions at ambient temperature.[239]

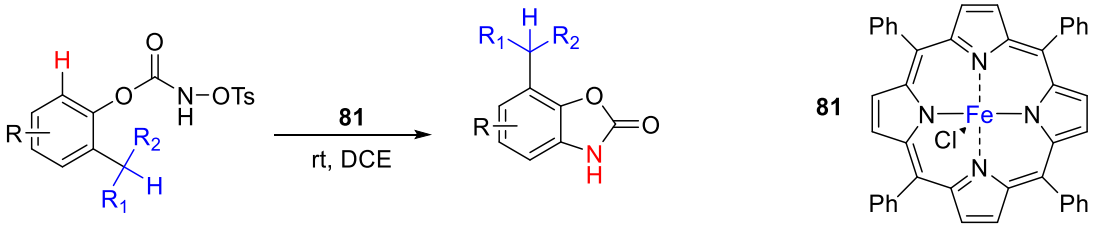

Scheme 5.19. Arene C-H amidation with the catalyst Fe(TPP)Cl.

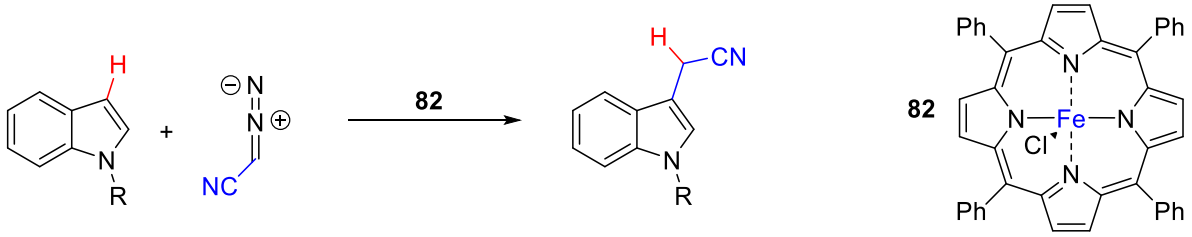

Scheme 5.20. Catalyzed reaction with the catalyst Fe(TPP)Cl.

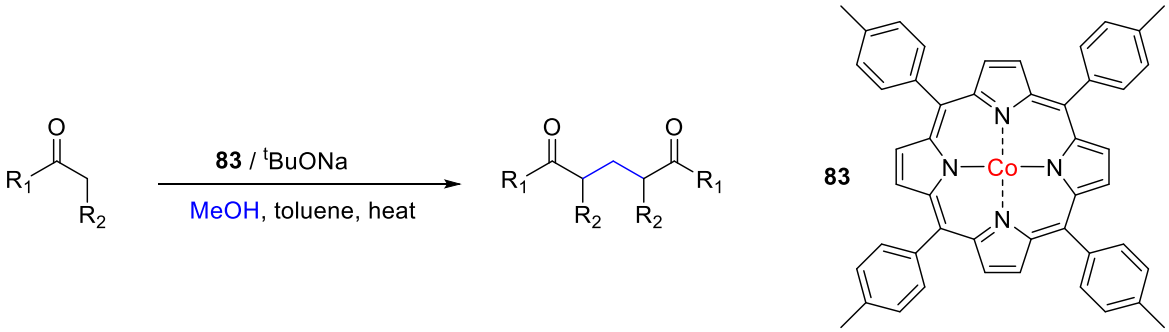

Scheme 5.21. Coupling reaction with a Co catalyst.

In Scheme 5.20, the development of iron porphyrin catalyzed reactions of diazoacetonitrile with N-heterocycles yielding important precursors of tryptamines, along with experimental mechanistic studies and proof-of-concept studies of an enzymatic process with the YfeX enzyme are described. By using readily available Fe(TPP)Cl, the highly efficient C-H functionalization of indole and indazole heterocycles is achieved. These transformations feature mild reaction conditions, excellent yields with broad functional group tolerance and can be conducted on a gram scale, and thus provide unique streamlined access to tryptamines.[240]

In Scheme 5.21, a novel cobalt(II)porphyrin-mediated acceptorless dehydrogenation of methanol is reported for the first time. A novel interrupted-borrowing hydrogen strategy for coupling of methanol and ketones using a bench stable Co(II)porphyrin complex is disclosed.[241]

In 2019, the Madsen group reported the development of manganese(III) porphyrin chloride complexes as catalysts for AD coupling reactions of alcohols and amines.[163] The reaction has been

used for the synthesis of imines, tertiary amines and quinolines using complex **84** and **85** as catalysts (Scheme 5.22 a and b). The mechanism for these transformations is assumed to include the initial formation of a manganese(III) alkoxide species, which is believed to undergo degradation into the aldehyde and a manganese(III) hydride complex. Subsequently, the alkoxide complex is regenerated by reaction with another alcohol molecule, completing the catalytic cycle. The main disadvantage of these transformations is that the reactions are running in mesitylene. Hence, a high temperature is needed for the reactions to proceed. In addition, in Scheme 5.22c, Vanadium(IV) tetraphenylporphyrin dichloride **86** has also been developed as a catalyst for the acceptorless dehydrogenation of alcohols.[242]

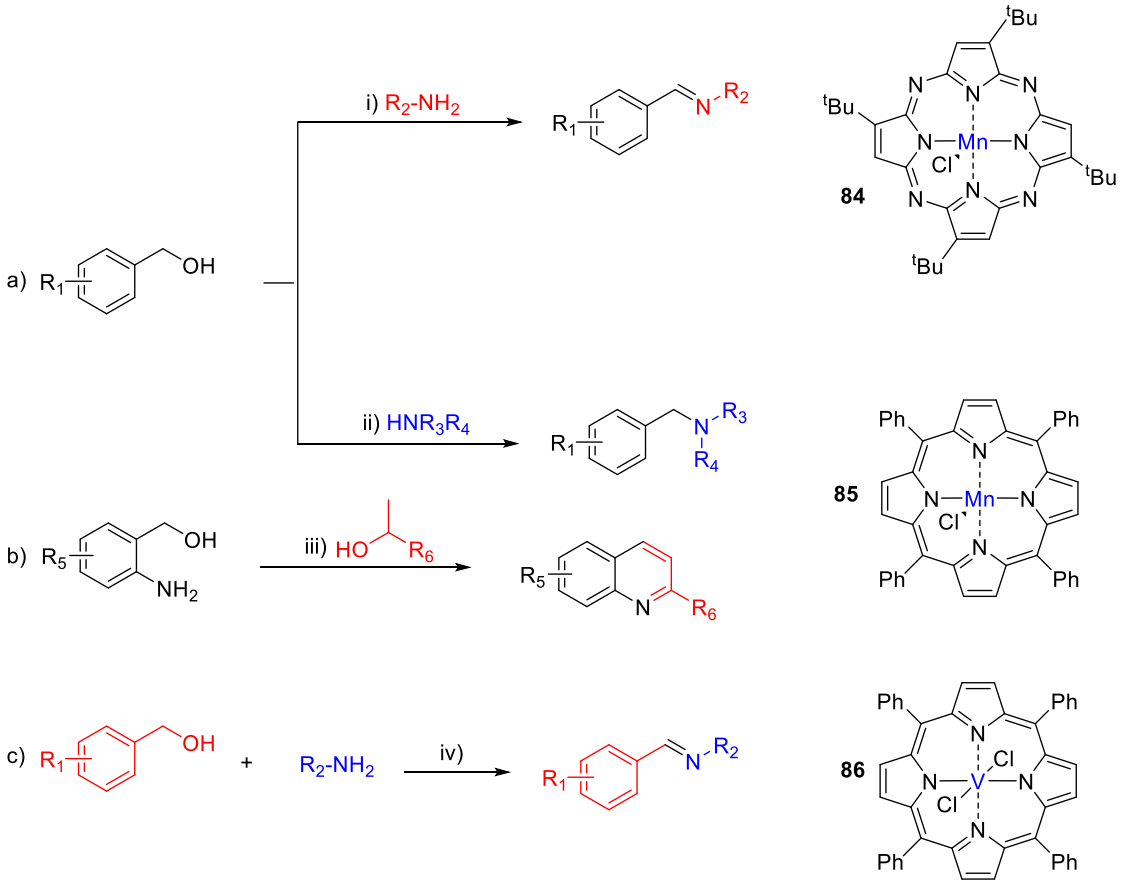

Scheme 5.22. Reagents and conditions: (i) 2 mol% **85**, 4Å MS, mesitylene (4 ml), 164 ºC, 48 h. (ii) 3 mol% **86**, 20% K_2CO_3, 4Å MS, mesitylene (4 ml), 164 ºC, 48 h. (iii) 5 mol% **86**, 20% pyridine, KOH, ^{t}BuOK, 4Å MS, mesitylene (4 ml), 164 ºC, 60 h. (iv) 5 mol% **87**, NaOH (0.20 mmol), 4Å MS (150 mg), toluene (2 ml), reflux, 48 h.

Inspired by the manganese(III) tetraazaporphyrin and vanadium(IV) porphyrin catalyzed dehydrogenative transformation of alcohols, speculations arise whether the manganese metal could be replaced with another Earth-abundant metal while keeping the catalytic activity of the complex?

5.2 Results and discussion

5.2.1 Catalyst design and optimization of the reaction conditions

Chromium(III) tetraphenylporphyrin chloride (Cr(TPP)Cl) is a well-established metal complex and has been applied in different reactions as a catalyst. In Scheme 5.23, the Claisen rearrangement of simple aliphatic allyl vinyl ethers catalyzed by Cr(TPP)Cl is described. The porphyrin-based Lewis acid catalyst can effectively accelerate the rearrangement via a concerted [3,3] pathway with a minimal degree of bond ionization of the substrates, providing the corresponding Claisen products in moderate to high yields and almost perfect regio-selectivity at a low catalyst loading.[243]

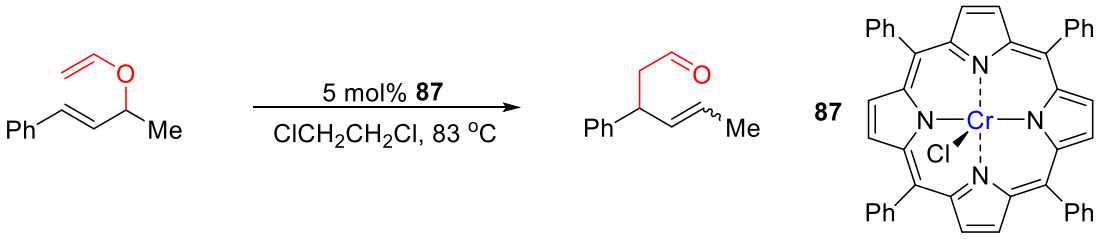

Scheme 5.23. Catalyzed Claisen rearrangement reaction with Cr(TPP)Cl.

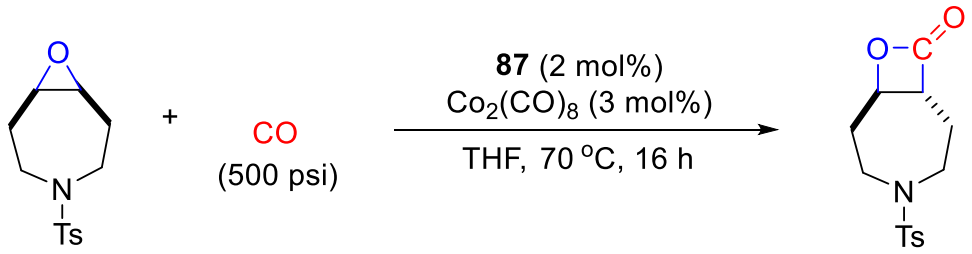

Scheme 5.24. Carbonylation with Cr(TPP)Cl.

In Scheme 5.24, a highly active catalytic system for the carbonylation of meso- and terminal epoxides to β-lactones is described. The active catalyst, analogous to Coates' catalyst, is generated in situ from commercially available Cr(TPP)Cl and $Co_2(CO)_8$. This practical system circumvents the preparation of air sensitive cobaltate salts, operates at a low catalyst loading, and allows the carbonylation of functionalized, sterically demanding and heterocyclic meso-epoxides. Cr(TPP)Cl, which has been reported to form the strongly Lewis acidic $[Cr(TPP)(L)_2]^+$ ion in the presence of epoxides was found to be the catalyst giving rise to high yields of the β-lactones.[244]

Inspired by the previous report from the Madsen group,[163,242] the complex Cr(TPP)Cl could have a good performance on the dehydrogenation of alcohols. Therefore, it is interesting to investigate commercially available Cr(TPP)Cl as a catalyst for the imination. In the initial experiments, the dehydrogenation of benzyl alcohol with cyclohexylamine was selected as a model reaction (Table 5.1).

Table 5.1. Optimization of chromium(III)-catalyzed alcohol dehydrogenation.[a]

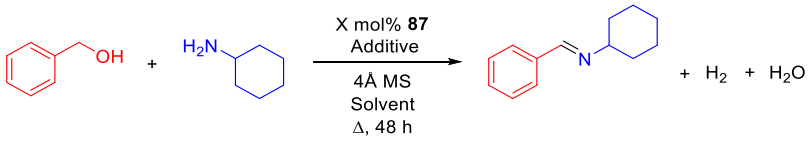

Entry	X	Additive	Solvent	Yield[%][b]
1	5	20% ^{t}BuOK	mesitylene (4 mL)	67
2	5	20% NaOH	mesitylene (4 mL)	quant.
3	5	20% Cs_2CO_3	mesitylene (4 mL)	74
4	5	20% K_2CO_3	mesitylene (4 mL)	47
5	5	20% KOH	mesitylene (4 mL)	75
6	5	20% Ca_3N_2	mesitylene (4 mL)	26
7	5	20% NaOH	toluene (4 mL)	28
8	5	20% NaOH	*o*-xylene (4 mL)	70
9	4	20% NaOH	mesitylene (4 mL)	89
10	3	20% NaOH	mesitylene (4 mL)	85
11	3	20% NaOH	mesitylene (2 mL)	82
12	0	20% NaOH	mesitylene (4 mL)	30
13	5	-	mesitylene (4 mL)	quant.
14	3	-	mesitylene (4 mL)	74
15	4	-	mesitylene (4 mL)	quant.
16	0	-	mesitylene (4 mL)	5
17	4	-	*o*-xylene (4 mL)	38
18	4	-	toluene (4 mL)	10
19	4	-	mesitylene (4 mL)	26[c]

[a] Reaction conditions: BnOH (1 mmol), $CyNH_2$ (1 mmol), catalyst Cr(TPP)Cl **87** (X mol%), additive, tetradecane (0.5 mmol, internal standard), 4Å MS (150 mg), solvent, reflux, 48 h. [b] Determined by GC. [c] without MS.

Different additives were investigated as shown in Table 5.1. Based on previous experience in the group, a base is usually chosen as an additive, which may be due to the elimination of HCl to form the active catalyst or to absorb the liberated H_2O.[167] Six different bases were applied in the reaction, respectively, and all gave different yields (entry 1-6). There was a high yield with NaOH, while a poor outcome was observed with Ca_3N_2. The calcium nitride salt is a rather unusual additive, but has given good results in iminations catalyzed manganese(III) salt complexes.[167] Two other low-boiling solvents were used (entry 7-8), but in both cases, a lower yield was obtained showing the importance of the reaction temperature. The yield was also lowered when the loading of the catalyst or the solvent volume was reduced (entry 9-11). Then two blank reactions were performed (entry 12-13), and a higher yield was obtained without the additive. This indicates that the additive is not necessary for this reaction. For further optimization, more control experiments were carried out (entry 14-19). The results showed that the reaction still had a good performance with a 4% loading of the catalyst in the solvent mesitylene. Thus, the effect of NaOH as an acid scavenger (and possible additional desiccant) appears to be very small in this case, and it was therefore decided to adopt the conditions with 4% of Cr(TPP)Cl in mesitylene for general use (entry 15). No side reactions were observed in any of the transformations in Table 5.1, where unreacted starting materials were the only other compounds that could sometimes be detected. As a result, it was decided to use 4% of Cr(TPP)Cl in refluxing mesitylene as the optimum protocol for the chromium-catalyzed dehydrogenative synthesis of imines.

5.2.2 Substrate scope and limitations

With the optimized conditions in hand, the procedure was processed with a variety of primary alcohols and amines to explore the substrate scope and limitations of the transformation. Cyclohexylamine was first reacted with different alcohols and the corresponding imines were purified by flash chromatography (Table 5.2). The product from benzyl alcohol was obtained in 86% isolated yield (entry 1). The influence of various groups in the para position of benzyl alcohol was subsequently investigated, where the *p*-methyl and *p*-methoxy-substituted substrates afforded 70% and 69% yield, respectively (entries 2 and 3). *p*-Methylthiobenzyl alcohol gave 69% yield of the imine, while *p*-phenylbenzyl alcohol furnished 68% yield (entries 4 and 5). *p*-Nitrobenzyl alcohol gave a lower yield. This group is problematic for dehydrogenation, giving that it can be reduced to an amine.[245–247] Yet, the imine was obtained in 62% yield (entry 6), and traces of several byproducts could be observed due to competitive reduction of the nitro group. The yield was 69% when the para-substituted group was trifluoromethyl on benzyl alcohol (entry 7). Next, four differ-

Table 5.2. Imination of alcohols with cyclohexylamine[a]

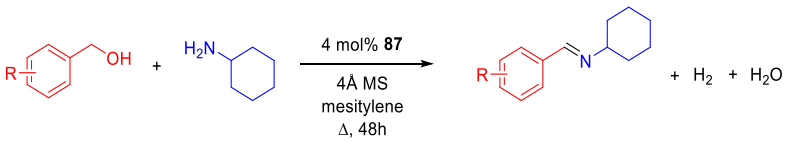

Entry	Alcohol	Imine	Yield[%][b]
1	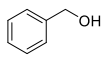	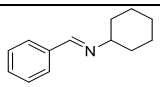	86
2	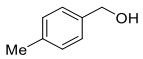	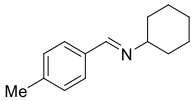	70
3	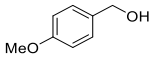	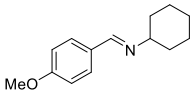	69
4	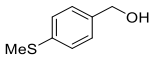	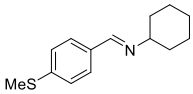	69
5	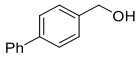	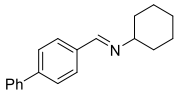	68
6	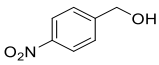	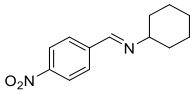	62
7	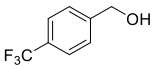	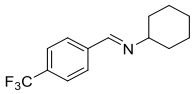	69
8	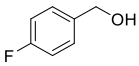	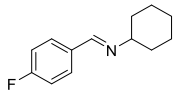	61
9	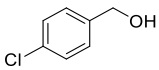	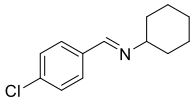	59
10	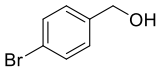	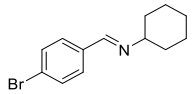	64
11	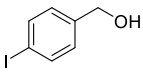	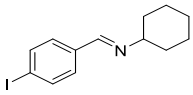	75
12	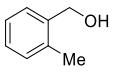	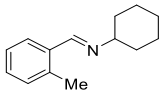	75
13	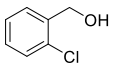	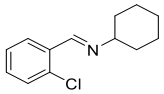	63
14	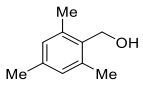	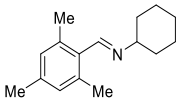	61
15	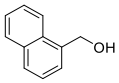	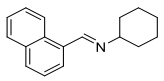	70

[a] Reaction conditions: alcohol (1 mmol), $CyNH_2$ (1 mmol), catalyst Cr(TPP)Cl **87** (0.04 mmol), 4Å MS (150 mg), mesitylene (4 ml), reflux, 48 h. [b] Isolated yield.

-ent *p*-halobenzyl alcohols gave 59-75% yield (entries 8-11) with some partial dehalogenation,[224] which could be observed in GC. In the latter case, small amounts of the starting alcohol could still be observed after the reaction. The ortho-substituted benzyl alcohols were also investigated. The *o*-methyl- and *o*-chlorobenzyl alcohol produced the corresponding imines in 75% and 63% yield, respectively (entry 12 and 13). A benzyl alcohol with three substituted groups was also explored and gave 61% yield (entry 14). In addition, a naphthalenemethanol gave the product in 70% yield (entries 15). Aliphatic primary alcohols, such as hexan-1-ol and 2-phenylethanol, were also subjected to the reaction conditions, but no conversion of the alcohol was observed.

Table 5.3. Imination of amines with benzyl alcohol.[a]

Entry	Amine	Imine	Yield[%][b]
1	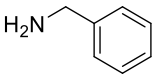	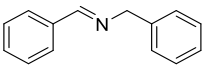	72
2	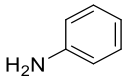	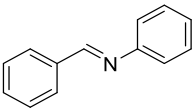	66
3	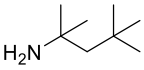	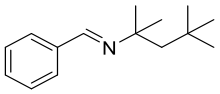	74
4	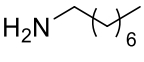	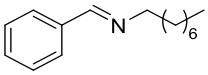	78
5	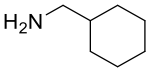	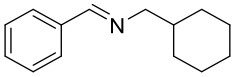	80
6	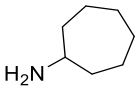	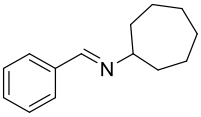	70
7	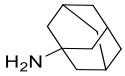	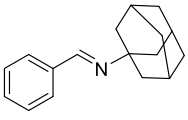	72
8	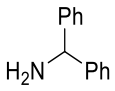	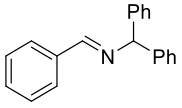	73
9	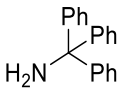	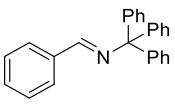	76

[a] Reaction conditions: BnOH (1 mmol), amine (1 mmol), catalyst Cr(TPP)Cl **87** (0.04 mmol), 4Å MS (150 mg), mesitylene (4 ml), reflux, 48 h. [b] Isolated yield.

Different amines were applied to the reaction with benzyl alcohol to study the influence of the substrate in the transformation (Table 5.3). Benzylamine afforded the imine in 72% yield (entry 1), while aniline only gave 66% yield due to the instability of the product (entry 2). Then different aliphatic amines were also employed. *t*-Octylmine and octylamine gave similar yields, 74% and 78%, respectively (entry 3 and 4). Cyclohexylmethanamine (entry 5) gave 80% yield of the imine, while the cycloheptylamine furnished 70% yield of the imine (entry 6). Then bulky amines were explored and gave similar yields (entry 7-9), which indicates that the steric hindrance had less of an influence, possibly because the imine formation occurs in the absence of the catalyst. Finally, it should be noted that imines are not highly stable to standard silica gel flash chromatography, but the problem could be circumvented by including NEt_3 in the column.

5.2.3 Exploration of the mechanism

Gas evolution

Based on our previous report, dihydrogen should be one of the byproducts, and the dehydrogenative pathway of the metal-catalyzed imination was verified by collecting the liberated hydrogen gas. The reaction was performed as in Table 5.1, entry 15, and the gas was collected in a burette. Finally, a total of 17 mL gas was collected, and then characterized by ^{1}H-NMR. The gas was dihydrogen as shown by the characteristic signal at 4.99 ppm, which confirms that the transformation takes place by an acceptorless dehydrogenative pathway. LCMS analysis of the mixture after the imination showed the Cr^{III}(TPP) cation in the experiment. No sign of any reduction of the porphyrin ligand was observed with complex Cr(TPP)Cl.

Deuterium labeling study

To further investigate the mechanism of the reaction, a deuterium labeling study was introduced (Scheme 5.25). When the reaction in Table 5.1, entry 15 was performed with $PhCD_2OH$ instead of $PhCH_2OH$, the product was exclusively PhCD=NCy with no evidence for any hydrogen incorporation into the benzylic position. The lack of isotope scrambling may indicate that the dehydrogenation takes place by a monohydride pathway.

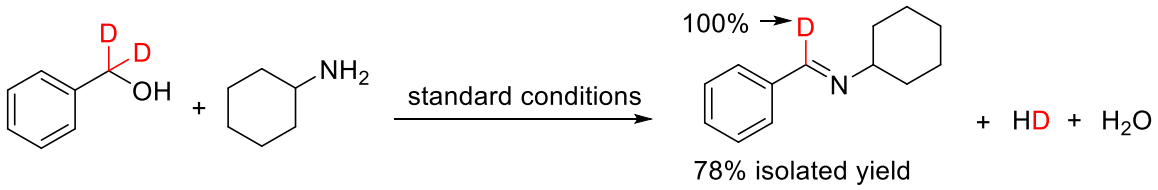

Scheme 5.25. Imination with benzyl alcohol-α,α-d_2.

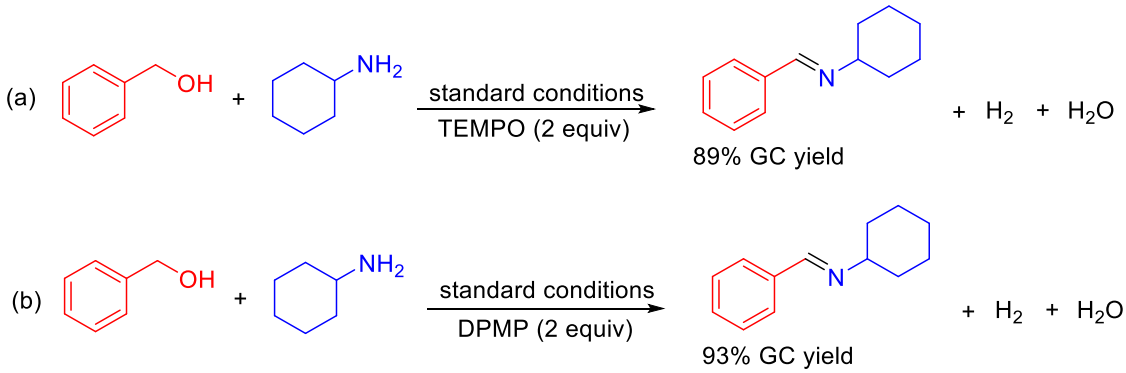

Scheme 5.26. Investigation of a possible radical reaction.

Investigation of a radical reaction

To elucidate whether the reaction proceeds by a radical mechanism, (2,2,6,6-tetramethylpiperidin-1-yl)oxyl (TEMPO) and 2,4-diphenyl-4-methyl-1-pentene (DPMP) were added to the reaction, respectively (Scheme 5.26), but there was no product formed based on TEMPO or DPMP. The results indicate that the acceptorless dehydrogenation did not take place through a radical reaction.

Kinetic isotope effect (KIE)

To obtain more details about the mechanism, the primary KIE was measured to investigate whether the hydride abstraction takes place in the rate-limiting step. The KIE was determined by measuring the initial rates with $PhCH_2OH$ and $PhCD_2OH$ in the reaction with cyclohexylamine. The measurements gave a KIE of 2.3 for the chromium-catalyzed protocol, which shows that the breakage of the benzylic C-H bond is a slow step in the transformation.

Hammett study

To gain more information about the reaction pathway, the studies were also supplemented by a Hammett study. Thus, at first six para-substituted benzyl alcohols (X = OCH_3, CH_3, F, Cl, CF_3 and NO_2) were allowed to compete with the parent benzyl alcohol in the imination of cyclohexylamine (Scheme 5.27). Benzyl alcohol (54.0 mg, 0.5 mmol), para-substituted benzyl alcohol (0.5 mmol) and cyclohexylamine (99.0 mg, 1.0 mmol) were placed in an oven-dried tube and subjected to the imination reaction following the general procedure for imine synthesis. For 5 h, a sample of 0.05 ml was prepared every 30 minutes, transferred to a GC vial, diluted to 1 mL with diethyl ether and then subjected to GCMS analysis to follow the formation of *N*-benzylidenecyclohexylamine and the 4-substituted *N*-benzylidenecyclohexylamine to determine k_{rel}. However, a new compound was detected in the GCMS chromatograms, and the compound was *N*-(3,5-dimethylbenzylidene)cyclohexylamine. The result indicated that there was some 3,5-dimethylbenzaldehyde in the reaction system, and it seemed that oxygen had been introduced into the reaction mixture, possible when taking out samples for GCMS analysis. Mesitylene can indeed be converted to 3,5-dimethylbenzaldehyde in the presence of oxygen,[248,249] and especially when the rather hard conditions employed in this case. Therefore, the desired Hammett plot for the imination of para-substituted benzyl alcohols was not obtained.

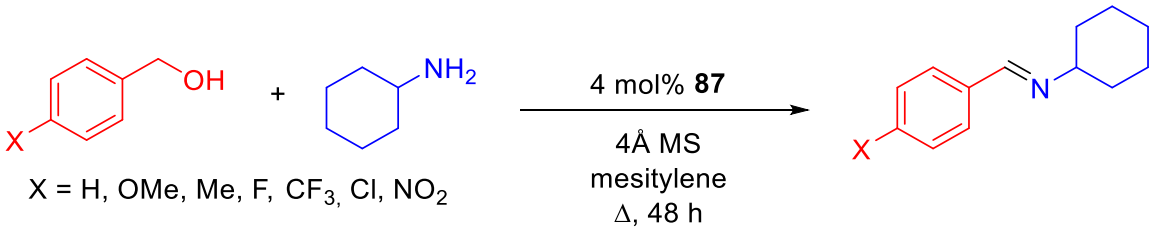

Scheme 5.27. Imination of cyclohexylamine with *p*-substituted benzyl alcohols as part of the Hammett study.

Identification of catalyst intermediate

In the former examples of dehydrogenative reactions with a manganese(III) porphyrin complex, the mechanism was thought to involve an alkoxide complex that is formed and degrades into the aldehyde and a metal hydride species.[163] Metal porphyrin alkoxide complexes do not contain an available coordination site for a classical β-hydride elimination, but a dissociative β-hydride abstraction pathway has been proposed in alkoxide complexes, where an open *cis* coordination site is not available.[250–253] The metal porphyrin alkoxide Mn(TPP)OBn species was detected by GCMS. In principle, the present chromium-catalyzed protocol could take place by this mechanism.

In an attempt to detect possible catalytic intermediates, an experiment was performed where 50 mmol of $PhCH_2OH$ and 10 mmol of NaH were mixed with 1 mmol of complex Cr(TPP)Cl in the absence of a solvent. The mixture was analyzed by LCMS after stirring for 30 min at room temperature, but potential benzyloxy metal porphyrin species could not be detected. A distillation head was then attached and the mixture was heated to 185 °C, which caused 2 mmol of benzyl alcohol/benzaldehyde with a ratio of 7:1 to distill off after 24 h. The experiment showed that the dehydrogenation was possible in the absence of the amine. The result may indicate that breakage of a metal-oxygen bond is not part of the catalytic cycle

Based on the former experiments and the fact that chromium is a more oxophilic metal than manganese,[254] there could be a different pathway operating with complex Cr(TPP)Cl. As introduced in Chapter 4, for many dehydrogenative reactions of alcohols with manganese, iron and cobalt complexes with multidentate ligands, the mechanisms have been shown to perform the dehydrogenation by an outer-sphere pathway with active participation from the ligand,[149, 160, 235] where the proton from the alcohol OH group and the hydride from the α-carbon are transferred to the ligand nitrogen atom and the metal center, respectively. Nothing indicates that a highly basic nitrogen atom is required in the ligand, and therefore in this dehydrogenative reaction with Cr(TPP)Cl, the pyrrole moieties of the porphyrin ligand could participate in this bifunctional pathway. Under acidic conditions, it is generally believed that demetallation of metal porphyrin complexes proceeds through diprotonation of two pyrrole groups to afford so-called sitting-atop complexes as intermediates, where the metal is located above the plane of the diprotonated porphyrin.[255,256] Even though monoprotonated metal porphyrins are not entirely well described, they can likewise be envisioned as intermediates.[257]

According to the experimental facts and physical observations, it is believed that the most plausible mechanism for the chromium-catalyzed dehydrogenation involves an available coordination site in complex Cr(TPP)Cl (Scheme 5.28).[258] The alcohol coordinates with complex **88**, and then hydride complex **90** is obtained through outer-sphere hydrogen abstraction from transition state **89** to regenerate complex **88** with the liberation of hydrogen gas. It should be noted that the aromatic 18 π-electron conjugated network of the porphyrin ring is not disrupted during the catalytic cycle. The pathway may indicate that first-row transition metals with porphyrin ligands perform the alcohol dehydrogenation by a similar mechanism as observed reactions with a PNP ligand.

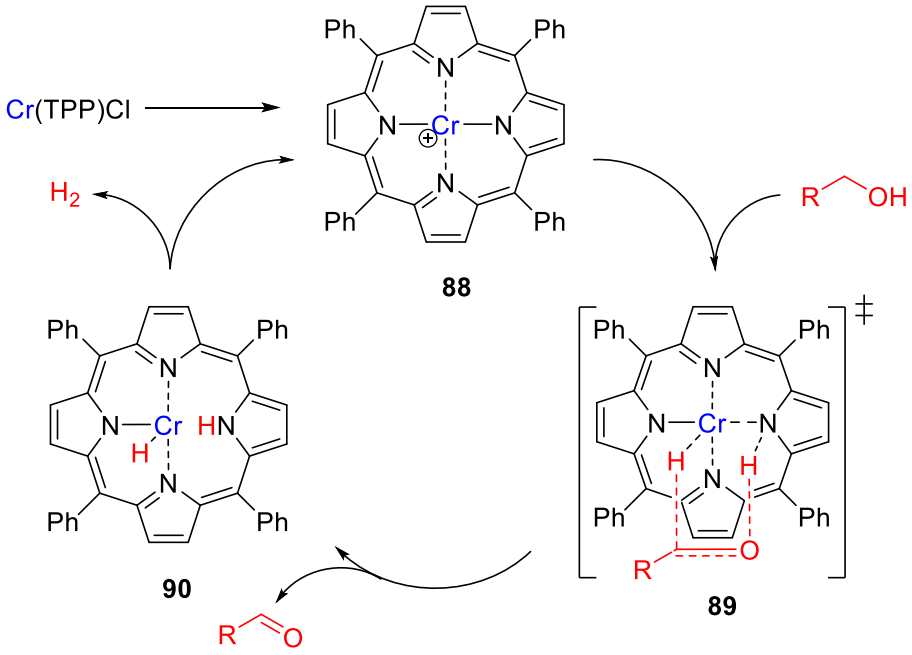

Scheme 5.28. Proposed mechanism for chromium porphyrin-catalyzed alcohol dehydrogenation.

5.3 Project conclusions

In conclusion, the first example of an acceptorless alcohol dehydrogenation with a chromium complex has been described. Cr(TPP)Cl mediates the coupling of alcohols and amines into imines and the transformation has been applied to a variety of substrates. The results show that chromium complexes may be useful alternatives to other catalysts based on Earth-abundant metals when developing alcohol dehydrogenation reactions. The mechanism with Cr(TPP)Cl is proposed to involve a metal-ligand bifunctional pathway where two hydrogen atoms from the alcohol are transferred to the metal porphyrin complex followed by the elimination of hydrogen gas. Further investigations into the mechanism for these transition metal porphyrin-catalyzed dehydrogenations of alcohols by DFT calculations are ongoing in the group.

5.4 Experimental section

5.4.1 General experimental methods

All commercial reagents were purchased from Sigma-Aldrich, Strem or Fluorochem and used as received. NMR spectra were recorded at 400 MHz for ^{1}H-NMR and 101 MHz for ^{13}C-NMR on a Bruker Ascend 400 MHz spectrometer. Chemical shift values (δ) are reported in ppm relative to the residual solvent signal in $CDCl_3$ (δ_H 7.26 ppm, δ_C 77.2 ppm) while coupling constants (*J*) are given in Hz. High resolution mass spectra were recorded using ESI with TOF detection. GCMS was carried out on a Shimadzu GCMS-QP2010S instrument fitted with an Equity 5, 30m×0.25mm×0.25µm column. Ionisation was performed by electronic impact (EI, 70 eV) and helium as the carrier gas. LCMS was performed on a Waters ACQUITY UPLC system equipped with PDA and SQD2 electrospray MS detector. Column: Thermo accucore C18 (2.6 µm, 2.1×50mm). Column temperature: 50 ºC. Flowrate 0.6 mL/min. Solvent A: 5 mM NH_4OAc in water, solvent B: 5 mM NH_4OAc in acetonitrile/water 95/5. Flash column chromatography was performed using silica gel 60 (0.035-0.070 mm particle size) saturated with NEt_3. Mesitylene was dried over molecular sieves (4Å) while toluene was obtained by using a Pure Solv™ Micro solvent purification system. The water content of the solvents and liquid reagents was measured on a Karl-Fischer apparatus. All experiments were carried out under a nitrogen flow using Schlenk flask techniques except for the synthesis of the catalyst.

5.4.2 General procedure for imine synthesis

Chromium complex **87** (28.0 mg, 0.04 mmol) and pre-activated 4Å molecular sieves (150 mg) were placed in an oven-dried tube, and then it was placed in a Radleys carousel. Vacuum was applied and the flask was then filled with nitrogen gas (repeated 3 times). Degassed fresh mesitylene (4 ml) was added and the reaction mixture was heated to reflux. Alcohol (1 mmol), amine (1 mmol) and tetradecane (0.5 mmol as internal standard) were added by a syringe, and the reaction was refluxed with stirring under a flow of nitrogen for 48 h. The mixture was cooled to room temperature and the solvent removed under reduced pressure. The crude product was purified by silica gel column chromatography (hexane with 2% NEt_3) to afford the desired imine.

5.4.3 Gas development

The catalyst Cr(TPP)Cl (28.0 mg, 0.04 mmol) and 4Å molecular sieves (150 mg) were placed in an oven-dried Schlenk tube. The tube was subjected to vacuum, and then filled with nitrogen gas (repeated 3 times). Degassed mesitylene (4 ml) was added and the reaction mixture was heated to reflux. Benzyl alcohol (108 mg, 1 mmol) and cyclohexylamine (99 mg, 1 mmol) were added. The Schlenk tube was connected with a tube, and the other end of the tube was connected to the bottom of a burette filled with water. The bottom of the burette was further connected to a water reservoir with a large surface area. A total of 17 mL gas was collected after the reaction was refluxed for 48 h. A GC sample of the reaction mixture showed 90% yield of the imine. The identity of the gas was established from a ^{1}H-NMR spectrum in toluene-d_8 displaying a signal at 4.99 ppm shown in Figure 5.1. Thus, 0.76 mmol of molecular hydrogen gas was collected according to the ideal gas law (76% of H_2 yield at a temperature of 25 °C).

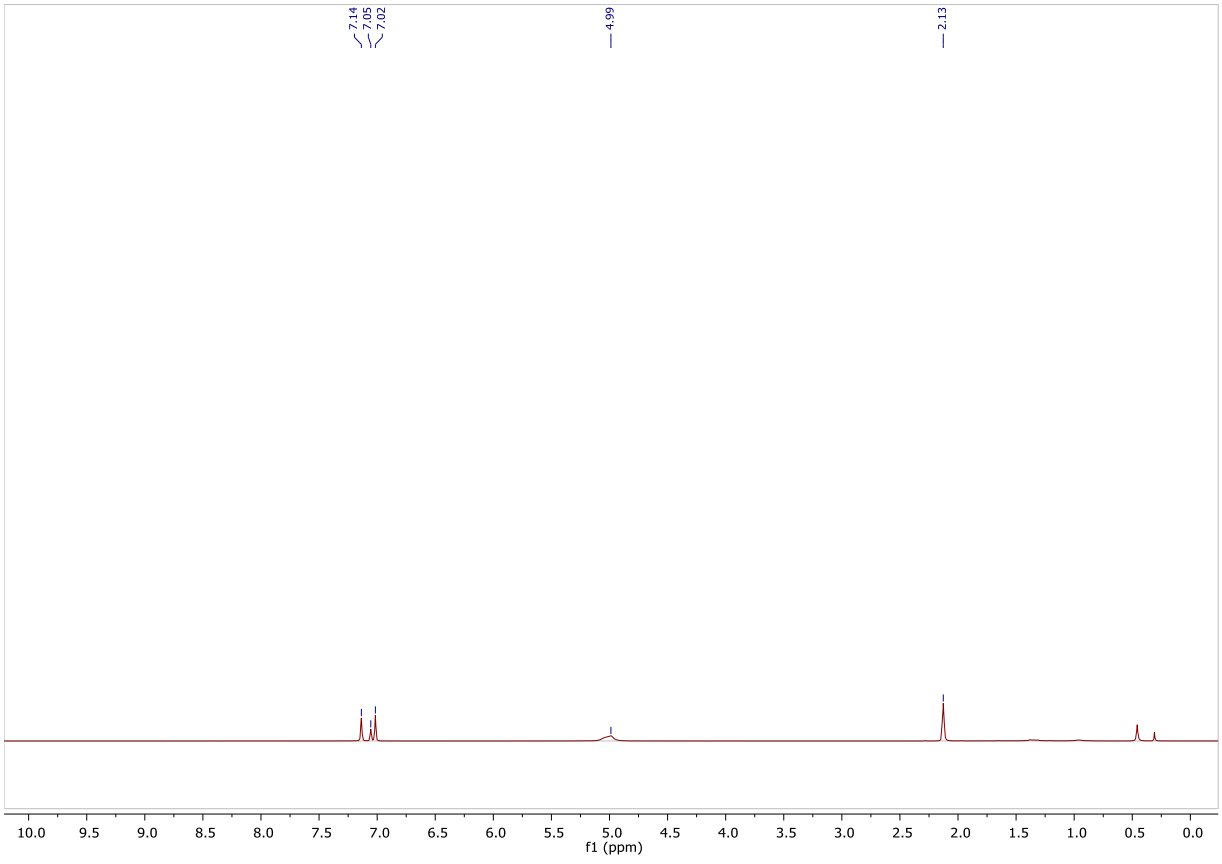

Figure 5.1. ^{1}H-NMR spectrum of collected gas (hydrogen).

5.4.4 Deuterium labelling study

Benzyl alcohol-α,α-d_2 (110 mg, 1.0 mmol) and cyclohexylamine (99.0 mg, 1.0 mmol) were placed in an oven-dried tube and subjected to the imination reaction following the general procedure for imine synthesis. After purification of the product imine (146.6 mg, 78%), examination of the ^{1}H-NMR spectrum revealed that the product imine was obtained as a pure deuterium-labeled imine and no hydrogen/deuterium scrambling had occurred. The ^{1}H-NMR spectrum is shown below.

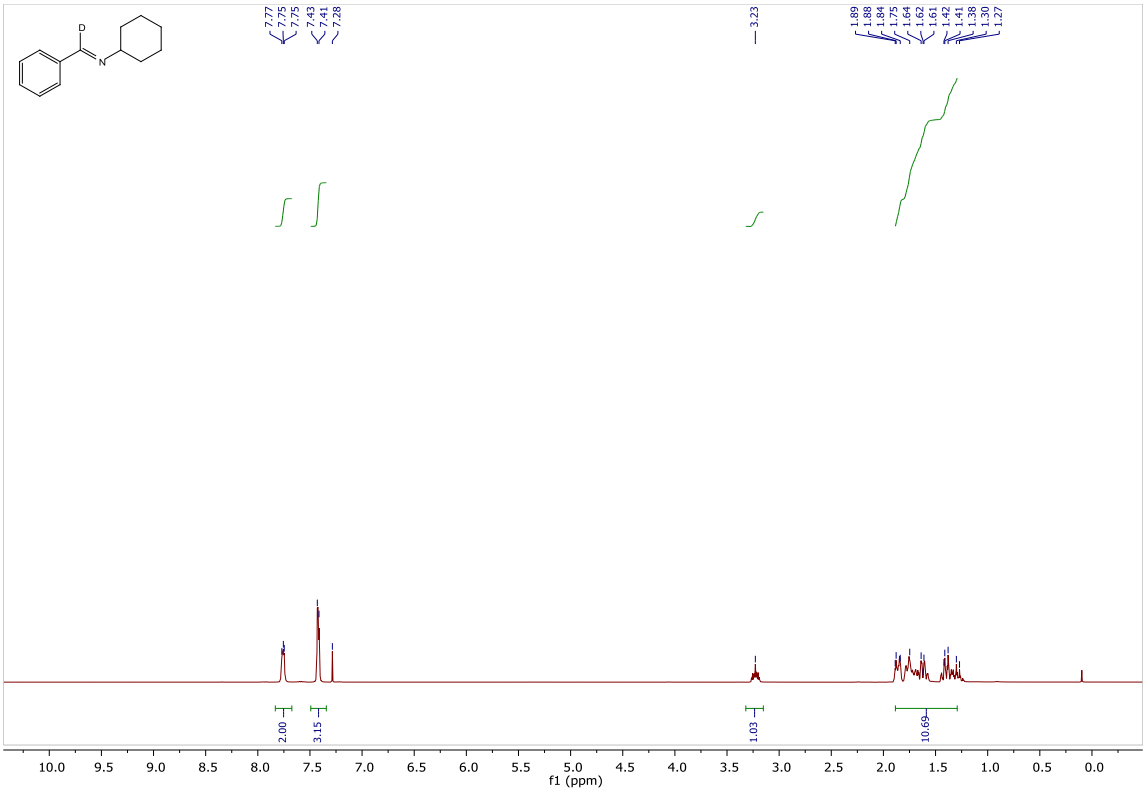

Figure 5.2. ^{1}H-NMR spectrum of *N*-benzylidenecyclohexylamine-α-d_1.

5.4.5 Kinetic isotope effect (KIE)

The reaction was performed as the general procedure for imine synthesis. An oven-dried tube was charged with the catalyst Cr(TPP)Cl (28 mg, 0.04 mmol) and 4Å molecular sieves (150 mg), and placed in a Radleys carousel on a hotplate. The tube was evacuated and then filled with N_2 gas (repeated 3 times). Freshly degassed mesitylene (4 mL) was injected into the tube followed by heating to 170 °C under a N_2 atmosphere. Benzyl alcohol (108 mg, 1.0 mmol), cyclohexylamine (99 mg, 1.0 mmol) and tetradecane (0.13 ml, 0.5 mmol) were added, and then the reaction was

monitored by GC for 5 h. A sample of 50 μL was removed every 30 minutes, transferred to a GC vial, diluted to 1 mL with diethyl ether and then subjected to GCMS analysis to follow the formation of *N*-benzylidenecyclohexylamine and determine the initial rate (r). The same procedure was performed by using benzyl alcohol-α,α-d_2 (110 mg, 1.0 mmol) instead of non-deuterated benzyl alcohol. Assuming that no by-product was formed, the initial rate for the transformation of benzyl alcohol was $r_H = 7.00\ 10^{-5}$, and the initial rate for the reaction of benzyl alcohol-α,α-d_2 was $r_D = 3.00\ 10^{-5}$, and thus the value of KIE (k_H/k_D) was 2.3.

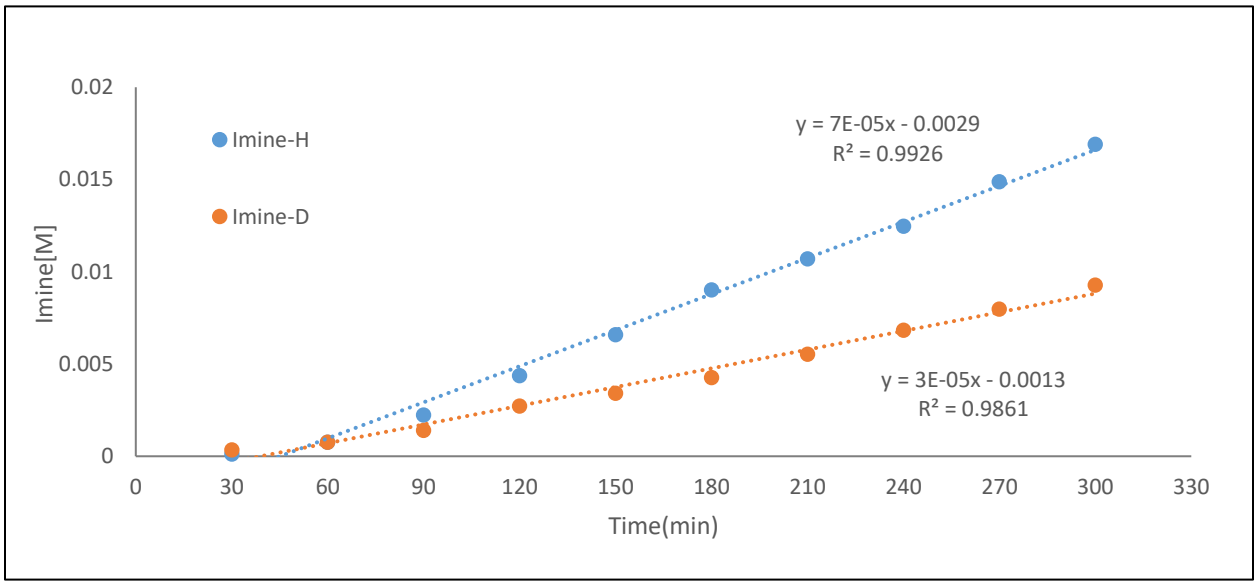

Figure 5.2. Determination of KIE by plotting the initial rates of the reaction involving benzyl alcohol and benzyl alcohol-α,α-d_2.

5.4.6 Identification of catalyst intermediate with LCMS

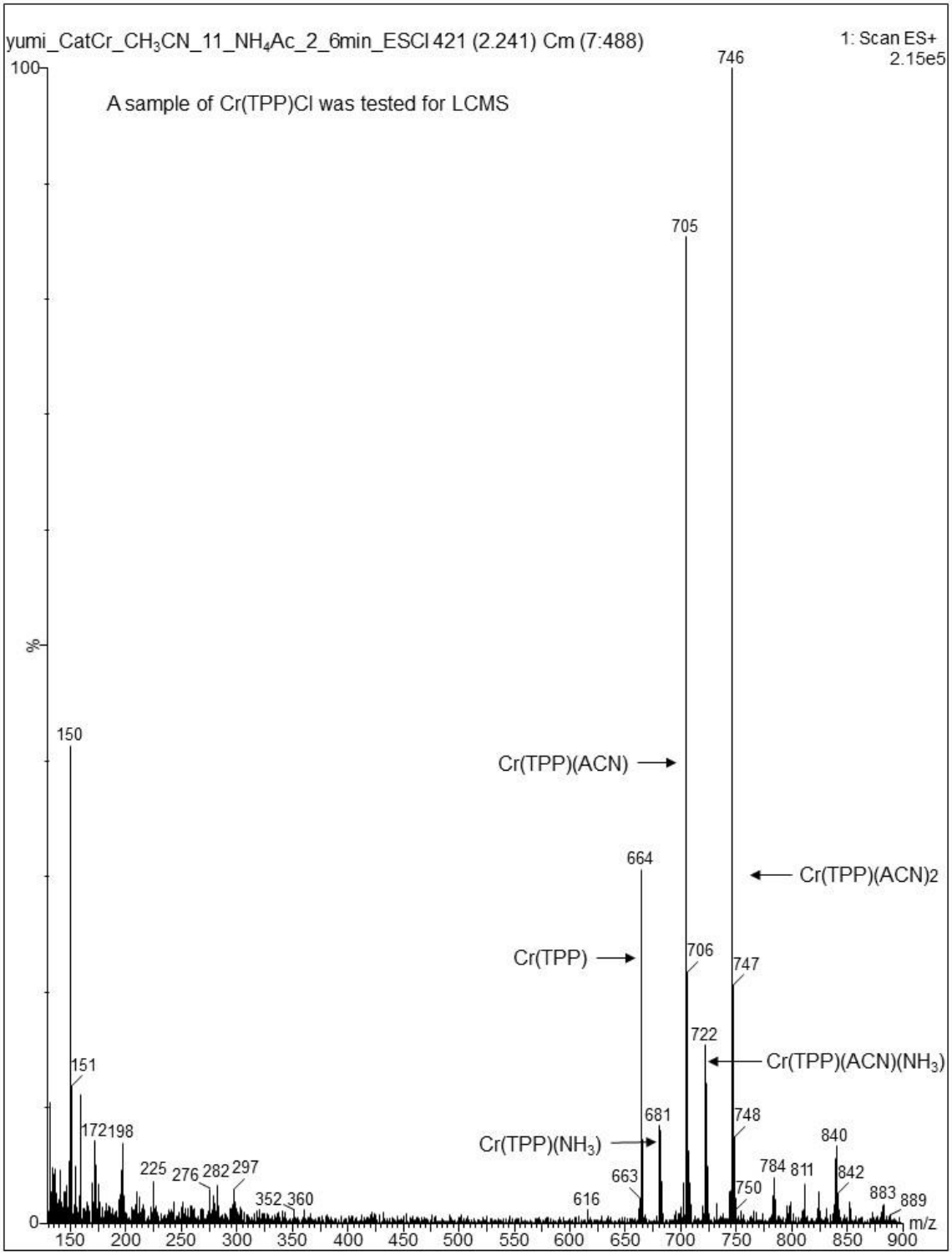

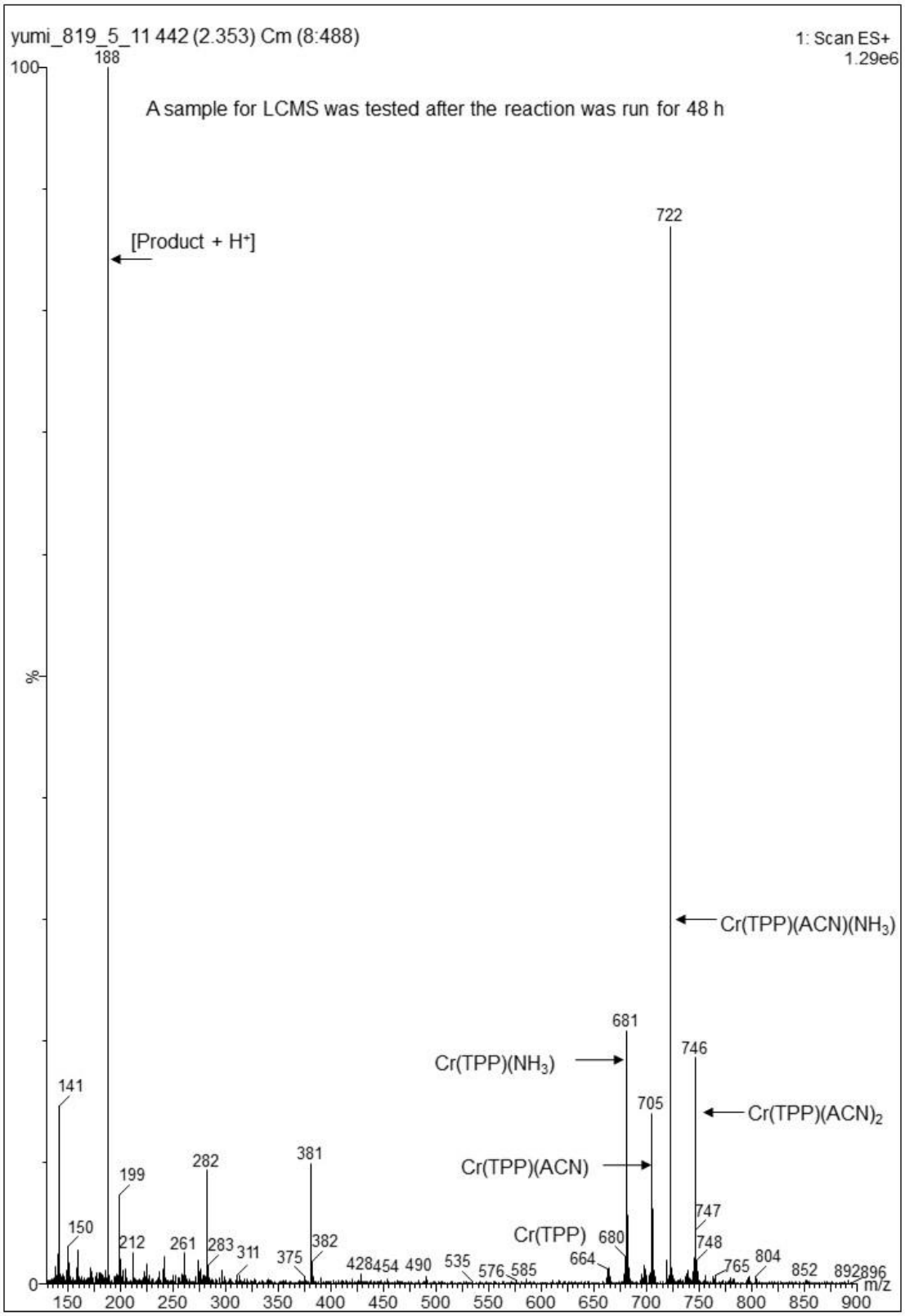
yumi_819_5_11 442 (2.353) Cm (8:488)
1: Scan ES+
1.29e6
A sample for LCMS was tested after the reaction was run for 48 h
[Product + H+]
Cr(TPP)(ACN)(NH3)
Cr(TPP)(NH3)
Cr(TPP)(ACN)2
Cr(TPP)(ACN)
Cr(TPP)
188
722
681
746
705
141
199
282
381
150
212
261
283
311
375
382
680
664
747
748
765
804
852
892896
%
m/z

5.4.7 Characterization data for imines

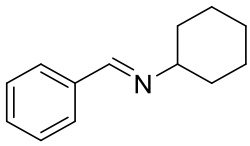

***N*-Benzylidenecyclohexylamine (Table 5.2, entry 1)**

Following the general procedure for imine synthesis, the product was isolated as a yellow liquid. Yield: 161.1 mg (86%). ^{1}H-NMR (400 MHz, $CDCl_3$) δ ppm: 8.34 (s, 1H), 7.80-7.70 (m, 2H), 7.45-7.38 (m, 3H), 3.26-3.15 (m, 1H), 1.88-1.29 (m, 10H). ^{13}C-NMR (101 MHz, $CDCl_3$) δ ppm: 158.6, 136.6, 130.3, 128.5, 128.1, 70.2, 34.4, 25.7, 24.8. MS: m/z = 187 $[M]^+$. NMR data are in accordance with literature values.[167]

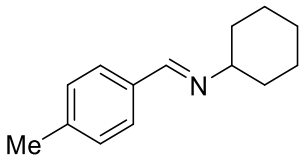

***N*-(4-Methylbenzylidene)-cyclohexylamine (Table 5.2, entry 2)**

Following the general procedure for imine synthesis, the product was isolated as a yellow liquid. Yield: 140.5 mg (70%). ^{1}H-NMR (400 MHz, $CDCl_3$) δ ppm: 8.30 (s, 1H), 7.64 (d, *J* = 7.9 Hz, 2H), 7.28 (d, *J* = 7.9 Hz, 2H), 3.26-3.15 (m, 1H), 2,40 (s, 3H), 1.90-1.26 (m, 10H). ^{13}C-NMR (101 MHz, $CDCl_3$) δ ppm:158.6, 140.6, 133.9, 129.2, 128.1, 70.0, 34.4, 25.7, 24.9, 21.5. MS: m/z = 201 $[M]^+$. NMR data are in accordance with literature values.[167]

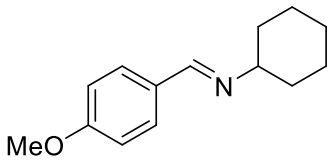

***N*-(4-Methoxybenzylidene)-cyclohexylamine (Table 5.2, entry 3)**

Following the general procedure for imine synthesis, the product was isolated as a yellow liquid. Yield: 149.3 mg (69%). ^{1}H-NMR (400 MHz, $CDCl_3$) δ ppm: 8.26 (s, 1H), 7.70 (d, *J* = 8.6 Hz, 2H), 6.93 (d, *J* = 8.7 Hz, 2H), 3.86 (s, 3H), 3.25-3.13 (m, 1H), 1.90-1.26 (m, 10H). ^{13}C-NMR (101 MHz, $CDCl_3$) δ ppm: 161.4, 158.0, 129.7, 113.9, 69.9, 55.4, 34.4, 25.7, 24.9. MS: m/z = 217 $[M]^+$. NMR data are in accordance with literature values.[167]

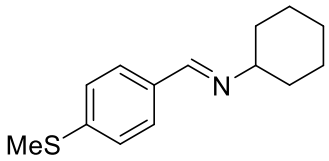

***N*-(4-Methylthiobenzylidene)-cyclohexylamine (Table 5.2, entry 4)**

Following the general procedure for imine synthesis, the product was isolated as a pale yellow liquid. Yield: 160.3 mg (69%). ^{1}H-NMR (400 MHz, $CDCl_3$) δ ppm: 8.27 (s, 1H), 7.69 (d, *J* = 7.7 Hz, 2H), 7.27 (d, *J* = 8.4 Hz, 2H), 3.25-3.17 (m, 1H), 2.53 (s, 3H), 1.90-1.26 (m, 10H). ^{13}C-NMR (101 MHz, $CDCl_3$) δ ppm: 158.0, 130.3, 128.4, 125.9, 124.0, 70.0, 34.4, 25.6, 24.9, 15.4. MS: m/z = 233 $[M]^+$. NMR data are in accordance with literature values.[167]

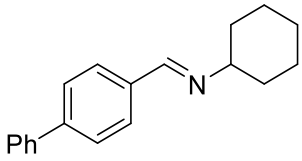

***N*-(4-Phenylbenzylidene)-cyclohexylamine (Table 5.2, entry 5)**

Following the general procedure for imine synthesis, the product was isolated as a pale yellow liquid. Yield: 180.2 mg (68%). ^{1}H-NMR (400 MHz, $CDCl_3$) δ ppm: 8.37 (s, 1H), 7.87-7.83 (m, 2H), 7.70-7.64 (m, 4H), 7.50-7.37 (m, 3H), 3.30-3.26 (m, 1H), 1.90-1.28 (m, 10H). ^{13}C-NMR (101 MHz, $CDCl_3$) δ ppm: 158.3, 143.1, 140.5, 135.5, 130.3, 128.6, 127.7, 127.1, 70.1, 34.4, 25.6, 24.9. MS: m/z = 263 $[M]^+$. NMR data are in accordance with literature values.[167]

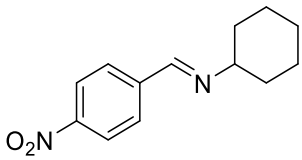

***N*-(4-Nitrobenzylidene)-cyclohexylamine (Table 5.2, entry 6)**

Following the general procedure for imine synthesis, the product was isolated as a pale yellow liquid. Yield: 144.1 mg (62%). ^{1}H-NMR (400 MHz, $CDCl_3$) δ ppm: 8.41 (s, 1H), 8.29 (d, *J* = 8.7 Hz, 2H), 7.98 (d, *J* = 8.7 Hz, 2H), 3.39-3.30 (m, 1H), 1.90-1.20 (m, 10H). ^{13}C-NMR (101 MHz, $CDCl_3$) δ ppm: 156.2, 148.8, 142.2, 128.7, 123.8, 70.2, 34.2, 25.6, 24.6. MS: m/z = 232 $[M]^+$. NMR data are in accordance with literature values.[167]

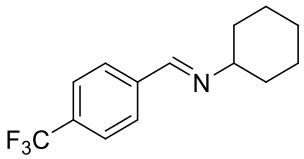

***N*-(4-Trifluoromethylbenzylidene)-cyclohexylamine (Table 5.2, entry 7)**

Following the general procedure for imine synthesis, the product was isolated as a white solid. Yield: 175.6 mg (69%). ^{1}H-NMR (400 MHz, $CDCl_3$) δ ppm: 8.38 (s, 1H), 7.86 (d, *J* = 8.2 Hz, 2H), 7.67 (d, *J* = 8.2 Hz, 2H), 3.30-3.24 (m, 1H), 1.90-1.29 (m, 10H). ^{13}C-NMR (101 MHz, $CDCl_3$) δ ppm: 157.1, 139.8, 132.1 (q, *J* = 32 Hz), 128.2, 125.6 (q, *J* = 4 Hz), 124.2 (q, *J* = 270 Hz), 70.1, 34.3, 25.6, 24.7. MS: m/z = 255 $[M]^+$. NMR data are in accordance with literature value.[167]

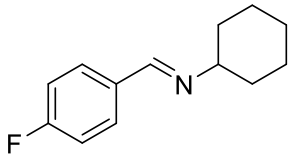

***N*-(4-Fluorobenzylidene)-cyclohexylamine (Table 5.2, entry 8)**

Following the general procedure for imine synthesis, the product was isolated as a yellow liquid. Yield: 125.1 mg (61%). ^{1}H-NMR (400 MHz, $CDCl_3$) δ ppm: 8.30 (s, 1H), 7.74 (dd, *J* = 8.6, 5.6 Hz, 2H), 7.10 (t, *J* = 8.6 Hz, 2H), 3.25-3.16 (m, 1H), 1.90-1.24 (m, 10H). ^{13}C-NMR (101 MHz, $CDCl_3$) δ ppm: 165.3 (d, *J* = 251 Hz), 157.2, 132.9, 129.9 (d, *J* = 8 Hz), 115.6 (d, *J* = 22 Hz), 69.9, 34.3, 25.6, 24.8. MS: m/z = 205 $[M]^+$. NMR data are in accordance with literature values.[167]

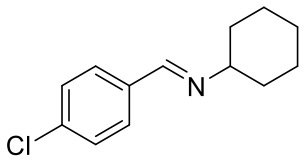

***N*-(4-Chlorobenzylidene)-cyclohexylamine (Table 5.2, entry 9)**

Following the general procedure for imine synthesis, the product was isolated as a white solid. Yield: 130.8 mg (59%). ^{1}H-NMR (400 MHz, $CDCl_3$) δ ppm: 8.29 (s, 1H), 7.72 (d, *J* = 8.4 Hz, 2H), 7.41 (d, *J* = 8.4 Hz, 2H), 3.29-3.19 (m, 1H), 1.90-1.26 (m, 10H). ^{13}C-NMR (101 MHz, $CDCl_3$) δ ppm: 157.3, 136.2, 135.1, 129.3, 128.8, 69.9, 34.3, 25.6, 24.8. MS: m/z = 221 $[M]^+$. NMR data are in accordance with literature values.[167]

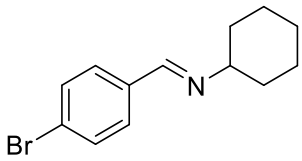

***N*-(4-Bromobenzylidene)-cyclohexylamine (Table 5.2, entry 10)**

Following the general procedure for imine synthesis, the product was isolated as a pale yellow solid. Yield: 170.2 mg (64%). ^{1}H-NMR (400 MHz, $CDCl_3$) δ ppm: 8.28 (s, 1H), 7.68-7.50 (m, 4H), 3.26-3.18 (m, 1H), 1.90-1.26 (m, 10H). ^{13}C-NMR (101 MHz, $CDCl_3$) δ ppm: 157.4, 135.4, 131.8, 129.5, 124.7, 69.9, 34.3, 25.6, 24.8. MS: m/z = 265 $[M]^+$. NMR data are in accordance with literature values.[167]

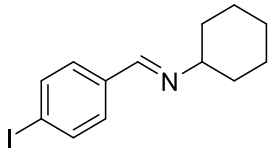

***N*-(4-Iodobenzylidene)-cyclohexylamine (Table 5.2, entry 11)**

Following the general procedure for imine synthesis, the product was isolated as a white solid. Yield: 223.6 mg (75%). ^{1}H-NMR (400 MHz, $CDCl_3$) δ ppm: 8.25 (s, 1H), 7.75 (d, *J* = 8.4 Hz, 2H), 7.47 (d, *J* = 8.4 Hz, 2H), 3.24-3.18 (m, 1H), 1.90-1.24 (m, 10H). ^{13}C-NMR (101 MHz, $CDCl_3$) δ ppm: 157.5, 137.7, 136.1, 130.8, 129.6, 96.8, 70.0, 34.4, 25.5, 24.7. MS: m/z = 313 $[M]^+$. NMR data are in accordance with literature values.[163]

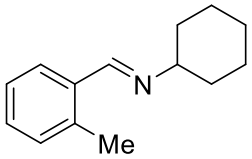

***N*-(2-Methylbenzylidene)-cyclohexylamine (Table 5.2, entry 12)**

Following the general procedure for imine synthesis, the product was isolated as a clear liquid. Yield: 150.1 mg (75%). ^{1}H-NMR (400 MHz, $CDCl_3$) δ ppm: 8.65 (s, 1H), 7.90 (dd, *J* = 7.6, 1.5 Hz, 1H), 7.32-7.16 (m, 3H), 3.25-3.19 (m, 1H), 2.52 (s, 3H), 1.92-1.28 (m, 10H). ^{13}C-NMR (101 MHz, $CDCl_3$) δ ppm: 157.1, 137.2, 134.6, 130.7, 129.9, 127.4, 126.2, 70.5, 34.5, 25.7, 24.8, 19.3. MS: m/z = 201 $[M]^+$. NMR data are in accordance with literature values.[163]

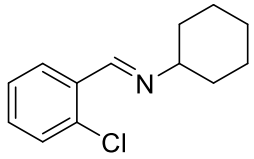

***N*-(2-Chlorobenzylidene)-cyclohexylamine (Table 5.2, entry 13)**

Following the general procedure for imine synthesis, the product was isolated as a clear liquid. Yield: 140.4 mg (63%). ^{1}H-NMR (400 MHz, $CDCl_3$) δ ppm: 8.76 (s, 1H), 8.08-8.00 (m, 1H), 7.45-7.25 (m, 3H), 3.35-3.27 (m, 1H), 1.90-1.35 (m, 10H). ^{13}C-NMR (101 MHz, $CDCl_3$) δ ppm: 155.4, 134.9, 133.6, 131.2, 129.7, 128.4, 126.9, 70.1, 34.4, 25.6, 24.7. MS: m/z = 221 $[M]^+$. NMR data are in accordance with literature values.[163]

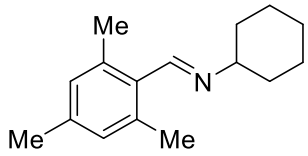

***N*-(2,4,6-Trimethylbenzylidene)benzylamine (Table 5.2, entry 14)**

Following the general procedure for imine synthesis, the product was isolated as a clear liquid. Yield: 140.2 mg (61%). ^{1}H-NMR (400 MHz, $CDCl_3$) δ ppm: 8.59 (s, 1H), 6.87 (s, 2H), 3.25-3.20 (m, 1H), 2.37 (s, 6H), 2.29 (s, 3H), 1.90-1.36 (m, 10H). ^{13}C-NMR (101 MHz, $CDCl_3$) δ ppm: 158.6, 138.3, 136.9, 130.5, 129.1, 70.8, 34.6, 25.7, 24.7, 21.1, 20.3. MS: m/z = 229 $[M]^+$. ^{1}H-NMR data are in accordance with literature values.[259]

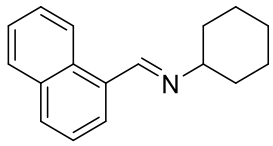

***N*-(1-Naphthalenylmethylene)-cyclohexylamine (Table 5.2, entry 15)**

Following the general procedure for imine synthesis, the product was isolated as a yellow liquid. Yield: 165.7 mg (70%). ^{1}H-NMR (400 MHz, $CDCl_3$) δ ppm: 9.02 (s, 1H), 8.91 (d, J = 8.5 Hz, 1H), 7.93-7.89 (m, 3H), 7.63-7.49 (m, 3H), 3.36-3.31 (m, 1H), 1.90-1.70 (m, 7H), 1.50-1.33 (m, 3H). ^{13}C-NMR (101 MHz, $CDCl_3$) δ ppm: 157.9, 133.8, 132.4, 131.2, 130.6, 128.6, 128.2, 126.9, 125.9, 125.3, 124.3, 70.9, 34.6, 25.7, 24.8. MS: m/z = 237 $[M]^+$. NMR data are in accordance with literature values.[167]

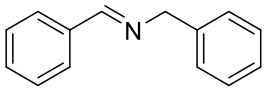

_N_-Benzylidenebenzylamine (Table 5.3, entry 1)

Following the general procedure for imine synthesis, the product was isolated as a clear liquid. Yield: 140.5 mg (72%). ^{1}H-NMR (400 MHz, $CDCl_3$) δ ppm: 8.45 (s, 1H), 7.88-7.85 (m, 2H), 7.48 (dd, *J* = 5.1, 1.9 Hz, 3H), 7.41 (d, *J* = 4.3 Hz, 4H), 7.32-7.26 (m, 1H), 4.87 (bs, 2H). ^{13}C-NMR (101 MHz, $CDCl_3$) δ ppm: 162.0, 139.3, 136.2, 130.8, 128.6, 128.3, 128.0, 127.0, 65.1. MS: m/z = 195 $[M]^+$. NMR data are in accordance with literature values.[163]

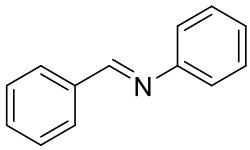

_N_-Benzylideneaniline (Table 5.3, entry 2)

Following the general procedure for imine synthesis, the product was isolated as a white solid. Yield: 120.1 mg (66%). ^{1}H-NMR (400 MHz, $CDCl_3$) δ ppm: 8.50 (s, 1H), 7.97-7.94 (m, 2H), 7.55-7.48 (m, 3H), 7.46-7.40 (m, 2H), 7.30-7.24 (m, 3H). ^{13}C-NMR (101 MHz, $CDCl_3$) δ ppm: 160.5, 152.0, 136.1, 131.4, 129.2, 128.8, 126.0, 120.9. MS: m/z = 181 $[M]^+$. NMR data are in accordance with literature values.[167]

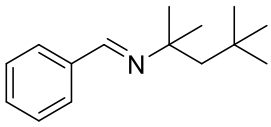

_N_-Benzylidene-*tert*-octylamine (Table 5.3, entry 3)

Following the general procedure for imine synthesis, the product was isolated as a clear liquid. Yield: 160.0 mg (74%). ^{1}H-NMR (400 MHz, $CDCl_3$) δ ppm: 8.27 (s, 1H), 7.82-7.76 (m, 2H), 7.45-7.40 (m, 3H), 1.72 (s, 2H), 1.35 (s, 6H), 0.99 (s, 9H). ^{13}C-NMR (101 MHz, $CDCl_3$) δ ppm: 154.4, 137.5, 130.0, 128.5, 127.9, 61.0, 56.6, 32.1, 31.8, 29.7. MS: m/z = 216 $[M-H]^+$. NMR data are in accordance with literature values.[167]

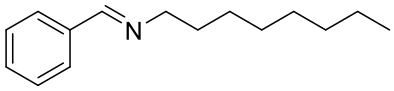

***N*-Benzylidene-octylamine (Table 5.3, entry 4)**

Following the general procedure for imine synthesis, the product was isolated as a yellow liquid. Yield: 170.6 mg (78%). ^{1}H-NMR (400 MHz, $CDCl_3$) δ ppm: 8.30 (d, 1H), 7.82-7.74 (m, 2H), 7.46-7.40 (m, 3H), 3.63 (t, *J* = 6.9 Hz, 2H), 1.75-7.70 (m, 2H), 1.39-1.27 (m, 10H), 0.93-0.89 (m, 3H). ^{13}C-NMR (101 MHz, $CDCl_3$) δ ppm: 160.7, 136.4, 130.4, 128.6, 128.0, 61.9, 31.9, 30.9, 29.4, 27.4, 22.7, 14.1. MS: m/z = 216 $[M-H]^+$. NMR data are in accordance with literature values.[167]

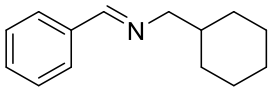

***N*-Benzylidene-cyclohexylmethylamine (Table 5.3, entry 5)**

Following the general procedure for imine synthesis, the product was isolated as a pale yellow liquid. Yield: 160.5 mg (80%). ^{1}H-NMR (400 MHz, $CDCl_3$) δ ppm: 8.25 (s, 1H), 7.79-7.72 (m, 2H), 7.46-7.40 (m, 3H), 3.49-3.48 (d, *J* = 6.2 Hz, 2H), 1.85-1.73 (m, 6H), 1.34-1.21 (m, 3H), 1.05-0.96 (m, 2H). ^{13}C-NMR (101 MHz, $CDCl_3$) δ ppm: 160.8, 136.4, 130.4, 128.6, 128.1, 68.7, 39.0, 31.5, 26.6, 26.1. MS: m/z = 201 $[M]^+$. ^{1}H-NMR data are in accordance with literature values.[70]

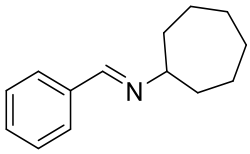

***N*-Benzylidene-cycloheptylamine (Table 5.3, entry 6)**

Following the general procedure for imine synthesis, the product was isolated as a clear liquid. Yield: 140.1 mg (70%). ^{1}H-NMR (400 MHz, $CDCl_3$) δ ppm: 8.28 (s, 1H), 7.80-7.70 (m, 2H), 7.45-7.40 (m, 3H), 3.40-3.36 (m, 1H), 1.88-1.60 (m, 12H). ^{13}C-NMR (101 MHz, $CDCl_3$) δ ppm: 157.8, 136.4, 130.3, 128.5, 128.1, 72.6, 36.3, 28.4, 24.8. MS: m/z = 201 $[M]^+$. ^{1}H-NMR data are in accordance with literature values.[260]

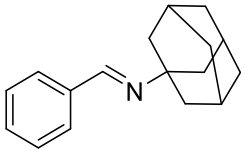

***N*-Benzylidene-1-adamantanylamine (Table 5.3, entry 7)**

Following the general procedure for imine synthesis, the product was isolated as a white solid. Yield: 172.0 mg (72%). ^{1}H-NMR (400 MHz, $CDCl_3$) δ ppm: 8.28 (s, 1H), 7.89 (bs, 2H), 7.49-7.41 (m, 3H), 2.22 (s, 3H), 1.91 (s, 6H), 1.80-1.72 (m, 6H). ^{13}C-NMR (101 MHz, $CDCl_3$) δ ppm: 154.9, 138.0, 130.1, 128.5, 127.9, 57.4, 43.2, 36.2, 29.6. MS: m/z = 239 $[M]^+$. NMR data are in accordance with literature values.[167]

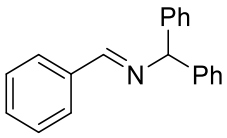

***N*-Benzylidene-1,1-diphenylmethylamine (Table 5.3, entry 8)**

Following the general procedure for imine synthesis, the product was isolated as a white solid. Yield: 198.8 mg (73%). ^{1}H-NMR (400 MHz, $CDCl_3$) δ ppm: 8.40 (s, 1H), 8.02-7.95 (m, 2H), 7.47-7.41 (m, 7H), 7.40-7.32 (m, 4H), 7.28-7.26 (m, 2H), 5.65 (s, 1H). ^{13}C-NMR (101 MHz, $CDCl_3$) δ ppm: 160.8, 143.9, 136.3, 130.8, 128.5, 127.8, 127.0, 77.9. MS: m/z = 271 $[M]^+$. NMR data are in accordance with literature values.[167]

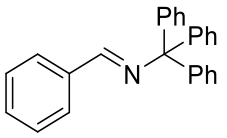

***N*-Benzylidene-1,1,1-triphenylmethylamine (Table 5.3, entry 9)**

Following the general procedure for imine synthesis, the product was isolated as a white solid. Yield: 265.3 mg (76%). ^{1}H-NMR (400 MHz, $CDCl_3$) δ ppm: 7.93-7.85 (m, 2H), 7.50-7.43 (m, 2H), 7.39-7.26 (m, 17H). ^{13}C-NMR (101 MHz, $CDCl_3$) δ ppm: 159.8, 145.7, 136.6, 130.8, 129.8, 128.6, 127.8, 126.8, 78.3. MS: m/z = 347 $[M]^+$. NMR data are in accordance with literature values.[167]

6. Vanadium-catalyzed dehydrogenation of alcohols to form imines

6.1 Background

6.1.1 Introduction to vanadium

Vanadium, the sixth most abundant transition metal in the Earth's crust and the 20th most abundant among all elements, has gained much attention in organic synthesis and catalysis. Vanadium is a fairly cheap metal with a price of around 16.70 €/kg and a worldwide production estimated at 73000 ton per year.[154,158] The common oxidation states of vanadium compounds range from 0 to +V and thereby it encompasses both reductive and oxidative transformations in synthetic chemistry. One of the key reactions that vanadium is known for is the modern sulfuric acid production, where V_2O_5 catalyzes the aerobic oxidation of sulfur dioxide to sulfur trioxide. This process was patented by Peregrine Phillips in 1831.[261]

Vanadium compounds have been used as catalysts in a variety of organic reactions, including oxidations of alkanes, alkenes, arenes, sulfur compounds, alcohols and carbonyl groups, as well as carbon-carbon and carbon-oxygen bond cleavage and formation, deoxydehydration, cyanation, and ring-opening metathesis polymerization.[262,263] Additionally, vanadium has been used to catalyze the aerobic oxidative synthesis of imines from alcohols and amines. However, limited attention has been drawn to the use of vanadium as catalysts in dehydrogenation reactions. Seemingly, the only examples involving vanadium-catalyzed nonoxidative dehydrogenation reactions include the dehydrogenation of light alkanes, such as propane catalyzed by $VO(Mes)_3$ supported on SiO_2, Al_2O_3 or TiO_2.[264–267]

To illustrate the applications of vanadium, several examples with vanadium complexes in different reactions are shown below.

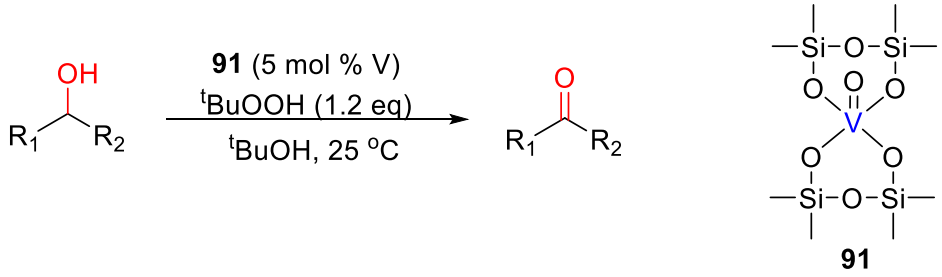

Scheme 6.1. Oxidation of alcohols with V/SiO_2.

In Scheme 6.1, the oxidation of alcohols to aldehydes and ketones has been described using silica-supported vanadium(IV) oxide (V/SiO_2) in the presence of *tert*-butyl hydroperoxide in *tert*-butyl alcohol at ambient temperature with quantitative yields. The procedure is simple, efficient, and environmentally benign.[268]

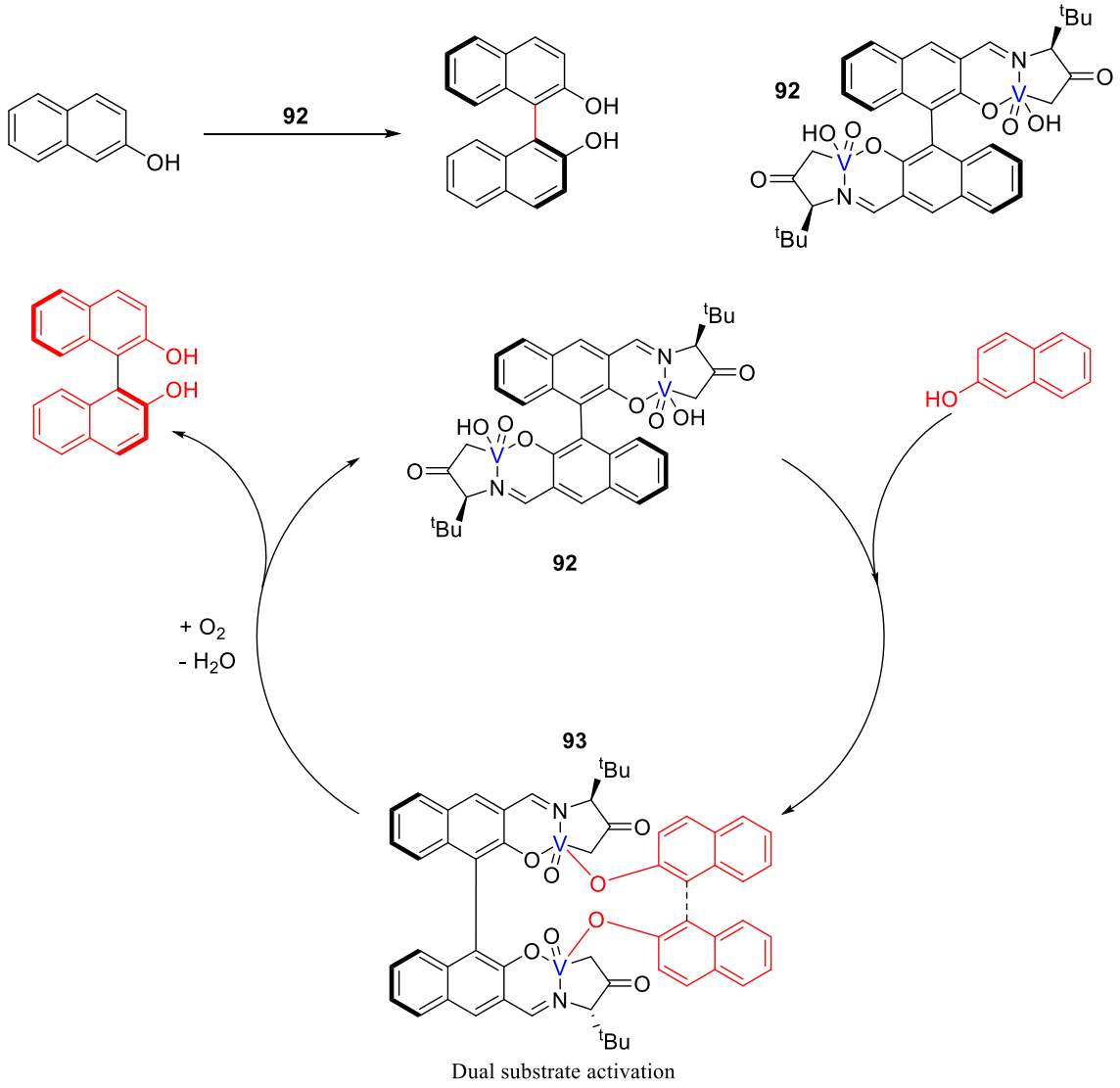

Scheme 6.2. Asymmetric coupling of 2-naphthol with oxygen in the presence of a chiral dinuclear vanadium complex as a catalyst.

In Scheme 6.2, in the presence of 5 mol% of a vanadium catalyst, the desired (*S*)-1,1'-bi-2-naphthol was obtained in 76% yield and with a high enantioselectivity of 91% ee after 24 h. When conducting the reaction at 0 °C at a somewhat prolonged reaction time of 72 h, a quantitative yield of the binaphthol accompanied by a high enantioselectivity of 90% ee was obtained.[269]

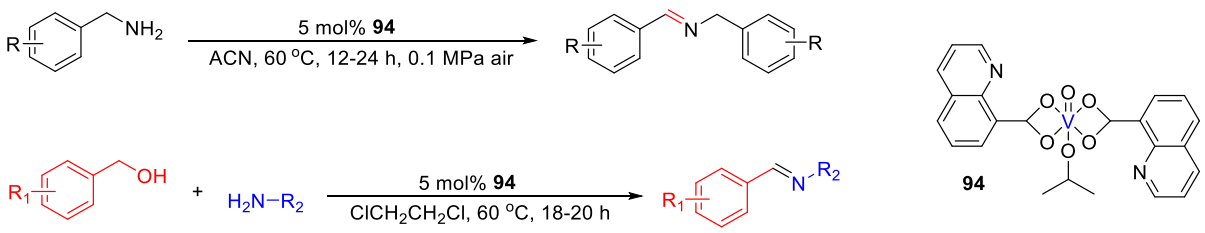

Scheme 6.3. Imination between amines and imination from alcohols and amines.

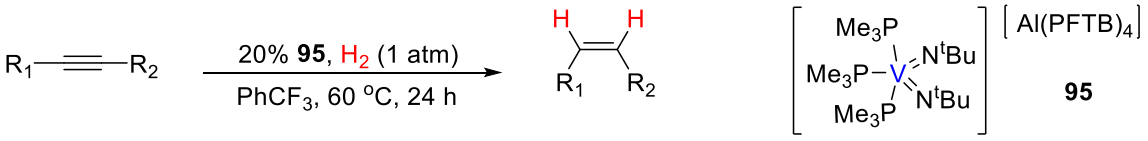

Scheme 6.4. Hydrogenation of alkynes with a vanadium catalyst.

In Scheme 6.3, the oxidation of primary amines to imines and the oxidation of alcohols and amines to imines with a vanadium catalyst were developed. Without an additive or promoter, various symmetrical and unsymmetrical imines were obtained in good to excellent yields (up to 98%) under mild conditions with air as an environmentally benign oxidant. This catalytic system is also effective for the synthesis of heteroatom-containing imines.[270]

In Scheme 6.4, the synthesis of the cationic vanadium bisimido complex **95** $[V(N^tBu)_2(PMe_3)_3][Al\text{-}(PFTB)_4]$ (PFTB = perfluoro-tert-butoxide) and its application to the selective catalytic hydrogenation of alkynes to *Z*-alkenes were reported.[271]

Vanadium(IV) compounds often exist as vanadyl derivatives with a VO^{2+} center. Consequently, most reported vanadium(IV) porphyrin complexes are oxovanadium compounds.[262] Nevertheless, vanadium(IV) porphyrin ditriflate complexes have been used as catalysts in different reactions.[272–274] Some examples are shown in Scheme 6.5.

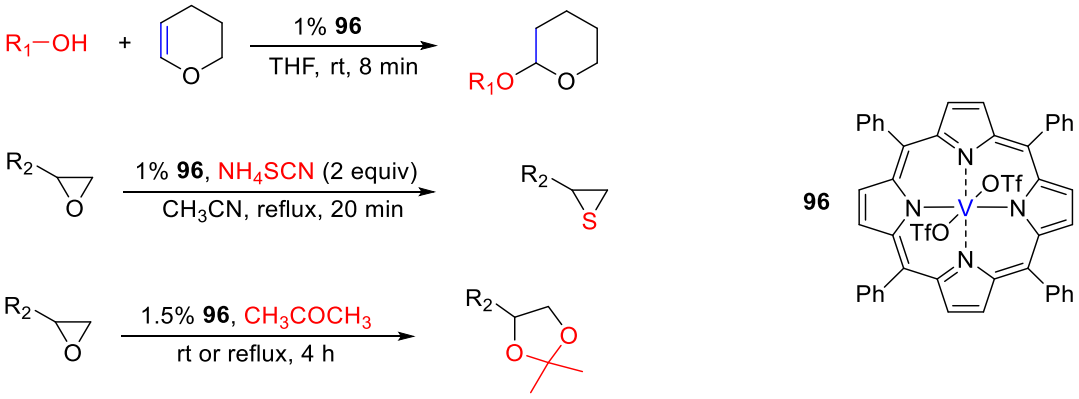

Scheme 6.5. Vanadium(IV) porphyrin-catalyzed reactions.

6.1.2 The salen ligand

Salen molecules have been studied for more than six decades, and refers to a tetradentate C_2-symmetric ligand synthesized from salicylaldehyde (sal) and ethylenediamine (en) (Scheme 6.6). It may also refer to a class of compounds, which are structurally related to the classical salen ligand, primarily bis-Schiff bases. Salen ligands are notable for coordinating a wide range of different metals, which they can often stabilize in various oxidation states.[275]

A metal salen complex is a coordination compound between a metal cation and a salen ligand. In 1990, Jacobsen and Katsuki independently published the first reports of salen used as ligands with manganese for asymmetric epoxidation reactions.[276] Since then, the area of metal-salen catalysis has expanded. A plethora of metal-salen complexes have been synthesized and used in a variety of catalyzed transformations.[277,278]

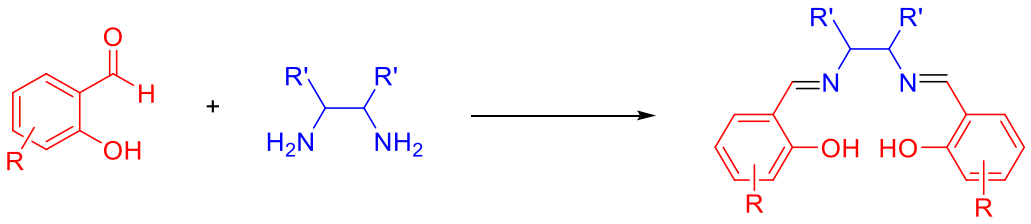

Scheme 6.6. General procedure to prepare salen ligands.

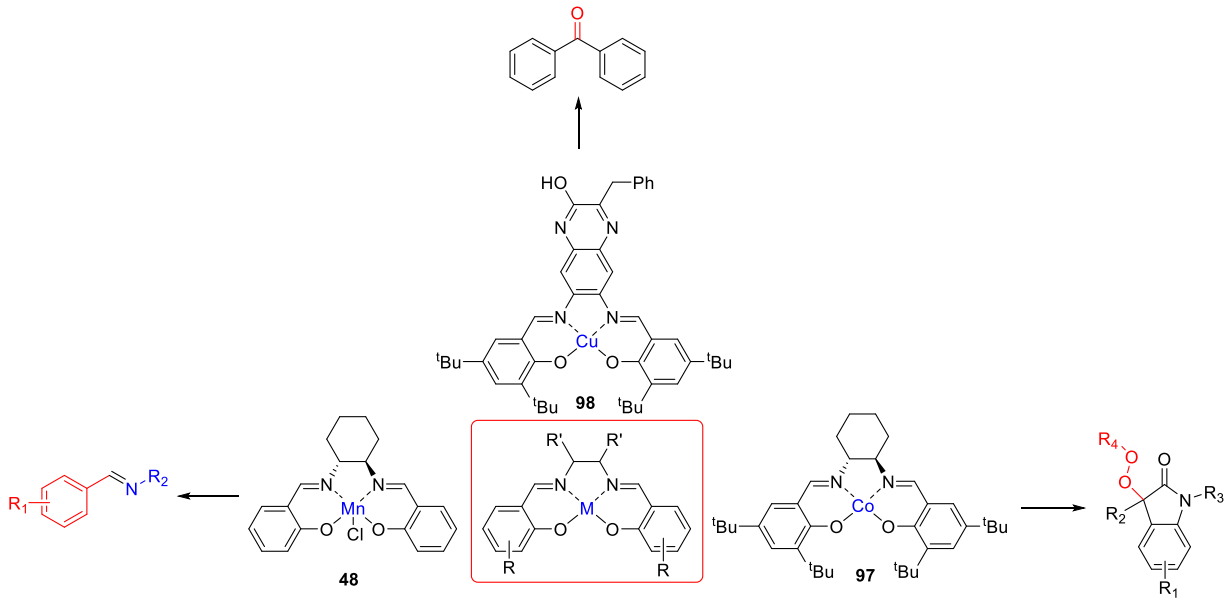

Scheme 6.7. Examples of the versatility of the metal salen complexes.

In Scheme 6.7, a manganese salen complex **48** catalyzes dehydrogenation of alcohols with amines to form imines.[167] A cobalt salen complex **97** catalyzes peroxidation of 2-oxindoles with hydroperoxides.[279] A copper salen complex **98** catalyzes oxidation of aryl methylenes.[280] The easy synthesis and modifications of the salen ligand framework have made it the platform of choice for the discovery of many new catalysts and reactions.

6.2 Results and discussion

6.2.1 Catalyst design and optimization of the reaction conditions

The position of vanadium in the periodic table of the elements is very close to that of manganese, and since the manganese salen chloride has a good performance on dehydrogenation of alcohols (Scheme 6.7), it would be interesting to investigate whether the corresponding vanadium salen complex would have a similar effect on the dehydrogenation of alcohols.

First, several derivatives of vanadium salen complexes were prepared to investigate the influence of the aryl substituent, the scaffold and the Schiff base functionality (Scheme 6.8). As mentioned previously, these vanadium salen complexes can be easily synthesized. The salen ligands were prepared by simple condensation between a salicylaldehyde derivative and a diamine. The complexes were prepared by mixing the ligand and an oxovanadium(IV) compound under aerobic conditions, and then reacted with $SOCl_2$ (Scheme 6.9). All the complexes were highly stable and can be stored at room temperature for more than 1 year without affecting the activity. It should be mentioned that although the vanadium salen dichloride complexes are stable, it is recommended to store them under inert atmosphere.

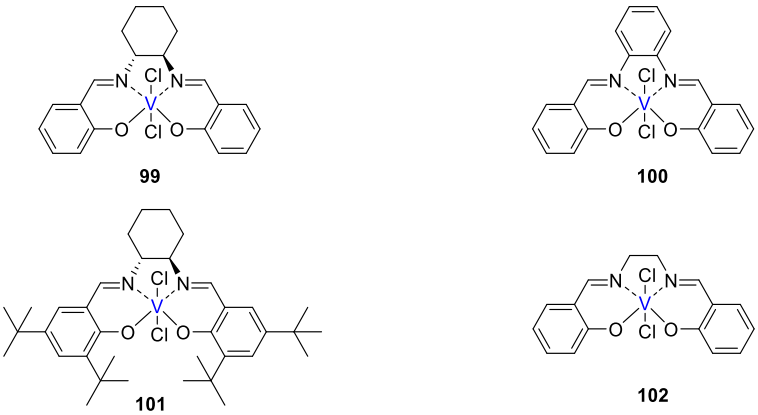

Scheme 6.8. Vanadium complexes used for dehydrogenative imine synthesis.

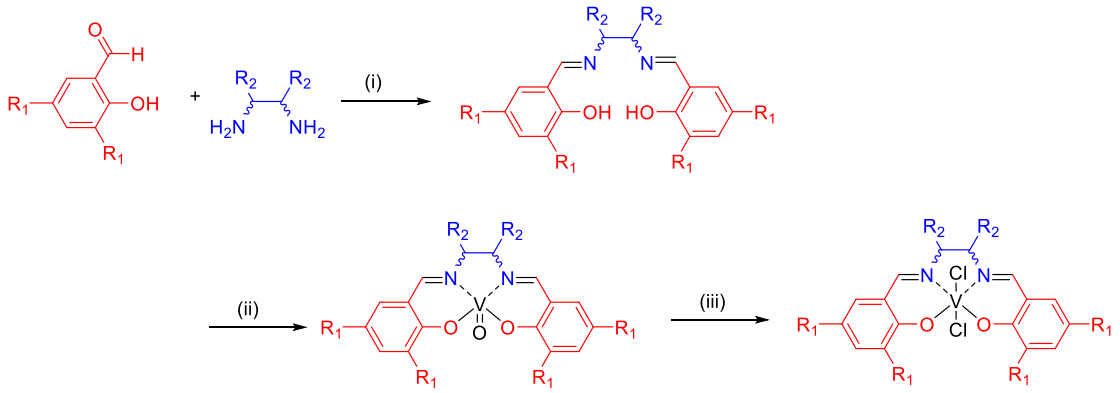

Scheme 6.9. Synthesis of various derivatives of vanadium salen dichloride complexes. Reagents and conditions: (i) EtOH, reflux, 4 h. (ii) $VO(acac)_2$, air, toluene, reflux, 18 h. (iii) $SOCl_2$, MeOH, reflux, 1 h.

Table 6.1. Optimization of vanadium(VI)-catalyzed alcohol dehydrogenation.[a]

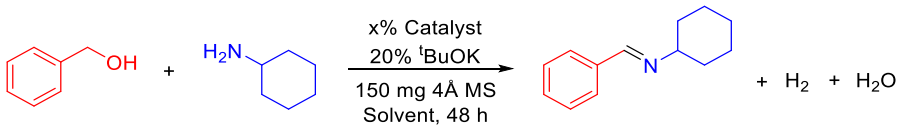

Entry	X	Catalyst	Additive	Solvent	Yield[%][b]
1	5	**99**	^{t}BuOK	mesitylene	21
2	5	**100**	^{t}BuOK	mesitylene	22
3	5	**101**	^{t}BuOK	mesitylene	36
4	5	**102**	^{t}BuOK	mesitylene	26
5	5	**99**	-	mesitylene	75
6	5	**100**	-	mesitylene	78
7	5	**101**	-	mesitylene	94
8	5	**102**	-	mesitylene	94
9	5	-	^{t}BuOK	mesitylene	53
10	5	-	-	mesitylene	4
11	5	**99**	^{t}BuOK	toluene	32
12	5	**100**	^{t}BuOK	toluene	13
13	5	**101**	^{t}BuOK	toluene	16
14	5	**102**	^{t}BuOK	toluene	10
15	5	**99**	-	toluene	61
16	5	**100**	-	toluene	77
17	5	**101**	-	toluene	62
18	5	**102**	-	toluene	34
19	0	-	^{t}BuOK	toluene	60
20	0	-	-	toluene	0

[a] Reaction conditions: BnOH (1 mmol), $CyNH_2$ (1 mmol), catalyst (0.0X mmol), ^{t}BuOK (0.2 mmol), tetradecane (0.5 mmol, internal standard), 4Å MS (150 mg), solvent, reflux, 48 h. [b] Determined by GC.

The synthesized complexes were investigated as catalysts for the dehydrogenative coupling of benzyl alcohol and cyclohexylamine using 5 mol% of the catalyst in refluxing mesitylene under a flow of N_2 (Table 6.1). 4Å molecular sieves (MS) were added to push the equilibrium in the direction of imine. Initially, ^{t}BuOK was employed as an additive, which may serve to activate the catalyst or absorb the liberated H_2O.[167] Different catalysts were applied to the reactions. From entry 1 to 8, it seemed that all catalysts did not have a good performance, while they performed well without ^{t}BuOK where a few catalysts did proceed smoothly without the use of base,[281–284] especially catalyst **101** and **102**. To lower the temperature of the reaction, all catalysts were also employed in toluene. From entry 11 to 18, it can be seen that the imination proceeded in lower yields. Blank reactions without any catalysts were performed for comparison (entry 19 and 20). To investigate the optimal conditions, complex **102** was chosen as the desired catalyst, since it has a simpler structure than that of complex **101**.

Table 6.2. Optimization vanadium(VI)-catalyzed alcohol dehydrogenation.[a]

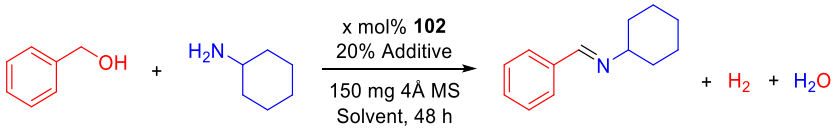

Entry	X	Catalyst	Additive	Solvent	Yield[%] [b]
1	5	**102**	PPh_3	toluene	68
2	5	**102**	Na_2SO_4	toluene	85
3	5	**102**	$MgSO_4$	toluene	93
4	5	**102**	Na_2CO_3	toluene	8
5	5	**102**	Na_2SO_3	toluene	89
6	5	**102**	NPh_3	toluene	70
7	5	**102**	K_2CO_3	toluene	30
8	5	**102**	Cs_2CO_3	toluene	11
9	5	**102**	LiCl	toluene	41
10	5	**102**	KOH	toluene	12
11	5	**102**	NaOH	toluene	6
12	5	**102**	Li_3N	toluene	24
13	5	**102**	Mg_3N_2	toluene	84
14	5	**102**	Ca_3N_2	toluene	17
15	5	**102**	NEt_3	toluene	64
16	3	**102**	$MgSO_4$	toluene	93
17	1	**102**	$MgSO_4$	toluene	71

[a] Reaction conditions: BnOH (1 mmol), $CyNH_2$ (1 mmol), catalyst **102** (0.0X mmol), additive (0.2 mmol), tetradecane (0.5 mmol, internal standard), 4Å MS (150 mg), toluene, reflux, 48h. [b] Determined by GC.

For further optimization, the influence of additives and the solvent were investigated (Table 6.2). A number of common additives were applied to the reaction in toluene. In Table 6.2, from entry 1 to 15, different additives were used in the reaction. It can be seen in Table 6.2 that for some strong

bases, such as KOH, NaOH, Li_3N and Ca_3N_2, the yields obtained were very low, while the yields were very high when $MgSO_4$, Na_2SO_4, Na_2SO_3 and Mg_3N_2 were employed in the reaction. The pK_a value and the cationic or anionic nature of the additive could influence the catalytic efficiencies of transition-metal catalysts.[285,286] By comparing the different results, $MgSO_4$ had a positive effect on the reaction as seen from the results of GC yields and was chosen as the additive. Then, the influence of the catalyst loading was explored. As shown in Table 6.2 (entry 16 and 17), the reaction also proceeded in a good yield when 3 mol% of catalyst **102** was employed. Based on the different observations in Table 6.1 and 6.2, the conditions of entry 16 in Table 6.2 were selected as the optimal conditions.

Table 6.3. Imination of alcohols with cyclohexylamine[a]

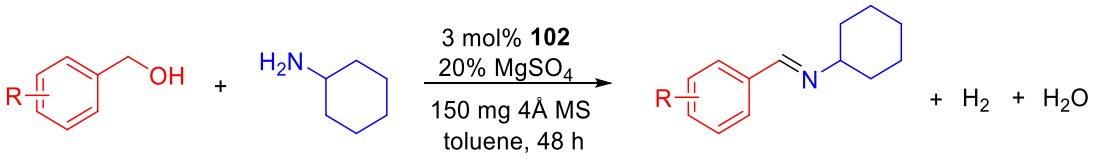

Entry	Alcohol	Imine	Yield[%][b]
1	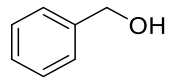	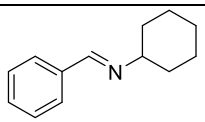	84
2	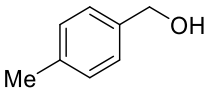	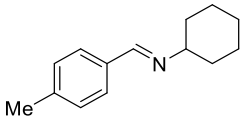	71
3	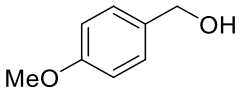	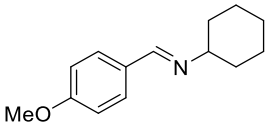	72
4	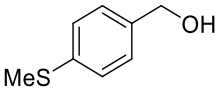	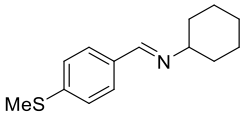	75
5	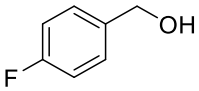	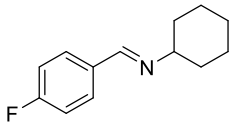	76
6	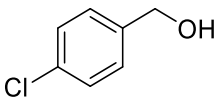	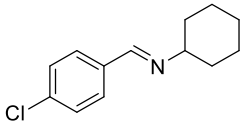	62
7	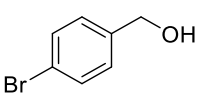	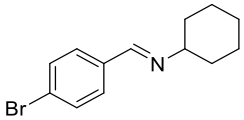	80
8	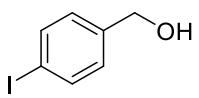	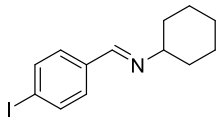	60

9	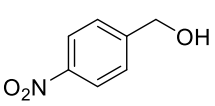	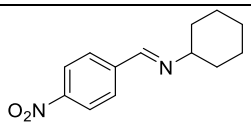	65
10	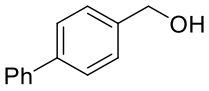	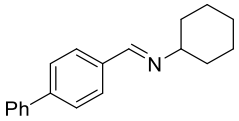	73
11	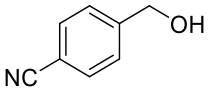	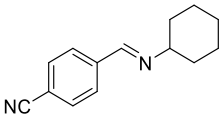	72
12	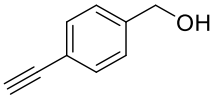	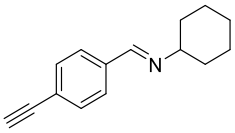	69
13	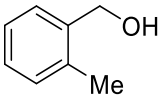	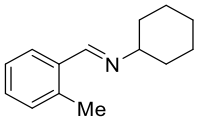	71
14	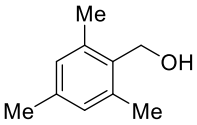	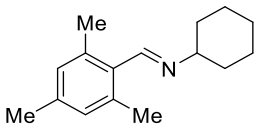	72
15	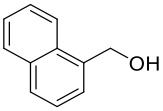	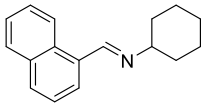	68
16	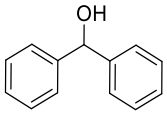	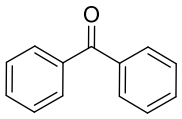	73
17	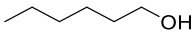	–	–
18	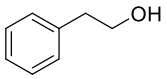	–	–

[a] Reaction conditions: alcohol (1 mmol), $CyNH_2$ (1 mmol), complex **102** (3 mol%), $MgSO_4$ (20 mol%), 4Å MS (150 mg), toluene (4 ml), reflux, 48 h. [b] Isolated yield.

6.2.2 Substrate scope and limitations

With the optimal conditions in hand, the substrate scope of the imination could be investigated. Different alcohols were first applied in the reaction with cyclohexylamine to explore their influence (Table 6.3). It should be noted that the desired imine was isolated by flash chromatography. For the model reaction (entry 1), the isolated yield of the product was 84%. Next, different benzyl alcohols with different substituted groups in the para position were investigated. The *p*-methyl, *p*-methoxy, and *p*-methythiobenzl alcohols all gave 71-75% (entry 2-4). Four

different halogen groups in the para-position of benzyl alcohol were explored. *p*-Fluoro- and *p*-chloro-substituents were also tolerated giving 76% and 62% yield (entry 5 and 6). The analogous *p*-bromo substrate gave a yield up to 80% (entry 7) whereas the *p*-iodo substrate gave 60% yield (entry 8). For these four halogen benzyl alcohols, there was some partial dehalogenation,[224] which could be observed in GC. *p*-Nitrobenzyl alcohol gave a low yield of 65%, which could be because the nitro group can be reduced to an amine,[245–247] while *p*-benzyl alcohol gave 73% yield. The reaction can tolerate benzyl alcohols with cyano and ethynyl group on the para position, and the yields were 72% and 69%, respectively (entry 11 and 12). The ortho-substituted and multiple substituted benzyl alcohols were also explored, and they gave similar yields (entry 13 and 14). In addition, 1-naphthalenemethanol afforded a 68% yield of the Schiff base product (entry 15).

A ketone was obtained, instead of an imine, when the diphenylmethanol was employed in the reaction (entry 16). Traditionally, a commonly used method for the preparation of imines is the condensation of an aldehyde or ketone with a primary amine as introduced in Chapter 3. However, harsh conditions (nonstoichiometric amounts of reagents, high reaction temperatures, added protic or Lewis acids, and/or long reaction times) are generally required for the preparation, when the carbonyl component is a ketone.[287,288] There are some mild and efficient routes to prepare the desired imine, such as a palladium-catalyzed diarylation of isocyanides with tetraaryllead compounds[289] and amination of cyclohexyl iodide with *N*-trimethylstannylated benzophenone imine.[290]

Aliphatic primary alcohols (hexan-1-ol and 2-phenylethanol) were also subjected to the reaction conditions, but no conversion of the alcohol was observed (entry 17 and 18).

Then different amines were also subjected to the reaction to investigate their influence (Table 6.4). Benzylamine and aniline gave similar yields of 62% and 61%, respectively (entry 1 and 2). *tert*-Octylamine gave 71% yield (entry 3) while octylamine gave 67% yield (entry 4). For hexyl-, cyclohexylmethyl- and cycloheptylamine, similar yields were obtained between 70% and 74% (entry 5-7). Then amines with a bulky group were explored. The more hindered amines (*R*)-1-phenylethyl-, 1-adamantyl-, diphenylmethylamine afforded imines in 70-74% yield (entry 8-10), which indicates that the steric hindrance had less of an influence, possibly because the imine formation occurs in the absence of the catalyst.

Table 6.4. Imination of amines with benzyl alcohol.[a]

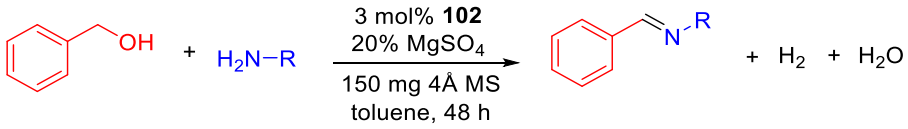

Entry	Amine	Imine	Yield[%][b]
1	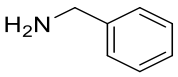	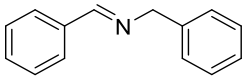	62
2	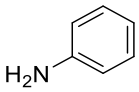	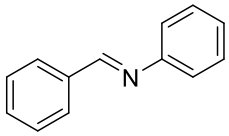	61
3	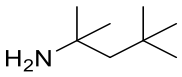	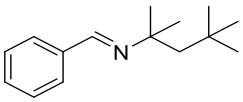	71
4	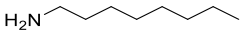	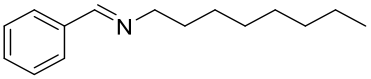	67
5	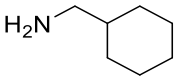	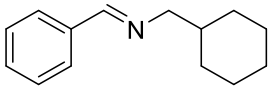	74
6	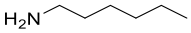	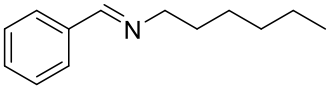	72
7	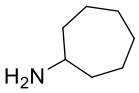	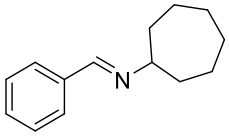	70
8	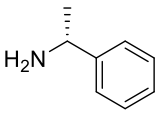	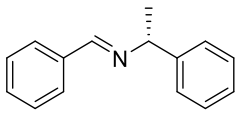	74
9	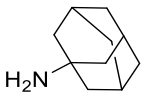	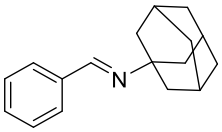	73
10	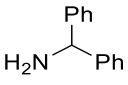	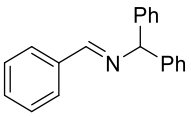	70

[a] Reaction conditions: BnOH (1 mmol), amine (1 mmol), complex **102** (3 mol%), $MgSO_4$ (20 mol%), 4Å MS (150 mg), toluene (4 ml), reflux, 48 h. [b] Isolated yield.

6.2.3 Exploration of the mechanism

Gas evolution

Based on our previous report, dihydrogen should be one of the byproducts, and the dehydrogenative pathway of the metal-catalyzed imination was verified by collecting the liberated hydrogen gas. The evolution of hydrogen gas was measured from the reaction in Table 6.2, entry 16, and the gas was collected in a burette. A total of 16 mL gas was collected, and then characterized through ^{1}H-NMR to be dihydrogen gas (δ 4.05 ppm), which confirms that the transformation takes place by an acceptorless dehydrogenative pathway.

Deuterium labeling study

To further investigate the mechanism of the reaction, a deuterium labelling study was conducted (Scheme 6.10). When the reaction in Table 6.2, entry 16 was performed with $PhCD_2OH$ instead of $PhCH_2OH$, the product was exclusively PhCD=NCy with no evidence for any hydrogen incorporation into the benzylic position. The lack of isotope scrambling may indicate that the dehydrogenation takes place by a monohydride pathway.

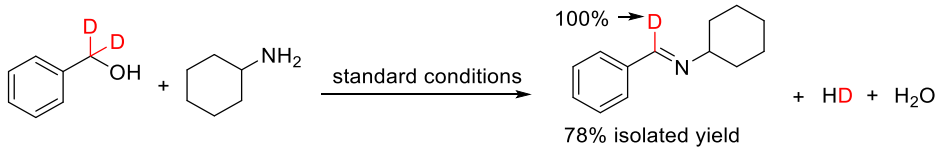

Scheme 6.10. Imination with benzyl alcohol-α,α-d_2.

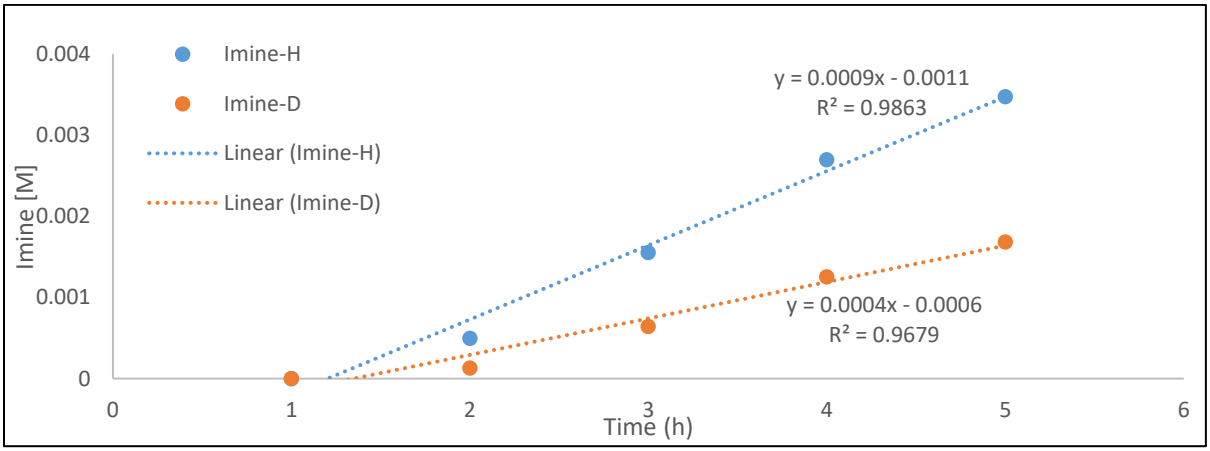

Figure 6.1. Determination of KIE by plotting the initial rates of the reaction involving benzyl alcohol and benzyl alcohol-α,α-d_2.

Kinetic isotope effect (KIE)

To obtain more details about the mechanism, the primary KIE was measured to investigate whether the hydride abstraction takes place in the rate-limiting step. The KIE was determined by measuring the initial rates with $PhCH_2OH$ and $PhCD_2OH$ in the reaction with cyclohexylamine. The measurements gave a KIE of 2.3, which shows that breakage of the benzylic C-H bond is a slow step in the transformation.

Catalyst deuterium labelling

In the former example of a dehydrogenative reaction with Mn(III) complex **48**, it was believed that the double bond between the C atom and the N atom in complex **48** could be reduced, and the species was indeed detected through LCMS.[167] The vanadium complex **102** has a similar structure as complex **48**, and thus it was thought that there could be a similar intermediate when complex **102** was applied in the dehydrogenation reaction. Some experiments were performed to investigate this suggestion.

Complex **102** (11.6 mg, 0.03 mmol), $MgSO_4$ (20.7 mg, 0.2 mmol) and molecular sieves (150 mg) were placed in an oven-dried tube, and then put in a carousel. The following steps were carried out as standard procedures. Just after the substrates were added, a sample was prepared and tested through LCMS. More LCMS samples were taken from the reaction and tested after 12 h, 24 h and 36 h. In the LCMS chromatograms, a catalyst elutes between 1.15 - 1.20 minutes with a dominant m/z of 334. This species corresponds to $[VO(salen)+H^+]$, indicating that catalyst **102** is converted to pre-catalyst **115** VO(salen) (seen in the experimental section). This may happen in the reaction mixture, where water is a byproduct of the condensation to form the imine. It may also happen during the LCMS test as water is present in the eluent. Importantly, no masses corresponding to either $V{=}O^{2+}$ or V^{4+} with a reduced ligand backbone like salan species **103** (Scheme 6.11) were identified. When the reaction was finished (48 h), a GC sample was prepared, and the yield was over 90%.

A similar experiment was performed with benzyl alcohol-α,α-d_2 (110 mg, 1.0 mmol) and cyclohexylamine (99.0 mg, 1.0 mmol) following the general procedure for imine synthesis. When the reaction time was 0 h, 12 h, 24 h and 36 h, a LCMS sample was prepared and tested. Again, the catalyst elutes between 1.15 - 1.20 minutes with a dominant m/z of 334 and no masses corresponding to salan species **104** (Scheme 6.11) were identified. This indicates that deuterium is not incorporated into the ligand. To further confirm this suggestion, HCl (aq) was added to the finished reaction and stirred for 10 min. The organic phase was collected, dried, concentrated, and

tested in GC, but no signal of salicyladehyde-α-d_1 was observed. To conclude, no incorporation of deuterium in the catalyst could be observed, which may indicate that the reaction with vanadium complex **102** proceeds through a different pathway than manganese complex **48**.

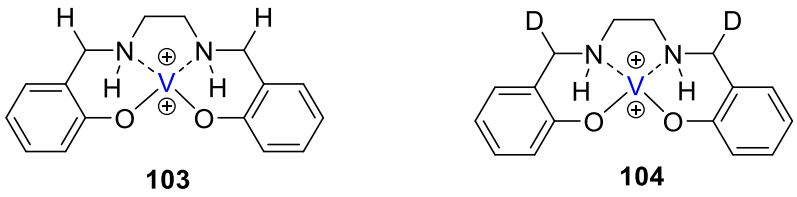

Scheme 6.11. Possible intermediates in the reactions.

Investigating the influence of VO(salen) (pre-catalyst 4)

As observed in the catalyst deuterium labelling experiments, catalyst **102** can be converted to complex **115**. To evaluate the catalytic activity of **115**, a comparison experiment with complex **115** was run. Two reactions with complex **115**, and one reaction with complex **102** were performed under the standard procedure (Table 6.5). A GC sample was prepared and tested when the reaction was finished, but the yield was less than 70%, which indicates that pre-catalyst **115** is a less active catalyst. LCMS samples of the reaction mixtures were prepared, and the [VO(salen)+H^+] species with an m/z of 334 were observed as expected.

Table 6.5. Investigating the performance of VO(salen) on dehydrogenation of alcohols.

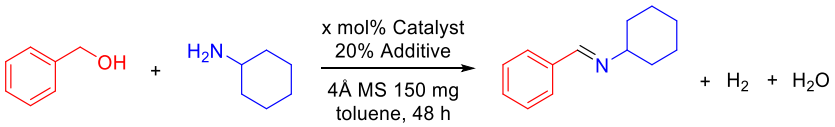

Entry	X	Catalyst	Additive	solvent	Yield[b]
1	3	VO(salen) (pre-catalyst **115**)	$MgSO_4$	toluene	68
2	3	VO(salen) (pre-catalyst **115**)	-	toluene	62
3	3	V(salen)Cl_2 (catalyst **102**)	$MgSO_4$	toluene	> 90

[a] Reaction conditions: BnOH (1 mmol), $CyNH_2$ (1 mmol), catalyst (0.0X mmol), $MgSO_4$ (0.2 mmol), tetradecane (0.5 mmol, internal standard), 4Å MS (150 mg), toluene (4 ml), reflux, 48 h. [b] Determined by GC.

From the above experiments, it can be seen that the double bond between the C atom and the N atom in the salen ligand was not reduced, and the metal salen ligand was not disrupted in complex

102 or pre-catalyst **115**. Pre-catalyst **115** also had an influence on the dehydrogenation of alcohols, but complex **102** performed better. Thus, it was believed that there could be a metal-ligand cooperation pathway, which is very similar to mechanisms shown in Scheme 4.11 and 5.27. Thus, the mechanism in Scheme 6.12 was proposed. Initially, complex **102** was activated in the solvent with the removal of two chlorides to obtain the active complex **105**, and then the alcohol coordinated with transition state complex **106** to afford the complex **107**. Complex **107** and the aldehyde were generated with outer-sphere hydrogen abstraction through complex **106**, and the complex **105** was regenerated with the liberation of hydrogen gas. The pathway is different from the proposed route for the dehydrogenation by manganese(III) salen complex **48** (Scheme 4.16), which may give a new idea that the catalysts based on different transition metals with salen ligands could proceed by different mechanisms on the dehydrogenation of alcohols.

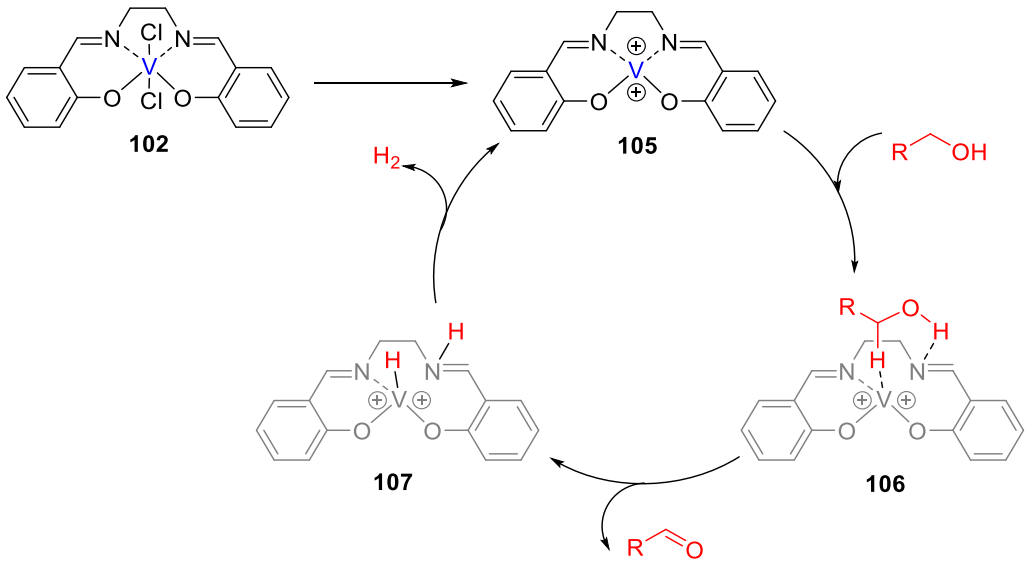

Scheme 6.11. Proposed mechanism for dehydrogenation of alcohols with complex **102**.

6.3 Project conclusions

In summary, a new catalyst for the acceptorless dehydrogenation of alcohols has been described. The vanadium(IV) salen complex mediates the formation of imines from alcohols and amines with the liberation of hydrogen gas. The catalyst can tolerate different alcohols and amines. The mechanism is believed to involve a bifunctional pathway, where both the metal and the ligand participate in the dehydrogenation reaction, and more investigations based on DFT will be carried out in the near future.

6.4 Experimental section

6.4.1 General experimental methods

NMR spectra were recorded at 400 MHz for ^{1}H-NMR and 100 MHz for ^{13}C-NMR on a Bruker Ascend 400 MHz spectrometer. Chemical shift values (δ) are reported in ppm relative to the residual solvent signal in $CDCl_3$ (δ_H = 7.26 ppm, δ_C = 77.2 ppm). High Resolution mass spectra were recorded using ESI with TOF detection. FT-IT was recorded on a Bruker ALPHA II. GCMS was carried out on a Shimadzu GCMS-QP2010S instrument fitted with an Equity 5, 30m×0.25mm×0.25µm column. Ionisation was performed by electronic impact (EI, 70 eV) and helium as the carrier gas. Flash column chromatography was performed using silica gel 60 (35-70 um particle size) saturated with NEt_3. All commercially available reagents were purchased from Sigma-Aldrich and were not further purified. Mesitylene was stored over activated 4Å molecular sieves and degassed with N_2 before being used. All experiments were carried out under a nitrogen flow using Schlenk flask techniques except when mentioned otherwise.

6.4.2 Procedure for ligand synthesis

Method A: A mixture of the diamine (3.8 mmol), K_2CO_3 (525 mg, 3.8 mmol) and water (2.5 mL) was stirred until complete dissolution, and then methanol (20 ml) was added. The reaction mixture was heated to reflux and a solution of salicylaldehyde (0.80 ml, 7.6 mmol) in methanol (8 ml) was added over 30 min. The reaction mixture was refluxed for an additional 4 h and then cooled to room temperature. The mixture was concentrated in vacuum and the residue was dissolved in ethyl acetate (15 ml), washed with water (8 ml), dried (Na_2SO_4) and concentrated under vacuum to give the desired ligand.[167,291]

Method B: The diamine (10 mmol) was dissolved in ethanol, and salicylaldehyde (2.44 g, 20 mmol) dissolved in ethanol (25 ml) was then added dropwise to the solution over 5 min, followed by heating the reaction to reflux for 2.5 h. The mixture was allowed to be cooled to room temperature, and the precipitated crystals were collected by filtration, washed with cold ethanol and dried under vacuum to give the desired ligand.[167,291]

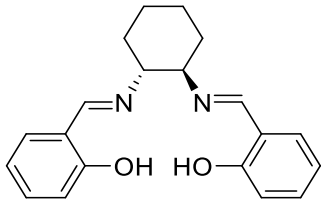

(1*R*,2*R*)-*N*,*N*'-Bis(salicylidene)-1,2-cyclohexanediamine (Ligand **108**)

The ligand was prepared according to method A: (1*R*,2*R*)-(+)-1,2-diaminocyclohexane L-tartrate was used as the diamine. The desired ligand was collected as a yellow oil (1.20 g, 98%). ^{1}H-NMR (400 MHz, $CDCl_3$) δ ppm: 13.32 (s, 2H), 8.26 (s, 2H), 7.29-7.23 (m, 2H), 7.17 (dd, *J* = 7.6, 1.6 Hz, 2H), 6.91 (d, *J* = 8.3 Hz, 2H), 6.79 (t, *J* = 7.5 Hz, 2H), 3.37-3.30 (m, 2H), 2.00-1.90 (m, 4H), 1.80-1.70 (m, 2H), 1.55-1.45 (m, 2H). ^{13}C-NMR (101 MHz, $CDCl_3$) δ ppm: 164.7, 160.9, 132.1, 131.5, 118.6, 116.8, 72.6, 33.1, 24.2. NMR data are in accordance with literature values.[167,292] FT-IR (neat) v/cm^{-1}: 2930, 2858, 1627, 1578, 1495, 1460, 1417, 1275, 1202, 1149, 846, 751, 662, 419. FT-IR data are in accordance with literature values.[292]

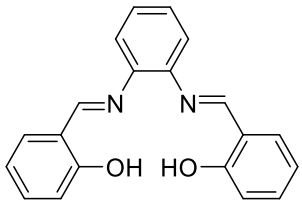

N,*N*'-Bis(salicylidene)-1,2-benzenediamine (Ligand **109**)

The ligand was prepared according to method B: 1,2-benzenediamine was used as the diamine. The desired ligand was collected as orange crystals (1.41 g, 90%). ^{1}H-NMR (400 MHz, $CDCl_3$) δ ppm: 13.05 (s, 2H), 8.67 (s, 2H), 7.44-7.35 (m, 6H), 7.29-7.24 (m, 2H), 7.08 (d, *J* = 8.2 Hz, 2H), 6.95 (td, *J* = 7.5, 1.1 Hz, 2H). ^{13}C-NMR (101 MHz, $CDCl_3$) δ ppm: 163.7, 161.4, 142.6, 133.4, 132.3, 127.7, 119.8, 119.2, 119.0, 117.6. NMR data are in accordance with literature values.[167,293] FT-IR (neat) v/cm^{-1}: 1609, 1559, 1479, 1275, 1189, 1149, 908, 758, 434. FT-IR data are in accordance with literature values.[294–296]

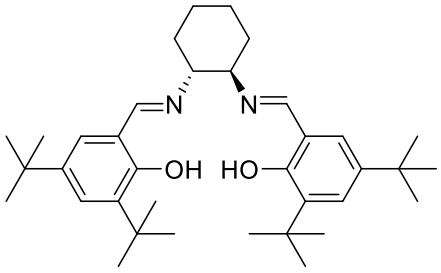

(1*R*,2*R*)-*N*,*N*'-Bis(3,5-di-*tert*-butylsalicylidene)-1,2-cyclohexanediamine (Ligand **110**)

The ligand was prepared according to method A: (1*R*,2*R*)-(+)-1,2-diaminocyclohexane L-tartrate and 3,5-di-*tert*-butylsalicylaldehyde were used. The desired ligand was collected as yellow crystals (1.17 g, 96%). ^{1}H-NMR (400 MHz, $CDCl_3$) δ ppm: 13.73 (s, 2H), 8.32 (s, 2H), 7.33 (s, 2H), 7.01 (s, 2H), 3.34 (s, 2H), 2.00-1.85 (m, 6H), 1.44 (s, 20H), 1.26 (s, 18H). ^{13}C-NMR (101 MHz, $CDCl_3$) δ ppm: 165.8, 158.0, 139.9, 136.3, 126.7, 126.0, 117.8, 72.4, 34.9, 34.0, 33.3, 31.4, 29.4, 24.4. NMR data are in accordance with literature values.[297] FT-IR (neat) v/cm^{-1}: 2949, 2905, 2861, 1629, 1591, 1468, 1437, 1361, 1269, 1173, 1135, 1084, 1037, 878, 728, 711, 644. FT-IR data are in accordance with literature values.[298]

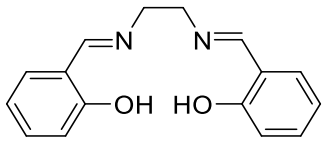

N,*N*'-Bis(salicylidene)ethylenediamine (Ligand **111**)

The ligand was prepared as method B: ethylene diamine and salicylaldehyde were used. The desired ligand was collected as yellow crystals (0.51 g, 95%). ^{1}H-NMR (400 MHz, $CDCl_3$) δ ppm: 13.22 (s, 2H), 8.39 (s, 2H), 7.32 (ddd, *J* = 8.4, 7.9, 1.7 Hz, 2H), 7.26 (dd, *J* = 7.9, 1.7 Hz, 2H), 6.96 (d, *J* = 8.3 Hz, 2H), 6.88 (td, *J* = 7.4, 1.0 Hz, 2H), 3.97 (s, 4H). ^{13}C-NMR (101 MHz, $CDCl_3$) δ ppm: 166.5, 162.0, 132.4, 131.5, 118.7, 118.6, 117.0, 59.8. NMR data are in accordance with literature values.[299] FT-IR (neat) v/cm^{-1}: 1609, 1576, 1495, 1460, 1417, 1280, 1198, 1148, 1040, 1020, 854, 740, 646, 557, 472. FT-IR data are in accordance with literature values.[300]

6.4.3 Procedure for pre-catalyst synthesis

Pre-catalysts **112-115** were prepared following the methods reported in the literature with slight modifications.[301–303] The ligand (1.1 equiv) was dissolved in methanol (20 ml), and heated to reflux (if there are some precipitate in the mixture, more methanol should be added until the ligand is completely dissolved in methanol). An excess of ligand was used to ensure its maximum complexation. A solution of 1 equivalent of $VO(acac)_2$ dissolved in 5 ml of methanol was added. After cooling to room temperature, the mixture was stirred for an additional 18 h. The precipitate was recovered by filtration, washed with cool methanol, and dried in vacuum to afford the corresponding pre-catalyst.

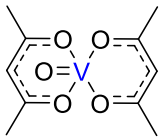

Vanadyl acetylacetonate ($VO(acac)_2$)

A green powder. FT-IR (neat) v/cm^{-1}: 1589, 1555, 1520, 1417, 1372, 1357, 1286, 1018, 995, 936, 798, 789, 685, 659, 609, 485, 424. FT-IR data are in accordance with literature values.[304,305]

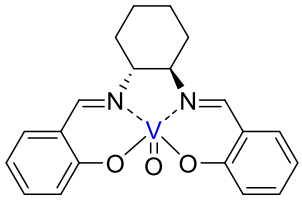

((1*R*,2*R*)-N, N'-Bis(salicylidene)cyclohexane-1,2-diamine)oxovanadium(IV) (Pre-catalyst **112**)

Ligand **108** (0.65 g) was applied in this procedure, and 0.70 g of the corresponding pre-catalyst was isolated as a cyan powder (yield 90%). FT-IR (neat) v/cm^{-1}: 2932, 2858, 1618, 1542, 1470, 1445, 1396, 1312, 1199, 1149, 988 (V=O), 908, 809, 754, 623, 569, 462, 422. FT-IR data are in accordance with literature values.[303,306]

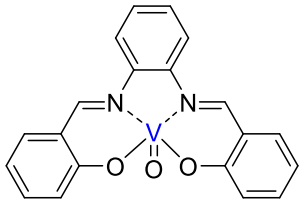

(*N*,*N*'-Bis(salicylidene)-1,2-benzenediamine)oxovanadium(IV) (Pre-catalyst **113**)

Ligand **109** (1.00 g) was applied in this procedure, and 1.12 g of the corresponding pre-catalyst was isolated as a green powder (yield 93%). FT-IR (neat) v/cm^{-1}: 1603, 1577, 1532, 1461, 1434, 1378, 1313, 1193, 1147, 977 (V=O), 811, 749, 624, 540, 503, 484, 446. FT-IR data are in accordance with literature values.[301–303]

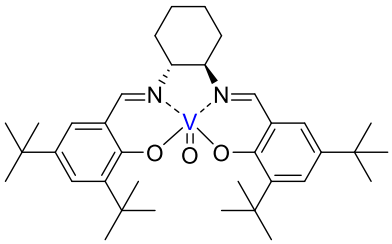

((1*R*,2*R*)-*N*,*N*'-Bis(3,5-di-*tert*-butylsalicylidene)-1,2-cyclohexanediamine)oxovanadium(IV) (Pre-catalyst **114**)

Ligand **110** (0.80 g) was applied in this procedure, and 0.68 g of the corresponding pre-catalyst was isolated as a yellow-green powder (yield 90%). FT-IR (neat) v/cm^{-1}: 2947, 2905, 2864, 1627, 1601, 1531, 1426, 1385, 1345, 1313, 1250, 1199, 1170, 979 (V=O), 836, 186, 748, 561, 542, 488. FT-IR data are in accordance with literature values.[301,302,307]

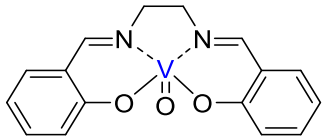

(*N*,*N*'-Bis(salicylidene)ethylenediamine)oxovanadium(IV) (Pre-catalyst **115**)

Ligand **111** (0.78 g) was applied in this procedure, and 0.86 g of the corresponding pre-catalyst was isolated as a black green powder (yield 95%). FT-IR (neat) v/cm^{-1}: 1613, 1532, 1445, 1387, 1333, 1298, 1146, 1146, 969 (V=O), 903, 798, 767, 626, 596, 457, 413. FT-IR data are in accordance with literature values.[301–306]

6.4.4 Procedure for synthesis of dichlorovanadium(IV) salen complexes

The complexes were prepared following a procedure in the literature.[308,309] The pre-catalyst (2 mmol) was added to dry toluene (30 ml), and the mixture heated to reflux. Distilled $SOCl_2$ (1.2 equiv, 2.4 mmol, 0.18 ml) was added, and the reaction was refluxed for 30 min. An excess of $SOCl_2$ was used to ensure complete conversion. When the mixture was cooled down to room temperature, a new crystalline deep blue solid precipitated. The corresponding catalyst was obtained by filtration, washed with dry toluene, and dried in vacuum.

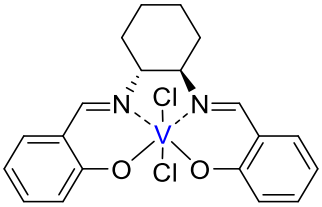

Dichloro((1*R*,2*R*)-*N*,*N*'-bis(salicylidene)cyclohexane-1,2-diamine)vanadium(IV) (Complex **99**)

0.70 g pre-catalyst **112** was used, and 0.76 g black catalyst was prepared (yield 99%). FT-IR (neat) v/cm^{-1}: 2951, 2921, 1593, 1546, 1440, 1392, 1303, 1273, 1152, 908, 828, 768, 650, 491, 441. The peak at 988 of V=O stretch had disappeared by comparison with the IR of pre-catalyst **112**.

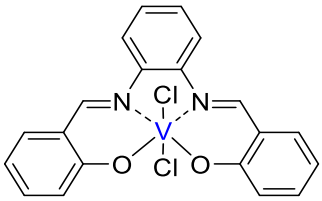

Dichloro(*N*,*N*'-bis(salicylidene)-1,2-benzenediamine)vanadium(IV) (Complex **100**)

1.12 g pre-catalyst **113** was used, and 1.20 g brown catalyst was prepared (yield 94%). FT-IR (neat) v/cm^{-1}: 1593, 1575, 1536, 1465, 1435, 1377, 1305, 1276, 1210, 1148, 928, 875, 830, 754, 650, 545, 489, 442. The peak at 978 of V=O stretch had disappeared by comparison with the IR of pre-catalyst **113**.

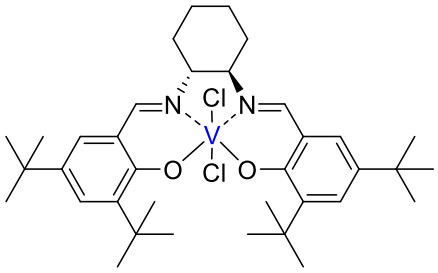

Dichloro((1*R*,2*R*)-*N*,*N'*-bis(3,5-di-*tert*-butylsalicylidene)-1,2-cyclohexanediamine)vanadium(IV) (Complex **101**)

1.08 g pre-catalyst **114** was used, and 1.00 g black catalyst was prepared (yield 85%). FT-IR (neat) v/cm^{-1}: 2949, 2906, 2867, 1596, 1541, 1463, 1391, 1364, 1338, 1297, 1270, 1241, 919, 887, 867, 848, 759, 583, 487. The peak at 979 of V=O stretch had disappeared by comparison with the IR of pre-catalyst **114**.

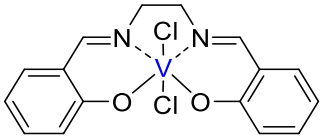

Dichloro(*N*,*N*'-bis(salicylidene)ethylenediamine) vanadium(IV) (Complex **102**)

0.78 g pre-catalyst **115** was used, and 0.86 g black catalyst was prepared (yield 95%). FT-IR (neat) v/cm^{-1}: 1600, 1545, 1440, 1388, 1272, 911, 817, 763, 643, 509, 446. The peak at 967 of V=O stretch had disappeared by comparison with the IR of pre-catalyst **115**.

6.4.5 General procedure for imine synthesis

Catalyst **102** (11.6 mg, 0.03 mmol), $MgSO_4$ (20.7 mg, 0.20 mmol) and 4Å molecular sieves (150 mg) were placed in an oven-dried tube, where after it was placed in a carousel. Vacuum was applied and the flask was then filled with nitrogen gas (repeated 3 times). Degassed toluene (4 mL) was added and the reaction mixture was heated to reflux. Alcohol (1 mmol), amine (1 mmol) and tetradecane (0.5 mmol, as internal standard) were added by a syringe, and the reaction was refluxed with stirring under a flow of nitrogen for 48 h. The mixture was cooled to room temperature and the solvent was removed in vacuum. The crude products were purified by silica gel column chromatography (hexane with 2% NEt_3) to afford the desired imines.

6.4.6 Gas development

Catalyst **102** (11.6 mg, 0.03 mmol), $MgSO_4$ (20.7 mg, 0.20 mmol), and 4Å molecular sieves (150 mg) were placed in an oven-dried Schlenk tube. The tube was subjected to vacuum and then filled with nitrogen gas (repeated 3 times). Degassed toluene (4 mL) was added and the reaction mixture were heated to reflux. Benzyl alcohol (108 mg, 1 mmol) and cyclohexylamine (99 mg, 1 mmol) were added. The Schlenk tube was connected with a tube and the other end of the tube was connected to the bottom of a burette filled with water. The bottom of the burette was further connected to a water reservoir with a large surface area. A total of 16 mL gas was collected after the reaction was refluxed for 48 h, and the GC yield of the reaction was more than 90%. The identity of the gas was established through a ^{1}H-NMR spectrum (Figure 6.2) in $CDCl_3$ where a peak at 4.05 ppm was obtained. Thus, the gas collected was hydrogen gas.

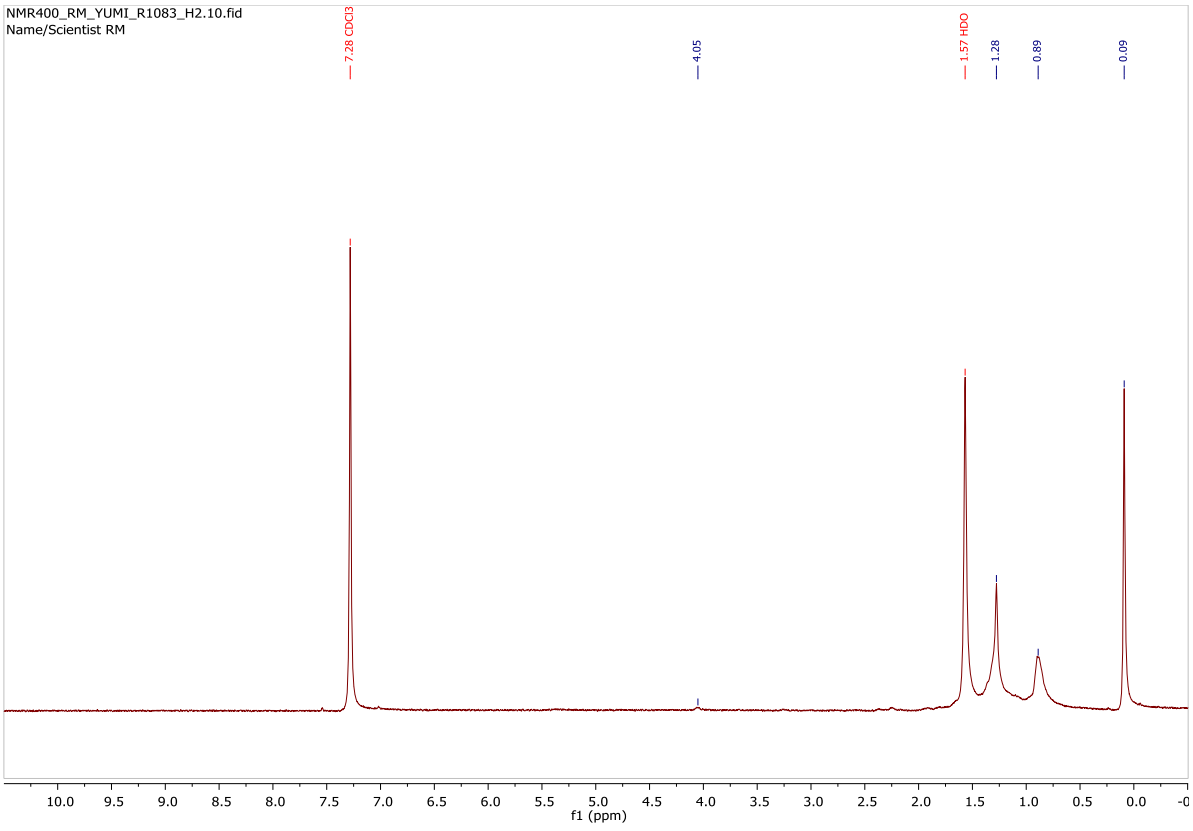

Figure 6.2. ^{1}H-NMR spectrum of collected gas (hydrogen).

6.4.7 Identifying the type of reaction

To investigate the type of the reaction, two standard reactions were set up, where 2,4-diphenyl-4-methyl-1-pentane (DPMP) and butylated hydroxytoluene (BHT) were applied in the reaction, respectively (Scheme 6.13). Two samples were prepared and tested in GC when the reactions were finished, but there were no other products obtained than the desired imine, which means that the reaction is not a radical reaction.

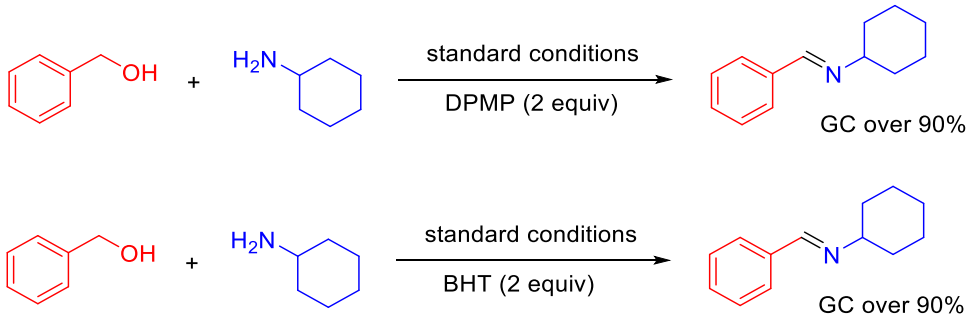

Scheme 6.13. Identifying the reaction type.

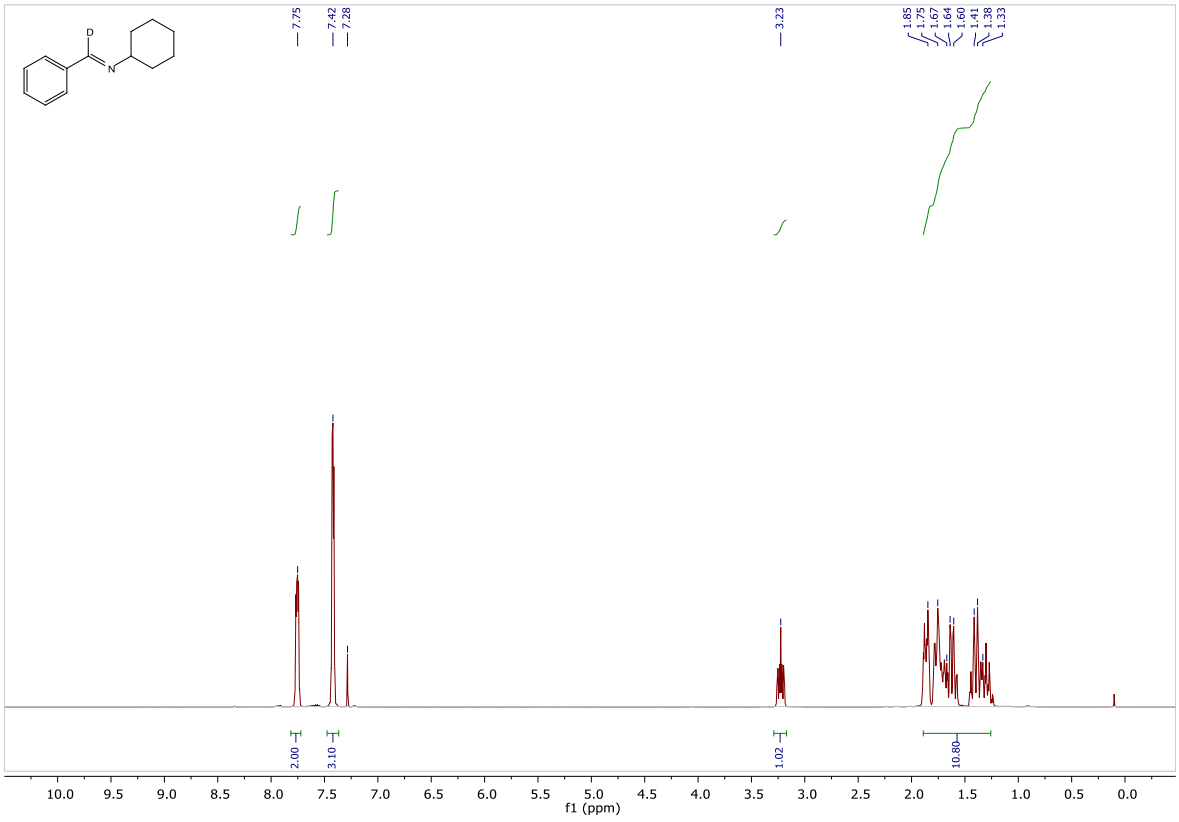

Figure 6.3. ^{1}H-NMR spectrum of *N*-benzylidenecyclohexylamine-α-d_1.

6.4.8 Deuterium labelling study

Benzyl alcohol-α,α-d_2 (110 mg, 1.0 mmol) and cyclohexylamine (99.0 mg, 1.0 mmol) were placed in an oven-dried tube and subjected to the imination reaction following the general procedure for imine synthesis. When the reaction was finished, the GCMS result showed that there was only one peak for the product, and the MS was 188, which means that there should be only one deuterium atom in the product. After purification of the product imine (137.2 mg, 73%), examination of the ^{1}H-NMR spectrum (Figure 6.3) revealed that the product imine was obtained as a pure deuterium-labeled imine and no hydrogen/deuterium scrambling had occurred.

6.4.9 Kinetic Isotope Effect (KIE)

To determine the kinetic isotope effect, the reaction was performed as the general procedure for imine synthesis. A dried tube was charged with catalyst **102** (11.6 mg, 0.03 mmol), $MgSO_4$ (20.7 mg, 0.2 mmol), and 4Å molecular sieves (150 mg) and placed in a Radleys carousel on a hotplate. The tube was evacuated and then filled with N_2 gas (repeated 3 times). Freshly degassed toluene (4 mL) was injected into the tube followed by heating to 120 °C under a N_2 atmosphere. Benzyl alcohol (108 mg, 1.0 mmol), cyclohexylamine (99 mg, 1.0 mmol) and tetradecane (0.13 ml, 0.5 mmol) were added, and then the reaction was monitored by GC for 5 h. A sample of 50 μL was removed every hour, transferred to a GC vial, diluted to 1 mL with diethyl ether and then subjected to GCMS analysis to follow the formation of *N*-benzylidenecyclohexylamine and determine the initial rate (r). The same procedure was performed using benzyl alcohol-α,α-d_2 (110 mg, 1.0 mmol) instead of non-deuterated benzyl alcohol. Assuming that no by-product was formed, the initial rate for the transformation of benzyl alcohol was $r_H = 9.00\ 10^{-4}$, and the initial rate for the reaction of benzyl alcohol-α,α-d_2 was $r_D = 4.00\ 10^{-4}$, and thus the value of the KIE (k_H/k_D) was 2.3.

6.4.10 Catalyst deuterium labelling

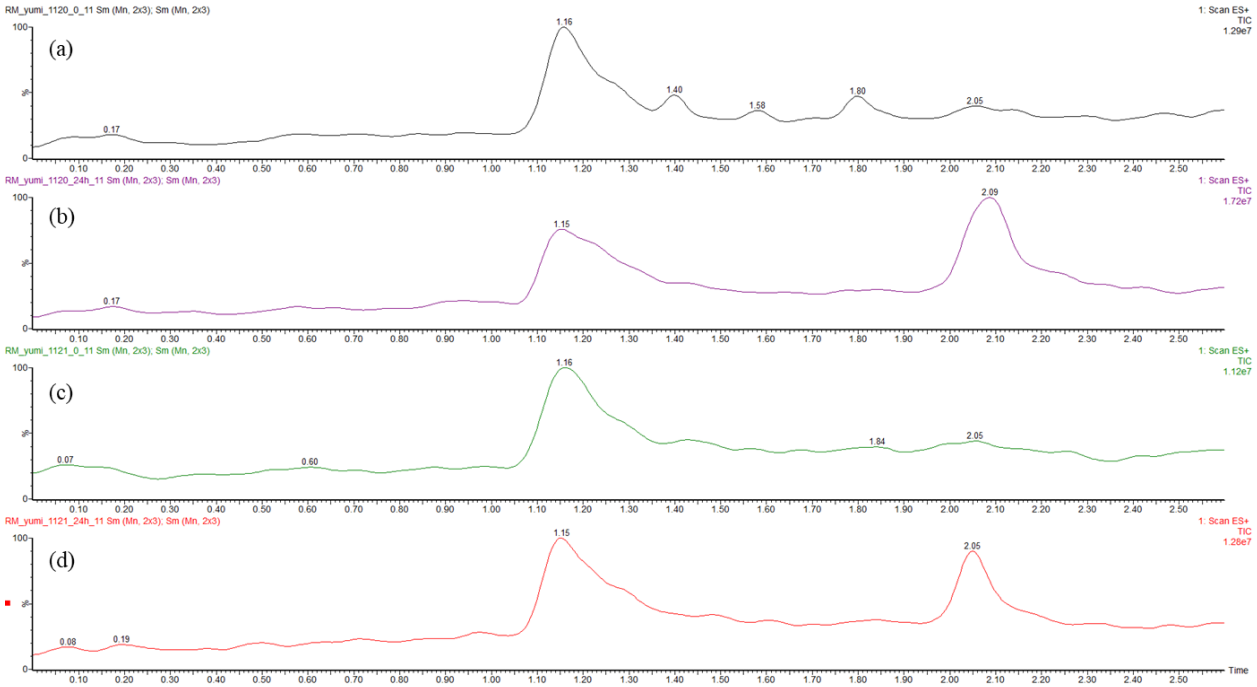

Figure 6.4. Different LCMS chromatograms: a) The sample from the reaction with BnOH at t = 0. b) The sample from the reaction with BnOH at t = 24 h. c) The sample from the reaction with BnOH-α,α-d_2 at t = 0. d) The sample from the reaction with BnOH-α,α-d_2 at t = 24 h.

The peak with retention time 2.10 min belongs to the product (*N*-benzylidenecyclohexylamine). The mass spectra of the catalyst region with retention time 1.15 - 1.20 min are presented in Figure 6.5.

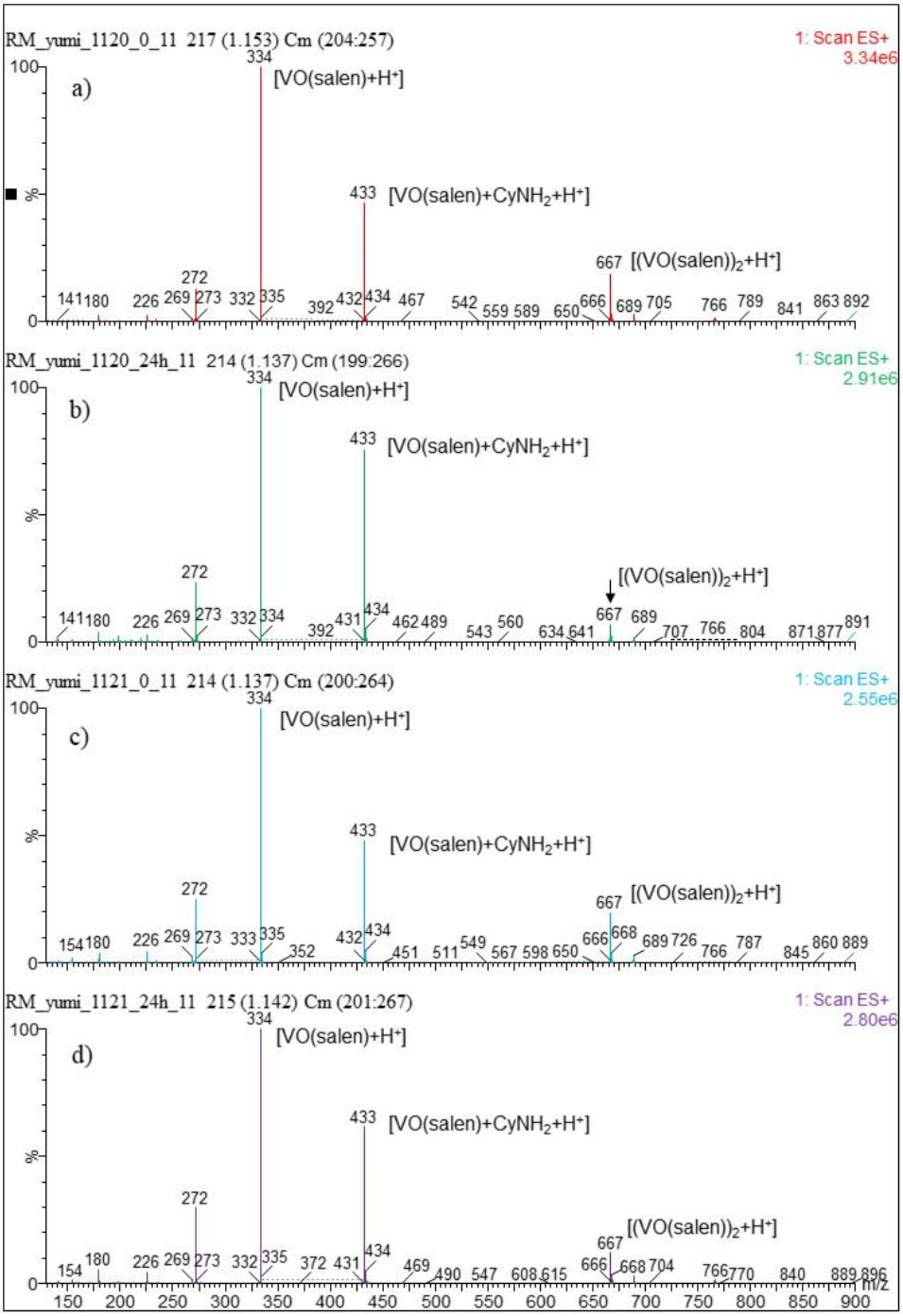

Figure 6.5. Mass spectra of the catalyst region with retention time 1.15 – 1.20 min. a) Reaction with catalyst **102** and BnOH at t = 0. b) Reaction with catalyst **102** and BnOH at t = 24 h. c) Reaction with catalyst **102** and BnOH-α,α-d_2 at t = 0. d) Reaction with catalyst **102** and BnOH-α,α-d_2 at t = 24 h.

The observed masses do not differ when BnOH-α,α-d_2 is used, and thus no incorporation of deuterium into the ligand could be detected.

6.4.11 Characterization data for imines

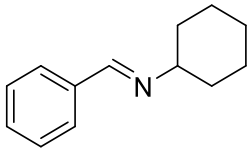

***N*-Benzylidenecyclohexylamine (Table 6.3, entry 1)**

Following the general procedure for imine synthesis, the product was isolated as a pale yellow liquid. Yield: 157.6 mg (84%). ^{1}H-NMR (400 MHz, $CDCl_3$) δ ppm: 8.34 (s, 1H), 7.78-7.73 (m, 2H), 7.45-7.39 (m, 3H), 3.26-3.19 (m, 1H), 1.90-1.27 (m, 10H). ^{13}C-NMR (100 MHz, $CDCl_3$) δ ppm: 158.6, 136.6, 130.3, 128.5, 128.1, 70.0, 34.4, 25.7, 24.8. MS: m/z = 187 $[M]^+$. NMR data are in accordance with literature values.[167]

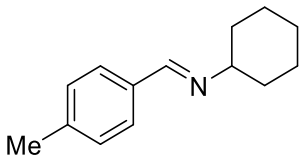

***N*-(4-Methylbenzylidene)-cyclohexylamine (Table 6.3, entry 2)**

Following the general procedure for imine synthesis, the product was isolated as a yellow liquid. Yield: 142.5 mg (71%). ^{1}H-NMR (400 MHz, $CDCl_3$) δ ppm: 8.30 (s, 1H), 7.64 (d, *J* = 7.9 Hz, 2H), 7.25 (d, *J* = 7.9 Hz, 2H), 3.22-3.17 (m, 1H), 2.40 (s, 3H), 1.89-1.26 (m, 10H). ^{13}C-NMR (100 MHz, $CDCl_3$) δ ppm: 158.5, 140.6, 134.0, 129.2, 128.0, 70.0, 34.4, 25.7, 24.9, 21.5. MS: m/z = 201 $[M]^+$. NMR data are in accordance with literature values.[167]

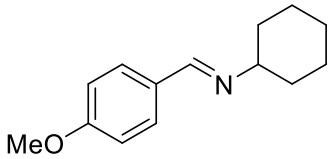

***N*-(4-Methoxybenzylidene)-cyclohexylamine (Table 6.3, entry 3)**

Following the general procedure for imine synthesis, the product was isolated as a yellow liquid. Yield: 157.2 mg (72%). ^{1}H-NMR (400 MHz, $CDCl_3$) δ ppm: 8.27 (s, 1H), 7.69 (d, *J* = 8.7 Hz, 2H), 6.93 (d, *J* = 8.5 Hz, 2H), 3.86 (s, 3H), 3.19-3.15 (m, 1H), 1.90-1.24 (m, 10H). ^{13}C-NMR (100 MHz, $CDCl_3$) δ ppm: 161.4, 158.0, 132.0, 129.6, 113.9, 69.9, 55.4, 34.5, 25.7, 24.9. MS: m/z = 217 $[M]^+$. NMR data are in accordance with literature values.[167]

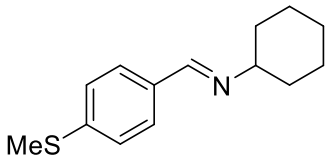

***N*-(4-Methylthiobenzylidene)-cyclohexylamine (Table 6.3, entry 4)**

Following the general procedure for imine synthesis, the product was isolated as a pale yellow liquid. Yield: 174.5 mg (75%). ^{1}H-NMR (400 MHz, $CDCl_3$) δ ppm: 8.28 (s, 1H), 7.66 (d, *J* = 8.3 Hz, 2H), 7.27 (d, *J* = 8.3 Hz, 2H), 3.21-3.17 (m, 1H), 2.52 (s, 3H), 1.90-1.24 (m, 10H). ^{13}C-NMR (100 MHz, $CDCl_3$) δ ppm: 157.9, 141.5, 133.4, 128.4, 125.9, 70.0, 34.4, 25.7, 24.9, 15.4. MS: m/z = 233 $[M]^+$. NMR data are in accordance with literature values.[167]

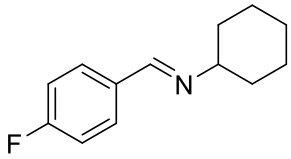

***N*-(4-Fluorobenzylidene)-cyclohexylamine (Table 6.3, entry 5)**

Following the general procedure for imine synthesis, the product was isolated as a yellow liquid. Yield: 155.4 mg (76%). ^{1}H-NMR (400 MHz, $CDCl_3$) δ ppm: 8.30 (s, 1H), 7.73 (dd, *J* = 8.6, 5.6 Hz, 2H), 7.10 (t, *J* = 8.6 Hz, 2H), 3.23-3.19 (m, 1H), 1.86-1.28 (m, 10H). ^{13}C-NMR (100 MHz, $CDCl_3$) δ ppm: 165.3 (d, *J* = 250 Hz), 157.1, 132.9, 129.9 (d, *J* = 10 Hz), 115.7 (d, *J* = 22 Hz), 69.9, 34.3, 25.6, 24.8. MS: m/z = 205 $[M]^+$. NMR data are in accordance with literature values.[167]

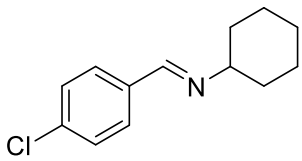

***N*-(4-Chlorobenzylidene)-cyclohexylamine (Table 6.3, entry 6)**

Following the general procedure for imine synthesis, the product was isolated as a white solid. Yield: 134.2 mg (62%). ^{1}H-NMR (400 MHz, $CDCl_3$) δ ppm: 8.29 (s, 1H), 7.68 (d, *J* = 8.4 Hz, 2H), 7.39 (d, *J* = 8.4 Hz, 2H), 3.24-3.19 (m, 1H), 1.90-1.25 (m, 10H). ^{13}C-NMR (100 MHz, $CDCl_3$) δ ppm: 157.2, 136.2, 135.1, 129.2, 128.8, 69.9, 34.3, 25.6, 24.8. MS: m/z = 221 $[M]^+$. NMR data are in accordance with literature values.[167]

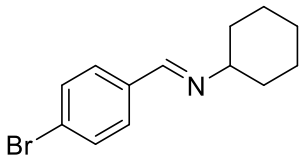

***N*-(4-Bromobenzylidene)-cyclohexylamine (Table 6.3, entry 7)**

Following the general procedure for imine synthesis, the product was isolated as a pale yellow liquid. Yield: 213.5 mg (80%). ^{1}H-NMR (400 MHz, CDCl3) δ ppm: 8.28 (s, 1H), 7.62 (d, *J* = 8.4 Hz, 2H), 7.55 (d, *J* = 8.5 Hz, 2H), 3.23-3.18 (m, 1H), 1.90-1.25 (m, 10H). ^{13}C-NMR (100 MHz, $CDCl_3$) δ ppm: 157.3, 135.5, 131.7, 129.5, 124.6, 70.0, 34.3, 25.6, 24.8. MS: m/z = 265 $[M]^+$. NMR data are in accordance with literature values.[167]

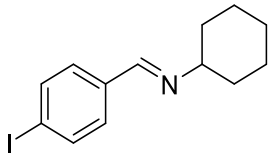

***N*-(4-Iodobenzylidene)-cyclohexylamine (Table 6.3, entry 8)**

Following the general procedure for imine synthesis, the product was isolated as a white solid. Yield: 189.3 mg (60%). ^{1}H-NMR (400 MHz, $CDCl_3$) δ ppm: 8.25 (s, 1H), 7.76 (d, *J* = 8.3 Hz, 2H), 7.47 (d, *J* = 8.3 Hz, 2H), 3.23-3.19 (m, 1H), 1.90-1.24 (m, 10H). ^{13}C-NMR (100 MHz, $CDCl_3$) δ ppm: 157.5, 137.7, 136.1, 129.6, 96.8, 70.0, 34.3, 25.6, 24.8. MS: m/z = 313 $[M]^+$. NMR data are in accordance with literature values.[163]

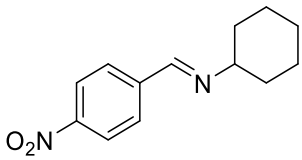

***N*-(4-Nitrobenzylidene)-cyclohexylamine (Table 6.3, entry 9)**

Following the general procedure for imine synthesis, the product was isolated as a pale yellow liquid. Yield: 142.3 mg (65%). ^{1}H-NMR (400 MHz, $CDCl_3$) δ ppm: 8.41 (s, 1H), 8.28 (d, *J* = 8.7 Hz, 2H), 7.91 (d, *J* = 8.7 Hz, 2H), 3.32-3.28 (m, 1H), 1.90-1.27 (m, 10H). ^{13}C-NMR (100 MHz, $CDCl_3$) δ ppm: 156.2, 148.8, 142.2, 128.7, 123.8, 70.2, 34.2, 25.6, 24.6. MS: m/z = 232 $[M]^+$. NMR data are in accordance with literature values.[167]

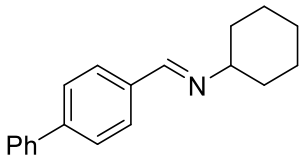

***N*-(4-Phenylbenzylidene)-cyclohexylamine (Table 6.3, entry 10)**

Following the general procedure for imine synthesis, the product was isolated as a pale yellow liquid. Yield: 192.0 mg (73%). ^{1}H-NMR (400 MHz, $CDCl_3$) δ ppm: 8.39 (s, 1H), 7.85-7.81 (m, 2H), 7.66-7.62 (m, 4H), 7.50-7.36 (m, 3H), 3.27-3.23 (m, 1H), 1.89-1.28 (m, 10H). ^{13}C-NMR (100 MHz, $CDCl_3$) δ ppm: 158.2, 143.1, 140.5, 135.6, 128.8, 128.5, 127.7, 127.1, 70.1, 34.4, 25.7, 24.9. MS: m/z = 263 $[M]^+$. NMR data are in accordance with literature values.[163]

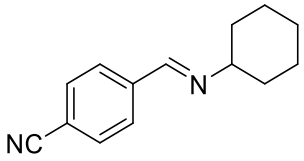

***N*-(4-Cyanobenzylidene)-cyclohexylamine (Table 6.3, entry 11)**

Following the general procedure for imine synthesis, the product was isolated as a clear liquid. Yield: 152.5 mg (72%). ^{1}H-NMR (400 MHz, $CDCl_3$) δ ppm: 8.35 (s, 1H), 7.84 (d, *J* = 8.1 Hz, 2H), 7.70 (d, *J* = 8.1 Hz, 2H), 3.28-3.26 (m, 1H), 1.89-1.26 (m, 10H). ^{13}C-NMR (100 MHz, $CDCl_3$) δ ppm: 156.6, 140.5, 132.3, 128.5, 118.6, 113.5, 70.0, 34.2, 25.6, 24.6. MS: m/z = 212 $[M]^+$. NMR data are in accordance with literature values.[34]

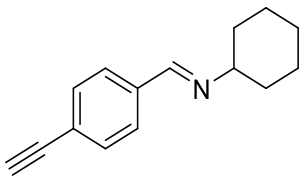

***N*-(4-Ethynyl)-cyclohexylamine (Table 6.3, entry 12)**

Following the general procedure for imine synthesis, the product was isolated as a clear liquid. Yield: 145.5 mg (69%). ^{1}H-NMR (400 MHz, $CDCl_3$) δ ppm: 8.31 (s, 1H), 7.71 (d, *J* = 8.2 Hz, 2H), 7.54 (d, *J* = 8.2 Hz, 2H), 3.24-3.22 (m, 1H), 3.18 (s, 1H), 1.89-1.28 (m, 10H). ^{13}C-NMR (100 MHz, $CDCl_3$) δ ppm: 157.7, 136.9, 132.3, 127.9, 123.9, 83.4, 78.7, 70.0, 34.3, 25.6, 24.8. MS: m/z = 211 $[M]^+$. NMR data are in accordance with literature values.[34]

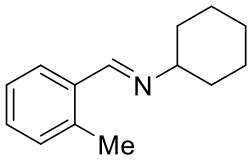

***N*-(2-Methylbenzylidene)-cyclohexylamine (Table 6.3, entry 13)**

Following the general procedure for imine synthesis, the product was isolated as a clear liquid. Yield: 142.3 mg (71%). ^{1}H-NMR (400 MHz, $CDCl_3$) δ ppm: 8.65 (s, 1H), 7.88 (dd, *J* = 7.5, 1.4 Hz, 2H), 7.30-7.15 (m, 3H), 3.25-3.21 (m, 1H), 2.52 (s, 3H), 1.87-1.30 (m, 10H). ^{13}C-NMR (100 MHz, $CDCl_3$) δ ppm: 157.0, 137.3, 134.7, 130.6, 129.9, 127.1, 126.2, 70.5, 34.5, 25.7, 24.8, 19.3. MS: m/z = 201 $[M]^+$. NMR data are in accordance with literature values.[163]

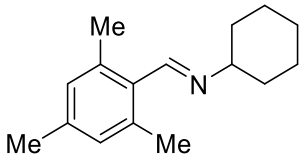

***N*-(2,4,6-Trimethylbenzylidene)-cyclohexylamine (Table 6.3, entry 14)**

Following the general procedure for imine synthesis, the product was isolated as a clear liquid. Yield: 165.0 mg (72%). ^{1}H-NMR (400 MHz, $CDCl_3$) δ ppm: 8.59 (s, 1H), 6.87 (s, 2H), 3.23-3.20 (m, 1H), 2.37 (s, 6H), 2.29 (s, 3H), 1.90-1.32 (m, 10H). ^{13}C-NMR (100 MHz, $CDCl_3$) δ ppm: 158.4, 138.2, 136.9, 131.9, 129.0, 70.9, 34.7, 25.7, 24.7, 21.1, 20.3. MS: m/z = 229 $[M]^+$. NMR data are in accordance with literature values.[163]

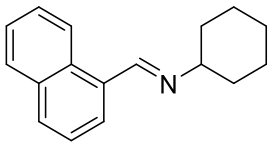

***N*-(1-Naphthalenylmethylene)-cyclohexylamine (Table 6.3, entry 15)**

Following the general procedure for imine synthesis, the product was isolated as a yellow liquid. Yield: 162.4 mg (69%). ^{1}H-NMR (400 MHz, $CDCl_3$) δ ppm: 9.02 (s, 1H), 8.91 (d, *J* = 8.5 Hz, 1H), 7.94-7.90 (m, 3H), 7.63-7.52 (m, 3H), 3.36-3.31 (m, 1H), 1.95-1.72 (m, 7H), 1.50-1.33 (m, 3H). ^{13}C-NMR (100 MHz, $CDCl_3$) δ ppm: 157.9, 133.8, 132.2, 131.4, 130.6, 128.6, 128.3, 126.9, 125.9, 125.3, 124.3, 70.9, 34.6, 25.8, 24.8. MS: m/z = 237 $[M]^+$. NMR data are in accordance with literature values.[167]

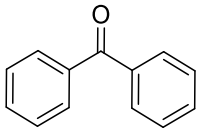

Benzophenone (Table 6.3, entry 16)

Following the general procedure for imine synthesis, the product was isolated as a clear liquid. Yield: 132.4 mg (73%). ^{1}H-NMR (400 MHz, $CDCl_3$) δ ppm: 7.85-7.83 (m, 4H), 7.65-7.59 (m, 2H), 7.54-7.48 (m, 4H). ^{13}C-NMR (100 MHz, $CDCl_3$) δ ppm: 196.8, 137.6, 132.4, 130.1, 128.3. MS: m/z = 182 $[M]^+$. NMR data are in accordance with literature values.[310]

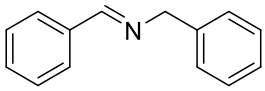

***N*-Benzylidenebenzylamine (Table 6.4, entry 1)**

Following the general procedure for imine synthesis, the product was isolated as a clear liquid. Yield: 121.3 mg (62%). ^{1}H-NMR (400 MHz, $CDCl_3$) δ ppm: 8.45 (s, 1H), 7.86-7.81 (m, 2H), 7.47 (dd, *J* = 5.1, 1.9 Hz, 3H), 7.39 (d, *J* = 4.3 Hz, 4H), 7.33-7.31 (m, 1H), 4.88 (s, 2H). ^{13}C-NMR (100 MHz, $CDCl_3$) δ ppm: 162.0, 139.3, 136.2, 130.8, 128.6, 128.3, 128.0, 127.0, 65.1. MS: m/z = 195 $[M]^+$. NMR data are in accordance with literature values.[163]

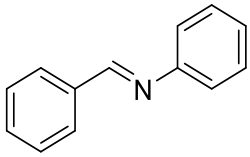

***N*-Benzylideneaniline (Table 6.4, entry 2)**

Following the general procedure for imine synthesis, the product was isolated as a white solid. Yield: 110.5 mg (61%). ^{1}H-NMR (400 MHz, $CDCl_3$) δ ppm: 8.49 (s, 1H), 7.98-7.94 (m, 2H), 7.54-7.49 (m, 3H), 7.46-7.41 (m, 2H), 7.30-7.24 (m, 3H). ^{13}C-NMR (100 MHz, $CDCl_3$) δ ppm: 160.4, 152.0, 136.1, 131.5, 129.2, 128.8, 126.0, 120.9. MS: m/z = 181 $[M]^+$. NMR data are in accordance with literature values.[167]

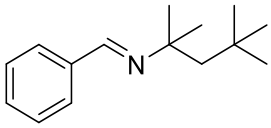

***N*-Benzylidene-*tert*-octylamine (Table 6.4, entry 3)**

Following the general procedure for imine synthesis, the product was isolated as a clear liquid. Yield: 153.4 mg (71%). ^{1}H-NMR (400 MHz, $CDCl_3$) δ ppm: 8.27 (s, 1H), 7.80-7.75 (m, 2H), 7.46-7.40 (m, 3H), 1.72 (s, 2H), 1.35 (s, 6H), 0.98 (s, 9H). ^{13}C-NMR (100 MHz, $CDCl_3$) δ ppm: 154.4, 137.4, 130.0, 128.5, 127.9, 61.0, 56.6, 32.1, 31.8, 29.7. MS: m/z = 216 $[M-H]^+$. NMR data are in accordance with literature values.[167]

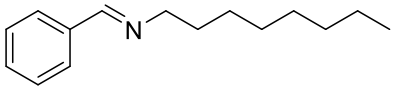

***N*-Benzylidene-octylamine (Table 6.4, entry 4)**

Following the general procedure for imine synthesis, the product was isolated as a yellow liquid. Yield: 145.6 mg (67%). ^{1}H-NMR (400 MHz, $CDCl_3$) δ ppm: 8.30 (s 1H), 7.76-7.74 (m, 2H), 7.46-7.42 (m, 3H), 3.64 (td, *J* = 7.0, 1.4 Hz, 2H), 1.75-1.71 (m, 2H), 1.39-1.29 (m, 10H), 0.91-0.89 (m, 3H). ^{13}C-NMR (100 MHz, $CDCl_3$) δ ppm: 160.7, 136.4, 130.4, 128.6, 128.0, 61.9, 31.9, 31.0, 29.5, 27.4, 22.7, 14.1. MS: m/z = 216 $[M-H]^+$. NMR data are in accordance with literature values.[167]

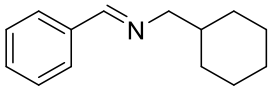

***N*-Benzylidene-cyclohexylmethylamine (Table 6.4, entry 5)**

Following the general procedure for imine synthesis, the product was isolated as a pale yellow liquid. Yield: 149.4 mg (74%). ^{1}H-NMR (400 MHz, $CDCl_3$) δ ppm: 8.25 (s, 1H), 7.76-7.74 (m, 2H), 7.46-7.42 (m, 3H), 3.49 (d, *J* = 6.4 Hz, 2H), 1.84-1.72 (m, 6H), 1.34-1.20 (m, 3H), 1.08-0.96 (m, 2H). ^{13}C-NMR (100 MHz, $CDCl_3$) δ ppm: 160.8, 136.4, 130.4, 128.6, 128.0, 68.7, 39.0, 31.5, 26.6, 26.1. MS: m/z = 201 $[M]^+$. NMR data are in accordance with literature values.[70]

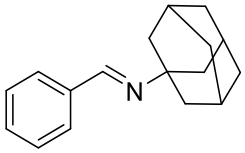

***N*-Benzylidene-1-adamantanylamine (Table 6.4, entry 6)**

Following the general procedure for imine synthesis, the product was isolated as a white solid. Yield: 175.5 mg (73%). ^{1}H-NMR (400 MHz, $CDCl_3$) δ ppm: 8.31 (s, 1H), 7.77 (bs, 2H), 7.43-7.40 (m, 3H), 2.20 (s, 3H), 1.85 (s, 6H), 1.83-1.70 (m, 6H). ^{13}C-NMR (100 MHz, $CDCl_3$) δ ppm: 154.9, 137.3, 130.1, 128.5, 127.9, 57.5, 43.2, 36.2, 29.6. MS: m/z = 239 $[M]^+$. NMR data are in accordance with literature values.[167]

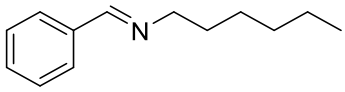

***N*-Benzylidene-hexylamine (Table 6.4, entry 7)**

Following the general procedure for imine synthesis, the product was isolated as a pale yellow solid. Yield: 136.2 mg (72%). ^{1}H-NMR (400 MHz, $CDCl_3$) δ ppm: 8.30 (s, 1H), 7.77-7.74 (m, 2H), 7.45-7.41 (m, 3H), 3.64 (td, *J* = 7.0, 1.2 Hz, 2H), 1.75-1.71 (m, 2H), 1.39-1.33 (m, 6H), 0.93-0.89 (m, 3H). ^{13}C-NMR (100 MHz, $CDCl_3$) δ ppm: 160.7, 136.4, 130.4, 128.6, 128.0, 61.9, 31.7, 31.9, 27.1, 26.4, 14.1. MS: m/z = 188 $[M-H]^+$. NMR data are in accordance with literature values.[311]

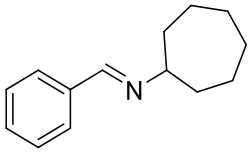

***N*-Benzylidenecycloheptylamine (Table 6.4, entry 8)**

Following the general procedure for imine synthesis, the product was isolated as a clear liquid. Yield: 140.3 mg (70%). ^{1}H-NMR (400 MHz, $CDCl_3$) δ ppm: 8.29 (s, 1H), 7.78-7.74 (m, 2H),7.45-7.40 (m, 3H), 3.40-3.36 (m, 1H), 1.84-1.61 (m, 12H). ^{13}C-NMR (101 MHz, $CDCl_3$) δ ppm: 157.7, 136.7, 130.3, 128.5, 128.1, 72.6, 36.4, 28.4, 24.8. MS: m/z = 201 $[M]^+$. ^{1}H-NMR data are in accordance with literature values.[260]

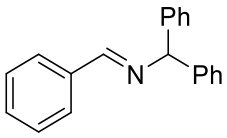

_N_-Benzylidene-1,1-diphenylmethylamine (Table 6.4, entry 9)

Following the general procedure for imine synthesis, the product was isolated as a white solid. Yield: 189.4 mg (70%). ^{1}H-NMR (400 MHz, $CDCl_3$) δ ppm: 8.46 (s, 1H), 7.89-7.85 (m, 2H), 7.46-7.40 (m, 7H), 7.40-7.31 (m, 4H), 7.30-7.25 (m, 2H), 5.63 (s, 1H). ^{13}C-NMR (100 MHz, $CDCl_3$) δ ppm: 160.8, 143.9, 136.3, 130.7, 128.5, 128.4, 127.7, 127.0, 77.9. MS: m/z = 271 $[M]^+$. NMR data are in accordance with literature values.[167]

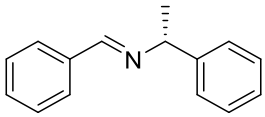

(R)-_N_-Benzylidene-1-phenylethylamine (Table 6.4, entry 10)

Following the general procedure for imine synthesis, the product was isolated as a clear liquid.

Yield: 154.5 mg (74%). $[\alpha]_D^{20}$ = -68.0 (c = 1.58, $CHCl_3$) (ref.[312] $[\alpha]_D^{27}$ = -64.7 (c = 1.0, $CHCl_3$). ^{1}H-NMR (400 MHz, $CDCl_3$) δ ppm: 8.42 (s, 1H), 7.86-7.81 (m, 2H), 7.51-7.26 (m, 8H), 4.60 (q, J = 6.6 Hz, 1H), 1.65 (d, J = 6.7 Hz, 3H). ^{13}C-NMR (101 MHz, $CDCl_3$) δ ppm: 159.5, 145.2, 136.5, 130.6, 128.6, 128.5, 128.3, 126.9, 126.7, 69.8, 24.9. MS: m/z = 209 $[M]^+$. NMR data are in accordance with literature values.[167]

7. Conclusion

The purpose of this project was to develop novel and inexpensive catalysts based on Earth-abundant transition metals for acceptorless dehydrogenative transformations of alcohols.

As a result, two novel catalysts based on chromium (complex **87**) and vanadium (complex **102**) have been developed for the dehydrogenative synthesis of imines, respectively. Catalyst **87** is the first example of a chromium(III) complex for acceptorless alcohol dehydrogenation. The reaction mechanism has been investigated thoroughly, and a MLC pathway has been proposed. Catalyst **102** constitutes an example of a vanadium catalyst for the acceptorless dehydrogenation of alcohols. Even though the reaction mechanism is not clear, the catalyst has a very good performance on the dehydrogenation of alcohols.

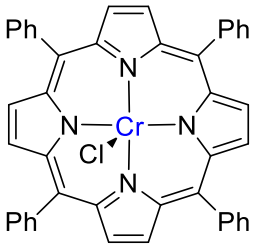

87

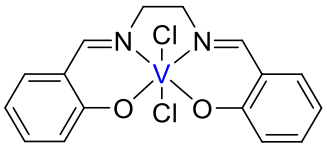

102

In summary, this study has contributed to two novel and more sustainable catalysts as an alternative to the traditional oxidants in organic synthesis.

8. Appendix

8.1 External stay at Haldor Topsøe A/S

The following work was performed at Haldor Topsøe A/S as an external stay under the supervision of manager Dr. Søren Tolborg and director Dr. Esben Taarning in R&D. The work was performed in collaboration with former Ph.D. students in the group, Fabrizio Bottaro and Simone V. Samuelsen.

Dehydrogenation and hydrogenation are vital reactions in organic chemistry. As mentioned in the thesis, many reactions involving dehydrogenation are introduced. Therefore, we decided to investigate whether the already described complexes **48**, **85-87** as well as complexes **116-120**, which either already has been investigated or is currently being investigated in the Madsen group for potential use as dehydrogenation catalysts (Scheme 8.1), could mediate the reduction of different unsaturated functional groups under a hydrogen atmosphere.

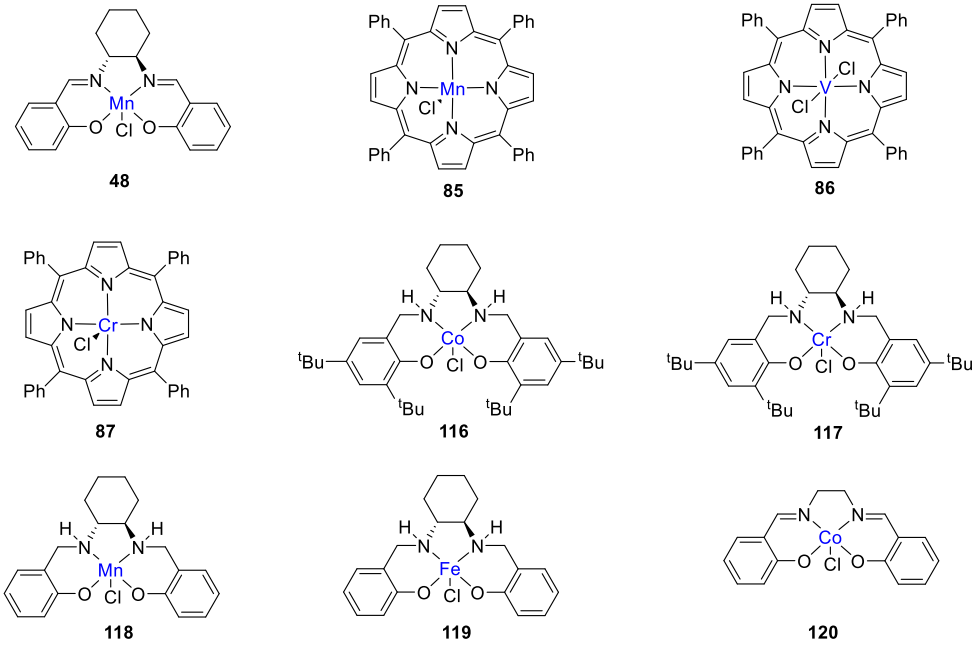

Scheme 8.1. Complexes investigated in hydrogenation reactions.

In our investigation, an ester, an imine, a ketone, and a nitrile were selected as substrates for our hydrogenation reactions. The reactions were carried out with 5% catalyst and 20% ^{t}BuOK under 50 bar of H_2 in refluxing toluene (Scheme 8.2).

Unfortunately, regardless of the harsh conditions, none of the complexes showed any activity in any of the four investigated transformations. Thus, although salen, salan and porphyrin complexes are able to catalyze the dehydrogenation of alcohols, they are unable to mediate the reverse hydrogenation reaction.

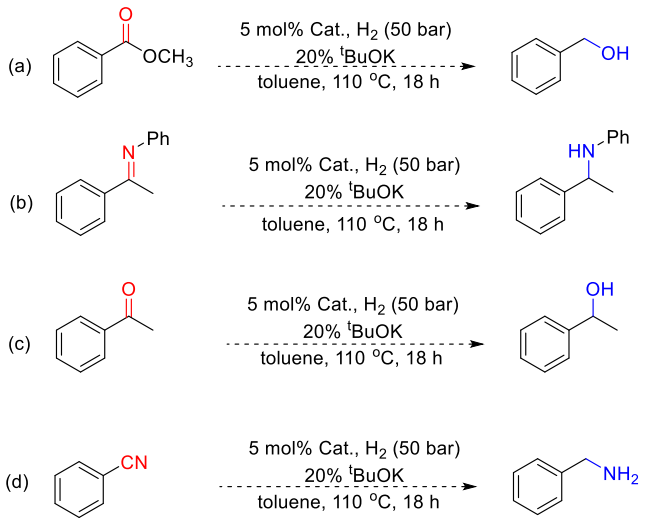

Scheme 8.2. Attempted hydrogenations of a) an ester, b) an imine, c) a ketone and d) a nitrile.

Experimental section

General experimental methods

All commercial reagents were purchased from Sigma-Aldrich or Strem Chemicals and used as received. GC-MS was carried out on a Shimadzu GCMS-QP2010S instrument fitted with an Equity 5.30m×0.25mm×0.25um column. All experiments were carried out under hydrogen pressure in a Parr reactor.

General procedure

Methyl benzoate (0.88 ml, 7 mmol), *N*-(α-methylhenzylidene)aniline (1365 mg, 7 mmol), acetophenone (0.84 ml, 7 mmol) or benzonitrile (0.72 ml, 7 mmol), complex (0.35 mmol), ^{t}BuOK (140 mg, 1.4 mmol), tetradecane (0.7 ml, as internal standard) and toluene (16 ml) were placed in an oven-dried Parr reactor. Vacuum was applied and the reactor was then filled with nitrogen gas (repeated three times) and subsequently with H_2 (50 bar). The reaction was stirred for 18 h, after wihch time the mixture was cooled to room temperature and the H_2 gas was carefully released. The reaction mixture was tested by GC-MS.

8.2 Other projects conducted

A project on the synthesis of ^{t}BuOK catalyzed α-alkylation of ketones from alcohols and acetylenes was also performed during my Ph.D. studies. However, it was unlucky that the Milstein group just reported the work in Angew. Chem. Int. Ed. three weeks in advance.[313]

8.2.1 Introduction

α-Alkylated ketones are a very important class of compounds, that have a wide range of pharmacological and physiological activities.[314–316] Traditionally, α-alkylated ketones are synthesized via α-alkylation of enolates derived from ketones with alkyl halides in the presence of at least a stoichiometric amount of a strong base.[317] However, these procedures suffer from the toxicity of alkyl halides and the generation of a great number of harmful waste salts.

Alternatively, alcohols can be efficiently used for the α-alkylation of ketones with a catalyst, where KOH and metal salts can be employed as the catalysts (Scheme 8.3 a and b).[313,318] However, these methods may require a stoichiometric catalyst, which could cause waste. There is a new trend to apply precious metal catalysts in the alkylation reactions (Scheme 8.3c).[319,320] Although used in low loadings, these organometallic complexes are expensive. Despite significant progress, this reaction is limited to ketones as the starting materials. Herein, a new C-C bond-forming reaction of benzyl alcohols with alkynes is explored in the presence of ^{t}BuOK as shown in Scheme 8.3d.

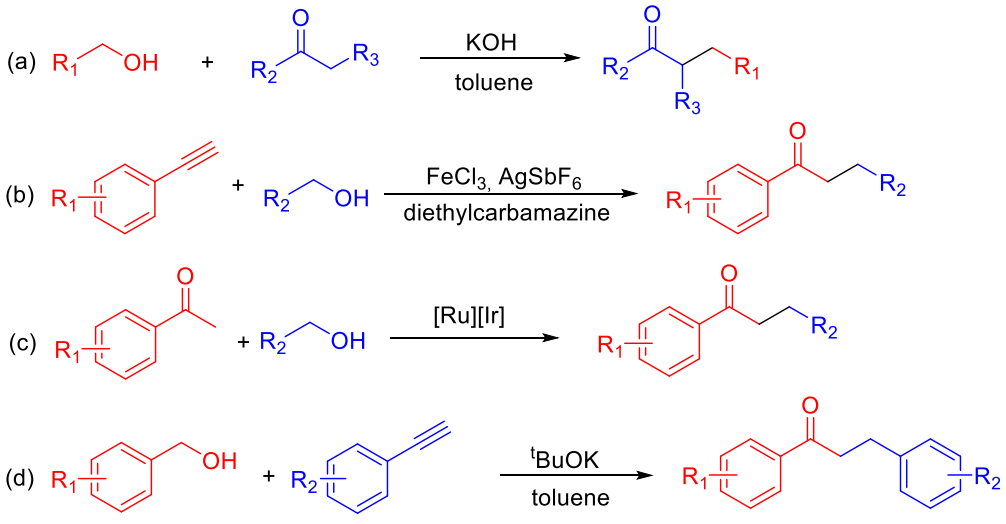

Scheme 8.3. a) C-alkylation of alcohols and ketones with KOH. b) C-alkylation of alcohols and alkyne. c) Precious metal catalyzed reaction of alcohols and ketones. d) Reaction discovered herein.

8.2.2 Optimization of the reaction conditions

Initially, benzyl alcohol (1 mmol) and phenyl acetylene (1 mmol) were selected as starting materials, and the reaction was run in toluene for 24 h with 5 mol% of catalysts **48** and **121** (Scheme 8.4). Three different bases were first employed in the reaction (entry 1-6), and it seemed that ^{t}BuOK had a positive influence on the reaction. To lower the reaction temperature, THF and acetonitrile were chosen as the solvent. However, there was no product detected (entry 7-10). It seemed that toluene was a suitable solvent in the reaction. Blank reactions were then performed (entry 11 and 12). There was still a good yield with only the base, which may indicate that the reaction does not need any catalyst, but only a base.

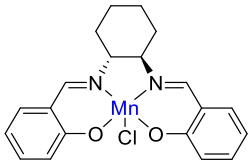

48

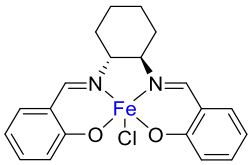

121

Scheme 8.4. Catalysts inverstigated for the coupling reaction.

Table 8.1. Optimization of the coupling reaction.[a]

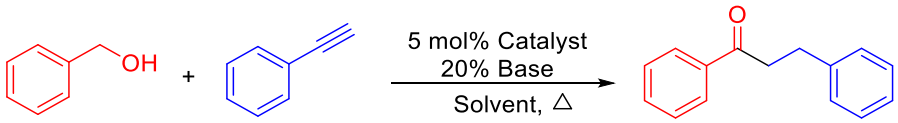

Entry	Catalyst	X	Base	Solvent	T/°C	t/h	Yield[%][b]
1	**48**	5	^{t}BuOK	toluene	120	24	43
2	**121**	5	^{t}BuOK	toluene	120	24	33
3	**48**	5	Cs_2CO_3	toluene	120	24	0
4	**121**	5	Cs_2CO_3	toluene	120	24	0
5	**48**	5	K_2CO_3	toluene	120	24	0
6	**121**	5	K_2CO_3	toluene	120	24	0
7	**48**	5	^{t}BuOK	THF	70	24	0
8	**121**	5	^{t}BuOK	THF	70	24	0
9	**48**	5	^{t}BuOK	CH_3CN	85	24	0
10	**121**	5	^{t}BuOK	CH_3CN	85	24	0
11	-	-	^{t}BuOK	toluene	120	24	51
12	-	-	-	toluene	120	24	0

[a] Reaction conditions: BnOH (1 mmol), PhCCH (1 mmol), catalyst (0.0X mmol), base (0.2 mmol), tetradecane (0.5 mmol, internal standard), solvent, reflux, 48 h. [b] Determined by GC.

To obtain improved conditions for the reaction, different bases were applied into the reaction without any catalyst (Table 8.2). From entry 1-3, three strong bases were used, and there was a high yield with ^{t}BuOK. There was still no conversion when the solvents with a low boiling point were employed in the reaction in the presence of ^{t}BuOK (entry 4 and 5). Thus, it seemed that ^{t}BuOK and toluene (high-boiling-point solvent) were the best choice.

Associate Professor Dr. Søren Kramer pointed out that the same results had just been published when I gave a presentation about the preliminary results of the coupling reaction at the Monday Morning Meeting at the department in March 2019, and then this project was abandoned.

Table 8.2. Optimization of the coupling reaction.[a]

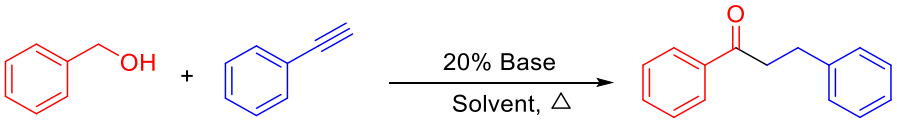

Entry	Base	Solvent	T/°C	t/h	Yield[%][b]
1	^{t}BuOK	toluene	120	24	51
2	KOH	toluene	120	24	43
3	NaOH	toluene	120	24	16
4	^{t}BuOK	THF	70	24	0
5	^{t}BuOK	CH_3CN	85	24	0

[a] Reaction conditions: BnOH (1 mmol), PhCCH (1 mmol), base (0.2 mmol), tetradecane (0.5 mmol, internal standard), solvent, reflux, 48h. [b] Determined by GC.

8.2.3 The article published by Milstein

In Milstein's report, the reaction could tolerate different benzyl alcohols and alkynes (Scheme 8.5), and the conditions were ^{t}BuOK (0.05 mmol), alcohol (1 mmol), alkyne (1 mmol), toluene (2 mL), 24 h, 125 °C. Product yields were determined by ^{1}H-NMR using mesitylene as an internal standard or as isolated yields. The reaction proceeded through a radical pathway (Scheme 8.6).

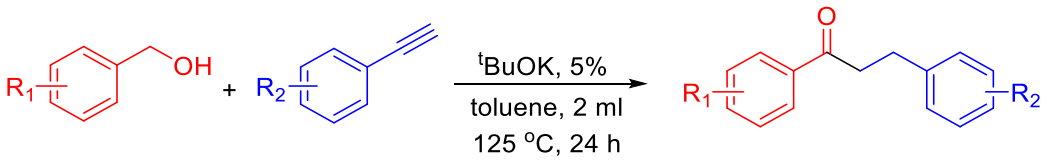

Scheme 8.5. Formation of α-alkylated ketones

Based on physical experiments and DFT calculations, a mechanism was proposed. It was suggested that the first step was the deprotonation of benzyl alcohol by ^{t}BuOK to form $PhCH_2OK$. The reaction was initiated by hydrogen-atom transfer (HAT) from $PhCH_2O^-$ to phenylacetylene to form radicals **122** and **123**.[321,322] In terms of the radical chain cycle, the alkoxide radical **122** inserted into phenylacetylene to form **124**. The radical **124** underwent a 1,2-hydrogen shift to form **125**, and **124** and **125** could then be converted into **126** through 1,3 and 1,2-hydrogen shifts, respectively. Radical **126** was related to radical **127** by resonance. Radical **127** could then be protonated by $PhCH_2OH$ to form the radical **128** and the $PhCH_2O^-$ anion. The $PhCH_2O^-$ anion could transfer a hydrogen radical to **128** to form **129** and regenerate **122**. The product could then be formed from **129** upon tautomerization. It was very likely that the reaction was driven by the highly favorable thermodynamics of the product formation, as the ΔG value of the overall reaction was found to be -36.5 kcal mol^{-1}. The values of ΔG presented herein were only for the purpose of comparing the relative energy of the intermediates, as potassium was excluded from the calculation for the sake of simplicity. It was believed that the stability of the radical intermediates, such as **122** and **124**, is critical for the formation of α-alkylated ketones, since the reaction scope was limited to benzylic alcohols, where the radicals derived from were stabilized by resonance with the phenyl ring.

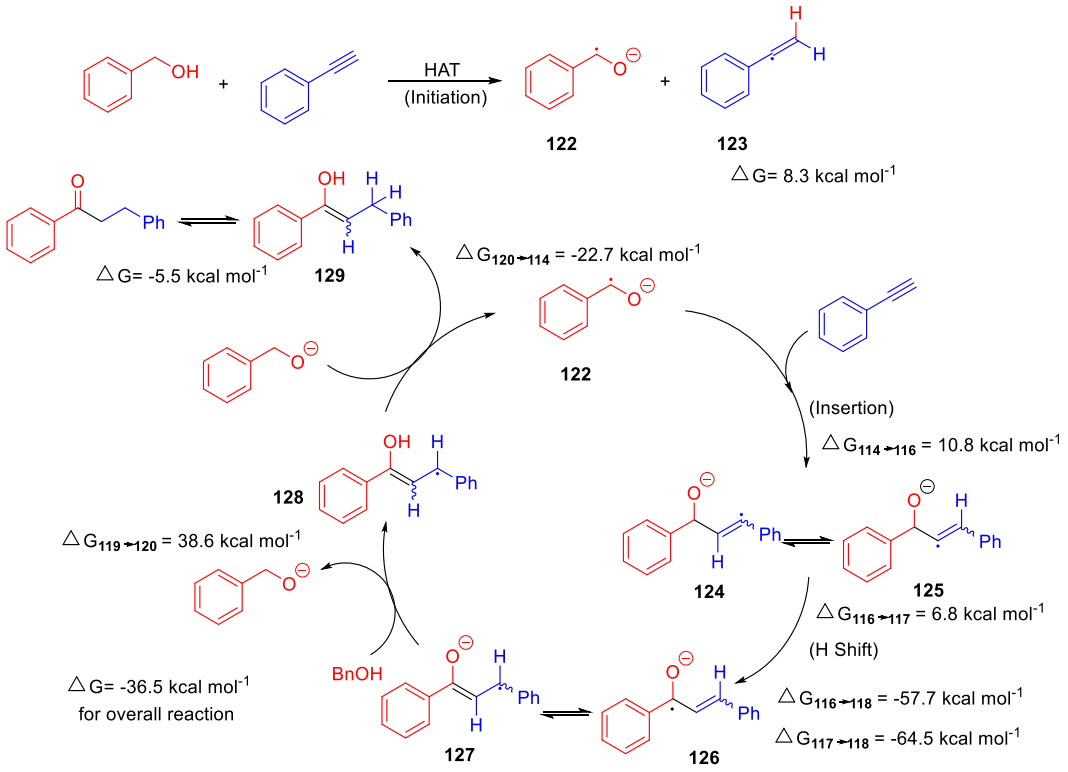

Scheme 8.6. Proposed mechanism for the reaction of benzyl alcohol and phenylacetylene with ^{t}BuOK

8.2.4 Supporting information

Take entry 1 in Table 8.2 as an example, a GCMS sample was prepared when the reaction was finished. From the results in Figure 8.1 and comparison with the standard compound, these peaks can be recognized: peak a, b, and c belong to phenyl acetylene, tetradecane and benzyl alcohol, respectively, while peak d, e and f belong to 1,3-diphenylpropan-1-ol, benzylacetophenone (1,3-diphenylpropan-1-one, desired product) and benzalacetophenone. For the product, the mass spectrum is shown in Figure 8.2, and the value of m/z is 210. The desired product was obtained through silica gel flash chromatography and analyzed by NMR. The characterization data of benzylacetophenone was as below: the product was isolated as a white solid. ^{1}H-NMR (400 MHz, $CDCl_3$) δ ppm: 7.99 (d, *J* = 7.7 Hz, 2H), 7.60 (t, *J* = 7.2 Hz, 1H), 7.48 (t, *J* = 7.0 Hz, 2H), 7.45-7.23 (m, 5H), 3.34 (t, *J* = 8.5, 6.9 Hz, 2H), 3.10 (t, *J* = 8.5, 6.9 Hz, 2H). ^{13}C-NMR (101 MHz, $CDCl_3$) δ ppm: 199.2, 141.3, 136.9, 133.1, 128.6, 128.5, 128.4, 128.0, 126.1, 40.5, 30.1. MS: m/z = 210 $[M]^+$. NMR data are in accordance with literature values.[323]

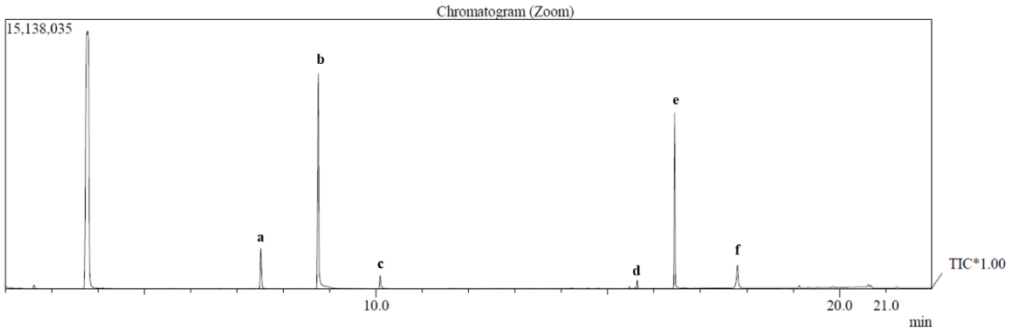

Figure 8.1. GC result of the reaction (entry 1 in Table 8.2).

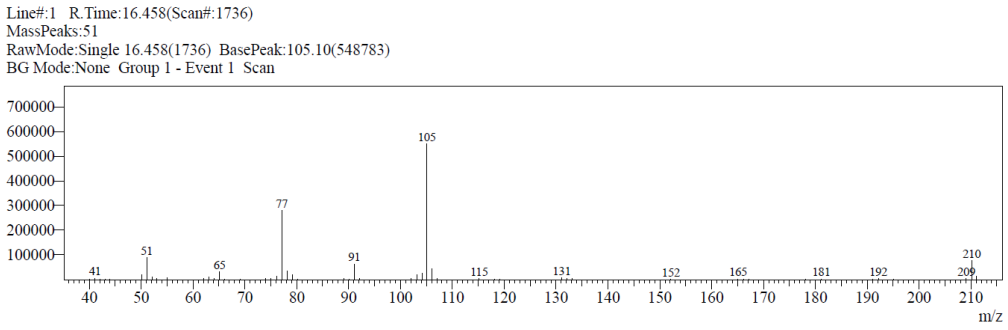

Figure 8.2. Mass spectrum of the compound e in Figure 8.1.

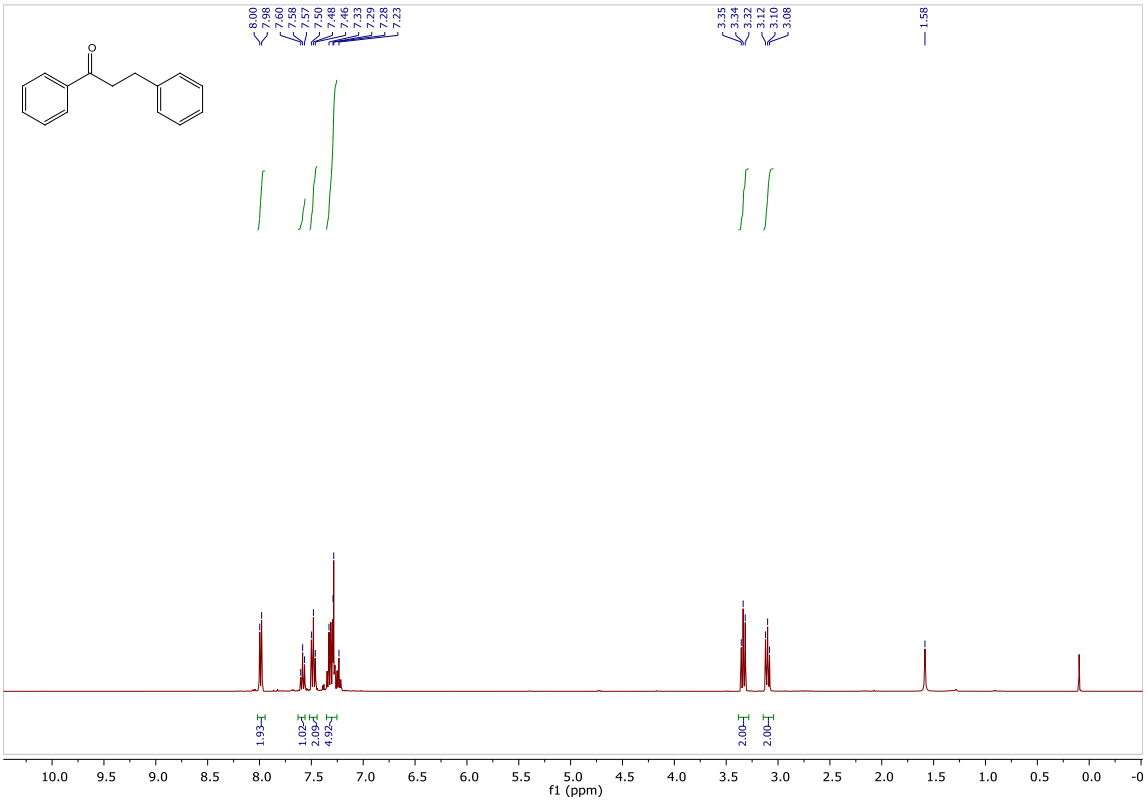
8.00
7.98
7.60
7.58
7.57
7.50
7.48
7.46
7.33
7.29
7.28
7.23
3.35
3.34
3.32
3.12
3.10
3.08
1.58
1.93
1.02
2.09
4.92
2.00
2.00
f1 (ppm)

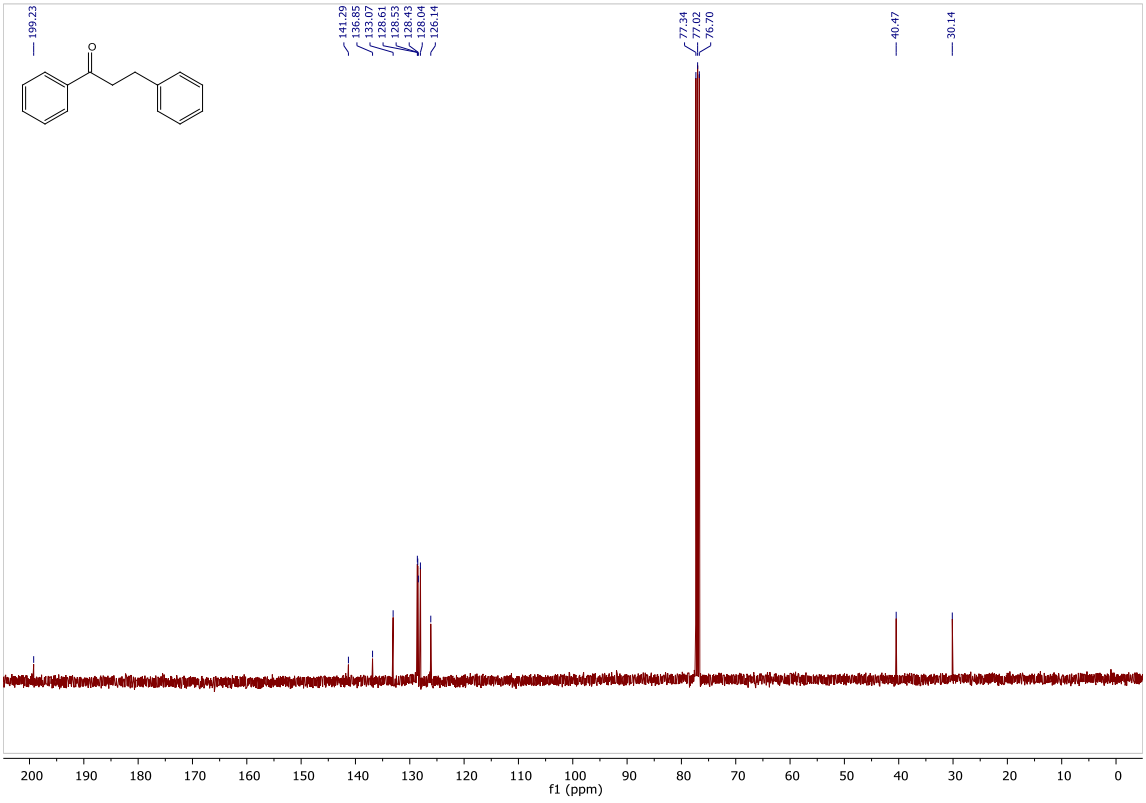
199.23
141.29
136.85
133.07
128.61
128.53
128.43
128.04
126.14
77.34
77.02
76.70
40.47
30.14
f1 (ppm)

8.2.5 Limitation of this project.

When optimizing the conditions for the ^{t}BuOK catalyzed coupling between alcohols and acetylenes, some combinations with different substrates were also performed in the reaction (Scheme 8.7). When benzyl alcohol and an aliphatic acetylene (1-heptyne) were subjected to the reaction, it was thought that compound **130** would be obtained, but there was no product. In addition, it was believed that compound **131** would be obtained when an aliphatic alcohol (1-heptanol) and phenyl acetylene were employed in the reaction. A GCMS sample was tested when the reaction was finished, and the results are shown in Figure 8.3 and 8.4.

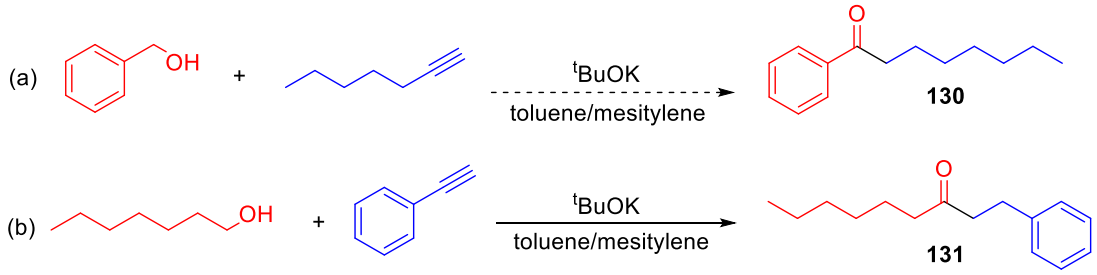

Scheme 8.7. Combination with different substrates for the coupling reaction.

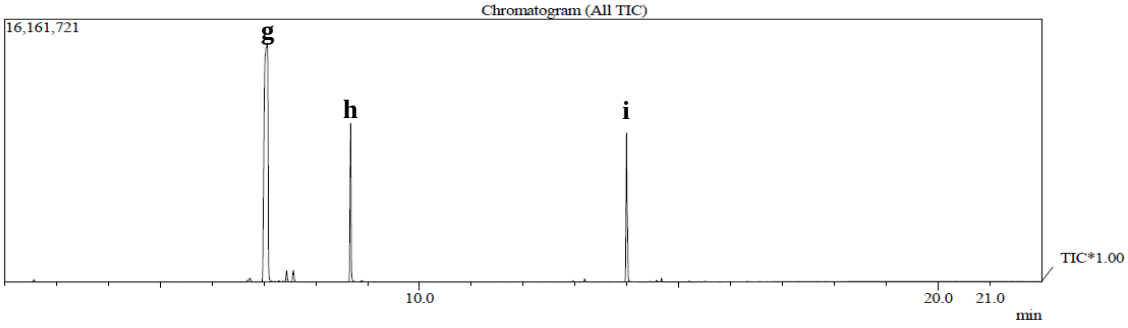

Figure 8.3. GC result of the reaction in Scheme 8.7b.

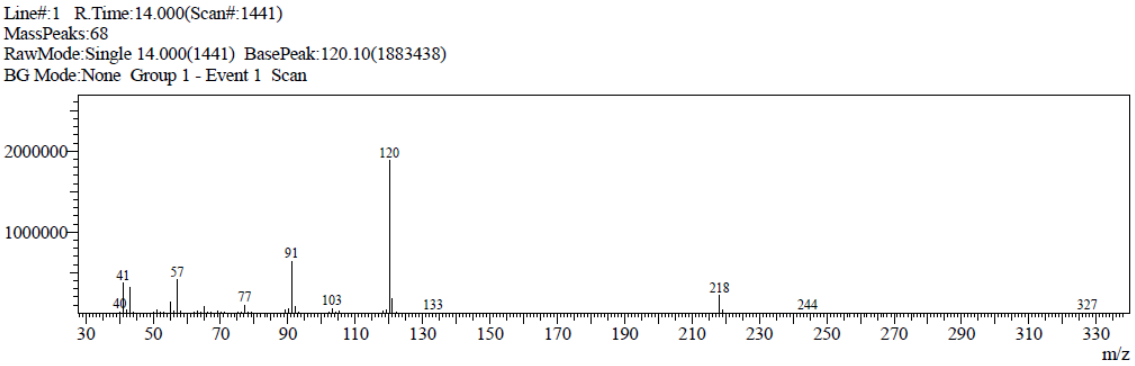

Figure 8.4. Mass spectra of the compound i in Figure 8.3.

In Figure 8.3, there were three peaks: g, h, and i, and they were solvent, internal standard and desired product, respectively. From Figure 8.4, it can be seen that the m/z value of compound i was 218, which was the same as the m/z of compound **123**. The product was isolated through silica gel flash chromatography and 50.0 mg of the product was obtained as a pale liquid. The product was analyzed by NMR, and the ^{1}H-NMR and the ^{13}C-NMR spectra are shown below. From the NMR spectra, it can be recognized that the product was an ether, and not a ketone, and the structure was (*Z*)-2-(heptyloxy)ethenyl benzene (Scheme 8.8), because the *J* coupling constant of the H atoms on the C-C double bond was 7.0.[324] Thus, the synthesis of *Z*-vinyl ethers seemed a good project. However, it turned out to be a known reaction[325–327] and no further optimization was therefore performed.

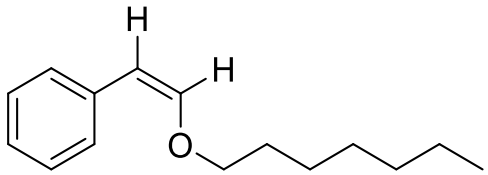

Scheme 8.8. Structure of (*Z*)-2-(heptyloxy)ethenyl benzene.

The NMR characterization data of (*Z*)-2-(heptyloxy)ethenyl benzene were shown here: ^{1}H-NMR (400 MHz, $CDCl_3$) δ ppm: 7.66-7.57 (m, 2H), 7.31 (dd, *J* = 8.4, 7.1 Hz, 2H), 7.22-7.09 (m, 1H), 6.23 (d, *J* = 7.0 Hz, 1H), 5.23 (d, *J* = 7.0 Hz, 1H), 3.94 (t, *J* = 6.6 Hz, 2H), 1.75 (dq, *J* = 8.2, 6.6 Hz, 2H), 1.51-1.42 (m, 2H), 1.38-1.27 (m, 6H), 0.96-0.87 (m, 3H). ^{13}C-NMR (101 MHz, $CDCl_3$) δ ppm: 146.9, 136.2, 128.1, 128.1, 125.5, 105.3, 73.8, 31.7, 29.9, 29.0, 25.8, 22.6, 14.1. MS: m/z = 218 $[M]^+$.

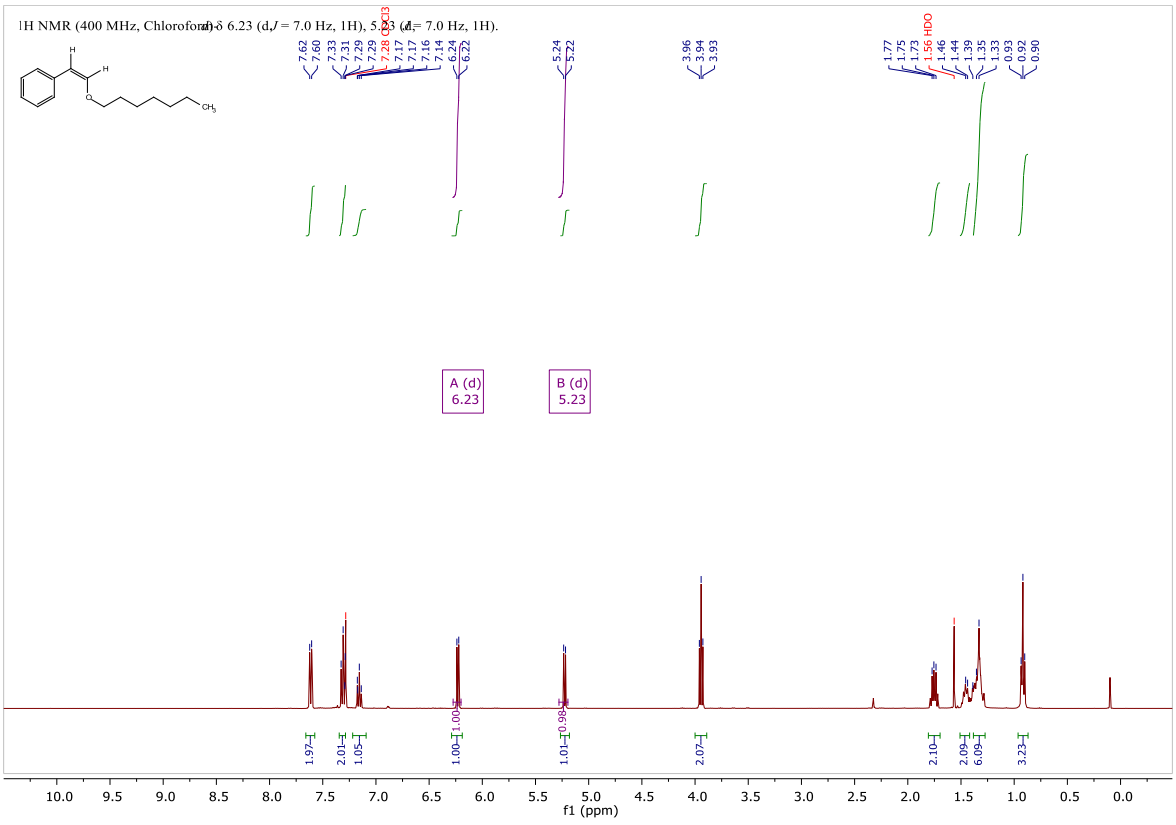
1H NMR (400 MHz, Chloroform-d) δ 6.23 (d, J = 7.0 Hz, 1H), 5.23 (d, J = 7.0 Hz, 1H).
A (d) 6.23
B (d) 5.23
f1 (ppm)

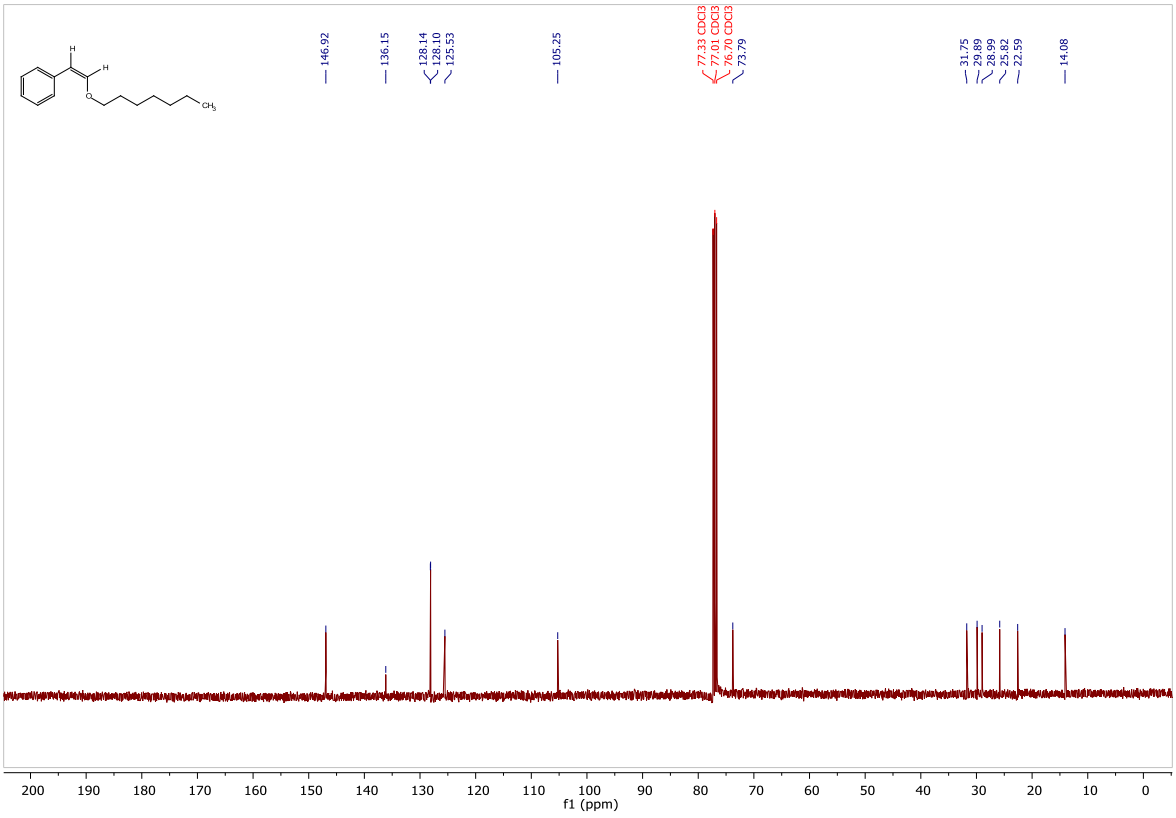
f1 (ppm)

8.3 Conference list

1. **Aug. 23 2021** the Danish Chemical Society Annual Meeting 2021, University of Copenhagen, Copenhagen, Denmark
2. **Sept. 30 - Oct. 2 2020** the Reaxys PhD Prize Symposium 2020 (webinar), The Netherlands
3. **Jan. 31 - Feb. 1 2020** the Torkil Holm Symposium 2020, Copenhagen, Denmark
4. **Nov. 11-15 2019** Poster presentation at the Organic Chemistry in the Pharmaceutical, Agrochemical and Contract Manufacturing Industries (OCPACMI) 2019 on Transition-Metal-Free Direct Alkylation of Amides with Alcohols Using Potassium tert-Butoxide, Kobra Azizi, Yulong Miao, Robert Madsen, University of Copenhagen, Copenhagen, Denmark
5. **July 21-25 2019** 20th IUPAC International Symposium on Organometallic Chemistry Directed Towards Organic Synthesis (OMCOS 20), Heidelberg University, Heidelberg, Germany
6. **June 27 2019** the Danish Chemical Society Annual Meeting 2019, University of Copenhagen, Copenhagen, Denmark
7. **May 3-4 2019** Træf for Organisk Kemi Studerende (TOKS) XVII, University of Copenhagen, Copenhagen, Denmark
8. **2018 - 2020** Oral and poster presentations at the annual Ph.D. Symposium organized by the Department of Chemistry, Technical University of Denmark, Denmark.

8.4 Journal publication list

1. Yulong Miao, Simone V. Samuelsen, Robert Madsen, Vanadium- and Chromium-Catalyzed Dehydrogenative Synthesis of Imines from Alcohols and Amines, *Organometallics* **2021**, 40, 1328-1335.

2. Yulong Miao, Robert Madsen, Vanadium(IV) Salen-Catalyzed Dehydrogenation of Alcohols and Amines to Form Imines (in preparation).

ORGANOMETALLICS

pubs.acs.org/Organometallics Article

Vanadium- and Chromium-Catalyzed Dehydrogenative Synthesis of Imines from Alcohols and Amines

Yulong Miao, Simone V. Samuelsen, and Robert Madsen*

Cite This: *Organometallics* 2021, 40, 1328−1335 Read Online

ACCESS | Metrics & More | Article Recommendations | Supporting Information

ABSTRACT: Vanadium(IV) tetraphenylporphyrin dichloride and chromium(III) tetraphenylporphyrin chloride have been developed as catalysts for the acceptorless dehydrogenation of alcohols. The catalysts have been applied to the direct synthesis of imines in overall good yields from a variety of alcohols and amines. The transformations are proposed to proceed by metal−ligand bifunctional pathways with an outer-sphere transfer of two hydrogen atoms from the alcohol to the metal porphyrin complexes. The results show that vanadium and chromium catalysts can also be employed for the dehydrogenation of alcohols with the release of hydrogen gas, and they may represent valuable alternatives to other catalysts based on Earth-abundant metals.

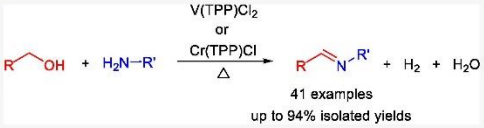

INTRODUCTION

Metal-catalyzed acceptorless dehydrogenation of alcohols has emerged as a powerful protocol in the formation of the C−N and C−C bonds since no stoichiometric oxidants are employed and only water and/or hydrogen gas are produced as byproducts.[1] The reactions proceed by the initial formation of the carbonyl compound, which then reacts with different N- and C-nucleophiles to form new functional groups and heterocyclic structures. The transformations were first catalyzed by metal complexes based on the platinum group metals where especially ruthenium and iridium catalysts have gained widespread applications.[1] During the past decade, attention has shifted toward catalysts based on Earth-abundant first-row transition metals where manganese, iron, cobalt, nickel, and copper complexes have been widely employed.[2,3] Vanadium complexes, however, have never been used to catalyze the acceptorless dehydrogenation of alcohols while only one example exists where a chromium(III) pincer complex was shown to catalyze the alkylation of amines with alcohols.[4]

Vanadium is the 12th most abundant metal in the Earth's crust and is mainly produced as V_2O_5 on an industrial scale with a price of \$10−30/kg.[5] Vanadium compounds are relatively nontoxic since the concentration of vanadium in the human body is around 40 nM.[6] Chromium is the 13th most abundant metal with a price of about \$10/kg and is predominately used for the production of stainless steel.[7] Trivalent chromium compounds show a low order of toxicity in humans (contrary to hexavalent species) due to their poor ability to pass through cell membranes.[8] In homogeneous catalysis, vanadium and chromium complexes are predominately used as Lewis acids and to mediate oxidations with stoichiometric oxidants.[9] Reactions with hydrogen gas are rare and only in a few cases have vanadium[10] and chromium[11] complexes been shown to catalyze the hydrogenation of alkenes and alkynes.

We have recently developed manganese(III) porphyrin complexes as catalysts for the acceptorless dehydrogenation of alcohols and applied the reaction in the synthesis of imines, tertiary amines, and quinolines by the condensation of alcohols and amines.[12] The alcohol dehydrogenation constitutes a new reaction for manganese(III) porphyrin complexes and the discovery inspired the idea that other metal porphyrin complexes may be able to catalyze the same reaction.[13]

Herein, we describe vanadium(IV) and chromium(III) porphyrin complexes as catalysts for the coupling of alcohols and amines into imines.[14] This constitutes the first example of a vanadium-catalyzed alcohol dehydrogenation and the first case where a chromium complex has been used to catalyze the liberation of hydrogen gas from alcohols.

RESULTS AND DISCUSSION

The studies began with the preparation of four vanadium(IV) porphyrin dichloride complexes **A**−**D** (Figure 1) from the corresponding oxovanadium(IV) compounds by treatment with $SOCl_2$.[15] The four porphyrin ligands were selected since reactions with these ligands were the highest yielding in the corresponding manganese-catalyzed protocol.[12] Benzyl alcohol and cyclohexylamine were selected as the substrates for the initial experiments, and in the first experiment, the trans-

Received: March 2, 2021
Published: April 28, 2021

https://doi.org/10.1021/acs.organomet.1c00123
Organometallics 2021, 40, 1328−1335

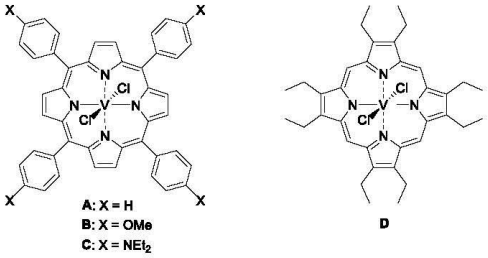

Figure 1. Structure of vanadium(IV) porphyrin complexes **A**–**D**.

formation was performed with 5% of tetraphenylporphyrin (TPP) complex **A** in refluxing mesitylene to afford *N*-benzylidene cyclohexylamine (**1**) in 51% gas chromatography (GC) yield with some alcohol and amine remaining (Table 1, entry 1). No improvement in the yield was observed when electron-donating groups were placed on the ligand (as in **B** and **C**) or when octaethylporphyrin complex **D** was employed (entries 2–4). Very little imine formation was detected when the porphyrin complexes were omitted (entry 5). Thus, complex **A** was selected for further optimization where the influence of additives and the solvent was studied.

Table 1. Optimizing Vanadium-Catalyzed Dehydrogenation[a]

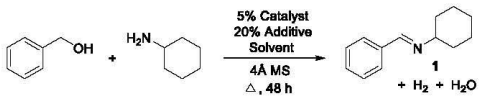

entry	catalyst	additive	solvent	yield (%)[b]
1	A		mesitylene	51
2	B		mesitylene	45
3	C		mesitylene	27
4	D		mesitylene	46
5			mesitylene	5
6	A	NaOH	mesitylene	68
7	A	Cs_2CO_3	mesitylene	72
8	A	Li_3N	mesitylene	75
9	A	Mg_3N_2	mesitylene	56
10	A	Ca_3N_2	mesitylene	24
11	A	Cs_2CO_3	toluene	10
12	A	Li_3N	toluene	35
13	A	NaOH	toluene	69
14	A	NaOH	toluene[c]	94
15	A	NaOH[d]	toluene	70
16	A	NaOH[e]	toluene	29
17[f]	A	NaOH	toluene	67
18	A	LiOH	mesitylene	59
19[g]	A	NaOH	toluene[c]	69

[a]Conditions: BnOH (1 mmol), $CyNH_2$ (1 mmol), catalyst (0.05 mmol), additive (0.2 mmol), tetradecane (0.5 mmol, internal standard), 4 Å MS (150 mg), solvent (4 mL), reflux, and 48 h. [b]GC yield based on the internal standard. [c]With 2 mL of the solvent. [d]With 0.3 mmol of NaOH. [e]With 0.1 mmol of NaOH. [f]With 0.025 mmol of **A**. [g]Without 4 Å MS.

A number of common additives such as LiCl, $MgBr_2$, KOH, Et_3N, Na_2SO_4, and $MgSO_4$ gave lower yields of the imine (results not shown). However, with NaOH, Cs_2CO_3, and Li_3N, the yield improved notably to 68–75% (entries 6–8). We have previously used the nitride salts Mg_3N_2 and Ca_3N_2 as additives in iminations,[16] but in this case, they both proved less effective (entries 9 and 10). Further reactions with Cs_2CO_3 and Li_3N revealed that toluene as the solvent gave a poor yield (entries 11 and 12). With NaOH, on the other hand, a similar outcome was obtained in toluene (entry 13) and the yield improved significantly with a lower amount of the solvent (entry 14). Changing the amount of NaOH or decreasing the catalyst loading resulted in lower imine yields (entries 15–17). The same was observed when LiOH was used as the additive or when the molecular sieves were omitted from the reaction (entries 18 and 19). The lower imine yields were always caused by the incomplete conversion of the alcohol and the amine and no byproducts were observed. Thus, the optimum conditions for the imination employ 5% of complex **A** and 20% of NaOH in refluxing toluene with equimolar amounts of the alcohol and the imine.

The protocol was then applied to different alcohols and amines to explore the substrate scope of the vanadium-catalyzed transformation where the products were isolated by flash chromatography (Table 2). First, a number of alcohols were reacted with cyclohexylamine, which afforded 93% yield of the parent imine **1** while *p*-methyl-, *p*-methoxy-, and *p*-methylthiobenzyl alcohols gave 65–82% yield of imines **2**–**4**. Electron-withdrawing nitro and trifluoromethyl groups in the para position of benzyl alcohol gave rise to imines **5** and **6** in 94 and 77% yield, respectively. *p*-Chloro-, *p*-bromo-, and *p*-iodobenzyl alcohols furnished compounds **7**–**9** in 70–82%, with no sign of a competing dehalogenation. 1-Naththylmethanol afforded imine **10** in 84% yield while cinnamyl alcohol gave unsaturated Schiff base **11** in 89% yield without any accompanying hydrogenation of the C=C bond.

Then, the imination was carried out with several other amines in the reaction with benzyl alcohol, which gave imines **12** and **13** in 62 and 74% yield, respectively, in the coupling with *tert*-octyl- and *n*-octylamine. The hindered amines 1-adamantylamine and benzhydrylamine furnished imines **14** and **15** in 61 and 92% yield while optically pure (*R*)-1-phenylethylamine afforded chiral imine **16** with no sign of racemization. Finally, the less nucleophilic aniline was reacted with benzyl alcohol to give *N*-benzylidene aniline (**17**) in 57% yield. No byproducts could be detected by gas chromatography–mass spectrometry (GC–MS) in any of the reactions in Table 2; however, in some cases, small amounts of the amine remained after the transformation. Aliphatic alcohols, on the contrary, such as hexan-1-ol and hex-5-en-1-ol did not react in the imination. Benzylic alcohols are dehydrogenated more readily than aliphatic alcohols, and this reactivity difference has also been observed in iminations with other metal catalysts.[2,16,17] The reaction could be scaled up to a gram scale where 8 mmol of benzyl alcohol and cyclohexylamine were transformed into 1.1 g (76%) of *N*-benzylidene cyclohexylamine (**1**) under optimized conditions. Notably, vanadium complex **A** performs the transformation at a lower temperature (i.e., 110 °C) than the previously developed manganese(III) porphyrin complex at 164 °C.[12]

Prompted by these promising results, it was also decided to investigate the commercially available chromium(III) tetraphenylporphyrin chloride (**E**) (Figure 2) as a catalyst for imination. Again, the initial experiments were carried out with benzyl alcohol and cyclohexylamine in refluxing mesitylene (Table 3). Notably, with 5% of complex **E** complete

https://doi.org/10.1021/acs.organomet.1c00123
Organometallics 2021, 40, 1328–1335

Table 2. Vanadium-Catalyzed Imine Formation from Alcohols and Amines[a]

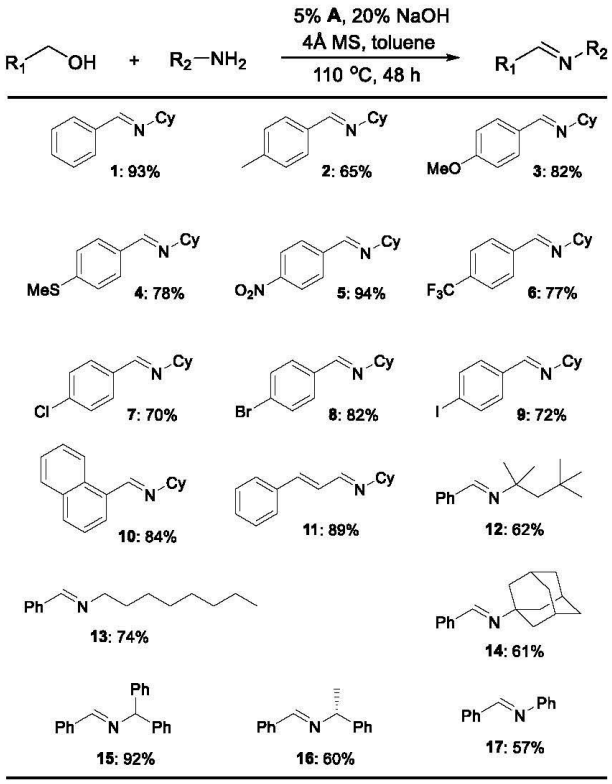

[a]Reaction conditions: alcohol (1 mmol), amine (1 mmol), **A** (0.05 mmol), NaOH (0.2 mmol), 4 Å MS (150 mg), toluene (2 mL), reflux, and 48 h (isolated yields).

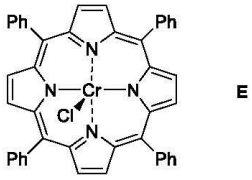

E

Figure 2. Structure of chromium(III) tetraphenylporphyrin chloride (E).

conversion into *N*-benzylidene cyclohexylamine (**1**) was observed (entry 1) while the yield decreased to 74 with 3% of the catalyst (entry 2). A number of additives were then included, which in most cases led to lower yields of the imine (entries 3−7). With 20% of NaOH, however, a quantitative yield of the product was again obtained (entry 8) while the yield decreased with lower loadings of the catalyst (entries 9 and 10) and lower boiling solvents (entries 11 and 12). Interestingly, the imination with 4% of **E** in mesitylene and in the absence of an additive also gave the product in quantitative yield (entry 13) while poor yields were obtained in xylene and toluene (entries 14 and 15). A desiccant is important for the imine formation since the transformation without molecular sieves only produced 28% yield of the Schiff base (entry 16). Thus, the effect of NaOH as an acid scavenger (and possible additional desiccant) appears to be very small in this case, and it was therefore decided to adopt the conditions with 4% of **E** in mesitylene for general use (entry 13). No side reactions were observed in any of the transformations in Table 3, where unreacted starting materials were the only other compounds that could sometimes be detected.

The optimized conditions were then applied to various alcohols and amines to investigate the substrate scope of the chromium-catalyzed protocol (Table 4). *N*-Benzylidene cyclohexylamine (**1**) was isolated in 86% yield while the imination of cyclohexylamine with *p*-methyl-, *p*-methoxy-, *p*-methylthio-, and *p*-phenylbenzyl alcohol afforded products **2**, **3**, **4**, and **18** in 68−70% yield. Electron-withdrawing *p*-nitro and *p*-trifluoromethyl groups gave rise to imines **5** and **6** in 68 and 62% yield, respectively, whereas the four *p*-halo-substituted benzyl alcohols furnished imines **19**, **7**, **8**, and **9** in 59−75% yield. Ortho-substituted *o*-methyl-, *o*-chloro-, and 2,4,6-trimethylbenzyl alcohol produced the resulting imines **20**−**22** in 61−75%

https://doi.org/10.1021/acs.organomet.1c00123
Organometallics 2021, 40, 1328−1335

Table 3. Optimizing Chromium-Catalyzed Dehydrogenation[a]

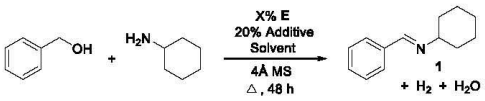

entry	X	additive	solvent	yield (%)[b]
1	5		mesitylene	quant.
2	3		mesitylene	74
3	5	Cs_2CO_3	mesitylene	74
4	5	K_2CO_3	mesitylene	47
5	5	KO*t*Bu	mesitylene	67
6	5	KOH	mesitylene	75
7	5	Ca_3N_2	mesitylene	26
8	5	NaOH	mesitylene	quant.
9	4	NaOH	mesitylene	89
10	3	NaOH	mesitylene	85
11	5	NaOH	xylene	70
12	5	NaOH	toluene	28
13	4		mesitylene	quant.
14	4		xylene	38
15	4		toluene	10
16[c]	4		mesitylene	26

[a]Conditions: BnOH (1 mmol), $CyNH_2$ (1 mmol), E (0.0X mmol), additive (0.2 mmol), tetradecane (0.5 mmol, internal standard), 4 Å MS (150 mg), solvent (4 mL), reflux, and 48 h. [b]GC yield based on the internal standard. [c]Without 4 Å MS.

yield while 1-naphthylmethanol generated Schiff base **10** in 70% yield. Likewise, the dehydrogenation was applied to several amines in the reaction with benzyl alcohol where *tert*-octyl-, *n*-octyl-, benzyl-, cycloheptyl-, and cyclohexanemethylamine gave rise to the corresponding imines **12**, **13**, **23**, **24**, and **25** in 70−80% yield. The more hindered amines 1-adamantyl-, benzhydryl-, and tritylamine afforded imines **14**, **15**, and **26** in 72−76% yield, whereas aniline furnished Schiff base **17** in 66% yield. No side reactions were observed during the imine syntheses in Table 4, although small amounts of unreacted amine could be detected in some cases. No reaction occurred when the aliphatic alcohol hexan-1-ol was reacted with cyclohexylamine under optimized conditions.

The dehydrogenative pathways of the two metal-catalyzed iminations were verified by collecting the liberated hydrogen gas. In the vanadium-catalyzed protocol, the experiment in Table 1, entry 14, was performed in a closed two-chamber system where the other compartment contained diphenylacetylene and Pd/C in methanol.[17] The experiment showed a reduction of diphenylacetylene to *cis*-stilbene after the imine reaction had completed and thus confirms the evolution of hydrogen gas during the transformation. In the chromium-catalyzed protocol, the experiment in Table 3, entry 13, was repeated and the liberated gas collected in a burette. A total of 17 mL (0.76 mmol) was obtained from the reaction of 1 mmol of substrates and the gas was shown to be dihydrogen, which again verifies the acceptorless dehydrogenative pathway of the transformation. Liquid chromatography−mass spectrometry (LCMS) analysis of the two reaction mixtures after the imination showed the $(TPP)Cr^{III}$ cation in the experiment with complex **E** while no clear catalyst-derived species could be detected in the reaction with complex **A**. No sign of any reduction of the porphyrin ligand was observed with complex **E**.[18] Control experiments revealed that the vanadyl complex (TPP)V = O could be detected by LCMS, but this compound was not observed in the analysis of the vanadium-catalyzed transformation. When the reactions in Table 1, entry 14, and Table 3, entry 13, were performed with $PhCD_2OH$ instead of $PhCH_2OH$, the product was in both cases exclusively PhCD = NCy with no evidence for any hydrogen incorporation into the benzylic position. The lack of isotope scrambling may indicate that the two dehydrogenations take place by monohydride (monodeuteride) pathways.

The primary kinetic isotope effect (KIE) was determined for both metal-catalyzed transformations by measuring the initial rates with $PhCH_2OH$ and $PhCD_2OH$ in the reaction with cyclohexylamine. The measurements gave a KIE of 2.5 for the vanadium-catalyzed reaction and 2.3 for the chromium-catalyzed protocol, which shows that breakage of the benzylic C−H bond is a slow step in the two transformations. No radical intermediates appear to be involved in the catalytic cycles since the presence of 1 equiv of the radical scavengers cyclohexa-1,4-diene and 2,4-diphenyl-4-methylpent-1-ene had no influence on the yield of the imine under the optimized conditions in Table 1, entry 14, and Table 3, entry 13, and the two scavengers were not converted during the transformations.[19] In an attempt to detect possible catalytic intermediates, two experiments were performed where 50 mmol of $PhCH_2OH$ and 10 mmol of NaH were mixed with 1 mmol of either complex **A** or complex **E** in the absence of a solvent. After stirring for 30 min at room temperature, both mixtures were analyzed by LCMS, but potential benzyloxy metal porphyrin species could not be detected.[20] Distillation heads were then attached and the mixtures heated to 185 °C, which caused 2 mmol of benzyl alcohol/benzaldehyde to distil off after 24 h in both cases (as an 11/1 mixture with complex **A** and a 7/1 mixture with complex **E**). These experiments show that the dehydrogenations are possible in the absence of the amine.

In our dehydrogenation with a manganese(III) porphyrin complex, we proposed a mechanism where an alkoxide complex is formed and degrades into the aldehyde and a metal hydride species.[12] Metal porphyrin alkoxide complexes do not contain an available coordination site for a classical β-hydride elimination, but a dissociative β-hydride abstraction pathway has been proposed in alkoxide complexes where an open cis coordination site is not available.[21] In principle, the present vanadium- and chromium-catalyzed protocols could take place by this mechanism, although it has not been possible to detect any intermediate metal alkoxide species.

However, vanadium and chromium are both more oxophilic metals than manganese.[22] Still, the vanadium-catalyzed dehydrogenation takes place at a lower temperature than the manganese counterpart, i.e., in refluxing toluene as compared to refluxing mesitylene. This fact may indicate that breakage of a metal−oxygen bond is not part of the catalytic cycle and that a different pathway is operating with complexes **A** and **E**. In this context, it should be noted that many manganese, iron, and cobalt complexes with multidentate ligands have been shown to perform the dehydrogenation by an outer-sphere pathway with active participation from the ligand.[16,23] In this metal−ligand bifunctional mechanism, the proton from the alcohol OH group and the hydride from the α-carbon are transferred to the ligand nitrogen atom and the metal center, respectively. Nothing indicates that a highly basic nitrogen atom is required in the ligand and thus the pyrrole moieties of the porphyrin ligand could participate in this bifunctional

https://doi.org/10.1021/acs.organomet.1c00123
Organometallics 2021, 40, 1328−1335

Table 4. Chromium-Catalyzed Imine Formation from Alcohols and Amines[a]

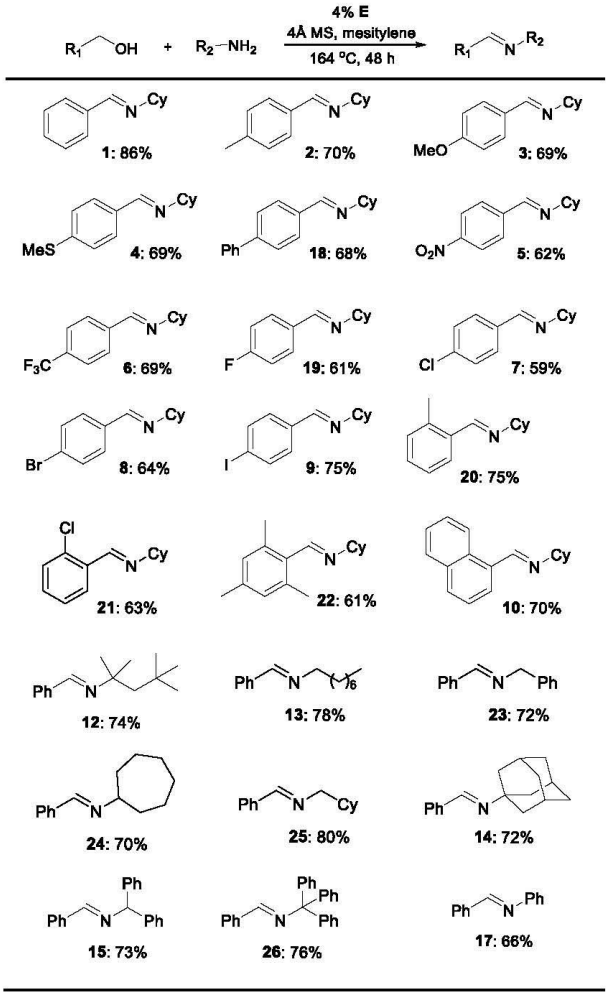

[a]Reaction conditions: alcohol (1 mmol), amine (1 mmol), E (0.04 mmol), 4 Å MS (150 mg), mesitylene (4 mL), reflux, and 48 h (isolated yields).

pathway. It is generally believed that demetallation of metal porphyrin complexes under acidic conditions proceeds through diprotonation of two pyrrole groups to afford so-called sitting-atop complexes as intermediates where the metal is located above the plane of the diprotonated porphyrin.[24] Monoprotonated metal porphyrins are poorly described[25] but can likewise be envisioned as intermediates.

Accordingly, we believe the most plausible mechanism for the present vanadium- and chromium-catalyzed dehydrogenation involves the formation of complex **F** with an available coordination site where the ligand X can be chloride, alcohol, or amine (Scheme 1).[26] Outer-sphere hydrogen abstraction through transition state **G** then affords hydride complex **H** from which hydrogen gas can be liberated to regenerate complex **F**. It should be noted that the aromatic 18 π-electron-conjugated network of the porphyrin ring is not disrupted during the catalytic cycle. The pathway resembles our previously proposed route for dehydrogenation by a manganese(III) salen complex[16b] and may indicate that first-row transition metals with tetradentate salen and porphyrin ligands perform the alcohol dehydrogenation by a similar mechanism.

■ CONCLUSIONS

In summary, we have described the first example of an acceptorless alcohol dehydrogenation with a vanadium and a chromium complex. V(TPP)Cl_2 and Cr(TPP)Cl mediate the

https://doi.org/10.1021/acs.organomet.1c00123
Organometallics 2021, 40, 1328−1335

Scheme 1. Proposed Mechanism for Vanadium and Chromium Porphyrin-Catalyzed Alcohol Dehydrogenation

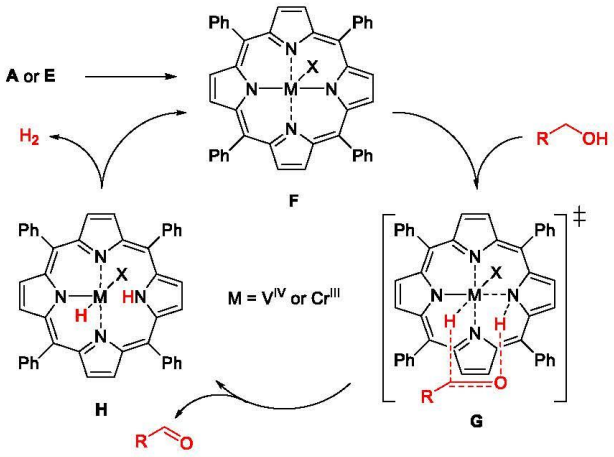

coupling of alcohols and amines into imines with the liberation of hydrogen gas, and the transformations have been applied to a variety of substrates. The results show that vanadium and chromium complexes may be useful alternatives to other catalysts based on Earth-abundant metals when developing alcohol dehydrogenation reactions. The mechanism with V(TPP)Cl_2 and Cr(TPP)Cl is proposed to involve a metal–ligand bifunctional pathway where two hydrogen atoms from the alcohol are transferred to the metal porphyrin complex, followed by elimination of hydrogen gas. Further investigations into the mechanism for these transition-metal porphyrin-catalyzed dehydrogenations of alcohols are ongoing in the group.

EXPERIMENTAL SECTION

General Procedure for Imine Synthesis with V(TPP)Cl_2 (A). Vanadium complex **A** (36.7 mg, 0.05 mmol), NaOH (8.0 mg, 0.20 mmol), and preactivated 4 Å molecular sieves (150 mg) were placed in an oven-dried tube, whereafter it was placed in a Radley carousel. A vacuum was applied and the flask was then filled with N_2 (repeated three times). Anhydrous toluene (2 mL) was added and the reaction mixture was heated to reflux. The alcohol (1 mmol), the amine (1 mmol), and tetradecane (0.5 mmol as an internal standard) were added by a syringe, and the reaction was refluxed with stirring under a flow of N_2 for 48 h. The mixture was cooled to room temperature and the solvent removed in vacuo. The crude product was purified by silica gel column chromatography (hexane/Et_3N, 98:2) to afford the desired imine.

General Procedure for Imine Synthesis with Cr(TPP)Cl (E). Chromium complex E (28.0 mg, 0.04 mmol) and preactivated 4 Å molecular sieves (150 mg) were placed in an oven-dried tube, whereafter they were placed in a Radley carousel. A vacuum was applied and the flask was then filled with N_2 (repeated three times). Degassed mesitylene (4 mL) was added and the reaction mixture heated to reflux. The alcohol (1 mmol), the amine (1 mmol), and tetradecane (0.5 mmol as an internal standard) were injected into the carousel tube by a syringe, and the reaction was refluxed with stirring under a flow of N_2 for 48 h. The mixture was cooled to room temperature and the solvent removed in vacuo. The crude product was purified by silica gel column chromatography (hexane/Et_3N, 98:2) to afford the desired imine.

ASSOCIATED CONTENT

Supporting Information

The Supporting Information is available free of charge at https://pubs.acs.org/doi/10.1021/acs.organomet.1c00123.

Experimental procedures; deuterium labeling studies; and compound characterization data and copies of ^1H and ^{13}C NMR spectra (PDF)

AUTHOR INFORMATION

Corresponding Author

Robert Madsen – *Department of Chemistry, Technical University of Denmark, 2800 Kgs. Lyngby, Denmark;* orcid.org/0000-0002-2576-1004; Email: rm@kemi.dtu.dk

Authors

Yulong Miao – *Department of Chemistry, Technical University of Denmark, 2800 Kgs. Lyngby, Denmark*

Simone V. Samuelsen – *Department of Chemistry, Technical University of Denmark, 2800 Kgs. Lyngby, Denmark*

Complete contact information is available at: https://pubs.acs.org/10.1021/acs.organomet.1c00123

Notes

The authors declare no competing financial interest.

ACKNOWLEDGMENTS

Y.M. and S.V.S. gratefully acknowledge the China Scholarship Council (CSC) and the Technical University of Denmark, respectively, for PhD fellowships. In addition, we thank the Independent Research Fund Denmark—Technology and Production Sciences for financial support.

REFERENCES

(1) (a) Corma, A.; Navas, J.; Sabater, M. J. Advances in One-Pot Synthesis through Borrowing Hydrogen Catalysis. *Chem. Rev.* **2018**, *118*, 1410–1459. (b) Huang, F.; Liu, Z.; Yu, Z. C-Alkylation of Ketones and Related Compounds by Alcohols: Transition-Metal-Catalyzed Dehydrogenation. *Angew. Chem., Int. Ed.* **2016**, *55*, 862–

875. (c) Gunanathan, C.; Milstein, D. Applications of Acceptorless Dehydrogenation and Related Transformations in Chemical Synthesis. *Science* **2013**, *341*, No. 1229712.
(2) (a) Reed-Berendt, B. G.; Polidano, K.; Morrill, L. C. Recent advances in homogeneous borrowing hydrogen catalysis using earth-abundant first row transition metals. *Org. Biomol. Chem.* **2019**, *17*, 1595−1607. (b) Irrgang, T.; Kempe, R. 3d-Metal Catalyzed N- and C-Alkylation Reactions via Borrowing Hydrogen or Hydrogen Autotransfer. *Chem. Rev.* **2019**, *119*, 2524−2549. (c) Filonenko, G. A.; van Putten, R.; Hensen, E. J. M.; Pidko, E. A. Catalytic (de)hydrogenation promoted by non-precious metals − Co, Fe and Mn: recent advances in an emerging field. *Chem. Soc. Rev.* **2018**, *47*, 1459−1483.
(3) In one case, a zinc compound has also been shown to catalyze the acceptorless alcohol dehydrogenation, see: Monda, F.; Madsen, R. Zinc Oxide-Catalyzed Dehydrogenation of Primary Alcohols into Carboxylic Acids. *Chem. - Eur. J.* **2018**, *24*, 17832−17837.
(4) Kallmeier, F.; Fertig, R.; Irrgang, T.; Kempe, R. Chromium-Catalyzed Alkylation of Amines by Alcohols. *Angew. Chem., Int. Ed.* **2020**, *59*, 11789−11793.
(5) Polyak, D. E. *2017 Minerals Yearbook − Vanadium*; US Geological Survey, Reston, VA, 2020; pp 81.1−81.11.
(6) Rehder, D. Implications of vanadium in technical applications and pharmaceutical issues. *Inorg. Chim. Acta* **2017**, *455*, 378−389.
(7) Schulte, R. F. *2017 Minerals Yearbook − Chromium*; US Geological Survey, Reston, VA, 2020; pp 17.1−17.21.
(8) Vincent, J. B. *The Nutritional Biochemistry of Chromium(III)*; Elsevier, Amsterdam, 2019; pp 361−370.
(9) (a) Langeslay, R. R.; Kaphan, D. M.; Marshall, C. L.; Stair, P. C.; Sattelberger, A. P.; Delferro, M. Catalytic Applications of Vanadium: A Mechanistic Perspective. *Chem. Rev.* **2019**, *119*, 2128−2191. (b) North, M. *Sustainable Catalysis: With Non-Endangered Metals, Parts 1 and 2*; RSC Green Chemistry Series; The Royal Society of Chemistry, Cambridge, 2016; Vol. 38, pp 250−277. (c) Sutradhar, M.; Martins, L. M. D. R. S.; Guedes da Silva, M. F. C.; Pombeiro, A. J. L. Vanadium complexes: Recent progress in oxidation catalysis. *Coord. Chem. Rev.* **2015**, *301*−*302*, 200−239. (d) Bandini, M.; Cozzi, P. G.; Umani-Ronchi, A. [Cr(Salen)] as a "bridge" between asymmetric catalysis, Lewis acids and redox processes. *Chem. Commun.* **2002**, 919−927.
(10) (a) Sohn, H.; Camacho-Bunquin, J.; Langeslay, R. R.; Ignacio-de Leon, P. A.; Niklas, J.; Poluektov, O. G.; Liu, C.; Conell, J. G.; Yang, D.; Kropf, J.; Kim, H.; Stair, P. C.; Ferrandon, M.; Delferro, M. Isolated, well-defined organovanadium(III) on silica: single-site catalyst for hydrogenation of alkenes and alkynes. *Chem. Commun.* **2017**, *53*, 7325−7328. (b) Tanabe, K. K.; Ferradon, M. S.; Siladke, N. A.; Kraft, S. J.; Zhang, G.; Niklas, J.; Poluektov, O. G.; Lopykinski, S. J.; Bunel, E. E.; Krause, T. R.; Miller, J. T.; Hock, A. S.; Nguyen, S. T. Discovery of Highly Selective Alkyne Semihydrogenation Catalysts Based on First-Row Transition-Metallated Porous Organic Polymers. *Angew. Chem., Int. Ed.* **2014**, *53*, 12055−12058. (c) La Pierre, H. S.; Arnold, J.; Toste, F. D. Z-Selective Semihydrogenation of Alkynes Catalyzed by a Cationic Vanadium Bisimido Complex. *Angew. Chem., Int. Ed.* **2011**, *50*, 3900−3903.
(11) (a) Gregori, B. J.; Nowakowski, M.; Schoch, A.; Pöllath, S.; Zweck, J.; Bauer, M.; von Wangelin, A. J. Stereoselective Chromium-Catalyzed Semi-Hydrogenation of Alkynes. *ChemCatChem* **2020**, *12*, 5359−5363. (b) Camacho-Bunquin, J.; Siladka, N. A.; Zhang, G.; Niklas, J.; Poluektov, O. G.; Nguyen, S. T.; Miller, J. T.; Hock, A. S. Synthesis and Catalytic Hydrogenation Reactivity of a Chromium Catecholate Porous Organic Polymer. *Organometallics* **2015**, *34*, 947−952. (c) Vasil'ev, A. A.; Serebryakov, E. P. Stereospecific 1,4-*cis*-hydrogenation of conjugated dienes, dienynes, and dienediynes catalyzed by chromium carbonyl complexes in stereocontrolled syntheses of physiologically active olefins. *Russ. Chem. Bull.* **2002**, *51*, 1341−1361. (d) Chandiran, T.; Vancheesan, S. Hydrogenation of conjugated dienes catalysed by η^6−arenetricarbonylchromium complexes. *J. Mol. Catal.* **1994**, *88*, 31−42. (e) Kramarz, W.; Kurek, S. S. A Chromium Catalyst Derived from Triallylchromium Active for Alkene Hydrogenation. *J. Mol. Catal.* **1985**, *33*, 305−310.
(12) Azizi, K.; Akrami, S.; Madsen, R. Manganese(III) Porphyrin-Catalyzed Dehydrogenation of Alcohols to form Imines, Tertiary Amines and Quinolines. *Chem. - Eur. J.* **2019**, *25*, 6439−6446.
(13) In addition, iron phthalocyanine catalyzes the alkylation of indoles and amines with benzylic alcohols and an in situ generated iron porphyrin complex mediates the transfer hydrogenation of ketones with isopropanol, see: (a) Di Gregorio, G.; Mari, M.; Bartoccini, F.; Piersanti, G. Iron-Catalyzed Direct C3-Benzylation of Indoles with Benzyl Alcohols through Borrowing Hydrogen. *J. Org. Chem.* **2017**, *82*, 8769−8775. (b) Bala, M.; Verma, P. K.; Sharma, U.; Kumar, N.; Singh, B. Iron phthalocyanine as an efficient and versatile catalyst for *N*-alkylation of heterocyclic amines with alcohols: one-pot synthesis of 2-substituted benzimidazoles, benzothiazoles and benzoxazoles. *Green Chem.* **2013**, *15*, 1687−1693. (c) Enthaler, S.; Spilker, B.; Erre, G.; Junge, K.; Tse, M. K.; Beller, M. Biomimetic transfer hydrogenation of 2-alkoxy- and 2-aryloxyketones with iron-porphyrin catalysts. *Tetrahedron* **2008**, *64*, 3867−3876.
(14) For reviews on the synthesis of imines from alcohols and amines, see: (a) Chen, B.; Wang, L.; Gao, S. Recent Advances in Aerobic Oxidation of Alcohols and Amines to Imines. *ACS Catal.* **2015**, *5*, 5851−5876. (b) Patil, R. D.; Adimurthy, S. Catalytic Methods for Imine Synthesis. *Asian J. Org. Chem.* **2013**, *2*, 726−744.
(15) Richard, P.; Poncet, J. L.; Barbe, J. M.; Guilard, R.; Goulon, J.; Rinaldi, D.; Cartier, A.; Tola, P. Vanadium(IV) Porphyrins: Synthesis and Spectrochemical Characterization of Dihalogenovanadium(IV) Porphyrins. Extended *X*-Ray Absorption Fine Structural Study of Dibromo(2,3,7,8,12,13,17,18-octaethylporphyrinato)vanadium(IV). *J. Chem. Soc., Dalton Trans.* **1982**, 1451−1456.
(16) (a) Bottaro, F.; Madsen, R. In Situ Generated Cobalt Catalyst for the Dehydrogenative Coupling of Alcohols and Amines into Imines. *ChemCatChem* **2019**, *11*, 2707−2712. (b) Samuelsen, S. V.; Santilli, C.; Ahlquist, M. S. G.; Madsen, R. Development and mechanistic investigation of the manganese(III) salen-catalyzed dehydrogenation of alcohols. *Chem. Sci.* **2019**, *10*, 1150−1157.
(17) Azizi, K.; Madsen, R. Molybdenum-Catalyzed Dehydrogenative Synthesis of Imines from Alcohols and Amines. *ChemCatChem* **2018**, *10*, 3703−3708.
(18) An oxovanadium(IV) porphyrin complex has been shown to react reversibly with hydrogen gas and without a catalyst to form the corresponding chlorin complex, see: Vandeneeckoutte, F.; Hubaut, R.; Pietrzyk, S.; Des Courieres, T.; Grimblot, J. Thermal Equilibrium Between Vanadyloctaethylporphyrin and Hydrogenated Porphyrin During the Hydrodemetallation Process. *React. Kinet. Catal. Lett.* **1991**, *45*, 191−198.
(19) Recently, we have shown that benzylic radicals can be formed under basic conditions in refluxing mesitylene and participate in a C−C-bond-forming reaction, see: Azizi, K.; Madsen, R. Radical condensation between benzylic alcohols and acetamides to form 3-arylpropanamides. *Chem. Sci.* **2020**, *11*, 7800−7806.
(20) To the best of our knowledge, vanadium(IV) and chromium(III) porphyrin alkoxide complexes have not previously been characterized.
(21) (a) Gusev, D. G. Revised Mechanisms of the Catalytic Alcohol Dehydrogenation and Ester Reduction with the Milstein PNN Complex of Ruthenium. *Organometallics* **2020**, *39*, 258−270. (b) Smythe, N. A.; Grice, K. A.; Williams, B. S.; Goldberg, K. I. Reductive Elimination and Dissociative β-Hydride Abstraction from Pt(IV) Hydroxide and Methoxide Complexes. *Organometallics* **2009**, *28*, 277−288. (c) Fafard, C. M.; Ozerov, O. V. Retardation of β-hydrogen elimination in PNP Pincer complexes of Pd. *Inorg. Chim. Acta* **2007**, *360*, 286−292. (d) Blum, O.; Milstein, D. Hydride elimination from an iridium(III) alkoxide complex: a case in which a vacant *cis* coordination site is not required. *J. Organomet. Chem.* **2000**, *593*−*594*, 479−484.
(22) Kepp, K. P. A Quantitative Scale of Oxophilicity and Thiophilicity. *Inorg. Chem.* **2016**, *55*, 9461−9470.

https://doi.org/10.1021/acs.organomet.1c00123
Organometallics 2021, 40, 1328−1335

(23) (a) Dub, P. A.; Gordon, J. C. Metal-Ligand Bifunctional Catalysis: The "Accepted" Mechanism, the Issue of Concertedness, and the Function of the Ligand in Catalytic Cycles Involving Hydrogen Atoms. *ACS Catal.* **2017**, *7*, 6635−6655. (b) Khusnutdinova, J. R.; Milstein, D. Metal-Ligand Cooperation. *Angew. Chem., Int. Ed.* **2015**, *54*, 12236−12273. (c) Morris, R. H. Exploiting Metal-Ligand Bifunctional Reactions in the Design of Iron Asymmetric Hydrogenation Catalysts. *Acc. Chem. Res.* **2015**, *48*, 1494−1502.

(24) (a) De Luca, G.; Romeo, A.; Scolaro, L. M.; Ricciardi, G.; Rosa, A. Sitting-Atop Metallo-Porphyrin Complexes: Experimental and Theoretical Investigations on Such Elusive Species. *Inorg. Chem.* **2009**, *48*, 8493−8507. (b) Shen, Y.; Ryde, U. The structure of sitting-atop complexes of metalloporphyrins studied by theoretical methods. *J. Inorg. Biochem.* **2004**, *98*, 878−895.

(25) A two-electron reduced nickel(II) porphyrin complex has been shown by DFT calculations to react with a proton at the pyrrole nitrogen. A further reaction with an additional proton generated H_2, see: Wu, Z.-Y.; Wang, T.; Meng, Y.-S.; Rao, Y.; Wang, B.-W.; Zheng, J.; Gao, S.; Zhang, J.-L. Enhancing the reactivity of nickel(II) in hydrogen evolution reactions (HERs) by β-hydrogenation of porphyrinoid ligands. *Chem. Sci.* **2017**, *8*, 5953−5961.

(26) In solution, complex E prefers to coordinate an additional ligand such as an alcohol or an amine, see: Chatterjee, C.; Chisholm, M. H. Influence of the Metal (Al, Cr, and Co) and the Substituents of the Porphyrin in Controlling the Reactions Involved in the Copolymerization of Propylene Oxide and Carbon Dioxide by Porphyrin Metal(III) Complexes. 2. Chromium Chemistry. *Inorg. Chem.* **2012**, *51*, 12041−12052.

https://doi.org/10.1021/acs.organomet.1c00123
Organometallics 2021, 40, 1328−1335

9. Bibliography

(1) Barta, K.; Ford, P. C. *Acc. Chem. Res.* **2014**, *47* (5), 1503–1512.

(2) Tuck, C. O.; Perez, E.; Horvath, I. T.; Sheldon, R. A.; Poliakoff, M. *Science* **2012**, *337* (6095), 695–699.

(3) Baruah, J.; Nath, B. K.; Sharma, R.; Kumar, S.; Deka, R. C.; Baruah, D. C.; Kalita, E. *Front. Energy Res.* **2018**, *6*, 1–19.

(4) Pera-Titus, M.; Shi, F. *ChemSusChem* **2014**, *7* (3), 720–722.

(5) Li, M. F.; Yang, S.; Sun, R. C. *Bioresour. Technol.* **2016**, *200*, 971–980.

(6) Muñoz, C.; Baeza, J.; Freer, J.; Mendonça, R. T. *J. Ind. Microbiol. Biotechnol.* **2011**, *38* (11), 1861–1866.

(7) Huijgen, W. J. J.; Smit, A. T.; de Wild, P. J.; den Uil, H. *Bioresour. Technol.* **2012**, *114*, 389–398.

(8) Reisinger, M.; Tirpanalan, Ö.; Huber, F.; Kneifel, W.; Novalin, S. *Bioresour. Technol.* **2014**, *170*, 53–61.

(9) Ostovareh, S.; Karimi, K.; Zamani, A. *Ind. Crops Prod.* **2015**, *66* (1), 170–177.

(10) Obama, P.; Ricochon, G.; Muniglia, L.; Brosse, N. *Bioresour. Technol.* **2012**, *112*, 156–163.

(11) Wildschut, J.; Smit, A. T.; Reith, J. H.; Huijgen, W. J. J. *Bioresour. Technol.* **2013**, *135*, 58–66.

(12) Amiri, H.; Karimi, K. *Bioprocess Biosyst. Eng.* **2015**, *38* (10), 1959–1972.

(13) Huijgen, W. J. J.; Smit, A. T.; Reith, J. H.; Uil, H. Den. *J. Chem. Technol. Biotechnol.* **2011**, *86* (11), 1428–1438.

(14) Hideno, A.; Kawashima, A.; Endo, T.; Honda, K.; Morita, M. *Bioresour. Technol.* **2013**, *132*, 64–70.

(15) Zhang, Q.; Tu, Z.; Wang, H.; Huang, X.; Shi, Y.; Sha, X.; Xiao, H. *J. Agric. Food Chem.* **2014**, *62* (12), 2522–2530.

(16) Yu, H.; You, Y.; Lei, F.; Liu, Z.; Zhang, W.; Jiang, J. *Bioresour. Technol.* **2015**, *187*, 161–166.

(17) Hii, K. L.; Yeap, S. P.; Mashitah, M. D. *J. Korean Soc. Appl. Biol. Chem.* **2012**, *55* (4), 507–514.

(18) Gandolfi, S.; Ottolina, G.; Consonni, R.; Riva, S.; Patel, I. *ChemSusChem* **2014**, *7*, 1991–1999.

(19) Wang, K.; Yang, H.; Guo, S.; Tang, Y.; Jiang, J.; Xu, F.; Sun, R. C. *Process Biochem.* **2012**, *47* (10), 1503–1509.

(20) Schiff, H. *Justus Liebigs Ann. Chem.* **1864**, *131*, 118–119.

(21) Patil, R. D.; Adimurthy, S. *Asian J. Org. Chem.* **2013**, *2* (9), 726–744.

(22) Mukherjee, A.; Nerush, A.; Leitus, G.; Shimon, L. J. W.; Ben David, Y.; Espinosa Jalapa, N. A.; Milstein, D. *J. Am. Chem. Soc.* **2016**, *138* (13), 4298–4301.

(23) Chen, B.; Wang, L.; Gao, S. *ACS Catal.* **2015**, *5* (10), 5851–5876.

(24) Rao, V. K.; Reddy, S. S.; Krishna, B. S.; Naidu, K. R. M.; Raju, C. N.; Ghosh, S. K. *Green Chem. Lett. Rev.* **2010**, *3* (3), 217–223.

(25) Bálint, E.; Tajti, Á.; Ádám, A.; Csontos, I.; Karaghiosoff, K.; Czugler, M.; Ábrányi-Balogh, P.; Keglevich, G. *Beilstein J. Org. Chem.* **2017**, *13*, 76–86.

(26) Müller, T. E.; Hultzsch, K. C.; Yus, M.; Foubelo, F.; Tada, M. *Chem. Rev.* **2008**, *108* (9), 3795–3892.

(27) Huang, J. M.; Zhang, J. F.; Dong, Y.; Gong, W. *J. Org. Chem.* **2011**, *76* (9), 3511–3514.

(28) Park, Y. J.; Jo, E. A.; Jun, C. H. *Chem. Commun.* **2005**, *1* (9), 1185–1187.

(29) Smith, G. E. P.; Bergstrom, F. W. *J. Am. Chem. Soc.* **1934**, *56* (10), 2095–2098.

(30) K. C. Gulati; S. R. Seth; K. Venkataraman. *Org. Synth.* **1935**, *15*, 70.

(31) Payette, J. N.; Yamamoto, H. *J. Am. Chem. Soc.* **2008**, *130* (37), 12276–12278.

(32) Wong, Y. C.; Parthasarathy, K.; Cheng, C. H. *Org. Lett.* **2010**, *12* (8), 1736–1739.

(33) Huang, J.; Yu, L.; He, L.; Liu, Y. M.; Cao, Y.; Fan, K. N. *Green Chem.* **2011**, *13* (10), 2672–2677.

(34) Pelletier, G.; Bechara, W. S.; Charette, A. B. *J. Am. Chem. Soc.* **2010**, *132* (37), 12817–12819.

(35) Ishiyama, T.; Oh-e, T.; Miyaura, N.; Suzuki, A. *Tetrahedron Lett.* **1992**, *33* (31), 4465–4468.

(36) Reyes-Sánchez, A.; Cañavera-Buelvas, F.; Barrios-Francisco, R.; Cifuentes-Vaca, O. L.; Flores-Alamo, M.; García, J. J. *Organometallics* **2011**, *30* (12), 3340–3345.

(37) Tobisu, M.; Yamaguchi, S.; Chatani, N. *Org. Lett.* **2007**, *9* (17), 3351–3353.

(38) Reddy, C. V.; Kingston, J. V.; Verkade, J. G. *J. Org. Chem.* **2008**, *73* (8), 3047–3062.

(39) Ritter, J. J. *J. Am. Chem. Soc.* **1933**, *55* (8), 3322–3326.

(40) Sabatier P., Mailhe A., H. C. R. *Seances Acad. Sci.* **1909**, *148*, 898.

(41) Valot, F.; Fache, F.; Jacquot, R.; Spagnol, M.; Lemaire, M. *Tetrahedron Lett.* **1999**, *40* (19), 3689–3692.

(42) Sheldon, R. A. *Chem. Soc. Rev.* **2012**, *41* (4), 1437–1451.

(43) Sheldon, R. A. *Chem. Commun.* **2008**, 29, 3352-3365.

(44) Watson, A. J. A.; Williams, J. M. J. *Science* **2010**, *329* (5992), 635–636.

(45) Collins, J. C.; Hess, W. W.; Frank, F. J. *Tetrahedron Lett.* **1968**, *9* (30), 3363–3366.

(46) Dess, D. B.; Martin, J. C. *J. Org. Chem.* **1983**, *48* (22), 4155–4156.

(47) Omura, K.; Swern, D. *Tetrahedron* **1978**, *34* (11), 1651–1660.

(48) Griffith, W. P.; Ley, S. V.; Whitcombe, G. P.; White, A. D. *J. Chem. Soc., Chem. Commun.* **1987**, 1625–1627.

(49) Pier L. A.; Fernando M.; Silvio Q. *Org. Synth.* **1990**, *69*, 212.

(50) Keirs, D.; Overton, K. *J. Chem. Soc., Chem. Commun.* **1987**, 1660–1667.

(51) Nicolaou, K. C.; Mathison, C. J. N.; Montagnon, T. *J. Am. Chem. Soc.* **2004**, *126* (16), 5192–5201.

(52) Highet, R. J.; Wildman, W. C. *J. Am. Chem. Soc.* **1955**, *77* (16), 4399–4401.

(53) Ohtani, B.; Osaki, H.; Nishimoto, S.; Kagiya, T. *Chem. Lett.* **1985**, *14* (7), 1075–1078.

(54) Lang, X.; Ma, W.; Zhao, Y.; Chen, C.; Ji, H.; Zhao, J. *Chem. Eur. J.* **2012**, *18* (9), 2624–2631.

(55) Furukawa, S.; Ohno, Y.; Shishido, T.; Teramura, K.; Tanaka, T. *ACS Catal.* **2011**, *1* (10), 1150–1153.

(56) Park, J. H.; Ko, K. C.; Kim, E.; Park, N.; Ko, J. H.; Ryu, D. H.; Ahn, T. K.; Lee, J. Y.; Son, S. U. *Org. Lett.* **2012**, *14* (21), 5502–5505.

(57) Largeron, M.; Chiaroni, A.; Fleury, M. B. *Chem. Eur. J.* **2008**, *14* (3), 996–1003.

(58) Okimoto, M.; Takahashi, Y.; Numata, K.; Nagata, Y.; Sasaki, G. *Synth. Commun.* **2005**, *35* (15), 1989–1995.

(59) Samec, J. S. M.; Éll, A. H.; Bäckvall, J. E. *Chem. Eur. J.* **2005**, *11* (8), 2327–2334.

(60) Liu, L.; Wang, Z.; Fu, X.; Yan, C. H. *Org. Lett.* **2012**, *14* (22), 5692–5695.

(61) Wendlandt, A. E.; Stahl, S. S. *Org. Lett.* **2012**, *14* (11), 2850–2853.

(62) Kamal, A.; Devaiah, V.; Laxma Reddy, K.; Shankaraiah, N. *Adv. Synth. Catal.* **2006**, *348* (1–2), 249–254.

(63) Donthiri, R. R.; Patil, R. D.; Adimurthy, S. *Eur. J. Org. Chem.* **2012**, 4457–4460.

(64) Liu, L.; Zhang, S.; Fu, X.; Yan, C. H. *Chem. Commun.* **2011**, *47* (36), 10148–10150.

(65) Jiang, L.; Jin, L.; Tian, H.; Yuan, X.; Yu, X.; Xu, Q. *Chem. Commun.* **2011**, *47* (38), 10833–10835.

(66) Geng, L.; Jian, W.; Jing, P.; Zhang, W.; Yan, W.; Bai, F. Q.; Liu, G. *J. Catal.* **2019**, *377*, 145–152.

(67) Kang, Q.; Zhang, Y. *Green Chem.* **2012**, *14* (4), 1016–1019.

(68) Geng, L.; Song, J.; Zhou, Y.; Xie, Y.; Huang, J.; Zhang, W.; Peng, L.; Liu, G. *Chem. Commun.* **2016**, *52* (92), 13495–13498.

(69) Wang, K.; Gao, W.; Jiang, P.; Lan, K.; Yang, M.; Huang, X.; Ma, L.; Niu, F.; Li, R. *Mol. Catal.* **2019**, *465*, 43–53.

(70) Zhang, Y.; Lu, F.; Zhang, H. Y.; Zhao, J. *Catal. Lett.* **2017**, *147* (1), 20–28.

(71) Wan, Y.; Ma, J. Q.; Hong, C.; Li, M. C.; Jin, L. Q.; Hu, X. Q.; Hu, B. X.; Mo, W. M.; Sun, N.; Shen, Z. L. *Chin. Chem. Lett.* **2018**, *29* (8), 1269–1272.

(72) Chen, B.; Li, J.; Dai, W.; Wang, L.; Gao, S. *Green Chem.* **2014**, *16* (6), 3328–3334.

(73) Blackburn, L.; Taylor, R. J. K. *Org. Lett.* **2001**, *3* (11), 1637–1639.

(74) Wang, C.; Chen, C.; Han, J.; Zhang, J.; Yao, Y.; Zhao, Y. *Eur. J. Org. Chem.* **2015**, 2972–2977.

(75) Xu, J.; Zhuang, R.; Bao, L.; Tang, G.; Zhao, Y. *Green Chem.* **2012**, *14* (9), 2384–2387.

(76) Biswas, S.; Dutta, B.; Mullick, K.; Kuo, C. H.; Poyraz, A. S.; Suib, S. L. *ACS Catal.* **2015**, *5* (7), 4394–4403.

(77) Kegnæs, S.; Mielby, J.; Mentzel, U. V.; Christensen, C. H.; Riisager, A. *Green Chem.* **2010**, *12* (8), 1437–1441.

(78) Poreddy, R.; García-Suárez, E. J.; Riisager, A.; Kegnæs, S. *Dalton Trans.* **2014**, *43* (11), 4255–4259.

(79) He, W.; Wang, L.; Sun, C.; Wu, K.; He, S.; Chen, J.; Wu, P.; Yu, Z. *Chem. Eur. J.* **2011**, *17* (47), 13308–13317.

(80) Tian, H.; Yu, X.; Li, Q.; Wang, J.; Xu, Q. *Adv. Synth. Catal.* **2012**, *354* (14–15), 2671–2677.

(81) Kwon, M. S.; Kim, S.; Park, S.; Bosco, W.; Chidrala, R. K.; Park, J. *J. Org. Chem.* **2009**, *74* (10), 2877–2879.

(82) Cui, W.; Zhaorigetu, B.; Jia, M.; Ao, W.; Zhu, H. *RSC Adv.* **2014**, *4* (6), 2601–2604.

(83) Bhattacharjee, J.; Sachdeva, M.; Panda, T. K. *Z. Anorg. Allg. Chemie* **2016**, *642* (17), 937–940.

(84) Tamura, M.; Tomishige, K. *J. Catal.* **2020**, *389*, 285–296.

(85) Sheldon, R. A. *Green Chem.* **2007**, *9* (12), 1273–1283.

(86) Galiano, F.; Castro-Muñoz, R.; Mancuso, R.; Gabriele, B.; Figoli, A. *Catalysts* **2019**, *9*, 614.

(87) de Vries, J. G.; Jackson, S. D. *Catal. Sci. Technol.* **2012**, *2*, 2009.

(88) Völksen, W. *Starch* **1949**, *1* (2), 30–36.

(89) Force, C.; Ages, M. *Stud. Surf. Sci. Catal.* **1993**, *79*, 3–21.

(90) Camia, A. *Catal. Lett.* **2000**, *67* (1), 1–4.

(91) Fadhel, A. Z.; Pollet, P.; Liotta, C. L.; Eckert, C. A. *Molecules* **2010**, *15* (11), 8400–8424.

(92) Stork, T.; Answer, E.; Dilemma, H.; York, N. *Org. Process Res. Dev.* **2006**, *10* (3), 683–684.

(93) Werner, A. *Ber. Dtsch. Chem. Ges.* **1911**, *44* (2), 1887–1898.

(94) *https://www.nobelprize.org/prizes/chemistry/1913/werner/facts* (accessed April **2021**).

(95) Erkey, C. *Supercrit. Fluid Sci. Technol.* **2011**, *1*, 1–10.

(96) Langmuir, I. *Science* **1921**, *54* (1386), 59–67.

(97) William B. Jensen. *Chem. Educ. Today* **2005**, *81*, 28.

(98) Kaupp, M. *Angew. Chem. Int. Ed.* **2001**, *40* (19), 3535–3565.

(99) Klaue, A.; Kruck, M.; Friederichs, N.; Bertola, F.; Wu, H.; Morbidelli, M. *Ind. Eng. Chem. Res.* **2019**, *58* (2), 886–896.

(100) Kianinia, Y.; Khalesi, M. R.; Abdollahy, M.; Hefter, G.; Senanayake, G.; Hnedkovsky, L.; Darban, A. K.; Shahbazi, M. *Minerals* **2018**, *8* (3), 1–13.

(101) Corriu, R. J. P.; Masse, J. P. *J. Chem. Soc., Chem. Commun.* **1972**, 144a.

(102) Tamao, K.; Sumitani, K.; Kumada, M. *J. Am. Chem. Soc.* **1972**, *94*, 4374–4376.

(103) de Meijere, A.; Meyer, F. E. *Angew. Chem. Int. Ed.* **1995**, *33*, 2379–2411.

(104) Beletskaya, I. P.; Cheprakov, A. V. *Chem. Rev.* **2000**, *100* (8), 3009–3066.

(105) Mc Cartney, D.; Guiry, P. J. *Chem. Soc. Rev.* **2011**, *40* (10), 5122–5150.

(106) Sonogashira, K. *J. Organomet. Chem.* **2002**, *653* (1–2), 46–49.

(107) Gazvoda, M.; Virant, M.; Pinter, B.; Košmrlj, J. *Nat. Commun.* **2018**, *9*, 4814.

(108) King, A. O.; Okukado, N.; Negishi, E. I. *J. Chem. Soc., Chem. Commun.* **1977**, 683–684.

(109) Gavryushin, A.; Kofink, C.; Manolikakes, G.; Knochel, P. *Org. Lett.* **2005**, *7* (22), 4871–4874.

(110) Zhou, J.; Fu, G. C. *J. Am. Chem. Soc.* **2003**, *125* (48), 14726–14727.

(111) Negishi, E.; King, A. O.; Okukado, N. *J. Org. Chem.* **1977**, *42* (10), 1821–1823.

(112) Stille, J. K. *Angew. Chem. Int. Ed.* **1986**, *25* (6), 508–524.

(113) Miyaura, N.; Yamada, K.; Suzuki, A. *Tetrahedron Lett.* **1979**, *20* (36), 3437–3440.

(114) Miyaura, N.; Suzuki, A. *J. Chem. Soc., Chem. Commun.* **1979**, 866–867.

(115) Suzuki, A. *J. Organomet. Chem.* **1999**, *576* (1–2), 147–168.

(116) Hatanaka, Y.; Hiyama, T. *J. Org. Chem.* **1988**, *53* (4), 918–920.

(117) Denmark, S. E.; Regens, C. S. *Acc. Chem. Res.* **2008**, *41* (11), 1486–1499.

(118) Forero-Cortés, P. A.; Haydl, A. M. *Org. Process Res. Dev.* **2019**, *23* (8), 1478–1483.

(119) Chinchilla, R.; Nájera, C. *Chem. Soc. Rev.* **2011**, *40* (10), 5084–5121.

(120) McGlacken, G. P.; Fairiamb, I. J. S. *Eur. J. Org. Chem.* **2009**, 4011–4029.

(121) Dobson, A.; Robinson, S. D. *Inorg. Chem.* **1977**, *16* (1), 137–142.

(122) McAuliffe, C. A.; Perry, W. D. *Inorg. Chim. Acta* **1975**, *12* (1), 29–30.

(123) Charman, H. B. *J. Chem. Soc. B* **1970**, 584–587.

(124) Charman, H. B. *J. Chem. Soc. B Phys. Org.* **1967**, 629–632.

(125) Imai, H.; Nishiguchi, T.; Fukuzumi, K. *J. Org. Chem.* **1974**, *39* (12), 1622–1627.

(126) Yang, X. *ACS Catal.* **2013**, *3* (12), 2684–2688.

(127) Gnanaprakasam, B.; Zhang, J.; Milstein, D. *Angew. Chem. Int. Ed.* **2010**, *49* (8), 1468–1471.

(128) Musa, S.; Fronton, S.; Vaccaro, L.; Gelman, D. *Organometallics* **2013**, *32* (10), 3069–3073.

(129) Saha, B.; Wahidurrahaman, S. M.; Daw, P.; Sengupta, G.; Bera, J. K. *Chem. Eur. J.* **2014**, *20* (21), 6542–6551.

(130) Tanabe, Y.; Kuriyama, S.; Arashiba, K.; Nakajima, K.; Nishibayashi, Y. *Organometallics* **2014**, *33* (19), 5295–5300.

(131) Musa, S.; Shaposhnikov, I.; Cohen, S.; Gelman, D. *Angew. Chem. Int. Ed.* **2011**, *50* (15), 3533–3537.

(132) Huckabee, B. K.; Lin, S.; Smith, T. L.; Stuk, T. L. *Org. Process Res. Dev.* **2000**, *4* (6), 594–595.

(133) Stevens, C. V.; Vekemans, W.; Moonen, K.; Rammeloo, T. *Tetrahedron Lett.* **2003**, *44* (8), 1619–1622.

(134) Casarrubios, L.; Pérez, J. A.; Brookhart, M.; Templeton, J. L. *J. Org. Chem.* **1996**, *61* (24), 8358–8359.

(135) Panda, S.; Saha, R.; Sethi, S.; Ghosh, R.; Bagh, B. *J. Org. Chem.* **2020**, *85* (23), 15610–15621.

(136) Cheung, H. W.; Li, J.; Zheng, W.; Zhou, Z.; Chiu, Y. H.; Lin, Z.; Lau, C. P. *Dalton Trans.* **2010**, *39* (1), 265–274.

(137) Alós, J.; Bolaño, T.; Esteruelas, M. A.; Oliván, M.; Oñate, E.; Valencia, M. *Inorg. Chem.* **2014**, *53* (2), 1195–1209.

(138) Thiyagarajan, S.; Gunanathan, C. *ACS Catal.* **2017**, *7* (8), 5483–5490.

(139) Zhu, Z. H.; Li, Y.; Wang, Y. B.; Lan, Z. G.; Zhu, X.; Hao, X. Q.; Song, M. P.

Organometallics **2019**, *38* (9), 2156–2166.

(140) Thiyagarajan, S.; Gunanathan, C. *ACS Catal.* **2018**, *8* (3), 2473–2478.

(141) Yadav, V.; Landge, V. G.; Subaramanian, M.; Balaraman, E. *ACS Catal.* **2020**, *10* (2), 947–954.

(142) Chakraborty, P.; Garg, N.; Manoury, E.; Poli, R.; Sundararaju, B. *ACS Catal.* **2020**, *10* (14), 8023–8031.

(143) Kong, Y. Y.; Wang, Z. X. *Asian J. Org. Chem.* **2020**, *9* (8), 1192–1198.

(144) Kashiwame, Y.; Kuwata, S.; Ikariya, T. *Organometallics* **2012**, *31* (23), 8444–8455.

(145) Jana, A.; Reddy, C. B.; Maji, B. *ACS Catal.* **2018**, *8* (10), 9226–9231.

(146) Borghs, J. C.; Tran, M. A.; Sklyaruk, J.; Rueping, M.; El-Sepelgy, O. *J. Org. Chem.* **2019**, *84* (12), 7927–7935.

(147) Jayaprakash, H.; Guo, L.; Wang, S.; Bruneau, C.; Fischmeister, C. *Eur. J. Org. Chem.* **2020**, 4326–4330.

(148) Hashiguchi, S.; Fujii, A.; Takehara, J.; Ikariya, T.; Noyori, R. *J. Am. Chem. Soc.* **1995**, *117* (28), 7562–7563.

(149) Bertoli, M.; Choualeb, A.; Lough, A. J.; Moore, B.; Spasyuk, D.; Gusev, D. G. *Organometallics* **2011**, *30* (13), 3479–3482.

(150) Esteruelas, M. A.; Lezáun, V.; Martínez, A.; Oliván, M.; Onate, E. *Organometallics* **2017**, *36* (15), 2996–3004.

(151) Nishimura, T.; Onoue, T.; Ohe, K.; Uemura, S. *J. Org. Chem.* **1999**, *64* (18), 6750–6755.

(152) Muzart, J. *Tetrahedron* **2003**, *59* (31), 5789–5816.

(153) Wang, X.; Wang, C.; Liu, Y.; Xiao, J. *Green Chem.* **2016**, *18* (17), 4605–4610.

(154) Gandeepan, P.; Müller, T.; Zell, D.; Cera, G.; Warratz, S.; Ackermann, L. *Chem. Rev.* **2019**, *119* (4), 2192–2452.

(155) *https://www.ema.europa.eu/en/documents/scientific-guideline/guideline-specification-limits-residues-metal-catalysts-metal-reagents_en.pdf* (accessed April **2021**).

(156) Zoroddu, M. A.; Aaseth, J.; Crisponi, G.; Medici, S.; Peana, M.; Nurchi, V. M. *J. Inorg. Biochem.* **2019**, *195*, 120–129.

(157) McCall, A. S.; Cummings, C. F.; Bhave, G.; Vanacore, R.; Page-Mccaw, A.; Hudson, B. G. *Cell* **2014**, *157* (6), 1380–1392.

(158) *https://www.visualcapitalist.com/all-the-worlds-metals-and-minerals-in-one-visualization/* (accessed April **2021**).

(159) Li, H.; Hall, M. B. *ACS Catal.* **2015**, *5* (3), 1895–1913.

(160) Chakraborty, S.; Das, U. K.; Ben-David, Y.; Milstein, D. *J. Am. Chem. Soc.* **2017**, *139*

(34), 11710–11713.

(161) Chakraborty, S.; Gellrich, U.; Diskin-Posner, Y.; Leitus, G.; Avram, L.; Milstein, D. *Angew. Chem. Int. Ed.* **2017**, *56* (15), 4229–4233.

(162) Bauer, J. O.; Chakraborty, S.; Milstein, D. *ACS Catal.* **2017**, *7* (7), 4462–4466.

(163) Azizi, K.; Akrami, S.; Madsen, R. *Chem. Eur. J.* **2019**, *25* (25), 6439–6446.

(164) Tursky, M.; Lorentz-Petersen, L. L. R.; Olsen, L. B.; Madsen, R. *Org. Biomol. Chem.* **2010**, *8* (24), 5576–5582.

(165) Monrad, R. N.; Madsen, R. *Org. Biomol. Chem.* **2011**, *9* (2), 610–615.

(166) Maggi, A.; Madsen, R. *Organometallics* **2012**, *31* (1), 451–455.

(167) Samuelsen, S. V.; Santilli, C.; Ahlquist, M. S. G.; Madsen, R. *Chem. Sci.* **2019**, *10* (4), 1150–1157.

(168) Sølvhøj, A.; Madsen, R. *Organometallics* **2011**, *30* (21), 6044–6048.

(169) Azizi, K.; Madsen, R. *ChemCatChem* **2018**, *10* (17), 3703–3708.

(170) Prokopchuk, D. E.; Morris, R. H. *Organometallics* **2012**, *31* (21), 7375–7385.

(171) Nguyen, D. H.; Trivelli, X.; Capet, F.; Paul, J. F.; Dumeignil, F.; Gauvin, R. M. *ACS Catal.* **2017**, *7* (3), 2022–2032.

(172) Nguyen, D. H.; Trivelli, X.; Capet, F.; Swesi, Y.; Favre-Réguillon, A.; Vanoye, L.; Dumeignil, F.; Gauvin, R. M. *ACS Catal.* **2018**, *8* (5), 4719–4734.

(173) Peña-López, M.; Piehl, P.; Elangovan, S.; Neumann, H.; Beller, M. *Angew. Chem. Int. Ed.* **2016**, *55* (48), 14967–14971.

(174) Mastalir, M.; Glatz, M.; Gorgas, N.; Stöger, B.; Pittenauer, E.; Allmaier, G.; Veiros, L. F.; Kirchner, K. *Chem. Eur. J.* **2016**, *22* (35), 12316–12320.

(175) Mastalir, M.; Glatz, M.; Pittenauer, E.; Allmaier, G.; Kirchner, K. *J. Am. Chem. Soc.* **2016**, *138* (48), 15543–15546.

(176) Fertig, R.; Irrgang, T.; Freitag, F.; Zander, J.; Kempe, R. *ACS Catal.* **2018**, *8* (9), 8525–8530.

(177) Deibl, N.; Kempe, R. *Angew. Chem. Int. Ed.* **2017**, *56* (6), 1663–1666.

(178) Chakraborty, S.; Lagaditis, P. O.; Förster, M.; Bielinski, E. A.; Hazari, N.; Holthausen, M. C.; Jones, W. D.; Schneider, S. *ACS Catal.* **2014**, *4* (11), 3994–4003.

(179) Koehne, I.; Schmeier, T. J.; Bielinski, E. A.; Pan, C. J.; Lagaditis, P. O.; Bernskoetter, W. H.; Takase, M. K.; Würtele, C.; Hazari, N.; Schneider, S. *Inorg. Chem.* **2014**, *53* (4), 2133–2143.

(180) Chakraborty, S.; Brennessel, W. W.; Jones, W. D. *J. Am. Chem. Soc.* **2014**, *136* (24), 8564–8567.

(181) Bielinski, E. A.; Lagaditis, P. O.; Zhang, Y.; Mercado, B. Q.; Würtele, C.; Bernskoetter, W. H.; Hazari, N.; Schneider, S. *J. Am. Chem. Soc.* **2014**, *136* (29), 10234–10237.

(182) Bala, M.; Verma, P. K.; Kumar, N.; Sharma, U.; Singh, B. *Can. J. Chem.* **2013**, *91* (8), 732–737.

(183) Zhang, G.; Vasudevan, K. V.; Scott, B. L.; Hanson, S. K. *J. Am. Chem. Soc.* **2013**, *135* (23), 8668–8681.

(184) Bianchini, C.; Peruzzini, M.; Vacca, A.; Zanello, P.; Laschi, F.; Ottaviani, F. M. *Inorg. Chem.* **1990**, *29* (18), 3394–3402.

(185) Hebden, T. J.; St. John, A. J.; Gusev, D. G.; Kaminsky, W.; Goldberg, K. I.; Heinekey, D. M. *Angew. Chem. Int. Ed.* **2011**, *50* (8), 1873–1876.

(186) Camus, A.; Cocevar, C.; Mestroni, G. *J. Organomet. Chem.* **1972**, *39* (2), 355–364.

(187) Muetterties, E. L.; Watson, P. L. *J. Am. Chem. Soc.* **1976**, *98* (15), 4665–4667.

(188) Brewer, K. J.; Murphy, W. R.; Moore, K. J.; Eberle, E. C.; Petersen, J. D. *Inorg. Chem.* **1986**, *25* (14), 2470–2472.

(189) Pandey, B.; Xu, S.; Ding, K. *Org. Lett.* **2019**, *21* (18), 7420–7423.

(190) Paudel, K.; Xu, S.; Ding, K. *J. Org. Chem.* **2020**, *85* (23), 14980–14988.

(191) Paudel, K.; Xu, S.; Hietsoi, O.; Pandey, B.; Onuh, C.; Ding, K. *Organometallics* **2021**, *40* (3), 418–426.

(192) Rösler, S.; Ertl, M.; Irrgang, T.; Kempe, R. *Angew. Chem. Int. Ed.* **2015**, *54* (50), 15046–15050.

(193) Zhang, G.; Yin, Z.; Zheng, S. *Org. Lett.* **2016**, *18* (2), 300–303.

(194) Mastalir, M.; Tomsu, G.; Pittenauer, E.; Allmaier, G.; Kirchner, K. *Org. Lett.* **2016**, *18* (14), 3462–3465.

(195) Daw, P.; Ben-David, Y.; Milstein, D. *ACS Catal.* **2017**, *7* (11), 7456–7460.

(196) Daw, P.; Chakraborty, S.; Garg, J. A.; Ben-David, Y.; Milstein, D. *Angew. Chem. Int. Ed.* **2016**, *55* (46), 14373–14377.

(197) Mandal, S. *Int. J. Sci. Technol. Res.* **2020**, *9* (1), 3803–3807.

(198) Ahmad, J. U.; Figiel, P. J.; Räisänen, M. T.; Leskelä, M.; Repo, T. *Appl. Catal. A Gen.* **2009**, *371* (1–2), 17–21.

(199) Chakraborty, S.; Piszel, P. E.; Brennessel, W. W.; Jones, W. D. *Organometallics* **2015**, *34* (21), 5203–5206.

(200) Schrock, R. R.; Osborn, J. A. *J. Chem. Soc. D Chem. Commun.* **1970**, 567–568.

(201) Clapham, S. E.; Hadzovic, A.; Morris, R. H. *Coord. Chem. Rev.* **2004**, *248* (21–24), 2201–2237.

(202) Samec, J. S. M.; Bäckvall, J. E.; Andersson, P. G.; Brandt, P. *Chem. Soc. Rev.* **2006**, *35* (3), 237–248.

(203) Malacea, R.; Poli, R.; Manoury, E. *Coord. Chem. Rev.* **2010**, *254* (5–6), 729–752.

(204) Khusnutdinova, J. R.; Milstein, D. *Angew. Chem. Int. Ed.* **2015**, *54* (42), 12236–12273.

(205) Gunanathan, C.; Milstein, D. *Acc. Chem. Res.* **2011**, *44* (8), 588–602.

(206) Blum, Y.; Czarkie, D.; Rahamim, Y.; Shvo, Y. *Organometallics* **1985**, *4* (8), 1459–1461.

(207) Dub, P. A.; Gordon, J. C. *ACS Catal.* **2017**, *7* (10), 6635–6655.

(208) Noyori, R.; Ohkuma, T. *Angew. Chem. Int. Ed.* **2001**, *40* (1), 40–73.

(209) Morris, R. H. *Acc. Chem. Res.* **2015**, *48* (5), 1494–1502.

(210) *https://pubs.usgs.gov/fs/2010/3089/pdf/fs2010-3089.pdf* (accessed April **2021**).

(211) Baruthio, F. *Biol. Trace Elem. Res.* **1992**, *32* (1–3), 145–153.

(212) Ma, J.; Liu, S.; Kong, X.; Fan, X.; Yan, X.; Chen, L. *Res. Chem. Intermed.* **2012**, *38* (7), 1341–1349.

(213) Durandetti, M.; Nédélec, J. Y.; Périchon, J. *Org. Lett.* **2001**, *3* (13), 2073–2074.

(214) Chareonsiriwat, L.; Chavasiri, W. *Synth. Commun.* **2017**, *47* (4), 257–267.

(215) Bai, G. Y.; Dou, H. Y.; Qiu, M. De; He, F.; Fan, X. X.; Ma, Z. *Res. Chem. Intermed.* **2010**, *36* (5), 483–490.

(216) Dapurkar, S. E.; Kawanami, H.; Yokoyama, T.; Ikushima, Y. *Catal. Commun.* **2009**, *10* (6), 1025–1028.

(217) Yun, J. J.; Liu, X. Y.; Deng, W.; Chu, X. Q.; Shen, Z. L.; Loh, T. P. *J. Org. Chem.* **2018**, *83* (18), 10898–10907.

(218) Ling, L.; Chen, C.; Luo, M.; Zeng, X. *Org. Lett.* **2019**, *21* (6), 1912–1916.

(219) Bellan, A. B.; Kuzmina, O. M.; Vetsova, V. A.; Knochel, P. *Synthesis* **2017**, *49*, 188–194.

(220) Cong, X.; Tang, H.; Zeng, X. *J. Am. Chem. Soc.* **2015**, *137* (45), 14367–14372.

(221) Chen, C.; Liu, P.; Luo, M.; Zeng, X. *ACS Catal.* **2018**, *8* (7), 5864–5868.

(222) Weston, M. H.; Farha, O. K.; Hauser, B. G.; Hupp, J. T.; Nguyen, S. T. *Chem. Mater.* **2012**, *24* (7), 1292–1296.

(223) Tanabe, K. K.; Ferrandon, M. S.; Siladke, N. A.; Kraft, S. J.; Zhang, G.; Niklas, J.; Poluektov, O. G.; Lopykinski, S. J.; Bunel, E. E.; Krause, T. R.; Miller, J. T.; Hock, A. S.; Nguyen, S. T. *Angew. Chem. Int. Ed.* **2014**, *53* (45), 12055–12058.

(224) Hirscher, N. A.; Agapie, T. *Organometallics* **2017**, *36* (21), 4107–4110.

(225) Hirscher, N. A.; Perez Sierra, D.; Agapie, T. *J. Am. Chem. Soc.* **2019**, *141* (14), 6022–6029.

(226) Gregori, B. J.; Nowakowski, M.; Schoch, A.; Pöllath, S.; Zweck, J.; Bauer, M.; Jacobi von Wangelin, A. *ChemCatChem* **2020**, *12* (21), 5359–5363.

(227) Kallmeier, F.; Fertig, R.; Irrgang, T.; Kempe, R. *Angew. Chem. Int. Ed.* **2020**, *59* (29), 11789–11793.

(228) Chen, W.; Suenobu, T.; Fukuzumi, S. *Chem. Asian J.* **2011**, *6* (6), 1416–1422.

(229) Barona-Castaño, J.; Carmona-Vargas, C.; Brocksom, T.; de Oliveira, K. *Molecules* **2016**, *21*, 310.

(230) Chang, C. K.; Kuo, M.-S. *J. Am. Chem. Soc.* **1979**, *101* (12), 3413–3415.

(231) Cao, H.; Wang, G.; Xue, Y.; Yang, G.; Tian, J.; Liu, F.; Zhang, W. *ACS Macro Lett.* **2019**, 616–622.

(232) Adler, A. D.; Longo, F. R.; Kampas, F.; Kim, J. *J. Inorg. Nucl. Chem.* **1970**, *32* (7), 2443–2445.

(233) Gopalaiah, K. *Chem. Rev.* **2013**, *113* (5), 3248–3296.

(234) Baciocchi, E.; Gerini, M. F.; Lapi, A. *J. Org. Chem.* **2004**, *69* (10), 3586–3589.

(235) Groves, J. T.; Viski, P. *J. Am. Chem. Soc.* **1989**, *111* (22), 8537–8538.

(236) Ji, H. B.; Yuan, Q. L.; Zhou, X. T.; Pei, L. X.; Wang, L. F. *Bioorg. Med. Chem. Lett.* **2007**, *17* (22), 6364–6368.

(237) Irie, R.; Li, X.; Saito, Y. *J. Mol. Catal.* **1983**, *18* (3), 263–265.

(238) Li, A.; Pan, B.; Mu, C.; Wang, N.; Li, Y. L.; Ouyang, Q. *Synlett* **2021**, *32*, 679–684.

(239) Prasanthi, A. V. G.; Begum, S.; Srivastava, H. K.; Tiwari, S. K.; Singh, R. *ACS Catal.* **2018**, *8* (9), 8369–8375.

(240) Hock, K. J.; Knorrscheidt, A.; Hommelsheim, R.; Ho, J.; Weissenborn, M. J.; Koenigs, R. M. *Angew. Chem. Int. Ed.* **2019**, *58* (11), 3630–3634.

(241) Biswal, P.; Samser, S.; Nayak, P.; Chandrasekhar, V.; Venkatasubbaiah, K. *J. Org. Chem.* **2021**, *86* (9), 6744–6754.

(242) Miao, Y.; Samuelsen, S. V.; Madsen, R. *Organometallics* **2021**, *40* (9), 1328–1335.

(243) Takanami, T.; Hayashi, M.; Iso, K.; Nakamoto, H.; Suda, K. *Tetrahedron* **2006**, *62* (40), 9467–9474.

(244) Ganji, P.; Doyle, D. J.; Ibrahim, H. *Org. Lett.* **2011**, *13* (12), 3142–3145.

(245) Gunanathan, C.; Milstein, D. *Science* **2013**, *341*, 1229712.

(246) Corma, A.; Navas, J.; Sabater, M. J. *Chem. Rev.* **2018**, *118* (4), 1410–1459.

(247) Dobereiner, G. E.; Crabtree, R. H. *Chem. Rev.* **2010**, *110* (2), 681–703.

(248) Santra, S. K.; Szpilman, A. M. *J. Org. Chem.* **2021**, *86* (1), 1164–1171.

(249) Uygur, M.; Kuhlmann, J. H.; Pérez-Aguilar, M. C.; Piekarski, D. G.; García Mancheño, O. *Green Chem.* **2021**, *23* (9), 3392–3399.

(250) Gusev, D. G. *Organometallics* **2020**, *39* (2), 258–270.

(251) Smythe, N. A.; Grice, K. A.; Williams, B. S.; Goldberg, K. I. *Organometallics* **2009**, *28* (1), 277–288.

(252) Fafard, C. M.; Ozerov, O. V. *Inorg. Chim. Acta* **2007**, *360* (1), 286–292.

(253) Blum, O.; Milstein, D. *J. Organomet. Chem.* **2000**, *593–594*, 479–484.

(254) Kepp, K. P. *Inorg. Chem.* **2016**, *55* (18), 9461–9470.

(255) De Luca, G.; Romeo, A.; Scolaro, L. M.; Ricciardi, G.; Rosa, A. *Inorg. Chem.* **2009**, *48* (17), 8493–8507.

(256) Shen, Y.; Ryde, U. *J. Inorg. Biochem.* **2004**, *98* (5), 878–895.

(257) Wu, Z. Y.; Wang, T.; Meng, Y. S.; Rao, Y.; Wang, B. W.; Zheng, J.; Gao, S.; Zhang, J. L. *Chem. Sci.* **2017**, *8* (9), 5953–5961.

(258) Chatterjee, C.; Chisholm, M. H. *Inorg. Chem.* **2012**, *51* (21), 12041–12052.

(259) Verevkin, S. P.; Morgenthaler, J.; Rüchardt, C. *J. Chem. Thermodyn.* **1997**, *29* (10), 1175–1183.

(260) Richer, J.-C.; Perelman, D. *Can. J. Chem.* **1970**, *48* (4), 570–578.

(261) Cook, E. *Nature* **1926**, *117*, 419–421.

(262) Langeslay, R. R.; Kaphan, D. M.; Marshall, C. L.; Stair, P. C.; Sattelberger, A. P.; Delferro, M. *Chem. Rev.* **2019**, *119* (4), 2128–2191.

(263) Pellissier, H. *Coord. Chem. Rev.* **2015**, *284*, 93–110.

(264) Bulánek, R.; Čičmanec, P.; Sheng-Yang, H.; Knotek, P.; Čapek, L.; Setnička, M. *Appl. Catal. A Gen.* **2012**, *415–416*, 29–39.

(265) Chalupka, K.; Thomas, C.; Millot, Y.; Averseng, F.; Dzwigaj, S. *J. Catal.* **2013**, *305*, 46–55.

(266) Takahara, I.; Saito, M.; Inaba, M.; Murata, K. *Catal. Lett.* **2005**, *102* (3–4), 201–205.

(267) Szeto, K. C.; Loges, B.; Merle, N.; Popoff, N.; Quadrelli, A.; Jia, H.; Berrier, E.; De Mallmann, A.; Delevoye, L.; Gauvin, R. M.; Taoufik, M. *Organometallics* **2013**, *32* (21), 6452–6460.

(268) Rout, L.; Nath, P.; Punniyamurthy, T. *Adv. Synth. Catal.* **2007**, *349* (6), 846–848.

(269) Takizawa, S.; Gröger, H.; Sasai, H. *Chem. Eur. J.* **2015**, *21* (25), 8992–8997.

(270) Wang, L.; Chen, B.; Ren, L.; Zhang, H.; Lü, Y.; Gao, S. *Chin. J. Catal.* **2015**, *36* (1), 19–23.

(271) La Pierre, H. S.; Arnold, J.; Toste, F. D. *Angew. Chem. Int. Ed.* **2011**, *50* (17), 3900–3903.

(272) Taghavi, S. A.; Moghadam, M.; Mohammadpoor-Baltork, I.; Tangestaninejad, S.; Mirkhani, V.; Khosropour, A. R.; Ahmadi, V. *Polyhedron* **2011**, *30* (13), 2244–2252.

(273) Abdolmanaf Taghavi, S.; Moghadam, M.; Mohammadpoor-Baltork, I.; Tangestaninejad, S.; Mirkhani, V.; Khosropour, A. R. *Comptes Rendus Chim.* **2011**, *14* (12), 1095–1102.

(274) Taghavi, S. A.; Moghadam, M.; Mohammadpoor-Baltork, I.; Tangestaninejad, S.; Mirkhani, V.; Khosropour, A. R. *Inorg. Chim. Acta* **2011**, *377* (1), 159–164.

(275) Cozzi, P. G. *Chem. Soc. Rev.* **2004**, *33* (7), 410–421.

(276) Zhang, W.; Loebach, J. L.; Wilson, S. R.; Jacobsen, E. N. *J. Am. Chem. Soc.* **1990**, *112* (7), 2801–2803.

(277) Shaw, S.; White, J. D. *Chem. Rev.* **2019**, *119* (16), 9381–9426.

(278) Ugi, I. *Angew. Chem. Int. Ed.* **1982**, *21* (11), 810–819.

(279) Kong, D. L.; Cheng, L.; Yue, T.; Wu, H. R.; Feng, W. C.; Wang, D.; Liu, L. *J. Org. Chem.* **2016**, *81* (13), 5337–5344.

(280) Wu, X.; Gorden, A. E. V. *Eur. J. Org. Chem.* **2009**, 503–509.

(281) Landwehr, A.; Dudle, B.; Fox, T.; Blacque, O.; Berke, H. *Chem. Eur. J.* **2012**, *18* (18), 5701–5714.

(282) Corberán, R.; Peris, E. *Organometallics* **2008**, *27* (8), 1954–1958.

(283) Burling, S.; Whittlesey, M. K.; Williams, J. M. J. *Adv. Synth. Catal.* **2005**, *347* (4), 591–594.

(284) Long, J.; Zhou, Y.; Li, Y. *Chem. Commun.* **2015**, *51* (12), 2331–2334.

(285) Wang, D.; Astruc, D. *Chem. Rev.* **2015**, *115* (13), 6621–6686.

(286) Chen, S. J.; Lu, G. P.; Cai, C. *RSC Adv.* **2015**, *5* (17), 13208–13211.

(287) Seo, M. S.; Jang, S.; Jung, H.; Kim, H. *J. Org. Chem.* **2018**, *83* (23), 14300–14306.

(288) O'Donnell, M. J.; Polt, R. L. *J. Org. Chem.* **1982**, *47* (13), 2663–2666.

(289) Tran, C. C.; Kawaguchi, S. I.; Kobiki, Y.; Matsubara, H.; Tran, D. P.; Kodama, S.; Nomoto, A.; Ogawa, A. *J. Org. Chem.* **2019**, *84* (18), 11741–11751.

(290) Lamas, M.-C.; Vaillard, S. E.; Wibbeling, B.; Studer, A. *Org. Lett.* **2010**, *12* (9), 2072–2075.

(291) Tsygankov, A. A.; Chun, M. S.; Samoylova, A. D.; Kwon, S.; Kreschenova, Y. M.; Kim, S.; Shin, E.; Oh, J.; Strelkova, T. V.; Kolesov, V. S.; Zubkov, F. I.; Semenov, S. E.; Fedyanin, I. V.; Chusov, D. *Synlett* **2017**, *28*, 615–619.

(292) Szymkowiak, J.; Kwit, M. *Chirality* **2018**, *30* (2), 117–130.

(293) Godugu, K.; Yadala, V. D. S.; Pinjari, M. K. M.; Gundala, T. R.; Sanapareddy, L. R.; Nallagondu, C. G. R. *Beilstein J. Org. Chem.* **2020**, *16*, 1881–1900.

(294) Bi, J.; Dong, Y.; Meng, D.; Zhu, D.; Li, T. *Polymer* **2019**, *164*, 183–190.

(295) Wang, Q.; Yang, L.; Wu, J.; Wang, H.; Song, J.; Tang, X. *BioMetals* **2017**, *30* (1), 17–26.

(296) Aqlan, F. M.; Alam, M. M.; Asiri, A. M.; Zayed, M. E. M.; Al-eryani, D. A.; Al-zahrani, F. A. M.; El-shishtawy, R. M.; Uddin, J.; Rahman, M. M. *J. Mol. Liq.* **2019**, *281*, 401–406.

(297) Wang, Y.; Zhao, Y.; Zhu, S.; Zhou, X.; Xu, J.; Xie, X.; Poli, R. *Angew. Chem. Int. Ed.* **2020**, *59* (15), 5988–5994.

(298) Xi, X.; Shao, J.; Hu, X.; Wu, Y. *RSC Adv.* **2015**, *5* (98), 80772–80778.

(299) Cheng, J.; Li, Y.; Sun, R.; Liu, J.; Gou, F.; Zhou, X.; Xiang, H.; Liu, J. *J. Mater. Chem. C* **2015**, *3* (42), 11099–11110.

(300) Fallis, I. A.; Murphy, D. M.; Willock, D. J.; Tucker, R. J.; Farley, R. D.; Jenkins, R.; Strevens, R. R. *J. Am. Chem. Soc.* **2004**, *126* (48), 15660–15661.

(301) Shekaari, H.; Kazempour, A.; Khoshalhan, M. *Phys. Chem. Chem. Phys.* **2015**, *17* (3), 2179–2191.

(302) Coletti, A.; Whiteoak, C. J.; Conte, V.; Kleij, A. W. *ChemCatChem* **2012**, *4* (8), 1190–1196.

(303) Chang, C. J.; Labinger, J. A.; Gray, H. B. *Inorg. Chem.* **1997**, *36* (25), 5927–5930.

(304) Nenashev, R. N.; Mordvinova, N. E.; Zlomanov, V. P.; Kuznetsov, V. L. *Inorg. Mater.* **2015**, *51* (9), 891–896.

(305) Wang, W.; Li, N.; Tang, H.; Ma, Y.; Yang, X. *Mol. Catal.* **2018**, *453*, 113–120.

(306) Aranha, P. E.; Souza, J. M.; Romera, S.; Ramos, L. A.; dos Santos, M. P.; Dockal, E. R.; Cavalheiro, E. T. G. *Thermochim. Acta* **2007**, *453* (1), 9–13.

(307) Leung, W.-H.; Chan, E. Y. Y.; Chow, E. K. F.; Williams, I. D.; Peng, S.-M. *J. Chem. Soc., Dalton Trans.* **1996**, 1229–1236.

(308) Pasquali, M.; Marchetti, F.; Floriani, C. *Inorg. Chem.* **1979**, *18* (9), 2401–2404.

(309) Jezierski, A.; Raynor, J. B. *J. Chem. Soc., Dalton Trans.* **1981**, 1–7.

(310) Huang, T.; Chen, T.; Han, L. B. *J. Org. Chem.* **2018**, *83* (5), 2959–2965.

(311) Junor, G. P.; Romero, E. A.; Chen, X.; Jazzar, R.; Bertrand, G. *Angew. Chem. Int. Ed.* **2019**, *58* (9), 2875–2878.

(312) Yamada, H.; Kawate, T.; Nishida, A.; Nakagawa, M. *J. Org. Chem.* **1999**, *64* (24), 8821–8828.

(313) Xu, Q.; Chen, J.; Tian, H.; Yuan, X.; Li, S.; Zhou, C.; Liu, J. *Angew. Chem. Int. Ed.* **2014**, *53* (1), 225–229.

(314) Jana, R.; Pathak, T. P.; Sigman, M. S. *Chem. Rev.* **2011**, *111* (3), 1417–1492.

(315) Jong, Y. H.; Arnold, L. A.; Zhu, F.; Kosinski, A.; Mangano, T. J.; Setola, V.; Roth, B. L.; Guy, R. K. *J. Med. Chem.* **2009**, *52* (13), 3892–3901.

(316) Biswas, K.; Peterkin, T. A. N.; Bryan, M. C.; Arik, L.; Lehto, S. G.; Sun, H.; Hsieh, F. Y.; Xu, C.; Fremeau, R. T.; Allen, J. R. *J. Med. Chem.* **2011**, *54* (20), 7232–7246.

(317) Ma, J.; Wang, N.; Li, F. *Asian J. Org. Chem.* **2014**, *3* (9), 940–947.

(318) Jefferies, L. R.; Cook, S. P. *Tetrahedron* **2014**, *70* (27–28), 4204–4207.

(319) Jumde, V. R.; Gonsalvi, L.; Guerriero, A.; Peruzzini, M.; Taddei, M. *Eur. J. Org. Chem.* **2015**, 1829–1833.

(320) Ogawa, S.; Obora, Y. *Chem. Commun.* **2014**, *50* (19), 2491–2493.

(321) Suchand, B.; Satyanarayana, G. *Eur. J. Org. Chem.* **2017**, 3886–3895.

(322) Estes, D. P.; Norton, J. R.; Jockusch, S.; Sattler, W. *J. Am. Chem. Soc.* **2012**, *134* (37), 15512–15518.

(323) Tan, D. W.; Li, H. X.; Zhu, D. L.; Li, H. Y.; Young, D. J.; Yao, J. L.; Lang, J. P. *Org. Lett.* **2018**, *20* (3), 608–611.

(324) Graham, D. M.; Holloway, C. E. *Can. J. Chem.* **1963**, *41* (8), 2114–2118.

(325) Bellucci, G.; Chiappe, C.; Lo Moro, G. *Synlett* **1996**, *9*, 880–882.

(326) Winternheimer, D.; Shade, R.; Merlic, C. *Synthesis* **2010**, *15*, 2497–2511.

(327) Dang, Y.; Qu, S.; Wang, Z. X.; Wang, X. *Organometallics* **2013**, *32* (9), 2804–2813.